The Role of NPAS4 in Glucose Homeostasis

by

Paul Vincent Sabatini

BSc Hons, The University of Guelph, 2005

A THESIS SUBMITTED IN PARTIAL FULFILLMENT OF

THE REQUIREMENTS FOR THE DEGREE OF

DOCTOR OF PHILOSOPHY

in

THE FACULTY OF GRADUATE AND POSTDOCTORAL STUDIES

(Cell and Developmental Biology)

THE UNIVERSITY OF BRITISH COLUMBIA

(Vancouver)

July 2016

Abstract

Type 2 diabetes is characterized by hyperglycemia associated with reduced insulin secretion from pancreatic beta cells and impaired insulin sensitivity at peripheral target tissues. There is a growing body of evidence that supports the importance of bHLH-PAS domain transcription factors in promoting beta cell function. With the recent identification of neuronal PAS domain protein 4 (NPAS4) within the central nervous system, studies were undertaken to determine whether NPAS4 is expressed in beta cells, how its expression is regulated in response to changing environmental signals and uncover the functional significance of NPAS4 in the maintenance of glucose homeostasis.

Together, experiments within this thesis demonstrate that NPAS4 is expressed within the pancreatic beta cell and is rapidly upregulated in response to membrane depolarization and calcium influx. Further, this induction was impaired in a mouse model of beta cell dysfunction and within islets from individuals with T2D. Overexpression studies performed *in vitro* identified NPAS4 as a novel negative regulator of insulin expression and GLP-1 potentiated insulin secretion. Furthermore, NPAS4 protected beta cells from maladaptive cellular pathways that promote cell dysfunction and death; including endoplasmic reticulum stress and activation of HIF1α. Finally, the characterization of three different Npas4 mouse knockout models suggests that continued NPAS4 expression in the beta cell is required to maintain differentiation status and cellular function. An independent role for NPAS4 in the maintenance of glucose homeostasis was also discovered in other Pdx1-Cre expressing cells, likely within the hypothalamus. Together, the data suggest beta cells induce NPAS4

expression during periods of cellular activity and acts as a protective factor to protect cells in order to promote the maintenance of euglycemia.

Preface

Animal Studies were reviewed and approved by the University of British Columbia Committee on Animal Care under protocols A13-0184 and A14-0163.

P. Sabatini designed experiments with the guidance of F.C. Lynn. All experiments, animal monitoring, data analysis was performed by P. Sabatini with technical assistance provided by C. Nian and M. Kombo for mouse islet isolation, R. Uy for RNA extractions and E. Xu for mouse monitoring. The *in vivo* rat transfusion data presented in chapter 3 were performed in collaboration with Dr. Poitout and Dr. Zarrucki. The metabolic cage experiments and body mass composition determinations presented in chapter 5 and 6 were performed by C.K. Wong in collaboration with Dr. Gibson. Finally, the adeno-associated viral injections presented in Chapter 6 were performed by D. Dai in collaboration with Dr. Verchere.

Some data from this thesis have been previously published as described below.

1) The sections within the chapter 1, pertaining to the role of the bHLH-PAS domain proteins, HIF1α, ARNT, CLOCK and BMALI1 in beta cells has been published as Sabatini, P.V. & Lynn, F.C. (2015). All-encomPASsing regulation of beta-cells: PAS domain proteins in beta-cell dysfunction and diabetes. *Trends in Endocrinology and Metabolism.* 26(1): 49-57. P. Sabatini wrote the manuscript.

2) Data from chapters 3 and 4 has been previously published as Paul V. Sabatini, Nicole A.J. Krentz, Bader Zarrouki, Clara Y. Westwell-Roper, Cuilan Nian, Ryan A. Uy, A.M. James Shapiro, Vincent Poitout, and Francis C. Lynn. (2013). Npas4 Is a Novel Activity–Regulated Cytoprotective Factor in Pancreatic β-Cells.

Diabetes. 62(8): 2808-2820. P. Sabatini performed experiments, analyzed data and wrote the manuscript.

3) Data from chapter 3 has also been previously published as Thilo Speckmann, Paul V. Sabatini, Cuilan Nian, Riley G. Smith, and Francis C. Lynn. (2016). Npas4 transcription factor expression is regulated by calcium signalling pathways and prevents tacrolimus-induced cytotoxicity in pancreatic beta cells. *Journal of Biological Chemistry.* 291 (6) pp. 2682-2695. P. Sabatini performed the experiments and analyzed the data presented herein and edited the manuscript.

Table of Contents

List of Tables

List of Figures

List of Abbreviations

AAV	adeno-associated virus
Agrp	agouti–related peptide
Ahr	aryl hydrocarbon receptor
ANOVA	analysis of variance
AOC	area over the curve
ARC	arcuate hypothalamic nucleus
ARNT	aryl Hydrocarbon receptor nuclear translocator
ATP	adenosine triphosphate
AUC	area under the curve
BCA	bicinchoninic acid assay
bHLH	basic helix-loop-helix
BSA	bovine serum albumin
cAMP	cyclic adenosine monophosphate
cDNA	complementary deoxyribonucleic acid
ChIP	chromatin immunoprecipitation
CHW	chow diet
CMRL	connaught medical research laboratories
CNS	central nervous system
Cre	causes recombination (Cre recombinase)
Ddit3	DNA damage inducible transcript 3
DMEM	dulbecco's modified eagle's medium
DMSO	dimethyl sulfoxide

DNA	deoxyribonucleic acid
EGTA	ethylene glycol tetraacetic acid
ELISA	enzyme-linked immunosorbent assay
GABA	gamma-aminobutyric acid
Gapdh	glyceraldehyde-3-phosphate dehydrogenase
GFP	enhanced green fluorescent Protein
GIP-1	glucose-dependent insulinotropic peptide 1
GLP1	glucagon-like peptide 1
Gusb	glucuronidase beta
HbA1c	hemoglobin A1c
HFD	high fat diet
Hif1α	hypoxia inducible factor 1 alpha
I.P.	intra peritoneal
IAPP	islet amyloid polypeptide
IBMX	3-isobutyl-1-methylxanthine
ITT	insulin tolerance test
KATP	ATP sensitive potassium channel
KCl	potassium chloride
KO	knockout
KRBH	*krebs*-ringer bicarbonate hepes
Ldha	lactate dehydrogenase A
Loxp	locus of crossing over
MafA	V-Maf Avian Musculoaponeurotic Fibrosarcoma Oncogene Homolog A

Mct4	monocarboxylate transporter 4
MIN6	mouse insulinoma
MODY	mature onset diabetes of the young
MOI	multiplicity of infection
mTOR	mammalian target of rapamcyin
Neurod1	neurogenic differentiation 1
Npas4	neuronal PAS domain protein 4
NPY	neuropeptide Y
ODD	oxygen-dependent degradation domain
OGTT	oral glucose tolerance test
PAS	Period-Arnt-Sim domain
PBS	phosphate buffered saline
PCR	polymerase chain reaction
Pdk1	pyruvate dehydrogenase lipoamide kinase isozyme 1
Pdx1	pancreatic duodenal homeobox 1
PFA	paraformaldehyde
PI3K	Phosphoinositide 3-kinase
PIP_3	Phosphatidylinositol (3,4,5)-trisphosphate
POMC	proopiomelanocortin
PPAR	peroxisome proliferator-activated receptors
qPCR	quantitative polymerase chain reaction
RER	respiratory exchange ratio
Rgs2	regulator of G protein signaling 2

RIP	rat insulin promoter
RNA	ribonucleic acid
RPMI	roswell park memorial institute
SEM	standard error of the mean
Sox9	sex determining region Y (SRY)-related high mobility group (HMG) box 9
T2D	type 2 diabetes
TMX	tamoxifen
TUNEL	terminal deoxynucleotidyl transferase (TdT)-mediated dUTP nick end labeling
Vegfa	vascular endothelial growth factor A
Vhl	von Hippel Lindeau
WT	wildtype

Acknowledgements

I would like to acknowledge my supervisor Dr. Francis Lynn for his support and mentorship throughout my PhD studies. I also need to thank members of Lynn lab; Eric, Nicole Thilo, Cuilan, Mei and the numerous undergraduate students for their help with experiments and social interaction. I would like to thank the BC Transplantation Society, the University of British Columbia and the Canadian Diabetes association for stipend funding and the CIHR for partially funding experiments presented within this thesis. I am grateful for Drs. Greenberg, Ferrer, and Melton for providing mouse lines used herein.

I thank all the members of my PhD committee; Drs. Verchere, Hoffman, Ehses and Kieffer for all their input into this project. I am grateful for all the expertise shared by members of the Verchere, Lavoie, Gibson and Kieffer laboratories. I am also indebted to all members of the CFRI & UBC diabetes research groups, the CFRI islet and histology core services for their technical assistance.

Dedication

With deepest thanks for restoring hope, I dedicate this work to Mike Babcock and Jessica Sabatini

Chapter 1: Introduction

1.1 Beta cells and glucose homeostasis

The majority of the pancreas is comprised of either exocrine or endocrine cell types; with the endocrine cells found in clusters, termed the “islets of Langerhans”. These islets contain multiple cells types including but not limited to alpha, beta and delta cells which express glucagon, insulin and somatostatin, respectively. Within the human pancreas, there are approximately 1 million islets, with beta cells comprising about 54% of the endocrine cell population (1).

Alpha and beta cells have particular importance for maintaining blood glucose levels within a narrow range of 4-5.5 mM. Alpha cells secrete the peptide hormone glucagon as a homeostatic response to hypoglycemia (2) while beta cells secrete insulin as a critical response to hyperglycemia. Under low glucose conditions, beta cells remain in a resting state, with a membrane potential of ~-67mV and secrete little to no insulin (3). However, following a rise in circulating glucose levels, beta cell activity – the process of glucose metabolism, membrane depolarization, calcium influx and insulin secretion – is induced (3). At the cellular level, the insulin secretory process is divided into “triggering” and “amplifying” pathways (4). The triggering pathway involves glucose uptake and subsequent metabolism leading to a shift in the ratio of ATP to ADP. This closes ATP-sensitive potassium channels and leads to an accumulation of intracellular potassium ions. This build-up of potassium results in a loss of membrane polarization and opens voltage-gated L-type calcium channels. The resulting calcium influx triggers fusion of insulin vesicles with the cell membrane (5). The amplifying pathway results in insulin secretion through the production of metabolic intermediates from glucose and

fatty acid metabolism and their modulation of effector proteins (4). One example is evidence through the production of NADPH from glucose metabolism. NADPH then acts as a reducing agent for beta cell glutathione pools which reduces and activates SUMO1/Sentrin Specific Peptidase 1 (SENP1). Then, through an unknown mechanism, SENP1 enhances glucose-stimulated insulin secretion (6). While glucose has a major role in regulating insulin secretion, there are a number of other external signals, including fuel sources (7,8) and hormones (9,10) which add to the complexity of this regulation.

Following the secretion of insulin from the beta cell, insulin then binds to its receptor expressed on a variety of cell types including, but not limited to, adipocytes, hepatocytes and myocytes (11) and reduces blood glucose levels via increased glucose uptake, storage and metabolism and reducing glucose production through glycogenolytic and gluconeogenic pathways (12).

1.2 Diabetes Mellitus

Given the critical importance of insulin to the systemic response to hyperglycemia, it is perhaps unsurprising that impairments in insulin secretion or signaling impair glucose homeostasis. Diabetes Mellitus is a term applied to a number of metabolic diseases characterized by elevations in blood glucose levels and either an absolute or relative insufficiency in circulating insulin levels. Diabetes is clinically diagnosed by a fasting glucose level of >7mM, a glycolsylated hemoglobin a1c (HbA1c) level of >6.5% or glycemic values above 11mM following an OGTT (13). There are multiple subtypes of diabetes mellitus, which can be broadly distinguished by those caused by an absolute or relative insufficiency in circulating insulin levels. One common

feature of all types of diabetes is the long term sequelae which include damage to retinal capillary endothelial cells, renal mesangial cells and peripheral neurons, resulting in blindness, end stage renal disease, heart attacks and strokes (14).

The subtypes of diabetes caused by an absolute deficiency in insulin include type 1 diabetes, which accounts for 5-10% (15) of all diabetes cases and results from autoimmune destruction of pancreatic beta cells (16) and neonatal diabetes (17). One common feature shared between these forms of diabetes is that they are caused by either severe dysfunction or the destruction of beta cells and clearly demonstrate the importance of the beta cell for glucose homeostasis. However, these forms are much less prevalent than type 2 diabetes (T2D), which acts as the major contributor behind the global “diabetes epidemic” (18). In order to better understand, prevent, and treat T2D, continued study of the disease pathogenesis is required.

1.2.1 Type 2 diabetes: definition

While neonatal and type 1 diabetes are characterized by an absolute deficiency in circulating insulin levels; T2D is initially defined by the presence of peripheral insulin resistance and a relative deficiency of insulin. Furthermore, T2D generally, takes considerably longer to develop than other types of diabetes (13). Prior to the development of clinical T2D, individuals can remain in a state of “pre-diabetes”, characterized by mild glucose intolerance and slight elevations in fasting glucose, although there are some individuals with pre-diabetes that never develop T2D (19).

For the past twenty years, T2D has been the cause of growing concern for many reasons, primarily due to a dramatic rise in worldwide disease incidence. Current estimates have placed the global diabetes incidence at a staggering 387 million people;

with T2D accounting for 90% of this population (20). Alarmingly, this number is expected to increase by an additional 255 million over the next 20 years (21). Even more concerning is that previous prospective estimates on diabetes prevalence have underestimated future trends (21,22); leaving further questions as to how T2D will impact future generations. A second reason for further alarm, rooted in increased diabetes incidence, is the staggering costs to health care systems. The current estimated annual cost of diabetes in Canada is $12.2 billion, of which $2.1 billion are considered direct costs (23). The burden of diabetes to Canadian healthcare system is dwarfed by that in the United States where the annual costs of both diabetes and prediabetes has been estimated to be $322 billion (24). A third concern is the economic disparity in diabetes incidence and morbidity with individuals of lower socio-economic status have higher diabetes prevalence rates than those of middle or upper strata (25-27). Further, individuals with T2D in lower economic or education brackets have higher mortality rates than those of income matched controls (27,28). Together, these three concerns highlight the need to improve the understanding of T2D development and develop new options for the prevention and treatment of the disease.

1.2.2 The complex etiology of T2D

A major question that may be limiting therapeutic strategies, is how T2D progresses in humans. The use of various animal models have made it clear that the etiology of T2D is complex and involves the dysfunction of multiple glucoregulatory organs (29,30). For instance, the pancreatic alpha cells contribute to disease pathology as individuals with T2D have increased proportions of alpha cells (31,32) and elevated glucagon secretion (33,34). Additionally, dysfunction within adipose tissue has been

observed through altered production and secretion of the adipokines, resistin and adiponectin which are believed to contribute to insulin resistance in T2D (35,36). Furthermore, immune dysfunction also contributes to T2D pathology as individuals with T2D have increased circulating levels of proinflammatory cytokines (37) and elevated numbers of infiltrating immune cells in adipose and islets (38-40). Clinically, the antagonism of one proinflammatory cytokine, IL-1β, improved fasting glycemia in individuals with T2D (41); suggesting this cytokine is particularly relevant to T2D. Besides the contribution from these cell types, the central nervous system also plays critical roles in the maintenance of euglycemia.

1.2.3 Central control of glucose homeostasis

The importance of the central nervous system (CNS) in the regulation of glucose levels was initially observed in 1849 by Claude Bernard. Despite a long standing dearth of studies examining the role of the CNS in regulating glucose homeostasis, within the past ten years there has been a greater appreciation of the CNS as a glucoregulatory organ.

The ability of the CNS to regulate glucose levels is perhaps best highlighted through the study of insulin signaling within the hypothalamus. In seminal work by Obici *et al.* inhibiting hypothalamic insulin signaling, through blocking antibodies or insulin receptor antisense oligonucleotides, impaired the ability of peripherally delivered insulin to reduce hepatic glucose production (42). Conversely, stimulating hypothalamic insulin signaling through the infusion of insulin or an insulin receptor agonist, reduced endogenous glucose production in rats (42). Further studies have suggested that increased production of PIP_3, downstream of insulin receptor activation (42) maintains

neuronal K_{ATP} channels in an open state, which resulted in membrane hyperpolarization and reduced parasympathetic tone through the efferent vagus nerve (43-45).

Besides insulin, neurons within the hypothalamus also respond to leptin (46,47), fatty acids (48), glucose (49), glucagon (50) and GLP-1 (51) and in response reduce hepatic glucose production. This regulation of hepatic glucose output by the hypothalamus has been speculated to be mediated through a direct, brain-liver axis (52) as well as indirect pathways (46). Together, these studies highlight how the CNS, responding to numerous metabolic signals, regulates hepatic function to maintain euglycemia (45).

In a similar fashion to the neurons of the hypothalamus, the pancreatic beta cell also acts as a signaling nexus; incorporating multiple metabolic signals and in response, altering cellular function to promote glucose homeostasis.

1.3 Beta cells in T2D: dysfunction, dedifferentiation & death

While the pathogenesis of T2D is clearly complex, it is ultimately beta cell failure which permits the progression to clinical diabetes (53,54). One limiting factor hampering the beta cell compensatory response is increased levels of beta cell stress due to genetic and acquired susceptibilities (55).

Extensive research has identified environmental sources of beta cell stress relevant to T2D including, hyperglycemia, hyperlipidemia and elevated proinflammatory cytokines. Within the beta cell, these external stresses result in elevated levels of endoplasmic reticulum (ER) stress, oxidative stress and aggregation of islet amyloid polypeptide (IAPP). Exposure to prolonged elevated cellular stress levels within beta

cells leads to a number of beta cell defects including elevated apoptosis, cellular dysfunction and loss of maturation status (See Figure 1.1 for summary).

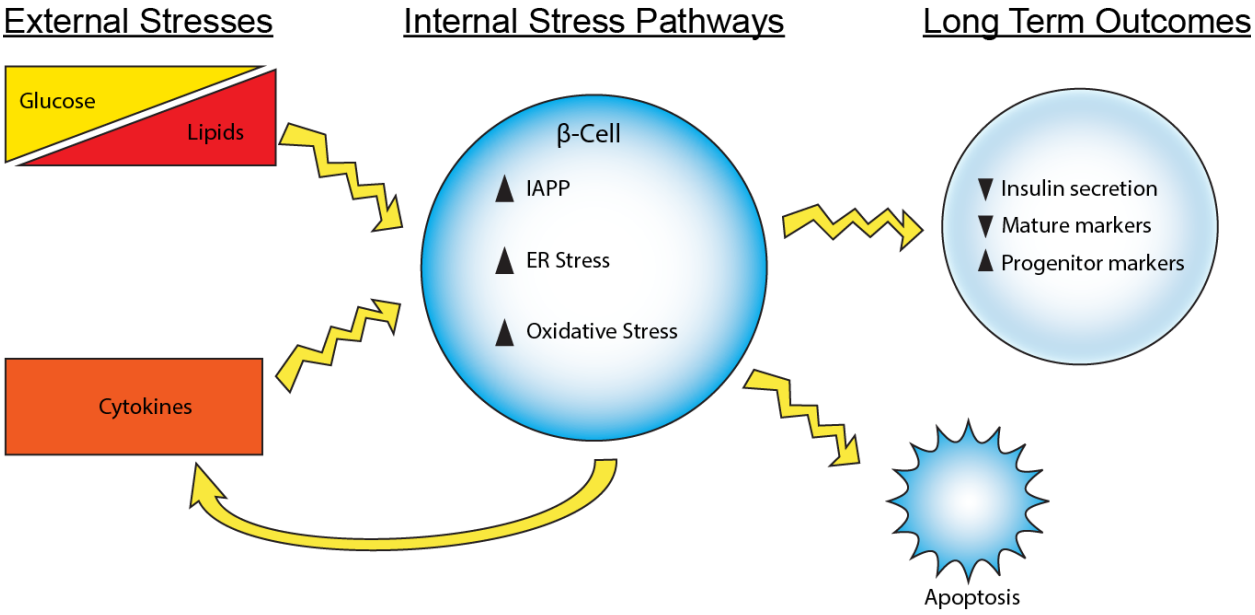

Figure 1.1: Model of beta cell stress in T2D.
A number of circulating factors in the diabetic milieu act as beta cell stressors (far left). The three best studied candidates are chronic hyperglycemia, hyperlipidemia (or a combination thereof) and increased levels of proinflammatory cytokines. These circulating factors increase beta cell stress levels (centre) through such pathways as increased IAPP production and aggregation, increased levels of ER or oxidative stress. Chronic beta cell stress results in cellular dysfunction, which can lead to a feed-forward loop and further exacerbate beta cell stress levels. Finally, prolonged cell stress reduces functional beta cell mass (far right) through increased rates of apoptosis or dedifferentiation as well as functional defects.

1.3.1 External source of beta cell stress in T2D

All cells are exposed to conditions which can induce cellular stress, defined as changes in the cells' environment which have the potential to damage cellular macromolecules, including: proteins, nucleic acids and lipids. In such circumstances, cell stress responses are activated to mitigate harm and restore homeostasis (56).

There are multiple theories that have attempted to describe environmental factors that initiate beta cell stress during the development of T2D.

One such hypothesis suggests that hyperglycemia may drive beta cell dysfunction or apoptosis. This is supported by the observation that culturing the INS1 immortalized beta cell line in 20 mM glucose for 48 hours reduced insulin expression and nuclear PDX1 protein levels compared with INS1 cells cultured in 5 mM glucose (57). Furthermore, incubating isolated human islets in 33 mM glucose for ten days reduced glucose stimulated insulin secretion compared with human islets cultured in 5 mM glucose (58). Besides reducing beta cell function, hyperglycemia is sufficient to induce beta cell apoptosis as islets from *Psammomys Obesus* cultured in either 11.1 mM or 33.3 mM glucose for ten days, had significantly increased beta cell apoptosis rates (59). This is also true within human islets, as a five day culture in 11 mM or 33.3 mM glucose significantly increased beta cell apoptosis, compared with human islets cultured in 5.5 mM glucose (58,60).

A second theory argues that an elevation in circulating lipid levels are responsible for the beta cell dysfunction in T2D. There has been a number of *in vivo* observations that support this position, including reduced insulin secretion (61) and insulin content (62) from beta cells of rats infused with lipids for 48 hours. Similarly, a 48 hour infusion of intralipid and heparin in humans also decreased circulating c peptide levels (63). There is also *in vitro* and *in vivo* evidence that the combination of elevated glucose and fatty acids act synergistically to induce beta cell dysfunction and cell death (64,65).

Finally, proinflammatory cytokines are also believed to contribute to the beta cell dysfunction and death in T2D as exposure to these cytokines *in vitro* can reduce glucose stimulated insulin secretion (66) and induce beta cell death (67,68). Also, antagonism of IL-1β in people with T2D improves beta cell function and glycemic control (41).

In all likelihood it is a combination of elevated glucose, lipids, cytokines as well as other factors contribute to beta cell dysfunction and death observed in T2D (69). These external sources of stress result in the activation of intracellular pathways within the beta cell resulting in their dysfunction.

1.3.2 Relevant intracellular cell stress pathways in beta cells in T2D

There are multiple pathways through which chronic exposure to environmental stress has been suggested to lead to a beta cell deficit in T2D, including, oxidative stress, ER stress and aggregation of amyloid oligomers. It is worth mentioning that these stress pathways are not mutually exclusive or distinct from one another; indeed, there seems to be a large degree of interplay between them. For instance, feeding antioxidants to the Akita mouse, a model of ER stress driven diabetes, resulted in improved glucose tolerance, suggesting beta cell ER stress increased oxidative stress within this model (70). In addition, human IAPP promotes the recruitment and activation of macrophages (71,72), and can induce beta cell ER stress (73), leading to further beta cell dysfunction.

Cells experience oxidative stress following the overproduction of reactive oxygen and reactive nitrogen species, which can damage membrane lipids, proteins and nucleic acids (74). These reactive species are produced by beta cells during normal glucose

metabolism and have important roles as signalling molecules required for glucose-stimulated insulin secretion (75). While most cells highly express antioxidant enzymes which can inactivate free radicals, beta cells express relatively low levels of many anti-oxidant proteins including catalase, glutathione peroxidase and superoxide dismutase (76). This may render them particularly vulnerable to oxidative stress (77). A role for oxidative stress in beta cell failure in T2D (78) is supported by elevations in the levels of the oxidative stress marker, 8-hydroxydeoxyguanosine within islets, urine and circulating mononuclear cells of people with T2D (79-81). Furthermore, overexpression of anti-oxidant genes; glutathione peroxidase and Cu/Zn superoxide dismutase in beta cells protected against the development of diabetes in mice (82,83).

Another pathway through which cell stress may lead to a beta cell deficit in T2D is the pathological aggregation of islet amyloid polypeptide (IAPP). Amyloid deposits are enriched in the islets of people with T2D (84-86). There are numerous deleterious effects of human IAPP overexpression (important as the rodent IAPP does not form aggregates (87)) including induction of ER stress and plasma membrane disruption (88,89). IAPP mediated impairments in beta cell function have also been observed in multiple *in vivo* studies in which human islets are transplanted in mice (89,90) or human IAPP is ectopically expressed in mouse or rat beta cells (91,92).

Additionally, it has been suggested that as secretory cells, beta cells are rendered more susceptible to ER stress, particularly under conditions requiring elevated insulin synthesis such as an insulin resistant state (93).

The ER facilitates protein synthesis, post-translational modification and proper folding, all while maintaining strict quality control (94). The folding capacity of the ER is

monitored by three transmembrane proteins, activating transcription factor -6 (ATF6), protein kinase RNA-like ER kinase (PERK), and inositol-requiring enzyme 1 (IRE1), which are normally bound to the ER chaperone, BiP within the ER lumen. However, in the presence of increased numbers of unfolded proteins, BiP dissociates from ATF6, PERK, and IRE1; resulting in activation of these three proteins and initiation of the unfolded protein response (UPR). In the case of ATF6, activation leads to its translocation from the ER membrane to the Golgi where the amino terminus is cleaved. Following this processing step, ATF6 translocates to the nucleus and regulates gene expression as a transcription factor. Following dissociation with BiP; the kinase domain of PERK is activated through homodimerization. One major target of activated PERK is eIF2a which when phosphorylated, decreases translational throughput to lighten ER burden. Finally, the endoribonuclease activity of IRE1 is induced following release form BiP and subsequent homodimerization (95). Activated IRE1 will degrade a large number of mRNAs and splices X-box binding protein 1 to render a mRNA for a functional transcription factor (96) (See Figure 1.3.2)

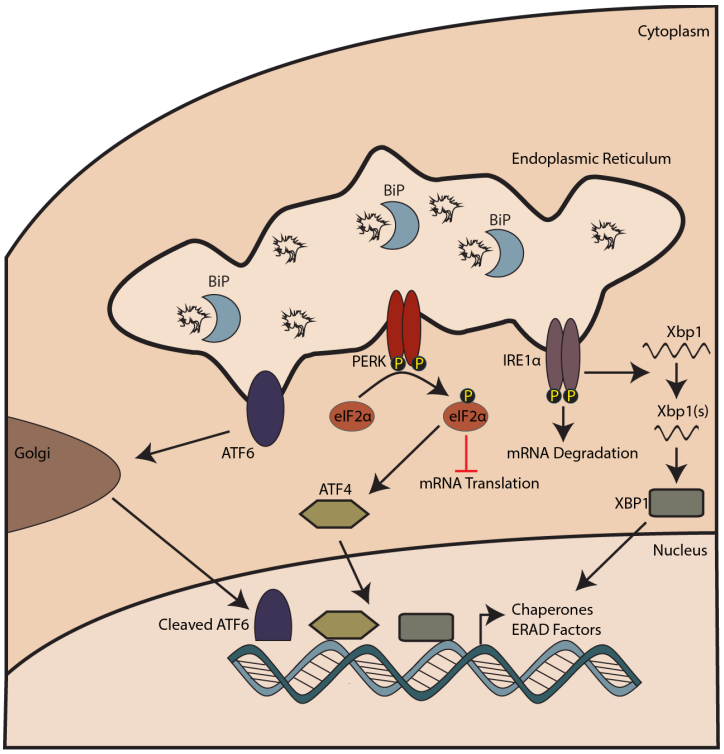

Figure 1.2: Schematic of UPR signaling.
BiP dissociates from ATF6, PERK and IRE1 in order to bind misfolded proteins; resulting in the activation of these three transmembrane proteins. Combined these three branches aim to restore ER homeostasis by increasing expression of ER chaperones and components of the ER-associated degradation (ERAD) pathway.

The desired outcome of the activated UPR is to restore ER homeostasis through increasing the expression of ER chaperones and enzymes that degrade improperly folded proteins while at the same time reducing ER burden by lowering transcription and translation rates (97). However, in the face of prolonged UPR activation that an apoptotic program is activated through the JNK pathway, increased expression of the pro-apoptotic transcription factor: DDIT3 (DNA Damage Inducible Transcript 3), and activation of caspase12 (94).

In support of a role of ER stress in beta cell dysfunction, expression of BiP and DDIT3 are elevated in islets from HFD-fed mice (98) and individuals with T2D (73,99)

and the ER is enlarged within beta cells of individuals with T2D (100). Numerous mouse models have demonstrated that a compromised UPR can result in diabetes as evidenced in the Akita mouse, which harbours a mutation within the insulin gene rendering it incapable of proper folding. This leads to a massive strain on the ER resulting in diabetes at an early age (101). Furthermore, reducing ER stress through the administration of a chemical ER chaperone (102) or through transgenic overexpression of BiP (103) in beta cells improved glycemic control in mouse models of T2D. The induction of the pro-apoptotic transcription factor, DDIT3, may be a critically important output of UPR signalling in T2D, as deletion of Ddit3 dramatically improved glucose tolerance of db/db and HFD-fed mice (104).

Within the diabetic beta cell, increased levels of IAPP aggregation, ER and oxidative stress likely all contribute to the elevated cellular stress levels. This likely impairs the ability of beta cells to compensate for increased metabolic demands resulting in the development of diabetes.

1.3.3 Outcomes of beta cell stress in T2D

The prolonged activation of beta cell stress pathways in T2D results in reduced functional beta cell mass, however, whether decreased numbers of beta cells or impaired cellular function drive this deficit is still a topic of debate (105,106). In support of the position that T2D results from and leads to decreased beta cell numbers, separate studies have observed significantly reduced numbers of beta cells in pancreata from people with T2D (86,107). This reduction may be driven by apoptosis as individuals with T2D have increased numbers of beta cells which are positive for the

apoptotic TUNEL stain (86) and have higher protein levels of cleaved Caspase-3 (108), an executioner caspase in the programmed cell death pathway (109).

As not every analysis of T2D pancreata have observed decreased beta cell numbers (32); it raises the possibility that cellular dysfunction acts as the primary contributor to the beta cell deficit in T2D. Confounding matters is that insulin immunostaining has been used to mark beta cells in every quantification study and as beta cells from individuals with T2D have reduced numbers of insulin granules (110,111), it has been suggested that there is an overestimation of beta cell loss in T2D (111). Further evidence of beta cell dysfunction in individuals with T2D are the observed reductions in insulin secretion (6) and impaired proinsulin processing (112) compared to healthy controls. Also, short periods of beta cell rest, achieved by administering the K_{ATP} channel opener, diazoxide (113,114) or somatostatin (115) to individuals with T2D, improved *in vivo* beta cell function. Given the short term nature of these interventions (up to five days of treatment) it is likely that these improvements are due to increased functional output as opposed to an increase in beta cell mass.

An alternative outcome of prolonged beta cell stress, which may explain the observed impaired cellular function and numbers in T2D, is a loss of beta cell differentiation status and reversion to a progenitor state, through a process termed “dedifferentiation” (116).

1.3.3.1 Altered beta cell differentiation status

Cellular differentiation had, for many years, been seen as a series of irreversible decisions that resulted in a terminally differentiated cell type (117). However, more recently, there has been a greater appreciation for the idea that differentiation requires

“positive control,” ie, the continued expression of factors which reinforce the functional capacity and differentiation status of the cell (117,118).

There have been a number of genetic studies in the past five years that have demonstrated the requirement of continued expression of certain “core” transcription factors for the maintenance of beta cell differentiation. For instance, it was understood that the transcription factor PDX1 is required for pancreas development (119,120). However, the ablation of Pdx1 in mature beta cells through the use of RIP-CreER transgenics dramatically reduced markers of mature beta cells, including *Insulin1, Insulin 2, Glut2, MafA and Nkx6.1* which was associated with increased expression of alpha cell markers such as glucagon, *MafB* and *Arx* (121). There was also a concomitant increase in rates of beta cell transdifferentiation to an alpha cell type (121). Similarly deletion of other transcription factors required for proper beta cell development including NKX6.1(122) and MAFA (123) result in beta cell transdifferentiation into other endocrine cell types (124,125).

These studies position PDX1, MAFA and NKX6.1 as central factors in the maintenance of beta cell differentiation, though likely more exist. Furthermore, under conditions of beta cell stress other transcription factors may also become critical for maintaining beta cell differentiation status; as evidenced in the FoxO1 beta cell knockout mouse. Under non stressed conditions, ablation of the transcription factor FoxO1 in beta cells did not alter beta cell identity or glucose homeostasis (126). However, in certain models of beta cell stress such as aging or multiparous pregnancies, FoxO1 null beta cells lost expression of multiple mature beta cell markers including *Pdx1*, *MafA*, *Glut2*, and *insulin*. Concordantly, the FoxO1 knockout beta cells

displayed increased levels of the endocrine progenitor marker, Neurogenin 3 (NGN3) and pancreatic progenitor marker, SOX9 (126).

A third pathway through which beta cell differentiation can be induced is through increased expression of transcription factors normally found within beta cell progenitors. One such model is the Vhl knockout mouse, which results in constitutively active hypoxia inducible factor 1α (HIF1α) and the upregulation of the HIF1α target, SOX9 (127). Normally expressed within pancreatic progenitor cells, the upregulation of SOX9 in the Vhl null beta cell results in decreased expression of mature beta cell markers and increased expression of other progenitor markers such as *HNF6* (127).

Chronic hyperglycemia has also been demonstrated to impact beta cell differentiation status. Mutation of the KIR6.2 subunit of the K_{ATP} channel, which rendered it insensitive to ATP binding and blocked glucose stimulated insulin secretion resulted in the rapid development of diabetes. Beta cells from these mutant mice had increased expression of the endocrine progenitor transcription factor, *Neurogenin 3*, and lineage tracing analysis suggested a small number of beta cells had transdifferentiated into alpha cells (128). Similarly, genetic ablation of insulin from beta cells resulted in severe diabetes, decreased expression of mature beta cell markers and resulted in beta cell transdifferentiation into glucagon expressing cells (129).

Together this research supports several mechanisms of beta cell dedifferentiation in mice; one is through decreased expression of core beta cell transcription factors. The second pathway of beta cell dedifferentiation is mediated through the loss of transcription factors required in conditions of chronic beta cell stress. The third mechanism is through increased expression of a transcription factor normally

found in progenitor cells and a final pathway seems to be driven through prolonged exposure to hyperglycemia.

While data from animal models of diabetes have suggested beta cell dedifferentiation is a major contributor to disease pathology, the role of dedifferentiation in T2D progression within humans is still controversial. Reduced expression of the transcription factors *Pdx1, Nkx6.1* and *MafA* has been observed in islets from individuals with T2D (130) and immunofluorescent examination of islets from individuals with T2D revealed reduced numbers of endocrine cells, marked by synaptophysin, which produced insulin (131). This was accompanied with increased numbers of alpha, delta and PP cells, possibly due to beta cell transdifferentiation to other endocrine cell types (131). However, a separate study could only detect rare dedifferentiated beta cells within the pancreas of individuals with T2D (132) and it was the authors' conclusion that they were unlikely a major contributor in diabetes pathology (132).

While the relevance of beta cell dedifferentiation in humans is still being explored, data collected from mouse models demonstrate this is a pathological contribution to diabetes phenotypes. These studies also strongly support the importance of transcription factors in promoting beta cell differentiation.

1.4 bHLH-PAS domain proteins in beta cells

The bHLH-PAS domain transcription factors are of particular importance to the beta cell as they have a conserved function as sensory proteins that are activated in response to various external stimuli (133) and can alter transcriptional programs to facilitate cellular responses to changing environmental conditions. As the sensory

capabilities of beta cells are of primary importance to their function, the bHLH-PAS domain proteins have a unique role in maintaining insulin secretion.

The PAS motifs were named after the three proteins within which they were originally found (Period, Arnt and Simple minded) and consist of smaller 70 amino acid PAS(A) and PAS(B) domains (133). The amino acid conservation between PAS domains is relatively low, but there is a shared secondary structure consisting of a five-stranded antiparallel beta sheet with flanking alpha helices (133).

The importance of bHLH-PAS transcription factors in beta cells is supported by multiple studies which demonstrate that altered function or expression levels of these proteins results in beta cell dysfunction (134). For instance, reduced function of the bHLH-PAS circadian rhythm defining proteins, CLOCK and BMAL1 resulted in impaired cellular function and glucose intolerance in mice (135-138). Besides the circadian rhythm, there are two other bHLH PAS domain transcription factors which have important roles within the beta cell: HIF1α and ARNT.

Given the importance of oxygen to energy metabolism, the ability to sense and respond to low oxygen availability is critical for cellular function and survival. The main factors involved in the cellular hypoxic response are the hypoxia inducible factors (HIF) 1α, 2a, 3a. These proteins contain proline residues in oxygen dependent degradation domains (ODDs), which, under normoxic conditions, are hydroxylated by oxygen dependent prolyl hydroxylase domain (PHD) containing enzymes (139). HIF1α hydroxylation promotes association with Von Hippel-Lindau (VHL), part of an E3 ubiquitin ligase protein complex (140) resulting in HIF1α ubiquitination and rapid degradation through the proteosomal pathway (141). In contrast, under hypoxic

conditions, the PHD containing enzymes are inactive; leading to HIF1α stabilization, nuclear translocation, and heterodimerization with its obligate heterodimerization partner, ARNT. The HIF1α-ARNT heterodimer then binds and promotes expression from hypoxic response elements (HREs) (142). Besides low oxygen, exposure to elevated glucose concentrations (143,144) have also been shown to lead to HIF1α stabilization in beta cells, possibly due to elevated free radical production (145-147). Overall, HIF proteins drive a transcriptional program which promotes angiogenesis, proliferation and shifts glucose metabolism away from oxygen dependent oxidative phosphorylation towards anaerobic glycolysis (148).

Animal studies have demonstrated the importance of HIF1α and ARNT in beta cells as the genetic ablation of either of these genes from mouse beta cells resulted in glucose intolerance and decreased *in vivo* insulin secretion (149,150). Similarly, knockdown of either *Hif1α* or *Arnt* in cultured beta cells resulted in reduced glucose stimulated insulin secretion (149-152). To assess the effects of increased HIF1α in beta cells *in vivo*, several studies have examined the effect of deleting von Hippel-Lindau from beta cells; which results in constitutively stabilized HIF1α. Knocking out Vhl with either RIP-Cre or Pdx1-Cre transgenic mice led to glucose intolerance at 12 weeks of age, associated with decreased insulin secretion *in vivo* (153,154). To circumvent any role of VHL in β-cell development, Pdx1CreER mice were used to knockout Vhl specifically in mature beta cells. Using this Cre mouse strain, Vhl knockout mice failed to mount an insulin response to a glucose challenge and became glucose intolerant 6-8 weeks following tamoxifen administration (155). While glucose intolerance is observed early in life, if allowed to age, beta cell Vhl null mice develop a more severe diabetic

phenotype mediated by increased SOX9 expression. This was associated with decreased expression of mature beta cell markers and increased rates of beta cell dedifferentiation and transdifferentiation (127).

These studies have demonstrated a critical role of many of the bHLH-PAS domain proteins in the maintenance of beta cell function and even differentiation status. Continued study of the uncharacterized bHLH-PAS domain proteins may provide deeper insight into the dysregulated pathways which occur during T2D progression.

1.5 Expression and function of Npas4 in the CNS

Originally identified in 2004 by two separate groups (156,157), Neuronal PAS domain protein 4 (NPAS4) is a basic helix-loop-helix PAS domain transcription factor and one of four members of the Npas4 family. In humans, the Npas4 gene consists of eight exons spanning approximately 5kb of chromosome 19 in the 11q13 locus and codes for an 802 amino acid protein.

Similar to other bHLH-PAS domain proteins, NPAS4 requires a heterodimerization partner for its transcriptional activity and use of a mammalian two-hybrid assay performed in 293 cells suggested that NPAS4 interacts ARNT1, ARNT2 and to a lesser degree BMAL1 (156). As a transcription factor, NPAS4 has been shown to be act as a repressor as well as an activator and preferentially binds to enhancer regions over promoters (158). Interestingly, it has been suggested that NPAS4 directly promotes its own expression (156,159). Two independent tissue surveys for *Npas4* mRNA expression have revealed that *Npas4* is present exclusively within the brain with the highest expression within the cortex, hippocampus, and olfactory bulb (156,157);

however, it should be noted that these studies did not examine *Npas4* expression within the pancreatic islet or the hypothalamus.

Studies within the brain have demonstrated that Npas4 expression is dynamic and altered in response to a number of stresses. For instance, *Npas4* mRNA within the hippocampus was decreased by 50% in mice following 4 weeks of social isolation (160), and in a model of stress wherein mice were maintained in a restraining device, hippocampal *Npas4* was reduced by ~40% within two hours (161). *Npas4* expression was also increased 12-fold in the frontal cortex in a model of central ischemia and subsequent reperfusion (162). In the neuroblastoma cell line, PC12, *Npas4* was significantly elevated by exposure to the SERCA inhibitor, thapsigargin, and exposure to oxidative and osmotic stress (163). Besides these stimuli, NPAS4 was also induced by membrane depolarization in hippocampal neurons (164). Induction of *Npas4* was subsequently demonstrated to be dependent on calcium influx and independent of *de novo* translation (165); classifying Npas4 as an activity regulated immediate early gene. There is also some evidence to suggest that *Npas4* was regulated in a circadian fashion as mRNA levels were increased over two-fold in the pars tuberalis of mice at 6PM compared to 6AM (166).

The first *in vivo* studies examining Npas4 function were performed using a germline knockout mouse which, while viable at birth, at 3 months of age had reduced survival. This was accredited to neuronal cell death as evidenced by increased TUNEL positive cells in the hippocampus. Further, while injection of kainate did not result in mortality in control mice, in age matched Npas4 null mice this led to a 38% mortality rate (163). In addition to its role promoting neuronal survival, NPAS4 has critical roles in

regulating the formation of inhibitory synapses. Knockdown of *Npas4* in dissociated rat hippocampal neurons significantly reduced the abundance of GABA receptors and the GABA producing enzyme, GAD65. Conversely, increased NPAS4 levels in hippocampal neurons resulted in elevated expression of the GABA receptors and GAD65 (164). NPAS4 also has important roles in memory formation, as global knockout mice had short and long term memory defects and deletion of Npas4 from the CA3 region of the hippocampus, similarly impaired long term memory formation (165).

These animal studies have emphasized an important role for NPAS4 in mouse neurobiology; however, to date there are scarce data on the role of NPAS4 in humans. The examination of 1000 human genotypes revealed 14 unique single nucleotide variants within the Npas4 gene. While 13 of these variants maintained transcriptional activity, one (F147S) had no transcriptional activity due to an inability to heterodimerize with ARNT (167). The loss of NPAS4 expression has also been implicated in the pathology of an intellectually disabled individual containing a 1mbp microdeletion on chromosome 19, which encompasses the Npas4 gene (168). These two studies raise the possibility of NPAS4 impacting human health; however, further studies are required.

1.6 Thesis objectives

In the progression of T2D, prolonged stress leads to reductions in beta cell functional mass, likely due to a combination of reduced cell numbers, functional capacity, loss of maturation status. To gain a better understanding of beta cell biology in pathophysiologic settings and to uncover novel dysregulated pathways within stressed beta cells, there is a need for continued identification of novel factors that regulate cell function, survival and differentiation.

The examination of bHLH-PAS domain transcription factors has supported a critical role of many of these proteins in the maintenance of beta cell function and even differentiation status. As a recently identified bHLH-PAS domain protein, the expression and function Neuronal PAS domain protein 4 (NPAS4) within beta cells is unknown. Previous research conducted on NPAS4 within the central nervous system has demonstrated the importance of NPAS4 in promoting cell viability and regulating critical cellular processes in neurons. Based on the shared similarities between neurons and beta cells and the importance of other bHLH-PAS domain transcription factors it is hypothesized that NPAS4 is expressed within the beta cells and has critical roles in promoting beta cell function in the face of diabetogenic stresses.

The overall objective of these studies is to determine how Npas4 expression is regulated within the beta cell under a variety of external stimuli and in turn, how NPAS4 acts to influence beta cell function, differentiation and survival. These objectives are addressed in two aims (illustrated in Figure 1.3).

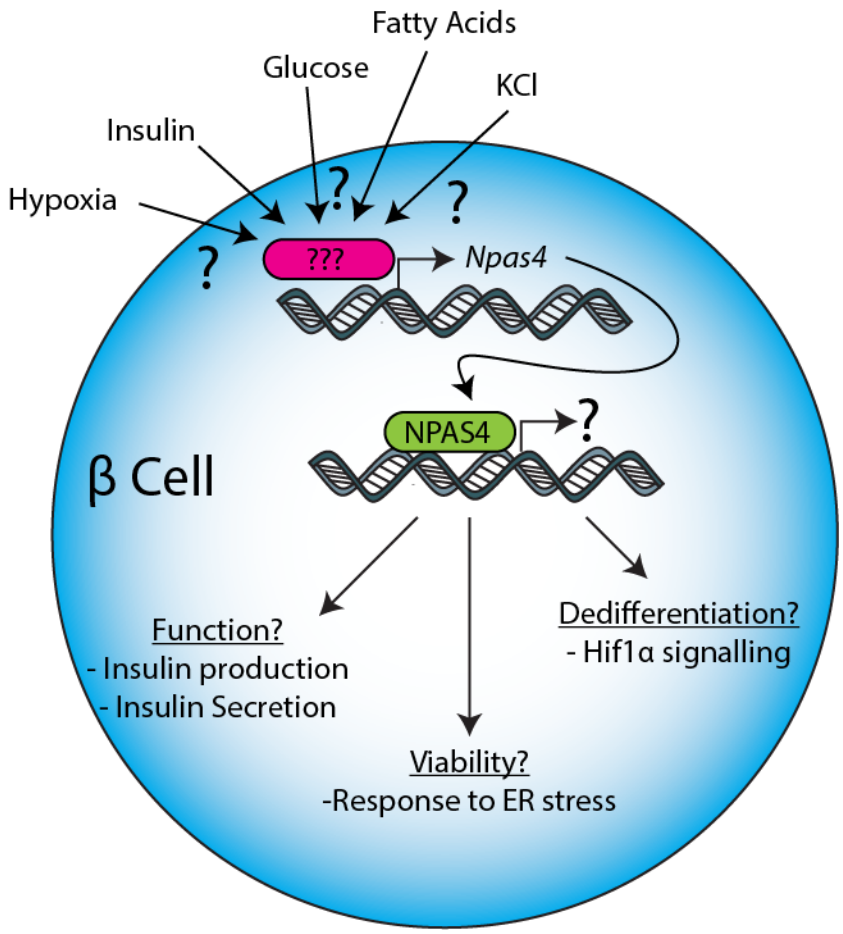

Figure 1.3: Illustration of thesis hypothesis.
The aims of this thesis are to determine how Npas4 is regulated within the beta cell and in turn how NPAS4 regulates various cellular processes relevant to the beta cell in type 2 diabetes pathogenesis.

The first aim, explored within chapter 3, characterizes the dynamics and regulation of beta cell Npas4 expression. This includes the role of various beta cell secretagogues in promoting Npas4 expression in both mouse and human beta cells and how conditions which may mimic the islet environment in T2D impacts Npas4 expression.

The second aim was to determine the functional significance of NPAS4 within beta cells and the role of NPAS4 in the promotion of glucose homeostasis. Within

chapter 4, NPAS4 mediated regulation of insulin production and secretion was examined through the use of *in vitro* overexpression and knockdown experiments. Similarly, *in vitro* studies in chapter 5 were performed to determine whether NPAS4 may impact beta cell responses to various diabetogenic stresses such as gluco(lipo)toxicity and HIF1α activation. With an understanding of which cellular processes NPAS4 may be impacting in beta cells, *in vitro*, the role of NPAS4 in the regulation of glucose homeostasis was examined in chapter 6 by ablating Npas4 from beta cells through the use of the Pdx1CreER transgenic mouse line. As Cre activity was detected within the hypothalamus of Pdx1CreER transgenic mice, two separate beta cell specific Npas4 knockout models were generated and characterized within chapter 7.

Collectively, this investigation highlights how beta cell activity and downstream activation of NPAS4 promote beta cell viability and function and further, how these pathways may be impaired in the development of T2D.

Chapter 2: Methods

2.1 In vitro studies

2.1.1 MIN6 cell culture

MIN6 cells were cultured in Dulbecco's modified Eagle's medium (DMEM) (Thermo Scientific) 25 mM glucose supplemented with 10% FBS, 1% penicillin (100 U/mL), streptomycin (100 µg/mL) and 2 mM L-glutamine (All reagents from Hyclone). Cells were split at a ratio of 1:3, twice a week and medium changed every two days.

For western blot experiments, MIN6 cells were plated in 6-well tissue culture plates (BD Falcon) at a density of $1.5x10^6$ cells/well. For insulin secretion experiments, MIN6 cells were plated in 12-well tissue culture plates (BD Falcon) at a density of $1.0x10^6$ cells/well. For RNA experiments, MIN6 cells were plated at a density of $3x10^5$ cells/well in a 24-well tissue culture plates (BD Falcon).

2.1.2 804G cell culture

804G cells were cultured in 5.5 mM glucose DMEM supplemented with 10% FBS, 1% penicillin, streptomycin and 2 mM L-glutamine. To harvest secreted matrix, 804G cells were cultured serum-free 5.5 mM glucose DMEM for 48 hours, media was then collected and centrifuged for 5 minutes at 300*g.* Supernatant was collected and filtered through a 0.2 µm bottle top filter and stored at -20°C.

2.1.3 Mouse islet isolation

Mice were sacrificed by cervical dislocation following isoflurane anesthesia. An incision was made into the abdominal cavity, the bile duct was then ligated using hemostatic forceps and 2-5 mL of Type XI collagenase (1000 U/mL dissolved in HBSS; Sigma) was injected into the pancreatic duct. The pancreas was then removed and

collected into a 50 mL conical tube and maintained on ice until digested. To digest the pancreas, whole pancreas was incubated in collagenase for 14 minutes in a 37°C water bath. The conical tube was then shaken for 5 minutes to disrupt the pancreas. Following disruption, the pancreas was centrifuged at 1200*g* and the supernatant discarded. The pellet was then re-suspended in RPMI and passed through a 70 µm nylon mesh filter to exclude exocrine tissue. The filtrand was then re-suspended in RPMI and passed once more through the 70 µM filter. The captured islets were then placed in a 10 cm cell culture dish in RPMI, supplemented with 10% FBS, glutamine and pen/strep. Islets were then handpicked under a dissecting microscope into a 10 cm tissue culture dish with 10 mL of islet culture media (11 mM glucose RPMI (Thermo Scientific) supplemented with 10% FBS, 1% penicillin (100 U/mL), streptomycin (100 µg/mL) and 2 mM L-glutamine) and allowed to recover overnight in a 37°C incubator.

2.1.4 Mouse islet culture

Following isolation, mouse islets were cultured in a 10 cm tissue culture plate (BD Falcon) in 11 mM glucose RPMI (Thermo Scientific) supplemented with 10% FBS, 1% penicillin (100 U/mL), streptomycin (100 µg/mL) and 2 mM L-glutamine. Every day, half of the medium was replaced with fresh RPMI.

2.1.5 Human Islet Culture

Human islets were obtained from the clinical islet core at the University of Alberta or from Dr. Patrick MacDonald at the University of Alberta. Upon receipt, islets were handpicked under a dissecting microscope into a 10 cm tissue culture dish with 10 mL of CMRL medium supplemented with 10% FBS, 1% penicillin (100 U/mL), streptomycin (100 µg/mL) and 2 mM L-glutamine and allowed to recover overnight.

2.1.6 Islet dispersion

For dispersion experiments, approximately 300 islets were centrifuged for 3 minutes at 300*g* in a 1.5 mL tube. Culture medium was removed, islets were washed once in PBS and 750 µL of 0.25% trypsin added. Islets were incubated in trypsin for 6 minutes and mixed via pipetting every two minutes. Trypsin digestion was stopped by transferring trypsin and dispersed islets into 10 mL of culture medium. The single cell suspension was pelleted by centrifugation for 3 minutes at 300*g*, medium removed and cells re-suspended in 3 mL culture medium. 500 µL of cell suspension, amounting to approximately 50000 cells, were then seeded onto 12-well plates.

2.1.7 Adenoviral transduction

Adenoviruses were constructed using the Adeasy protocol (169) which drives gene expression from a cytomegalovirus (CMV) promoter. One day after plating 0.3×10^6 MIN6 cells/well in a 24-well tissue culture plate, medium was aspirated from cells and DMEM growth medium containing Npas4 adenovirus or a fluorescent control virus (either Cerulean or eGFP) at an MOI of either 20 or 100, as indicated in the study, was added to cells for 2-4 hours before being removed and replaced with fresh culture medium.

To transduce dispersed islets, following overnight recovery in 12-well plates, islet culture media was aspirated and replaced with 400 µL of islet culture medium containing Npas4 adenovirus or a fluorescent control virus (either Cerulean or eGFP) at an MOI of 20. Islet culture media containing adenovirus was incubated with approximately 50000 islet cells for 24 hours prior to replacement with 500 µL of fresh islet culture medium.

For adenoviral infection of whole mouse islets, approximately 25 islets were placed in 50 µL of RPMI culture medium in a 1.5 mL microcentrifuge tube. Virus was added and gently mixed by pipetting. Islets were infected in this minimal volume for 30 minutes before being moved to a well of standard 24-well tissue culture plate containing 300 µL of RPMI growth medium. Islets were allowed to incubate in this medium overnight before half the medium was replaced with fresh islet culture medium.

2.1.8 Plasmid transfection and luciferase Assay

MIN6 cells were plated in 12-well plates at $8x10^5$ cells per well and the following day pFOX-RIP1-luciferase (170) or pFOX-luciferase promoterless (170) plasmid (1 µg each), Npas4-pcDNA3.1+ or pcDNA3.1+ (100 ng) and a renilla luciferase construct (50 ng) were complexed with Lipofectamine 2000 (2 µL lipofectamine/1 µg of DNA) (Life Technologies) for 20-30 minutes at room temperature in serum and antibiotic free high glucose DMEM. The Lipofectamine-DNA complex was added to MIN6 cells in serum and antibiotic free high glucose DMEM for six hours before being replaced with 500 µL of DMEM high glucose supplemented with 10% FBS. Forty-eight hours after transfection, cells were lysed with passive lysis buffer (Promega) and luciferase activity quantified with the dual luciferase reporter assay (Promega) and measured on a SpectraMax L luminometer (Molecular Devices). All firefly luciferase activity was normalized to renilla luciferase activity.

2.1.9 *In vitro* insulin secretion assay

For MIN6 cells, cells were transduced with adenovirus as described above. Following 48 hours of transduction, MIN6 cells were preincubated in 500 µL of *krebs*-ringer bicarbonate hepes (KRBH; 114 mM NaCl, 4.7 mM KCl, 1.2 mM KH2PO4, 20 mM

HEPES, 2.5 mM $CaCl_2$, 0.2% BSA and pH of 7.4) supplemented with 2.8 mM glucose for one hour. Following the pre-incubation, the buffer was replaced with either 500 µL of fresh KRBH supplemented with either 2.8 mM glucose, 25 mM glucose or 25 mM glucose with exendin-4 (between 5 and 50 nM) or forskolin (10 µM) (Sigma) and IBMX (100 µM) (Sigma) for a two hour stimulation. Buffer was then collected and centrifuged for 10 minutes at 5000*g* and the top 400 µL of supernatant was transferred to a 1.5 mL microcentrifuge tube and stored at -20°C. At the end of the insulin secretion assay, intracellular insulin was extracted by washing the cells once with 500 µL PBS, followed by the addition of 500 µL acid ethanol (1 M HCl in 75% ethanol in H_2O) and overnight incubation at 4°C. The following morning, the acid ethanol was carefully transferred from each well to a 1.5 mL microcentrifuge tube and centrifuged at 5000*g* for 10 minutes before the top 400 µL was transferred to a clean 1.5 mL microcentrifuge tube and stored at -20°C until assayed. Concentration of insulin in the media was assayed using a rodent insulin ELISA (Alpco) performed as per standard manufacturer's procedures. As a general rule, low glucose samples were diluted 2-5x, stimulated samples were diluted 15-20x and insulin totals were diluted 1000x for the insulin ELISA.

To determine insulin secretion in whole mouse islets, 12-well tissue culture plates were coated coated (400 µL) with the matrix secreted from the rat bladder carcinoma cell line, 804G that day before isolation (171). This matrix was then removed and washed with dH_2O three times and between 30 and 50 whole islets allowed to attach by placing them on top of the matrix and cultured in 500 µL islet culture medium overnight. The following day islets were infected with adenovirus by replacing the culture medium with 500 µL of culture medium containing either Npas4 or control adenovirus at an MOI

of 100:1. The islets were incubated with virus for 24 hours prior to virus containing media being replaced with 500 µL of fresh islet culture media. After a total of 48 hours infection, attached islets were washed once with 500 µL PBS and preincubated for one hour in 500 µL of 2.8 mM glucose in KRBH. Following the one-hour pre-incubation, 500 µL of fresh KRBH supplemented with 2.8mM glucose was added to the islets which were then incubated for one hour at 37°C. Subsequently, islets were then incubated in one hour increments at 37°C in KRBH supplemented with 2.8 mM glucose, 16 mM glucose and depending on the experiment either 40 mM KCl or 50 nM exendin-4 with 16 mM glucose. At the end of each hour, the buffer was collected, centrifuged at 500*g* for 10 minutes, the top 400 µL collected and stored at -20°C. At the end of the insulin secretion assay, intracellular insulin was extracted by washing islets once with 500 µL of PBS and incubating islets overnight at 4°C in 500 µL of acid ethanol. The following morning, acid ethanol from each well was collected in to a clean 1.5 mL microcentrifuge tube and centrifuged at 5000*g* for 10 minutes. The top 400 µL was then collected and stored at -20°C until assayed. Insulin determinations were performed using a rodent insulin ELISA (Alpco). As a general rule, basal glucose samples were diluted 2-fold, stimulated samples diluted 10-fold and insulin totals diluted 250-fold.

2.1.10 Depolarization of MIN6 and islet samples for expression analysis

For depolarization experiments, MIN6 cells were seeded into tissue culture plates at a density of 1.5×10^6 for 6-well plates (in 2 mL of MIN6 growth medium) or 3×10^5 for 24-well plates (in 0.5 mL MIN6 growth medium). One day after seeding, cells were transferred to 5 mM glucose DMEM (supplemented with FBS, penicillin, streptomycin and L-glutamine) for 16 hours. The next morning, cells were transferred to either fresh 5

mM glucose DMEM (supplemented with FBS, penicillin, streptomycin and L-glutamine) or 25 mM glucose DMEM (supplemented with FBS, penicillin, streptomycin and L-glutamine) with 40 mM KCl. MIN6 cells were maintained in either basal (fully supplemented 5 mM glucose DMEM) or stimulatory (fully supplemented 25mM glucose DMEM with 40 mM KCl) for up to 6 hours and harvested for either mRNA with 500 µL of TRIzol or protein with 60 µL NSRB.

To depolarize mouse islets, one day following isolation, between 20 and 50 islets were transferred to a 12-well tissue culture plate and preincubated in 500 µL of 2.8 mM glucose in KRBH for one hour before buffer replaced with either 500 µL of fresh KRBH supplemented with 2.8 mM glucose or 25 mM glucose. The length of the experiment is specified within each experiment but generally varied between two and six hours. At the conclusion of each experiment, islets were either harvested with 500 µL of TRIzol for mRNA quantification or 30 µL of NSRB for protein quantification.

To depolarize human islets for mRNA or protein expression, between 20 and 50 islets were put in a 12-well tissue culture plate and preincubated with 500 µL of 2.8mM glucose in KRBH for one hour before buffer was replaced with either 500 µL of fresh 2.8 mM glucose in KRBH or 25 mM glucose KRBH for two hours. At the conclusion of each experiment, islets were either harvested with 500 µL of TRIzol for mRNA quantification or 30 µL of NSRB for protein quantification.

2.1.11 Palmitate preparation

Palmitate was prepared by dissolving palmitic acid (Sigma) in 30 mM NaOH at 70°C, then complexed with 20% fatty acid free bovine serum albumin (BSA) (Sigma) at a molar ratio of 6:1. The complexed BSA-palmitate was then added to MIN6 or mouse

islet culture medium at indicated concentrations (ranging from 250 to 1000 μM). As a control, an equal volume of NaOH and BSA without palmitate was added to the culture medium.

2.1.12 Beta cell ER stress experiments

For MIN6 studies, cells were plated in either 6-well plates at a density of $1.5x10^6$ for protein quantifications or a 24-well plate at a density of $0.3x10^6$ for mRNA quantification. One day following passage, cells were then infected as described above. Forty-eight hours post adenoviral infection cells were treated (2 mL for 6-well plate or 0.5 mL for a 24-well plate) with either thapsigargin (concentrations varied from 0.05 μM to 1 μM), palmitate (concentrations varied from 250 μM to 1000 μM) or appropriate vehicle control (DMSO for thapsigargin and NaOH-BSA for palmitate) for 24 hours. At the conclusion of the experiment, cells were harvested with either 100 μL NRSB for protein quantification or 500 μL of TRIzol for mRNA quantification.

For ER stress studies in mouse islets, approximately 75 islets were infected as described above in a 12-well plate. Forty-eight hours post-infection, islets were treated with thapsigargin or palmitate for either 24 or 48 hours, respectively. At the conclusion of the experiment, islets were harvested with 500 μL of TRIzol for mRNA quantification.

2.1.13 Quantification of TUNEL positive MIN6 cells

To quantify terminal deoxynucleotidyl transferase (TdT)-mediated dUTP nick end labeling (TUNEL) positive cells, MIN6 were plated at a density of $0.3x10^6$ cells/well onto 10 mm glass cover slips placed in a 24-well plate. Cells were infected with adenovirus as described above and 48 hours post-transduction, MIN6 culture media was replaced with 500 μL culture media containing either 0,1 or 10 μM thapsigargin for 24 hours.

Cells were then washed once with 500 µL of PBS and fixed with 500 µL of 4% Paraformaldehyde (PFA) for ten minutes and assayed for single stranded DNA breaks with TUNEL staining (Roche) according to manufacturer's protocols. Following TUNEL staining, MIN6 cells were stained with DAPI (Life Technologies) for two hours. Coverslips were then washed and mounted onto glass microscope slides using Slow-fade Gold mounting media (Life Technologies). For quantification, two separate fields of view per coverslip were imaged using a 10x objective lens on an Olympus BX61 widefield fluorescent microscope. A minimum of 1500 MIN6 cells were then manually quantified by hand for TUNEL positivity and normalized to total cell count as measured by DAPI.

2.1.14 Stimulation of cAMP in MIN6 cells

MIN6 cells were plated in 24-well plates at a density of $0.3x10^6$ and infected with Ad-Npas4 or Ad-Cerulean as described above. Forty-eight hours post-infection, cells were washed once with 500 µL PBS and stimulated for 30 minutes at 37°C with 500 µL of KRBH with 10-fold serial dilutions of exendin-4 of concentrations between $1x10^{-7}$ M and $1x10^{-12}$ M. All samples were stimulated in the presence of 100 µM IBMX. Buffer was then removed and cells lysed with 200 µL of supplied lysis buffer (Applied Biosystems) and cAMP content measured with a cAMP ELISA (Applied Biosystems) according to manufacturer's protocol.

2.1.15 Hypoxia experiments

For experiments in which MIN6 cells were stimulated with KCl, cells were plated in either a 6-well plate for protein studies or 24-well plate for RNA studies at either $1.5x10^6$ cells/well or $0.3x10^6$ cells/well, respectively. The following day, cells were

transferred to 5.5 mM glucose culture media for 16 hours. MIN6 cells were then stimulated at either 20% or 1% O_2 levels in 5.5 mM DMEM or 25 mM DMEM supplemented with 40 mM KCl. At the conclusion of the experiments, cells were harvested in either 100 µL of NSRB for protein analysis or 500 µL of TRIzol for mRNA quantification.

For studies in which MIN6 cells were transduced with adenovirus, cells were plated and infected as described above in 24-well plates. Twenty-four hours post-transduction, cells were either maintained in a humidified incubator at 20% O_2 or transferred to a humidified incubator set at 1% atmospheric oxygen for six hours. At the conclusion of the experiments, cells were harvested with 500 µL of TRIzol for mRNA quantification.

For both human and mouse islets studies, either adenovirus-infected dispersed islets or uninfected whole islets were transferred to a hypoxic chamber at the specified oxygen levels (either 1% or 10% O_2) and time intervals (either a short term, two hour experiment or a longer term, 24-hour experiment). Similar to MIN6 experiments, a second plate of islets was maintained at 20% O_2 under identical experimental conditions. At the conclusion of the experiment, islets were harvested in 500 µL TRIzol for mRNA quantification or 50 µL NSRB for protein quantification.

2.1.16 RNA extraction & cDNA synthesis

To extract RNA from TRIzol samples, standard manufacturer's protocols were used. Briefly, 100 µL of chloroform (Sigma) was added to 500 µL of TRIzol, samples were then vortexed for 10 seconds and centrifuged at 10,000*g* for 10 minutes. Following phase separation, the top clear layer (generally 200 µL) was removed and added to 250

µL of isopropanol (Fischer Scientific), vortexed for 10 seconds and centrifuged for 15 minutes at 10,000*g*. The supernatant was removed and the pellet was washed twice with 1 mL of 70% ethanol in DEPC-H20. After the final wash, the supernatant was removed and the pellet was dried for two minutes before being re-suspended in molecular grade H_2O (Hyclone). In general, for $0.3x10^6$ cells the pellet was re-suspended in 20 µL. Once isolated, RNA was DNase (Ambion) treated for 30 minutes at 37°C according to manufacturer's instructions. RNA yield was quantified using a Nanodrop spectrophotometer. For reverse transcription, between 0.5-2 µg of RNA was used with addition of oligodT (200 ng/25 µL reaction volume) and random hexamer primers (10 µg/ 25 µL reaction volume) and with 22 U of Superscript III reverse transcriptase (Life Technologies). The following cDNA synthesis protocol was performed on an Eppendorf thermocycler: 10 minutes at 15°C, 10 minutes at 25°C, 15 minutes at 37°C, 45 minutes at 42°C, 10 minutes at 50°C, five minutes at 55°C and 3 s at 95°C.

2.1.17 Quantitative PCR

All qPCR was performed on a Viia7 (Life Technologies) using Taqman primer/probe sets (IDT). Samples were run in technical triplicates, using 40 ng of cDNA on a 384-well plate using fast run settings. Primer sequences are available in Table 1.5. All qPCR primers used FAM as the reporter dye and ZEN™ and IBFQ as quenchers. Relative quantification of transcripts was performed using ΔΔCT method using either beta glucuronidase (Gusb) or Rplp0 as a control gene.

2.1.18 Western blot

Cell lysates were obtained by adding 95°C non-standard reducing buffer (NSRB; 62.5 mM Tris buffer pH 6.8, 1 mM sodium vanadate, 0.2 mM sodium fluoride, 2% SDS, 10% glycerol) to cells followed by a 10 minute incubation at 100°C. Crude lysates were then sonicated (S-4000, Misonix) for 4 minutes (30 seconds on/30 seconds off at 85 amplitude), centrifuged at 10,000*g* for 10 minutes and supernatants were collected. Protein concentrations were obtained through BCA quantification (Pierce). Protein was then separated on either a 12 or 15% SDS/PAGE gel and transferred for 2 hours to a nitrocellulose membrane (Biorad). Membranes were blocked with 5% milk powder in TBST and probed with antibodies for NPAS4, GAPDH, PDX1, MAFA, NEUROD1, B ACTIN, RGS2 (details of primary antibodies available in Table 1.2) overnight at 4°C. Membranes were then probed with HRP conjugated secondary antibodies (details of secondary antibodies available in Table 2.3) and visualized using Luminata Crescendo (Millipore) and exposed to X-ray film. Protein quantification was performed by band densitometry using ImageJ (NIH) and normalized to loading control of β-ACTIN or GAPDH.

2.1.19 Chromatin immunoprecipitation

Ten million cells in a 10 cm tissue culture dish were washed in 10 mL of PBS and then incubated in growth medium with or without 40mM KCl for two hours. Cells were then fixed by addition of 1% formaldehyde in crosslinking buffer (0.1 M NaCl, 1 mM EDTA, 0.5 mM EGTA, 25 mM HEPES-KOH, pH 8.0) for 10 minutes at room temperature with gentle agitation on a standard rocker. Fixation was stopped with the addition of glycine to a final concentration of 125 mM and incubation continued for 5

minutes with gentle agitation. Cells were then washed three times with ice-cold PBS containing protease inhibitors (Complete EDTA-Free; Roche) and collected by scraping. Cells were pelleted by centrifugation at 2000*g* for 10 minutes at 4°C, PBS removed and pellets snap frozen in liquid nitrogen and stored at -80°C. Cells were lysed in 20 cell pellet volumes of L1 buffer (50 mM HEPES-KOH, pH 7.5, 140 mM NaCl, 1 mM EDTA, 10% glycerol, 0.5% NP-40, 0.25% Triton X-100, protease inhibitors) for 10 minutes at 4°C. The nuclei were pelleted by centrifugation at 3000*g* for 10 minutes at 4°C and then rinsed with 20 cell pellet volumes of L2 (200 mM NaCl, 1 mM EDTA, 0.5 mM EGTA, 10 mM Tris-HCl, pH 8.0, protease inhibitors) for 10 minutes at room temperature and then repelleted as above. Nuclei were resuspended in 5 cell pellet volumes of L3 (1 mM EDTA, 0.5 mM EGTA, 10 mM Tris-HCl pH 8.0, protease inhibitors) and sonicated in a Cup Horn sonicator (Misonix) at 80% power for 24 cycles 30s cycles on ice, which resulted in genomic fragments of 200-1kb in size. Insoluble material was removed by centrifugation at 20000*g* for 10 minutes at 4°C. The nuclear lysate was then adjusted to 1 mL by adding L3 buffer supplemented with 0.3 M NaCl, 1% Triton X-100, 0.1% deoxycholate. The lysate was then pre-cleared by adding 50uL of pre-rinsed sheep anti-rabbit Dynabeads (Invitrogen) and incubating at 4°C for 1 hour with agitation. After pre-clearing, 5% of the ChIP sample was set aside as input sample and the remainder of the lysate (950 µL) was incubated with 4 µg of antibody overnight at 4°C. The next day, 40 µL of pre-rinsed sheep anti-rabbit Dynabeads were added to the IPs and immunoprecipitation was carried out over a second night at 4°C. The bound beads were then washed twice for 5 minutes at 4°C with each: low salt buffer (150 mM NaCl, 0.1% SDS, 1% Triton X-100, 2 mM EDTA, 20 mM Tris-HCl, ph8.1); high salt buffer (500

mM NaCl, 0.1% SDS, 1% Triton X-100, 2 mM EDTA, 20 mM Tris-HCl, pH 8.1); LiCl buffer (0.25 M LiCl, 1% NP-40, 1% deoxycholate, 1 mM EDTA, 10 mM Tris-HCl pH 8.1); and TE (1 mM EDTA, 10 mM Tris-HCl pH 8.0). Immunoprecipitated materials were eluted from the beads by adding 200 µL of elution buffer (1% SDS, 0.1 M NaHCO3) and incubating the sample at 65°C with continuous vortexing for 1 hour; 150 µL of elution buffer was added to the input material and processed in parallel. Crosslinking was reversed by overnight incubation at 65°C with agitation and resultant DNA was phenol-chloroform purified, ethanol precipitated and re-suspended in 50 µL of TE. 1 µL was used for standard Taqman analyses.

2.1.20 Tissue processing for immunostaining

To collect pancreata, mice were anesthetized using isofluorane followed by cervical dislocation. The abdominal cavity was then opened, the right atrium cut open with fine scissors and 5 mL PBS injected with a 5 mL syringe into the left ventricle to clear blood cells from circulation. The left ventricle was then injected with 5 mL of 4% PFA. The pancreas was then collected and post-fixed with 4% PFA for an additional 16 hours at 4°C. The tissue was washed three times in PBS, transferred to 50% ethanol for 24 hours followed by an additional 24 hours in 70% ethanol. Tissue was then dehydrated through a series of ethanol steps including two 30 minute incubations in 95% ethanol, three 30 minute incubations in 100% ethanol, two 30 minute incubations in 100% xylenes and two 1 hour incubations in paraffin. Tissue was then embedded in paraffin using a Histocentre 2 (Thermo Shandon) and 5 µM sections collected on glass

microscope slides (Fischer Scientific) using Shandon Finesse microtome (Thermo Shandon).

To collect brain for cryosections, mice were sacrificed as above, and using a syringe pump, 30 mL of 4% PFA was perfused into the left ventricle at a rate of 0.9 mL/minute. The brain was then removed from the skull and post-fixed for 24 hours in 4% PFA. The brain was then transferred to 20% sucrose in H_2O solution for 24 hours followed by 24 hours in 30% sucrose. The brain was then embedded in NEG 50 cryomatrix (Thermo Scientific) and 20 μM sections collected with a cryostat and stored at -20°C until stained.

2.1.21 Immunofluorescent staining

Paraffin sections were rehydrated through a series of xylene and ethanol steps (two times for 3-minutes xylene; three times for 2-minutes in 100% ethanol; two times for 2 minutes in 95% ethanol; two times for 2 minutes in 75% ethanol; two times for 2 minutes in 50% ethanol). Antigen retrieval was performed on all paraffin slides by incubating in 95°C citrate buffer (10 mM sodium citrate, 0.05% Tween-20, pH 6) for 10 minutes. Sections were then allowed to cool to room temperature for one hour, washed three times with PBS, and blocked with 5% horse serum in PBS for one hour at room temperature. Primary antibodies (details listed in Table 2.4) were incubated on slides overnight at 4°C in 5% blocking solution. The following morning, slides were washed three times with PBS for a total of 15 minutes and incubated with fluorescently conjugated secondary antibody (dilutions listed in Table 2.5) and TO-PRO-3 (1:10,000; Life Technologies) nuclear dye for two hours. Slides were then washed three times in PBS for a total of 30 minutes and mounted with Slowfade Gold (Life Technologies).

For cryosections, slides were removed from -20°C and washed 3 times in PBS for a total of 15 minutes at room temperature. Antigen retrieval was performed on all slides as described above. Slides were then allowed to cool to room temperature, washed three times in PBS, individual sections circled with a PAP pen (Cedar Lane) and then blocked with 5% horse serum in PBS for one hour. Next, sections were incubated in primary antibody (listed, with dilutions, in Table 2.4) overnight. Sections were then washed three times with PBS for a total of 15 minutes, stained with secondary antibodies (details listed in Table 2.5) and TO-PRO-3, and mounted with Slowfade Gold as above.

2.1.22 Quantification of beta cell numbers

For quantification of beta cell number, pancreas was harvested, fixed and embedded in paraffin as described above. Subsequently, whole pancreas sections were stained for insulin on a minimum of four sections spaced 500 μM apart from at least three different mice per experimental group. Images were tiled on an Olympus BX61 widefield fluorescent microscope using a 10x objective lens. Beta cells were then automatically quantified using Cell Profiler and normalized to total pancreatic nuclei as determined by TO-PRO-3 staining.

2.1.23 Lineage tracing

At the endpoint of 32 weeks of age, pancreata was collected from control ($Npas4^{loxp/wt}$;$Rosa26^{mTmG/wt}$; $Pdx1CreER^{+}$) and knockout mice ($Npas4^{loxp/loxp}$;$Rosa26^{mTmG/wt}$;$Pdx1CreER^{+}$) for immunofluorescent staining as described above. A minimum of 50 islets from three different mice on three separate sections, spaced at least 500 μM apart were imaged using a SP8 confocal microscope with a 20x

objective lens. GFP labelled cells that were not insulin immunoreactive (Ins-/GFP+) or were glucagon immunoreactive (Gcg+/GFP+) were then quantified using Photoshop (Adobe) and normalized to total GFP labelled cells or total glucagon immunoreactive cells, respectively.

2.2 In vivo metabolic

2.2.1 Ethics

All procedures were carried out in accordance with and approved by University of British Columbia Animal Care Committee. For rat transfusion experiments, procedures were approved by l'Université de Montréal Animal Care Committee.

2.2.2 Mice

All mice were maintained on 12 hour light-dark cycles in temperature and humidity controlled rooms. Mice were housed in Optimouse cages (Animal Care Systems) with up to five males or females in a single cage with *ad libitum* access to food and water. Mice were weaned at 3 weeks of age and cage changes performed weekly. Only male mice were used for *in vivo* experiments. The details of all mouse strains used are available in Table 2.1.

2.2.3 Diets

Picolab Rodent diet 20 was used as the standard rodent chow. Fat, protein and carbohydrate constituted 13.2%, 24.6% and 62.1% caloric value (kcal%), respectively. For diet induced obesity studies in Chapter 5 and 6, Research Diet #D12331 was used in which fat, protein and carbohydrates comprised 58%, 16.4% and 25.5% of caloric value (kcal%), respectively.

2.2.4 *In vivo* rat transfusions

A full description of glucose infusions are described by Fontés et al (29). Briefly, indwelling catheters were inserted under general anesthesia into the left carotid artery and right jugular vein were tunneled subcutaneously and exteriorized at the base of the neck. The animals recovered for 5 days after surgery. Rats were randomized into two groups, receiving either 0.9% saline (Control) or 70% glucose transfusions. Initial glucose infusions rates were 3.3 mL kg^{-1} hr^{-1} and were adjusted to maintain glucose between 13.8 and16.7 mM over the 72 hour time course. Following infusion, islets were isolated, RNA extracted and reverse transcribed and qPCR analysis carried out as described above.

2.2.5 Tamoxifen administration

Tamoxifen was dissolved in corn oil at a concentration of 40 mg/mL through two minutes of sonication in a cup horn on a Misonix sonicator. Six week old mice were injected with three doses of 8 mg tamoxifen every other day over five days. Corn oil alone was used as vehicle control.

2.2.6 Embryonic pancreas isolation

Wild type C57Bl6 mice were used and noon on the day of plug discovery was considered embryonic day (e)0.5. At the desired embryonic day, pregnant dams were sacrificed by cervical dislocation following anesthesia by isoflurane. Embryos were then removed from the uterus and placed on ice cold PBS. The pancreas was harvested with the use of a dissecting scope and whole pancreas from individual embryos lysed in 1 mL of TRIzol. To ensure complete lysis, embryonic pancreas was finely processed with a set of narrow surgical scissors once in TRIzol.

2.2.7 Glucose tolerance test

Mice were fasted for 12 hours overnight. The following morning, a basal glucose measurement was taken by puncturing the saphenous vein with a 27½ gauge needle and assayed using a OneTouch UltraMini® handheld glucometer. Mice were then weighed and administered by oral gavage either a 2 g/kg glucose bolus from a 40% glucose stock (powdered glucose dissolved in sterile water) or 1 g/kg glucose bolus from a 20% glucose stock solution (powdered glucose dissolved in sterile water). Alternatively, one 2 g/kg glucose tolerance test was performed wherein glucose was administered into the intraperitoneal cavity with a 27½ gauge needle. Blood glucose was sampled at 15, 30, 60 and 90 minutes post glucose challenge. Area over the curve analysis was performed in Graphpad prism 6 using 0.0 as the baseline.

2.2.8 Plasma collection

For the collection of plasma for insulin or glucagon ELISA, whole blood was collected by puncturing the saphenous vein with a 27½ gauge needle and collection into a microcapillary tube. Blood was then transferred to a 1.5 mL microcentrifuge tube and stored on ice. Within 30 minutes of collection, whole blood was then centrifuged at 5000*g* for ten minutes at 4°C. Plasma was then collected, transferred to a new 1.5 mL tube and stored at -20°C until assayed using a rodent insulin ELISA (Alpco). For glucagon determinations, plasma was collected as above with the addition of aprotinin (Sigma) and KR-62436 hydrate (Sigma) and stored at -20°C until assayed using a glucagon ELISA (Mercodia).

2.2.9 Insulin tolerance test

Following a two hour fast, from 10AM-12PM PST, mice were weighed and a basal glucose measurement was taken from the saphenous vein. Subsequently, mice were injected with 0.75 U/kg of insulin (from a 150 mU/mL insulin stock, diluted in sterile PBS) directly into the peritoneal cavity. Blood glucose measurements were taken 15, 30, 60 and 90 minutes post-insulin injection. The change in blood glucose levels post-insulin injection were normalized to basal glucose levels. The net area over the curve analysis was performed in Prism 6 (Graphpad), using 1.0 as a baseline

2.2.10 Pyruvate and glycerol tolerance tests

Following an overnight fast of 12-hours, a basal glucose measurement was taken and mice were weighed. Mice were then IP injected with 2 g/kg of sodium pyruvate (from a 40% pyruvate stock solution prepared by dissolving powdered sodium pyruvate in sterile PBS) or 2 g/kg glycerol (from a 40% glycerol/sterile water stock). For pyruvate tolerance tests, blood glucose measurements were taken 15, 30 and 60 minutes post-pyruvate injection by puncturing the saphenous vein with a 27½ gauge needle. For glycerol tolerance tests, blood glucose was monitored at 15, 30, 60, 90 and 120 minutes post-glycerol injection. Area over the curve analysis was performed in Graphpad prism 6 using 0.0 as the baseline.

2.2.11 Body mass composition

Quantification of lean and fat mass was performed at 14 weeks of age in conscious animals using quantitative magnetic resonance (QMR) technology (EchoMRI-100 Echo Medical Systems) in collaboration with the laboratory of Dr. Bill Gibson.

2.2.12 Metabolic Cage monitoring

All metabolic cage analysis was carried out on 14 week old male mice. All mice were singly housed in metabolic cages (Lab-Master TSE Systems) for 24 hours to acclimatize prior to recordings. All calculated values for locomotor activity are based on measurements obtained over three days.

Spontaneous locomotor activity was analyzed by automatic recording of infrared beam breakage on the x,y and z axes by animals traveling within their cages. O_2 consumption and CO_2 production were measured via an open circuit indirect calorimetry system, with sensors sampling air from each cage once every 15 min (LabMaster TSE Systems). Metabolic activity (respiratory exchange ratio, RER) was calculated from the ratio of VCO2 (mL/h) produced to VO2 (mL/h) consumed throughout the day for each mouse. Food and water intakes were monitored every 15 minutes through weight sensors directly associated with food hopper or water bottle.

2.2.13 Streptozotocin preparation and administration to mice

Streptozotocin was dissolved in a 1:1 mixture of STZ buffer A (0.78 mL glacial acetic acid dissolved in 50 mL of sterile H_2O) and STZ buffer B (0.82 g sodium acetate dissolved in 50 mL sterile water) immediately prior to IP injection. STZ, at a dose of 25 mg/kg or equal volume of buffer control was injected 5 times into 4 month old C57BL6 mice for five consecutive days following a 4 hour fast from 10AM-2PM.

2.2.14 Intraductal AAV injections

Recombinant dsAAV6- RIP-Cre or AAV-RIP-Empty were generated at Children's Hospital of Pennsylvania. For the intraductal injections,$1.5x10^{10}$ viral genomes were injected into 8-9 week old male $Npas4^{flx/flx}$ mice into the pancreatic duct as previously

described (172). The week following the intraductal surgery, standard diet was replaced with HFD.

2.2.15 Statistical analysis

All statistical analysis was performed using Graphpad Prism 6 (Graphpad Software). All data is presented as the mean ± SEM. Statistical significance was determined using Student's t-test, or in the case of multiple comparisons, a one-way ANOVA with Dunnett's post-hoc test. All *in vivo* experiments were performed on at least two independent cohorts of mice.

Table 2.1: Mouse strains

Strain	Knockin	Source
Npas4^{loxp}	Y	Michael Greenberg (164)
Rosa26^{mTmG}	Y	Liqon Luo (173)
Pdx1CreER	N	Douglas Melton (174)
C57BL/6J	N	JAX (Stock # 000664)
Ins1^{Cre}	Y	Jorge Ferrer (175)

Table 2.2: Antibodies used for western blot

Target	Host	Source (Catalog #)	Dilution factor
GAPDH	Mouse	Sigma (G8795)	1:125000
HIF1α	Rabbit	Novus (NB100-15)	1:1000
MAFA	Mouse	Bethyl (IHC-00352)	1:5000
NEUROD1	Mouse	Cell Signaling (2833)	1:2000
NPAS4	Rabbit	Sigma (HPA039255)	1:1000
PDX1	Mouse	DSHB (F109-D12)	1:2000
RGS2	Chicken	Sigma (GW22245F)	1:1000
β-ACTIN	Mouse	Cell Signaling (8H10D10)	1:10000

Table 2.3: Secondary antibodies used for western blots

Target	Host	Source	Dilution factor
Mouse IgG	Goat	Jackson ImmunoResearch	1:3000
Rabbit IgG	Goat	Jackson ImmunoResearch	1:3000
Chicken IgG	Goat	Jackson ImmunoResearch	1:3000

Table 2.4: Primary antibodies for immunofluorescent staining

Target	Host	Source	Dilution factor
GLUCAGON	Mouse	Sigma(G2654)	1:2000
GFP	Rabbit	MBL(598)	1:500
INSULIN	Guinea Pig	Dako(A0564)	1:500

Table 2.5: Secondary antibodies for immunofluorescent staining

Target	Host	Source	Dilution factor
Rabbit IgG (Alexa Fluor 488)	Donkey	Jackson ImmunoResearch	1:250
Mouse IgG (Alexa Fluor 594)	Donkey	Jackson ImmunoResearch	1:450
Guinea Pig IgG (Alexa Fluor 594)	Donkey	Jackson ImmunoResearch	1:450

Table 2.6: Primer sequences for qPCR

All primers are targeted to mouse unless otherwise specified.

Target	Probe	Primer 1	Primer 2
Ddit3	CTTGACCCTGCGTCCCTAGCTTG	GCACCTATATGTCATCCCCAG	TGCGTGTGACCTCTGTTG
Gusb (Mouse)	TCTAGCTGGAAATGTTCACTGCCCTG	CACCCCTACCACTTACATCG	ACTTTGCCACCCTCATCC
GUSB (Human)	CAGATTCTAGGTGGGACGCAGGC	AGGTGATGGAAGAAGTGGTG	AGGATTTGGTGTGAGCGATC
Gusb (Rat)	TGGGCGATCAGCGTCTTGAAGTAAT	GGTCGTGATGTGGTCTGTG	TGTCTGGCGTCATATCTGGTATTG
Ins1	TGTTGGTGCACTTCCTACCCCTG	ATCAGAGACCATCAGCAAGC	GTTTGACAAAAGCCTGGGTG
Ins1 promoter	AGACCTAGCACCAGGCAAGTGTTT	GTGTTGATGTCCAATGAGTGC	CCCATTAAGGTGTCCAGGTG
Ins2	CCTCCACCCAGCTCCAGTTGT	TGATCTACAATGCCACGCTTC	GGCTTCTTCTACACACCCATG
Ins2 promoter	CAGGGAAGTGTTTGGAAACTGCAGC	GGACTAAGTAGAGGTGTTGA	CTGGACTTTGCTGTTTGACC
Ldha	AGCTCATCCGCCAAGTCCTTCATT	GCTCCCCAGAACAAGATTACAG	TCGCCCTTGAGTTTGTCTTC
LDHA (Human)	CCATTAGGTAACGGAATCGGGCTGA	CGTGTTATTGGAAGCGGTTG	TTCATTCCACTCCATACAGGC
MafA	ACTTCTCGCTCTCCAGAATGTGCC	AGTCGTGCCGCTTCAAG	CGCCAACTTCTCGTATTTCTCC
NeuroD1	TCATGAGTGCCCAGCTTAATGCCA	TCTTTCGATAGCCATTCGCATC	ATAGTGAAACTGACGTGCCTC
Npas4	CGTTGGTTCCCCTCCACTTCCAT	GTCTCAACATTCCCCTACGAAG	GACAATATGCCATACTTGAAGACG
NPAS4 (Human)	ACGCTTCTGCTCAACACTACCGC	GTCCTAATCTACCTGGGCTTTG	CCATCTCTGCCTGAATATCTCC
Npas4 (Rat)	CTTGAGCAGAGAGAAGCCCCGTG	ATGAGTCTTGCCTGCATCTAC	ACAAGTAGAAATCCAGGTAGTGC
Pdk1	TCGTGTTGAAACGTCCCGTGCT	GACTGTGAAGATGAGTGACCG	CAATCCGTAACCAAACCCAG
Pdx1	TTCCGCTGTGTAAGCACCTCCTG	GTACGGGTCCTCTTGTTTTCC	GATGAAATCCACCAAAGCTCAC
Rgs2	CTTGACCCTGCGTCCCTAGCTTG	GCACCTATATGTCATCCCCAG	TGCGTGTGACCTCTGTTG
Rgs2 enhancer	ATTCGCTCTGGTCAGGCTTGTGT	ATTGTCTTCCCACTGTCACG	GCTGTTTCCTCTATGAGCTGG
Rgs2 intron 1	AGCTCAGAACTAACAATGCAACGTCCA	TGTAGCTGAATAACGTCCACC	TCAACTCAAACATCTCCACCC
Rplp0	TGTCTTCCCTGGGCATCACGTC	TGACATCGTCTTTAAACCCCG	TGTCTGCTCCCACAATGAAG
Slc16a3	CCCCGTGGTGAGGTAGATCTGGATAA	CCTGTCATGCTTGTGGGTG	GGAAGGCTGGAAGTTGAGAG
Sox9 (Mouse)	AGGGTCTCTTCTCGCTCTCGTTCA	CAAGACTCTGGGCAAGCTC	GGGCTGGTACTTGTAATCGG
SOX9 (Human)	TCTGGAGACTTCTGAACGAGAGCGA	ACTTGCACAACGCCGAG	CTGGTACTTGTAATCCGGGTG
Vegfa	TTCCGGTGAGAGGTCTGGTTCC	GGCAGCTTGAGTTAAACGAA	TGGTGACATGGTTAATCGGTC

Chapter 3: Regulation of Npas4 in beta cells

3.1 Introduction

3.1.1 Calcium signaling in beta cells

The bHLH-PAS domain transcription factor, NPAS4, has been referred to as a "brain specific" transcription factor (161,162), where its expression regulated in response to a number of different stimuli such as calcium influx following membrane depolarization (164,165). Within beta cells, there are both intracellular and extracellular sources of calcium release, which may trigger the induction of *Npas4*. Extracellular calcium enters the beta cell mainly through L-type voltage dependent calcium channels but other channels such as T-type and P/Q-type calcium channels are required to elicit a full action potential in beta cells (3). There are also three intracellular calcium pools, distinguished based on their responsiveness to inositol triphosphate (IP_3), nicotinic acid adenine dinucleotide phosphate (NAADP) or ryanodine. NAADP responsive calcium pools within the beta cell are believed to be acidic vesicles such as lysosomes and insulin granules (176). Ryanodine receptors are found on the ER membrane and are responsible for calcium-induced calcium release (177). IP_3 receptors are found on the ER (178) and insulin granules (179) and are stimulated downstream of the activation of Gαq-coupled G protein receptors including GPR40 (8). This results in increased production of IP_3 which acts upon its receptor found within beta cells to trigger calcium release (178) (see figure 3.1)

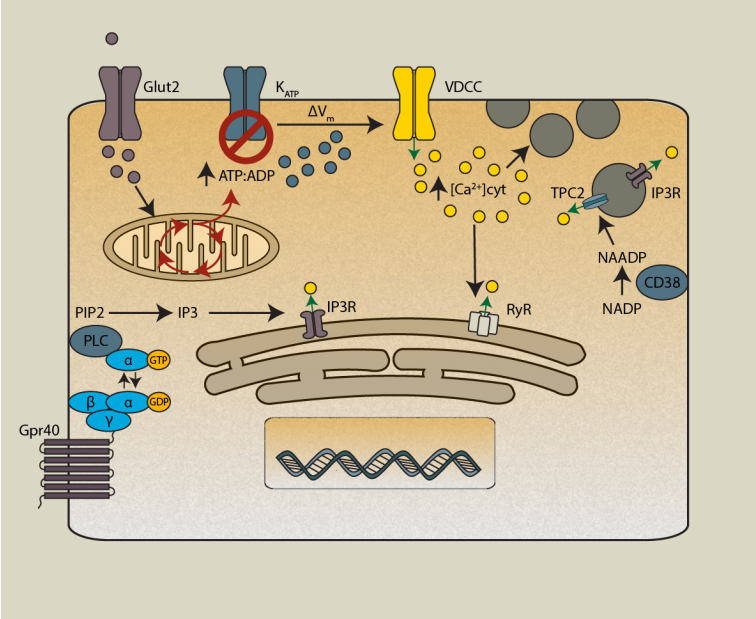

Figure 3.1: Schematic of sources of cytosolic calcium in beta cells.
Influx of extracellular calcium can be triggered by the metabolism of glucose, production of ATP and generation of ATP. This closes ATP dependent potassium (K_{ATP}) channels leading to depolarization and the opening of voltage dependent calcium channels (VDCC). Further there are three pools of intracellular calcium release; through IP3 receptors, ryanodine receptors and a NAADP responsive pool.

Following influx into the cytosol, calcium binds to and activates the calcium sensor protein, calmodulin, via four EF hand motifs (180). Calcium-bound calmodulin then interacts with, and activates, a large number of proteins, including a members of the calmodulin kinase (CamK) family of enzymes (181). Activated CamK then phosphorylate a number of dormant transcription factors including cAMP response element binding (CREB) protein (182). Calmodulin also activates the phosphatase, calcineurin, which dephosphosphorylates members of the NFAT family of transcription factors and MEF2 proteins; resulting in their nuclear localization (183). The activation of CREB, NFAT proteins and MEF2 leads to an initial wave of transcription of immediate early genes (IEGs). A large class of genes which are regulated by a specific stimuli (for instance, calcium) independent of *de novo* protein synthesis (184). As a calcium

regulated gene, it is likely that activation of one or more of these pathways are required for *Npas4* induction in neurons.

As the components of the calcium signaling pathway are expressed in beta cells (185) and many transcription factors found in neurons are also expressed within beta cells (186), it was hypothesized that NPAS4 is expressed within beta cells and regulated in a similar manner to that observed within neurons. Therefore, the studies within this chapter explore the regulation and dynamics of Npas4 expression.

3.2 Results

3.2.1 *Npas4* is expressed in beta cells & is activity regulated

As there have been no previous reports of *Npas4* expression in beta cells, the levels of *Npas4* in freshly isolated mouse islets was compared to that of other PAS domain proteins. Intriguingly, *Npas4* mRNA was readily detectable and was, in fact, similar in expression to other well-studied bHLH-PAS domain proteins including *Per1*, *Arnt* and *Hif1α*. Furthermore, of the four Npas family members, *Npas4* was the most highly expressed (Figure 3.2A). To determine when *Npas4* expression is activated during islet cell development, RNA was isolated from whole embryonic mouse pancreata between e(embryonic day) 10.5 and e18.5 and qPCR analysis performed. While detectable, compared to what was observed in adult mouse islets, *Npas4* expression was relatively low until e17.5, when *Npas4* levels increased approximately 10-fold compared to ~e16.5 and was comparable to what was observed in whole islets from adult mice (Figure 3.2B). These experiments are the first to demonstrate that *Npas4* is expressed outside the CNS.

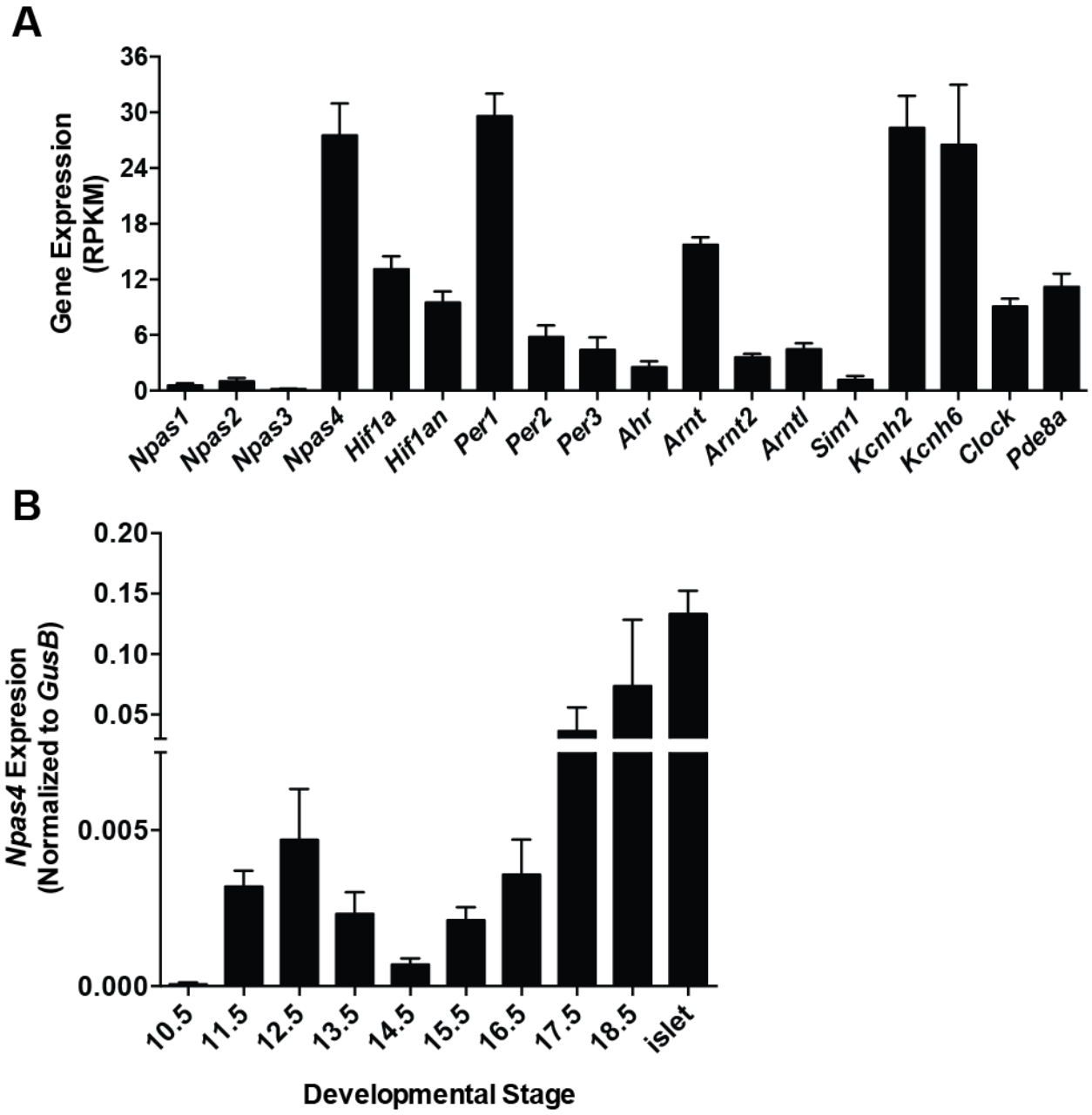

Figure 3.2: *Npas4* is expressed in pancreatic islets and the developing pancreas. *Npas4* expression in isolated islets from adult C57BL6 mice is higher than other Npas family members and comparable to many other bHLH-PAS domain transcription factors (n=3) (A). *Npas4* mRNA is detectable early in pancreas development but does not reach expression levels similar to those observed in isolated islets from adult mice until e17.5 (n=3-4) (B).

As *Npas4* expression is induced by membrane depolarization and calcium influx within neurons (165), beta cells were stimulated with depolarizing agents to determine

whether the same pathway might be conserved within beta cells. While a two-hour exposure to 25 mM glucose failed to induce *Npas4* message or protein levels in the MIN6 immortalized beta cell line (Figures 3.3A&D), exposure to 40 mM KCl led to a robust and rapid increase in *Npas4* message levels (Figure 3.3B). Similarly, NPAS4 protein expression was induced in MIN6 cells stimulated with KCl for two hours (Figures 3.3C&D). It is noteworthy that under basal conditions, NPAS4 protein was expressed at very low levels (Figure 3.3D), near or below the detection limit of western blots, despite the mRNA being readily detectable. As the MIN6 cells used in these experiments seemed resistant to the effects of high glucose, the effect of elevated glucose exposure was subsequently determined in primary mouse islets.

As glucose is the main physiologic inducer of beta cell depolarization, isolated mouse islets were stimulated *in vitro* with increasing concentrations of glucose for two hours and *Npas4* levels were assayed. In mouse islets, *Npas4* was increased by glucose in a concentration-dependent manner (Figure 3.4A); however, prolonged high glucose stimulation led to the gradual return to baseline levels (Figure 3.4B). Stimulating islets from human donors for two hours in high glucose led to a 40-fold increase in *NPAS4* mRNA (Figure 3.4C). NPAS4 protein levels were also increased following membrane depolarization with glucose or KCl in mouse islets (Figure 3.4D) and elevated glucose exposure increased NPAS4 levels in human islets from two separate donors (Figure 3.4E).

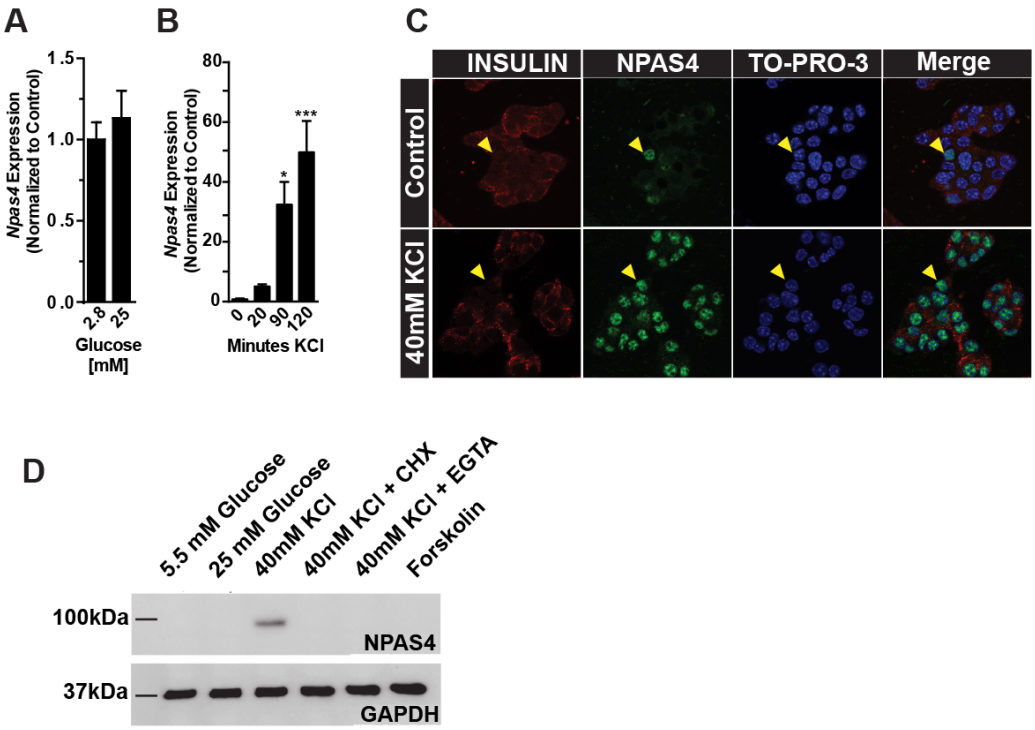

Figure 3.3: Npas4 is induced at the mRNA and protein level by KCl exposure in MIN6 cells.
In MIN6 beta cells, a two-hour high glucose (25 mM) exposure was not sufficient to induce *Npas4* (n=3) (A). However, depolarization with 40 mM KCl led to a time-dependent increase in *Npas4* levels over two hours (n=4) (B). Following a two-hour, 40 mM KCl stimulation, NPAS4 was induced in MIN6 cells and appeared to co-localize with the nuclear dye TO-PRO-3 (yellow arrow-heads) (C). NPAS4 induction was prevented by blocking of *de novo* protein biosynthesis with cycloheximide (CHX) or chelation of calcium with 5 mM EGTA, while application of 10 μM of the adenylate cyclase activator forskolin did not induce NPAS4 expression (D). Significance was established using two-tailed Student's t-tests or a one-way ANOVA with Dunnett's post-hoc analysis where applicable. *= $p \leq 0.05$; ** = $p \leq 0.01$; *** = $p \leq 0.001$.

To test whether glucose could induce *Npas4* levels *in vivo*, cannulas were placed within the carotid artery of rats and glucose infused at rates that maintained blood-glucose levels between 13.8 and 16.7mM for 72 hours. Alternatively, PBS was infused as a control. *Npas4* expression in freshly isolated islets from rats infused with glucose were 4-fold higher than saline controls (Figure 3.4F). Together, these data suggest that

in primary beta cells of different species, NPAS4 is induced by glucose exposure both *in vitro* and *in vivo*.

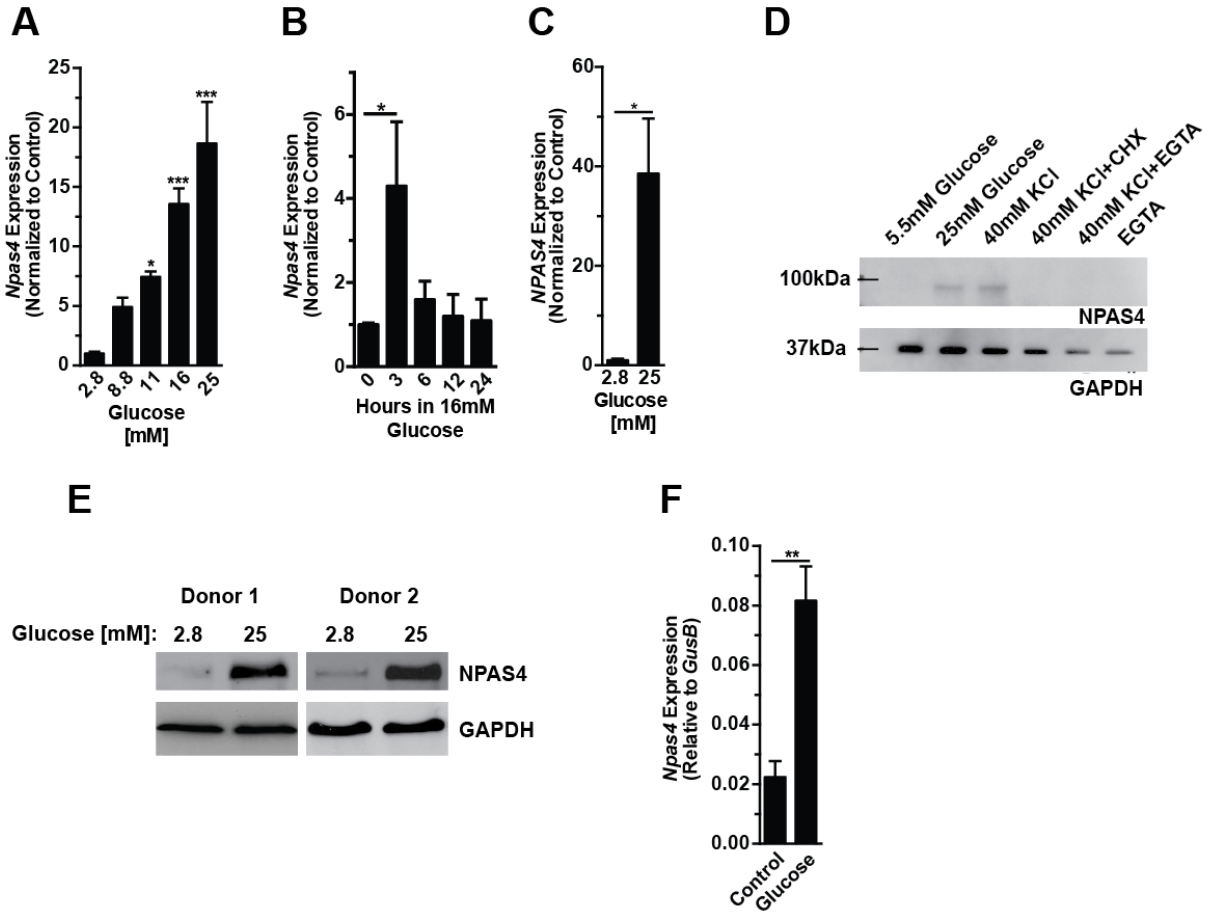

Figure 3.4: Elevated glucose exposure induces NPAS4 expression in murine and human islets.
During a two-hour stimulation, elevated glucose concentrations significantly increased *Npas4* expression in isolated mouse islets (n=3-8) (A). By six hours of exposure to 16 mM glucose, *Npas4* expression in isolated mouse islets returned to baseline (n=3-4) (B). *NPAS4* mRNA levels were significantly elevated by a two-hour exposure to 25 mM glucose in isolated human islets (n=4) (C). Similar to the induction observed at the mRNA level, NPAS4 was induced at the protein level in response to membrane depolarization in mouse (D) and human (E) islets. Following 72 hours of *in vivo* hyperglycemia (blood-glucose: 13.8-16.7 mM), *Npas4* was significantly increased in freshly isolated rat islets (n=4-5) (F). Significance was established using two-tailed Student's t-test or a one-way ANOVA with Dunnett's post-hoc analysis where applicable. n≥3 *= p≤ 0.05; ** = p≤ 0.01; *** = p≤ 0.001.

During KCl or glucose stimulation of beta cells, the influx of extracellular calcium through the voltage dependent calcium channel (VDCC) is a major source of cytosolic calcium. To determine whether stimulating ER calcium release in beta cells was sufficient to induce *Npas4* expression, MIN6 cells were incubated with two different ER calcium mobilizing agents, thapsigargin and palmitate. The sarco/endoplasmic reticulum calcium transport ATPase (SERCA) inhibitor, thapsigargin, blocks the reuptake of calcium into the ER which increases cytosolic calcium levels (187). In MIN6 cells, a two hour exposure to 1 μM thapsigargin increased *Npas4* mRNA by 10-fold (Figure 3.5A). A time-course of 1 μM thapsigargin exposure in MIN6 cells demonstrated two peaks in *Npas4* mRNA levels after 1 and 24 hours, respectively (Figure 3.5B) although only the second peak, present at 24 hours, could be appreciated at the protein level (Figure 3.5D). The fatty acid, palmitate also elevates intracellular calcium levels, in part, by acting through its receptor (GPR40) and downstream activation of the IP3 receptor on the ER membrane (188). Palmitate treated MIN6 cells had significantly elevated *Npas4* mRNA expression within the first hour of exposure (Figure 3.5C). Prolonged palmitate exposure led to the gradual decline in *Npas4* expression levels, although *Npas4* mRNA remained significantly elevated following 24 hours of high dose palmitate treatment (Figure 3.5C). Similar to what was observed at the message level, NPAS4 protein peaked in the first one to two hours of palmitate treatment and slowly returned to baseline levels (Figure 3.5E). In agreement with the findings in MIN6 cells (Figures 3.5A-E), treating mouse islets with thapsigargin or palmitate maximally increased *Npas4* expression by 12- and 5-fold, respectively (Figures 3.5F&G). These experiments

demonstrate that ER calcium release is sufficient to induce NPAS4 expression in beta cells.

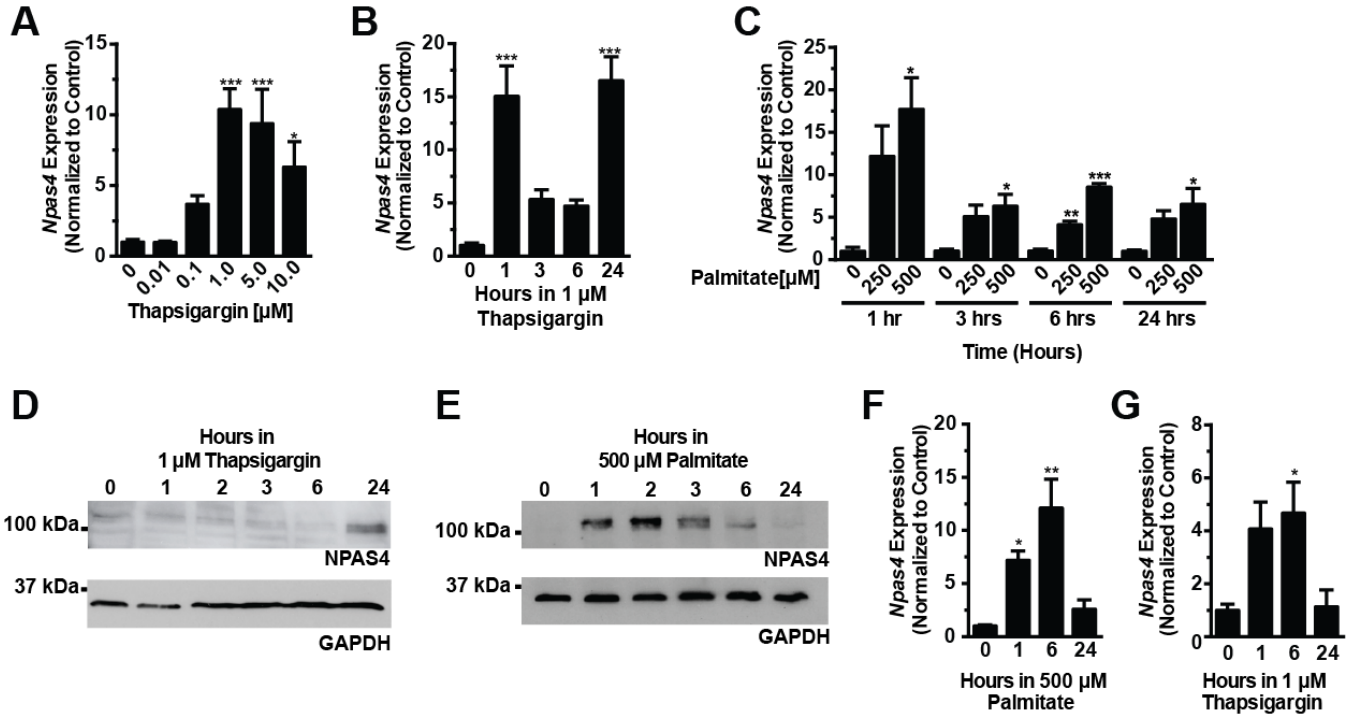

Figure 3.5: Thapsigargin and palmitate treatment increase NPAS4 expression in MIN6 cells and mouse islets.
Exposure to the SERCA pump inhibitor, thapsigargin, increased *Npas4* mRNA levels in a concentration (A) and time (B) dependent manner in MIN6 cells (n=3). Treatment with the fatty acid palmitate increased *Npas4* in both a time- and concentration-dependent manner (n=3) (C). Similar to induction of *Npas4* mRNA, both thapsigargin and palmitate increased NPAS4 protein levels in MIN6 cells (D&E). *Npas4* was also induced at the mRNA level in mouse islets in response to treatment with palmitate (F) and thapsigargin (G) (n=3). Significance was established using a one-way ANOVA with Dunnett's post-hoc analysis where applicable. *= p≤ 0.05; ** = p≤ 0.01; *** = p≤ 0.001.

Besides being upregulated by depolarization and ER calcium mobilizing agents, *Npas4* has previously been noted to be increased in response to oxidative stress in PC12 neuroblastoma cells (163). To assess the role of beta cell oxidative stress in the regulation of *Npas4* expression, MIN6 cells were treated with various concentrations of

hydrogen peroxide for two hours. However, across all doses administered, *Npas4* levels were not significantly altered (Figure 3.6A). To complement this *in vitro* experiment and examine the long term effects of oxidative stress insult, the beta cell toxin, streptozotocin (STZ), which mediates some of its cytotoxic effects through induction of oxidative stress (189-192), was used. Male wildtype C57BL6 mice were administered five doses of 25 mg/kg STZ and islets were isolated from these mice either 8 or 28 days following the final STZ dose. However, *Npas4* expression in islets from STZ-treated C57BL6 mice was not significantly different than islets from buffer-injected control mice (Figure 3.6B). Suggesting that Npas4 is strictly induced by calcium influx in beta cells.

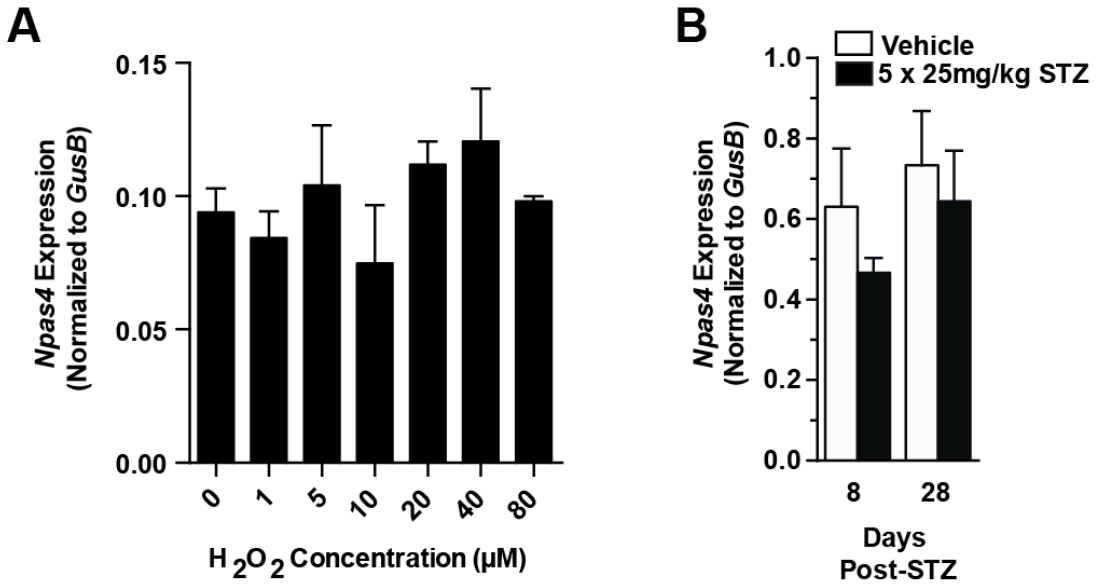

Figure 3.6: Beta cell *Npas4* expression is not altered by oxidative stress.
No change in *Npas4* expression levels were observed following a two hour exposure to increasing hydrogen peroxide concentrations (n=3) (A). *Npas4* expression was unchanged in freshly isolated islets from wildtype mice which were harvested either 8 or 28 days following multiple low dose STZ administration (5x25 mg/kg) or volume matched vehicle control (n=4-5) (B).

3.2.2 Dynamics and regulation of Npas4 induction in beta cells

To determine whether prolonged beta cell depolarization would lead to the continuous accumulation of Npas4 mRNA or protein, MIN6 cells were exposed to 40 mM KCl for up to six hours. However, past two hours, continued 40 mM KCl treatment led to a slow decline of Npas4 mRNA and protein levels (Figures 3.7A,C-D). The decline in Npas4 levels following a two-hour 40 mM KCl stimulation, could be accelerated by replacing the KCl medium, with non-stimulatory, 5.5 mM glucose DMEM (Figures 3.7B,E-F).

The accelerated decline of *Npas4* mRNA levels in MIN6 transferred to basal medium compared to *Npas4* levels maintained in KCl medium may be caused by reduced *de novo* Npas4 transcription or increased decay rates of *Npas4* mRNA. In order to examine mRNA decay rates under stimulatory or basal conditions, MIN6 cells were stimulated for two hours with KCl to induce *Npas4* before being transferred to either fresh 40 mM KCl-DMEM or basal DMEM with the transcriptional blocker, actinomycin D (ActD). While transcription was blocked in both the KCl and basal treatments, in the first two hours following KCl stimulation, *Npas4* expression levels were slightly but significantly elevated in MIN6 cells transferred to KCl-ActD medium compared to MIN6 cells transferred to Basal-ActD medium. Suggesting that beta cell activity results in the stabilization of *Npas4* mRNA. Analysis of the mRNA decay revealed an increased half-life of *Npas4* mRNA in stimulatory media (28.1 minutes) compared to basal media (12.6 minutes) (Figure 3.7F), suggesting that beta cell activity stabilizes *Npas4* mRNA.

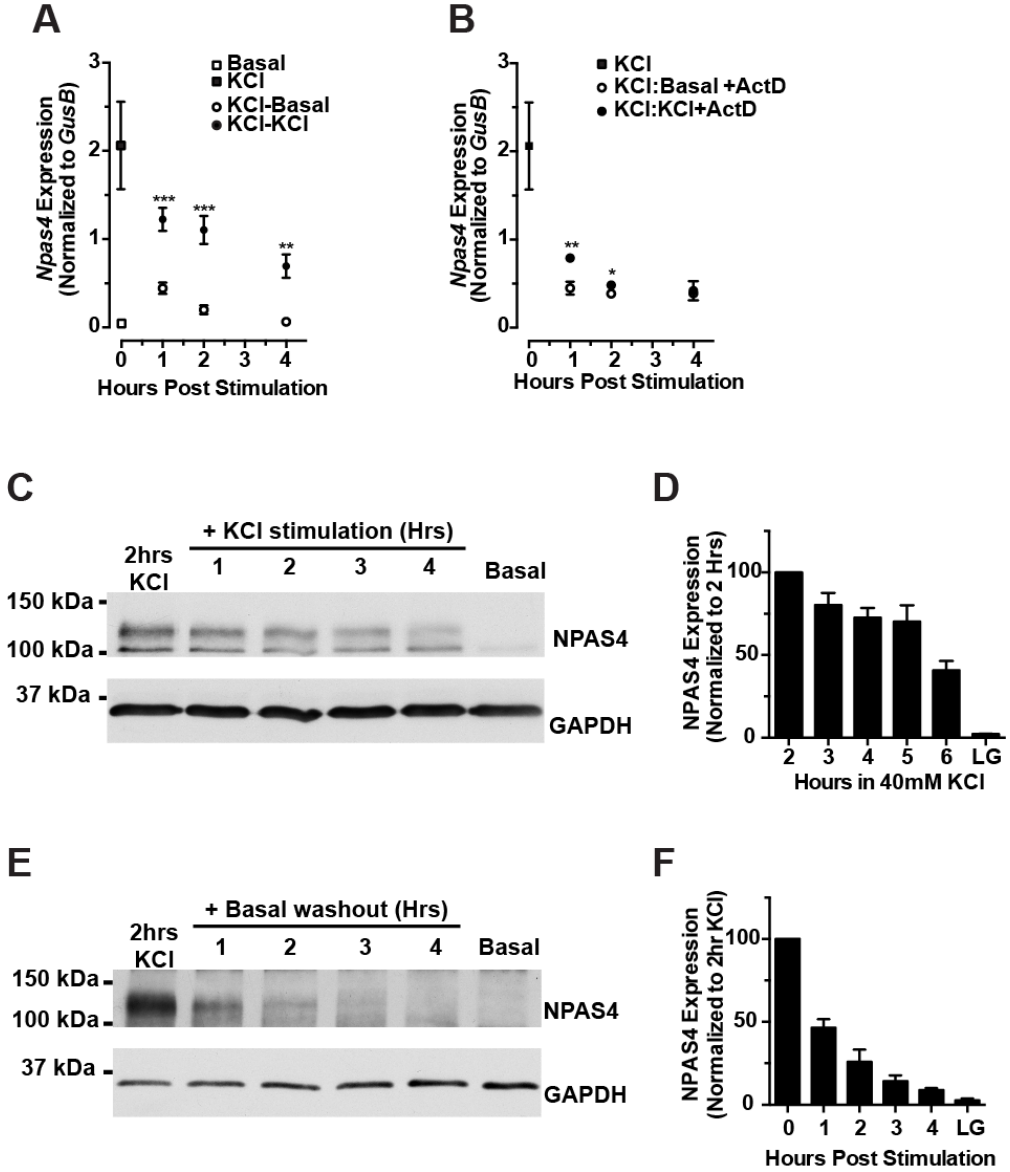

Figure 3.7: The decline in NPAS4 expression following a two hour KCl stimulation is accelerated by removal of stimulatory medium.
Prolonged exposure to 40 mM KCl led to the gradual reduction of Npas4 message (n=5) (A) and protein (n=3) (E&F) levels, while transfer to basal medium following a two hour KCl stimulation resulted in a more rapid reduction in Npas4 levels (n=3-5) (A,C&D). Examination of *Npas4* mRNA decay rates following a two-hour KCl stimulation with the addition of actinomycin D revealed that beta cell depolarization abated the decline of *Npas4* mRNA levels (n=4) (B). Significance was determined through a one-way ANOVA with Dunnett's post-hoc analysis. *= p≤ 0.05; ** = p≤ 0.01; *** = p≤ 0.001.

As chronic KCl stimulation led to a decline in *Npas4* induction, it was questioned whether a refractory period exists following an initial stimulation. To test this, MIN6 cells were exposed to two KCl stimulations, each of a two hour duration, separated by one to five hours of rest in basal medium. It appears that approximately five hours of rest following an initial stimulation is required to restore maximal *Npas4* induction as one, two and three hours of rest only resulted in a 50% induction when compared to the initial stimulus (Figure 3.8A).

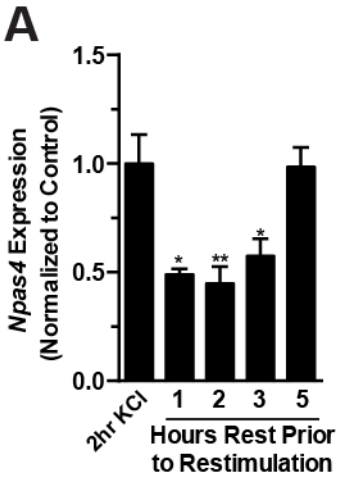

Figure 3.8: Restimulation of *Npas4* expression requires period of inactivity following depolarization of MIN6 cells.
In MIN6 cells, a second KCl stimulation after rest in basal medium did not induce *Npas4* to initial levels until 5 hours of intervening rest (n=4-8) (A). Significance was determined through a one-way ANOVA with Dunnett's post-hoc analysis. *= $p \leq 0.05$; ** = $p \leq 0.01$.

To begin to understand the mechanics behind the depolarization-dependent induction in *Npas4*, the role of calcium influx was interrogated through the use of the calcium chelator, EGTA. The presence of EGTA prevented KCl mediated induction of *Npas4*, suggesting depolarization-mediated *Npas4* expression is dependent on calcium influx (Figure 3.9A). A similar finding was observed at the protein level (Figure 3.3D). To further determine whether *Npas4* is induced in an immediate early fashion (independent

of *de novo* translation), MIN6 cells were stimulated with KCl in the presence of cycloheximide (CHX), which blocks translation of mRNAs (193). The increased *Npas4* mRNA levels following membrane depolarization occurred in the presence of cycloheximide (Figure 3.9B). Together, these experiments demonstrate that NPAS4 is an activity regulated, immediate early gene in beta cells.

As demonstrated above, both Npas4 mRNA and protein levels are induced following membrane depolarization and calcium influx. To determine whether both *de novo* transcription and *de novo* translation are required for the depolarization-dependent induction in NPAS4 protein levels, MIN6 cells were stimulated with 40 mM KCl in the presence of either actinomycin D or cycloheximide. Blocking *de novo* transcription with ActD completely inhibited the KCl-mediated induction of NPAS4 protein, likely precluding a large contribution of pre-existing *Npas4* mRNAs to the protein levels observed following KCl stimulation (Figure 3.9C). Similarly, blocking *de novo* protein translation with cycloheximide abrogated KCl-mediated NPAS4 protein induction in MIN6 cells (Figures 3.9D & 3.3D). These experiments demonstrate that following beta cell depolarization, both *de novo* transcription and translation are required to increase NPAS4 protein levels.

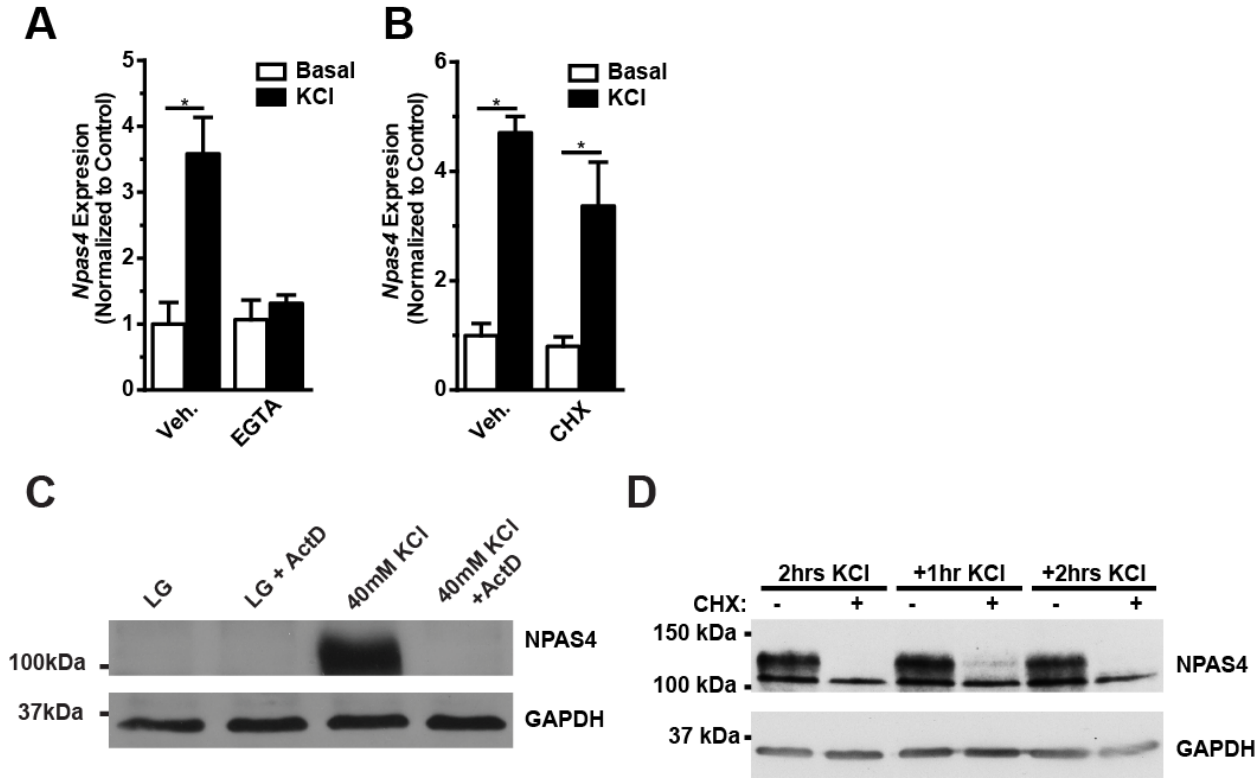

Figure 3.9: *Npas4* is induced by membrane depolarization in MIN6 cells in an immediate early fashion dependent on calcium influx.
Stimulating MIN6 cells with KCl in the presence of the calcium chelator, EGTA (A) but not the translational inhibitor cycloheximide (CHX) (B) inhibited *Npas4* mRNA induction (n=3). Blocking *de novo* transcription with actinomycin D (ActD) blunted the depolarization-dependent NPAS4 protein induction in MIN6 (C). In a similar fashion, blocking *de novo* translation with cycloheximide inhibited KCl-mediated NPAS4 expression in MIN6 cells (D). Blots in (C) and (D) are representative of three independent experiments. Significance was established using two-tailed Student's t-test. *= $p \leq 0.05$.

As membrane depolarization of beta cells results in both calcium influx and insulin secretion, it is possible that insulin promotes the induction of Npas4 in an autocrine/paracrine fashion. To determine whether the activity of Akt or mTOR, which constitute one arm of the insulin receptor signaling pathway (12) influenced KCl-mediated *Npas4* induction, MIN6 cells were stimulated in the presence of a pharmacologic inhibitor of Akt (Akt inhibitor VIII trifluoroacetate salt hydrate) or a mTOR

inhibitor (Rapamycin). Under basal conditions, Akt inhibition slightly but significantly increased *Npas4* levels (Figure 3.10A), while rapamycin had no impact on basal *Npas4* expression (Figure 3.10A). Under stimulatory conditions, high (10 μM) but not low (1 μM) concentration Akt inhibitor decreased *Npas4* levels by approximately 25% (Figure 3.10A). However, mTOR activity does not seem to be necessary for KCl-mediated *Npas4* expression as the presence of low or high concentration rapamycin did not alter *Npas4* mRNA levels (Figure 3.10A). Interestingly, when NPAS4 protein was assayed, high (10 μM) concentration Akt inhibition led to a more pronounced reduction in NPAS4 levels while rapamycin treatment had no significant impact (Figures 3.10B&C). While the direct effect of exogenous insulin on *Npas4* expression was not tested, these experiments suggest that intact insulin signaling and Akt activity is required for maximal induction of NPAS4 protein, through an mTOR independent pathway.

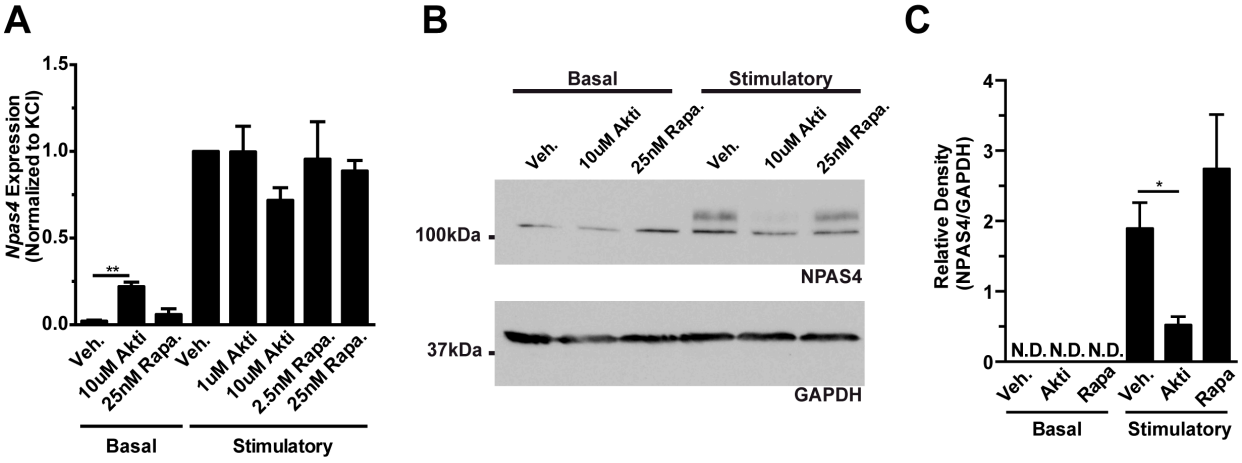

Figure 3.10: Inhibition of Akt but not mTOR reduces KCl-mediated NPAS4 induction in MIN6 cells.
Inhibiting the activity of Akt or mTOR does not dramatically dampen stimulatory (40 mM KCl) *Npas4* mRNA induction (n=3) (A). Blocking Akt but not mTOR substantially reduced NPAS4 protein induction in MIN6 cells (B&C). Significance was established using a two-tailed Student's t-test. (n=3) *= p≤ 0.05; ** = p≤ 0.01. N.D.= not detected.

3.2.3 Effect of hypoxia on Npas4 induction in beta cells

Reduced oxygen availability has dramatic effects on the expression levels of another bHLH-PAS domain transcription factor, HIF1α. Under normal oxygen levels, HIF1α is hydroxylation (139,194) by prolyl hydroxylase domain (PHD) enzymes and subsequently degraded (141), however, the paucity of oxygen reduces HIF1α hydroxylation and result in its stabilization. As the hypoxia experienced during ischemia may be responsible for the increased *Npas4* mRNA expression observed in the frontal cortex (162), the direct role of reduced oxygen availability on Npas4 expression within beta cells was assessed. In contrast to the robust increase in *Npas4* mRNA levels in MIN6 cells observed following KCl stimulation under control (20%) oxygen levels, stimulation in low (1%) oxygen significantly diminished *Npas4* induction (Figure 3.11A). The decreased *Npas4* mRNA was not dependent on stabilization of HIF1α as the presence of the PHD enzyme inhibitor, JNJ-42041935 (195), which stabilizes HIF1α (see Figure 5.5) did not significantly decrease *Npas4* levels under control oxygen conditions. In agreement to what was observed at the message level, NPAS4 protein was also reduced in the presence of KCl, under low oxygen conditions (Figures 3.11B&C); demonstrating that reduced oxygen availability reduced depolarization mediated NPAS4 expression in MIN6 cells.

To test whether hypoxia impaired Npas4 induction in primary tissue, C57BL6 mouse islets were stimulated for two hours in low or high glucose concentrations at either 20% or 1% environmental O_2 conditions. Under reduced oxygen conditions, stimulation of islets with high glucose significantly reduced *Npas4* expression compared to control oxygen levels (Figure 3.12A).

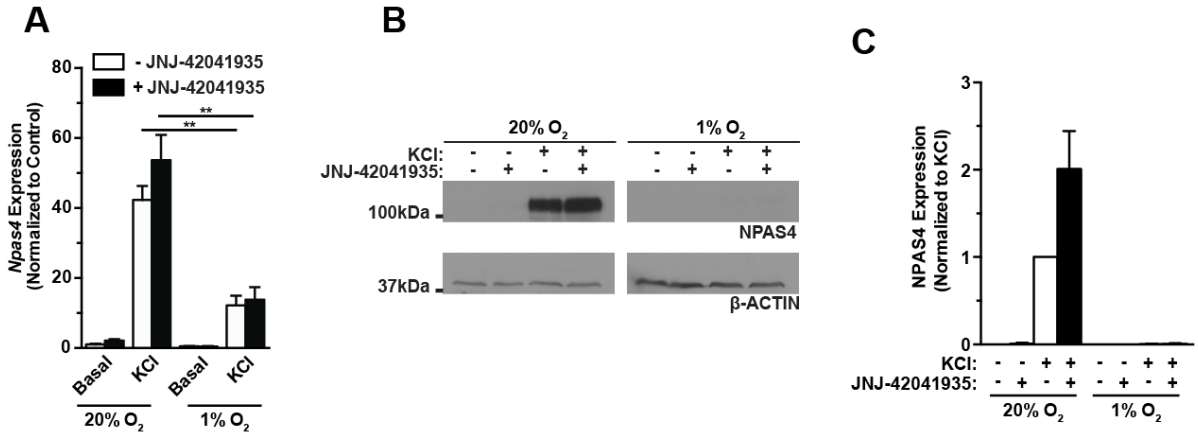

Figure 3.11: Reduced oxygen availability decreases NPAS4 induction in MIN6 cells.
Stimulation of MIN6 cells in low oxygen (1%) conditions significantly decreased KCl mediated *Npas4* induction compared to control environmental oxygen (20%) (n=3) (A). The presence of the PHD enzyme inhibitor JNJ-42041935 (black bars) did not similarly impact *Npas4* induction in 1% O_2 conditions (A). In agreement with what was observed at the mRNA level, low oxygen diminished KCl stimulated NPAS4 induction (n=3) (B&C). Significance was established using two-tailed Student's t-tests ** = p≤ 0.01.

Similar to the reduced *Npas4* expression in MIN6 cells and mouse islets, hypoxia also reduced NPAS4 protein induction by high glucose in human islets (Figure 3.12B). To determine whether a more chronic, mild hypoxic exposure would impact the expression of *Npas4* in beta cells, primary mouse islets were exposed to either 10% O_2 or 20% O_2 levels for 24 hours prior to a two-hour stimulation in either low or high glucose under 20% oxygen conditions. Mouse islets that had been exposed to 10% O_2 for 24 hours had significantly higher basal (2.8 mM glucose) and significantly decreased stimulatory (25 mM glucose) *Npas4* expression, compared to islets cultured in 20% O_2 (Figure 3.12C). These experiments in primary beta cells confirm the observed impairment in NPAS4 induction in MIN6 cells stimulated under hypoxia.

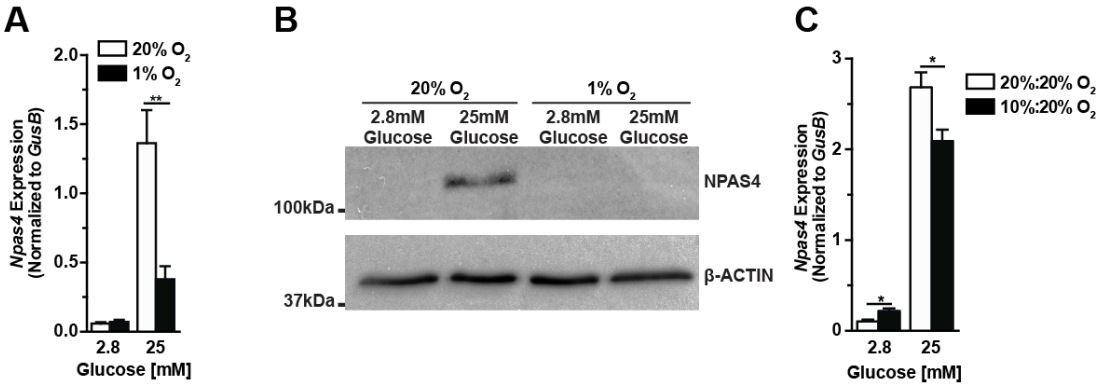

Figure 3.12: Glucose-mediated induction of Npas4 in primary islets is inhibited by low oxygen.
Two-hour high glucose stimulation in 1% O_2 conditions significantly diminished stimulatory *Npas4* expression in whole mouse islets compared to control oxygen conditions (n=6) (A). In one preparation of islets from a human cadaveric donor, NPAS4 protein induction was impaired by stimulation under low (1%) oxygen levels (n=1) (B). A 24-hour pretreatment in 10% O_2, increased *Npas4* expression under basal glucose and decreased *Npas4* expression under stimulatory glucose concentrations following a two-hour stimulation in 20% O_2 (n=4) (C). Significance was established using two-tailed Student's t-tests. *= $p \leq 0.05$; ** = $p \leq 0.01$.

The data from MIN6 cells and mouse islets suggest that reduced oxygen availability inhibited *Npas4* mRNA induction. To subsequently test whether low oxygen impacted preformed NPAS4 protein, MIN6 cells were stimulated for one hour under control oxygen conditions (20%) in 40 mM KCl (KCl) or 5.5 mM glucose DMEM (LG). For the second hour of the stimulation, half the cells were transferred to low oxygen conditions (1%) while the other half was maintained at control oxygen levels. Additionally, half the cells at each oxygen concentration were transferred to the opposite media type (i.e. cells stimulated for the first hour in LG were transferred to KCl; while cells stimulated with KCl for the first hour were transferred to LG). NPAS4 protein expression patterns matched what had been observed in earlier experiments in MIN6 cells maintained at 20% O_2 for the entire two-hour stimulation (Figure 3.13A). While MIN6 cells stimulated with KCl for the first hour of the stimulation (performed at control

oxygen levels) and subsequently transferred to low oxygen levels for the second hour still expressed detectable NPAS4 protein (Figure 3.13B; lanes 3&4). However, MIN6 cells incubated for the first hour in LG and then stimulated with KCl in 1% oxygen levels (Figure 3.13B; lane 2) had reduced NPAS4 protein levels compared to MIN6 cells stimulated for one hour with KCl in 20% O_2 (Figure 3.13A; lane 2). Together, these data suggest that low oxygen availability does not impact NPAS4 protein stability but rather NPAS4 biosynthesis.

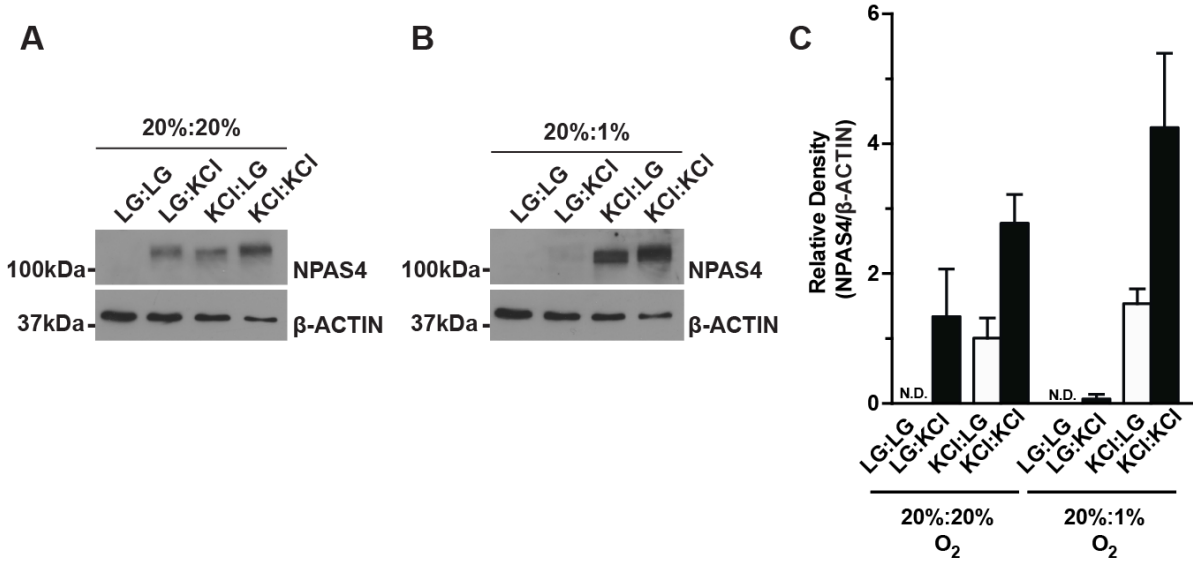

Figure 3.13: Exposure to low oxygen conditions does not dramatically impact preformed NPAS4 protein.
MIN6 cells were stimulated for one hour in either basal medium (LG) or 40mM KCl (KCl) medium under 20% O_2 conditions. Following one hour at 20% O_2, half the cells were maintained in 20% O_2 (A) and half transferred to 1% O_2 levels (B). Further, at each oxygen concentration, half the cells were maintained in the same media type for the second hour (i.e. LG:LG or KCl:KCl) and half transferred to the opposite media type (i.e. LG:KCl or KCl:LG). MIN6 cells stimulated with KCl under control oxygen levels and transferred to low oxygen had similar NPAS4 protein levels to MIN6 cells maintained at control oxygen. However, MIN6 cells stimulated with KCl for one-hour under low oxygen conditions had less NPAS4 protein compared to MIN6 cells stimulated with KCl for one-hour under control conditions. Representative blot from three individual experiments (n=3) (C).

3.2.4 Islet expression of Npas4 in diabetes

To examine a possible link between altered *Npas4* expression and *in vivo* beta cell dysfunction, seven week old, male C57BL6J mice were fed a high fat diet, or maintained on a standard chow diet, for 10 weeks. At which point islets were isolated and subjected to *in vitro* stimulation. Islets from HFD-fed mice had significantly reduced basal as well as high glucose and KCl stimulated *Npas4* expression (Figure 3.14A). To appreciate whether islet *NPAS4* expression was altered in humans with T2D, islets from donors diagnosed with T2D or healthy controls were stimulated for two hours in either low or high glucose. Compared to control islets, *NPAS4* expression in islets from individuals with T2D was elevated under low glucose conditions and decreased following exposure to high glucose; although these trends did not reach statistical significance (Figure 3.14B). However, while *NPAS4* could be significantly induced by high glucose exposure (an average 34-fold increase in control islets incubated in high versus low glucose), *NPAS4* islets from T2D donors was not significantly elevated following a two hour high glucose exposure (an average 2.8-fold increase in T2D islets incubated in high versus low glucose). These data from mice and humans suggest a correlation between dysregulated Npas4 expression and beta cell dysfunction.

3.3 Discussion

The experiments within chapter 3 set out to examine how a variety of external stimuli impact Npas4 expression in pancreatic beta cells. It was discovered that while expressed at very low levels under resting conditions, NPAS4 levels were increased in

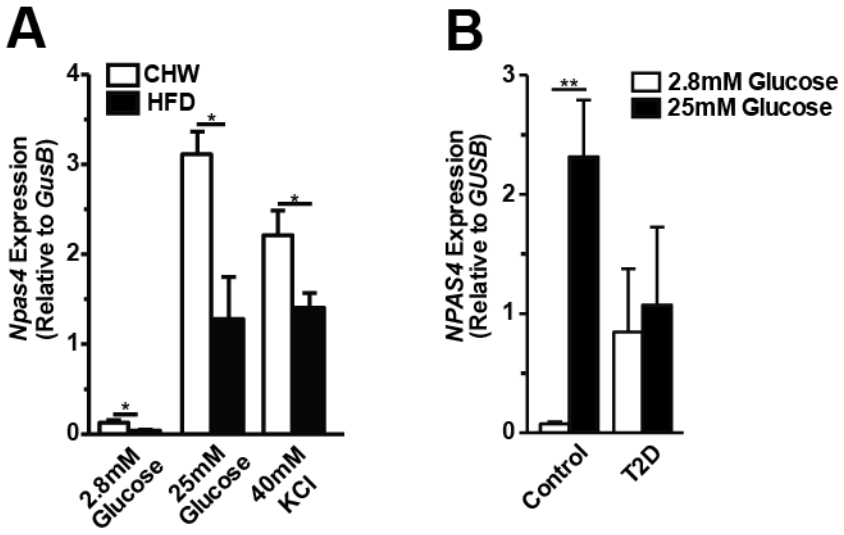

Figure 3.14: Npas4 expression is dysregulated in islets from HFD-fed mice and individuals with T2D.
Npas4 expression was significantly reduced in islets from male C57BL6 mice were fed a high fat diet (HFD) for ten weeks compared to age matched, control diet fed mice (CHW) (n=4) (A). There was a trend towards elevated *NPAS4* expression under low glucose conditions and elevated *NPAS4* expression following high glucose in islets from individuals diagnosed with T2D compared with islets from healthy (n=4) (B). Significance was established using two-tailed Student's t-tests *= p≤ 0.05; ** = p≤ 0.01.

response to membrane depolarization and mobilization of ER calcium in MIN6 cells and primary islets. In response to most stimuli, NPAS4 expression peaked at two hours of exposure with continued stimulation leading to a gradual return to baseline levels. Furthermore, the induction of NPAS4 could be inhibited by blocking Akt activity or reducing environmental oxygen conditions. These data are the first to demonstrate expression of NPAS4 in the pancreatic beta cell and highlight the dynamic nature of its regulation.

The induction of NPAS4 in beta cells in response to calcium mobilizing agents is in agreement with observations from the nervous system, where NPAS4 is potently induced by membrane depolarization and calcium influx (165). Stimulation of calcium signaling in beta cells by membrane depolarization results in the activation of the

transcription factors, CREB (196-198) and NFAT (199). These transcription factors act to promote insulin biosynthesis (200), proliferation (201-203) and survival (201) and disruption of CREB (196) or NFAT (204,205) activity *in vivo* results in impaired beta cell function and glucose homeostasis. As a recent publication demonstrated depolarization-dependent NPAS4 induction requires the action of Calcineurin and the Calmodulin kinases I,II&IV (206); it is possible that reduced NPAS4 contributes to the beta cell dysfunction caused by lack functional CREB or NFATs.

Besides a role for membrane depolarization in stimulating *Npas4* transcription, beta cell depolarization had a mild stabilizing effect on *Npas4* mRNA. Beta cell activity has previously been shown to more than double the half-life of *Insulin* mRNA when rat islets were cultured in 17 mM compared to 3.3 mM glucose (207). This effect may be mediated through the action of the RNA binding protein, polypyrimidine tract-binding protein which translocates from the nucleus to the cytoplasm (208) under high glucose conditions. Once in the cytoplasm, it is believed to bind to pyrimidine rich regions within the 3' untranslated region of *Insulin* mRNA, resulting in message stabilization (209-211). However, whether this mechanism explains *Npas4* mRNA stabilization remains untested.

While membrane depolarization regulated *de novo* transcription *Npas4* mRNA stability; the activity of Akt additionally regulated *Npas4* mRNA translation. This seemed to be the case as Akt inhibition had only a marginal effect on *Npas4* mRNA induction but completely abrogated the induction of NPAS4 protein levels; suggesting that *Npas4* mRNA translation also serves as an important step in the regulation of NPAS4 protein levels. This inhibition was not dependent on active mTOR, as rapamycin did not lead to

a similar reduction in NPAS4 protein levels. As activation of the insulin receptor is one pathway through which Akt is activated this data may suggest an autocrine/paracrine role for insulin-mediated beta cell NPAS4 expression. The role of autocrine/paracrine insulin activity within the beta cell is rather contentious, as it is believed that *in vivo* beta cells are not exposed to sufficient amounts of monomeric insulin to activate the insulin receptor (212). Furthermore, as neither exogenous insulin had any effect on *Npas4* expression levels (206) and as Akt activity can be modulated by numerous other pathways including calcium (213,214), more rigorous experiments are required to conclusively demonstrate a role for insulin signaling in NPAS4 induction.

Reduced atmospheric oxygen levels also significantly reduced NPAS4 expression following membrane depolarization in MIN6 cell, mouse and human islets. There is a lack of data examining the effect of hypoxic conditions on beta cell depolarization or calcium influx, however, within myocytes, hypoxia has been shown to hyperpolarize the cell membrane (215) and reduce KCl-stimulated calcium influx through L-type calcium channels (216). Regardless of the specific mechanism, blocking the production of NPAS4 under hypoxic conditions may be advantageous for beta cells. As both NPAS4 and HIF1α are dependent on heterodimerization with ARNT for transcriptional activity, the presence of both NPAS4 in hypoxia would likely dampen the hypoxic response by competing with HIF1α for ARNT. It is possible that NPAS4 expression is blocked in hypoxia in order to enhance HIF1α activity.

In order to determine whether changes in *NPAS4* expression correlated with beta cell dysfunction in humans; *NPAS4* expression was assessed in islets from individuals with T2D. In T2D islets, *NPAS4* levels tended to be higher under basal glucose

concentrations and lower under stimulatory glucose concentrations. However, the trends observed did not reach statistical significance. A similar *Npas4* expression pattern was observed in mouse islets pretreated with mild hypoxia for 24 hours prior to low or high glucose stimulation under normoxia; implicating activation of HIF1α in the disrupted expression of *NPAS4* in T2D. Indeed, it has been proposed that HIF1α is stabilized in beta cells, under conditions which resemble T2D, such as hyperglycemia (144) and in the diabetes mouse model, db/db (144). While the presence of islet hypoxia is unconfirmed in humans, it is possible that prolonged HIF1α activation *in vivo* blunts NPAS4 induction.

Finally, within the developing mouse pancreas, *Npas4* mRNA could be detected as early as e10.5; however, expression levels remained relatively low until e17.5 at which point they were similar to those observed in adult mouse islets. Intriguingly, transcriptome analysis of purified alpha and beta cells from human fetal (age 12-18 weeks) and adult (4-60 years of age) pancreas revealed that *NPAS4* was most highly expressed in fetal alpha cells, followed by fetal beta cells with the lowest expression observed in adult alpha and beta cells (217). This is contrast to the data from embryonic mice in which expression was generally lower in development than adult islets. However, one explanation is that the data presented in Figure 3.2 was from RNA extracted from whole mouse pancreas, which would dilute any signal from purified endocrine cells. This data from humans raises the possibility that NPAS4 may have functional significance in human endocrine cell development. Future experiments could identify the specific cell types in murine and human pancreatic development which

express NPAS4 and examine the effect of NPAS4 knockdown or overexpression on human beta cell development through stem cell differentiations.

In summary, these studies are the first to detail the expression of the bHLH-PAS domain transcription factor, NPAS4 within the pancreatic beta cell. NPAS4 expression is dynamic, being expressed at very low levels under basal conditions, but robustly induced in response to agents that increase cytosolic calcium levels. Based on the disruption of *NPAS4* expression in islets from individuals with T2D and the importance of beta cell calcium signaling pathways in promoting beta cell function and survival; the functional importance of NPAS4 must therefore be examined.

Chapter 4: *In vitro* regulation of insulin production and secretion by NPAS4

4.1 Introduction

In chapter 3, the expression of Npas4 was assayed in response to a variety of stimuli. These studies positioned NPAS4 as a depolarization-induced protein, however did not elucidate the functional significance of NPAS4 expression within the pancreatic beta cell. Therefore, the studies presented in chapter 4 aimed to understand how NPAS4 impacted insulin expression and secretion.

4.1.1 Regulation of the Insulin promoter

In mice, beta cells express two insulin genes, with the Insulin 2 gene being homologous to human insulin (218). The regulation of insulin expression is highly complex; with nearly a dozen transcription factor binding sites previously identified within the proximal promoter (219). Of all the transcription factors which promote insulin expression, the three of the most potent are pancreatic duodenal homeobox 1 (PDX1), neurogenic differentiation 1 (NEUROD1) and V-Maf Avian Musculoaponeurotic Fibrosarcoma Oncogene Homolog A (MAFA) (220). The insulin promoters are also regulated by silencers including c-Jun and CCAAT/Enhancer-binding Protein beta (219,221) .

The expression of insulin is also regulated by external factors such as glucose; with numerous *in vitro* and *in vivo* studies demonstrating an induction in insulin gene expression following high glucose exposure (222-227). The induction of insulin expression by glucose is at least partially dependent on calcium influx, as blocking calcium channels with verapamil significantly decreased the induction of insulin

promoter activity (200,228). Calcium may be mediating this effect through the downstream activation of NFAT proteins as NFAT2 is enriched at the insulin promoter following high glucose exposure to MIN6 cells or human islets (229). Further, inhibiting calcineurin with FK506 (tacrolimus) completely abrogated the induction of insulin promoter activity by either glucose or KCl in INS-1 cells (200) and transducing a constitutively active calcineurin into beta cells increased insulin promoter activity under basal and high glucose conditions (200). Whether factors downstream of NFAT, such as NPAS4, contribute to the regulation of insulin transcription has not been as well studied.

4.1.2 Incretin potentiated insulin secretion

In the postprandial state, insulin secretion is stimulated through exposure to ingested nutrients, including, glucose, free fatty acids and amino acids (230). Additionally, exposure to the incretin hormones, Glucose-dependent insulinotropic polypeptide (GIP) and glucagon like peptide-1 (GLP-1), potentiates nutrient induced secretion (231). Produced by cells within the intestinal tract (232), both GIP and GLP-1 are secreted into circulation in response to digestive products and neural stimulation (232). These hormones then act through seven transmembrane, G-protein coupled receptors, expressed on cells within the heart, brain, stomach, adipose and islets (233). Following ligand binding, the GIP and GLP receptors undergo conformational changes resulting in the interaction and activation of the heterotrimeric G-protein subunit, $G\alpha_S$ through the guanine-nucleotide exchange factor (GEF) activity of the receptor (234). GTP-bound $G\alpha_S$ results in the stimulation of adenylate cyclase activity, leading to the increased production of cAMP. Within beta cells, increased cAMP production acts to potentiate

glucose-stimulated insulin secretion through a PKA-dependent and a PKA-independent pathway (234).

Within the central nervous system, NPAS4 has been shown to positive regulate the synthesis and release of the neurotransmitter, Gamma-aminobutyric acid (GABA) (165,235). Based on this observation, a series of *in vitro* experiments were undertaken to examine how NPAS4 influenced the production and secretion of insulin.

4.2 Results

4.2.1 NPAS4 negatively regulates insulin expression in beta cells

As glucose promotes both insulin expression and NPAS4 induction in beta cells, it was hypothesized that NPAS4 may be one factor that promotes insulin gene transcription under conditions of beta cell activity. To test whether elevated NPAS4 expression increased insulin expression in beta cells, MIN6 cells were transduced with either an adenovirus expressing Npas4 (Ad-Npas4) or a control virus, expressing cerulean fluorescent protein (Ad-Cerulean). Adenoviral transduction in MIN6 cells resulted in supraphysiologic increases in NPAS4 protein expression, 48 hours post-infection (Figure 4.1A). Following 48 hours of infection, the Ad-Npas4 transduced MIN6 cells had significantly reduced *Insulin 1* (62% of control) and *Insulin 2* (69% of control) message levels along with reduced insulin protein (43% control) (Figures 4.2A-C). Similarly, transducing whole mouse islets with Ad-Npas4 resulted in significant reductions in *Insulin1*, *Insulin 2* mRNA and total insulin protein content (Figures 4.2 D-F).

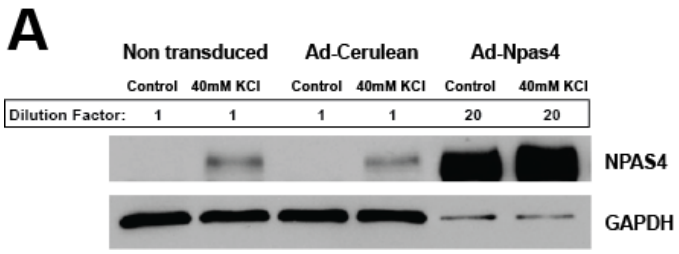

Figure 4.1: Transduction of MIN6 cells with Ad-Npas4 leads to supraphysiologic NPAS4 expression.
Following 48 hours of viral transduction with either control (Ad-Cerulean) or Npas4 (Ad-Npas4) adenovirus, MIN6 cells were stimulated for 2 hours in basal or 40mM KCl media. Non virally transduced cells are included as a control. NPAS4 protein levels were assayed through western blot (A). Representative blot from three independent experiments.

Conversely, to determine whether decreased NPAS4 expression would lead to elevated insulin levels, MIN6 cells were transfected with either small interfering RNAs (siRNA) targeting *Npas4* (siNpas4) or control siRNAs (siControl). The siRNAs targeting *Npas4*, reduced palmitate-mediated induction of NPAS4 expression, 48 hours following siRNA transfection in a concentration-dependent manner (Figure 4.2G). MIN6 cells transfected with siNpas4 had 50% higher expression levels of *insulin 1* and *insulin 2* levels compared to cells transfected with control siRNA (Figures 4.2H&I). These data demonstrate that through an unknown mechanism, NPAS4 acts to decrease *Insulin 1* and *Insulin 2* gene expression. To determine if the decreased insulin mRNA levels observed following NPAS4 overexpression were due to decreased transcription rates, insulin promoter activity was subsequently assessed using a luciferase assay.

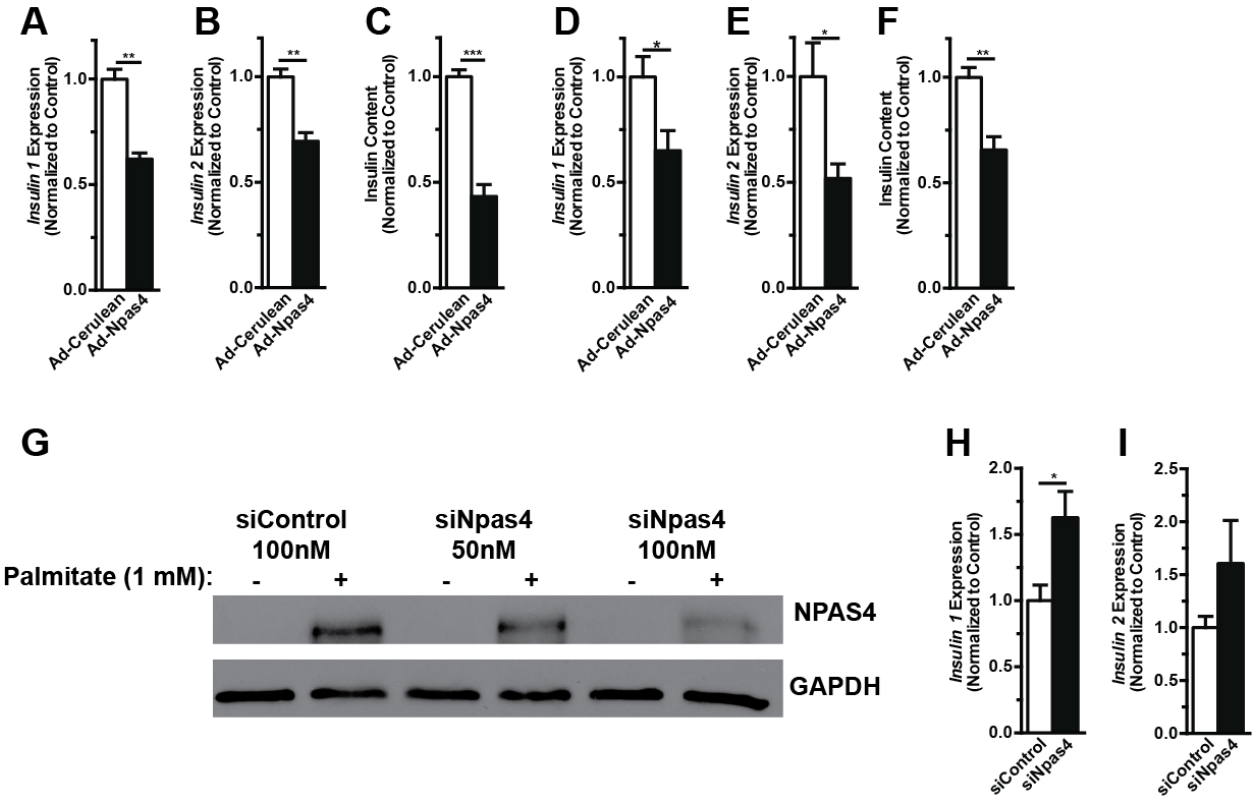

Figure 4.2: NPAS4 suppresses insulin gene transcription in mouse beta cells. Adenoviral overexpression of Npas4 for 48 hours in MIN6 cells significantly decreased expression of *Insulin 1* (n=3) (A) and *Insulin 2* (n=3) (B) message levels and total insulin content (n=3) (C). 48 hour adenoviral overexpression of Npas4 in mouse pancreatic islets (D-F) significantly decreased expression of *Insulin 1* (n=3-4) (D) and *Insulin 2* (n=3-4) (E) as well as total islet insulin content (n=3) (F). Transfecting siRNAs targeting Npas4(SiNpas4) into MIN6 cells reduced palmitate mediated NPAS4 induction (n=1) (G). SiNpas4 transfected MIN6 cells had increased expression of *Insulin 1* and *Insulin 2* (n=4-5) (H&I). * $p \leq 0.05$; ** $p \leq 0.01$; *** $p \leq 0.001$. Significance was established using a two-tailed Student's t-test.

Luciferase activity in MIN6 cells transfected with a rat insulin 1 promoter (RIP1)-driven luciferase reporter plasmid was markedly elevated (Figure 4.3A) compared to a promoterless luciferase construct (-Luciferase). However, co-transfection of the RIP1-luciferase plasmid with an Npas4 expression construct (pcDNA3.1+Npas4) significantly reduced luciferase activity (Figure 4.3A) suggesting that NPAS4 acts to reduce insulin transcription in MIN6 cells.

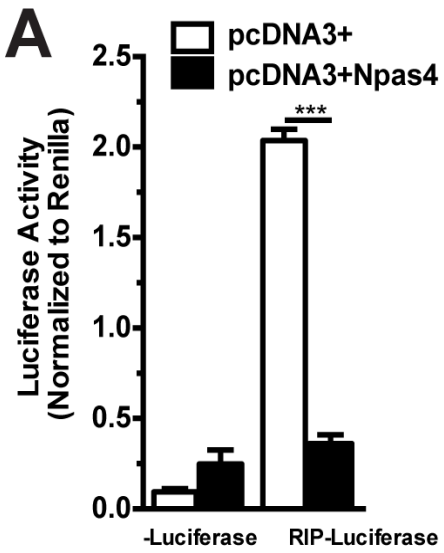

Figure 4.3: NPAS4 reduces rat insulin 1 promoter activity in MIN6 cells. Co-transfection of a Npas4 expression plasmid (pcDNA3+Npas4) with a rat insulin promoter luciferase construct (RIP1-Luciferase) in MIN6 cells significantly reduced luciferase activity 48 hours' post-transfection (n=3) (A). *** $p \leq 0.001$. Significance was established using a two-tailed Student's t-test.

To examine the possibility of NPAS4 directly regulating insulin promoter activity, chromatin immunoprecipitation (ChIP) experiments were performed. Following a 2-hour depolarization with KCl, endogenous NPAS4 was enriched 11-fold at the Insulin 1 promoter and by 15-fold at the Insulin 2 promoter compared with non-depolarized cells (primer sequences for ChIP experiments are available in Table 2.4 and a diagram of primer binding sites within the insulin promoter is available in appendix A) (Figure 4.4A). These ChIP experiments suggest that NPAS4 is directly inhibiting insulin promoter activity during periods of high beta cell activity.

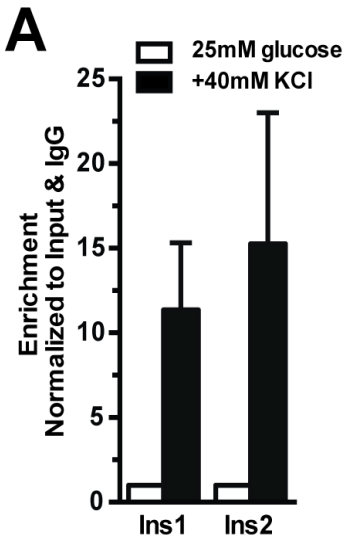

Figure 4.4: NPAS4 is enriched at both the mouse Insulin 1 and Insulin 2 promoter following membrane depolarization with KCl in MIN6 cells.
NPAS4 protein levels were enriched at both the insulin 1 and insulin 2 promoters in MIN6 cells following a two hour depolarization with 40mM KCl (n=3) (A).

To further determine whether elevated NPAS4 expression had an indirect effect on insulin levels, the expression of the three main promoters of insulin expression: Pdx1, Neurod1 and MafA, was examined. While Npas4 overexpression in MIN6 cells did not alter the mRNA levels of Pdx1 or Neurod1 (Figures 4.5A&B), both were significantly reduced at the protein level (Figures 4.5D,E,G&H). Interestingly, MafA mRNA and protein levels were increased by 3-4 fold in Npas4 transduced MIN6 cells (Figures 4.5C,F&I). In addition to the direct regulation of insulin promoter activity by NPAS4, the reduced protein expression of NEUROD1 and PDX1 would suggest that Npas4 transduction may also indirectly negatively regulate insulin expression.

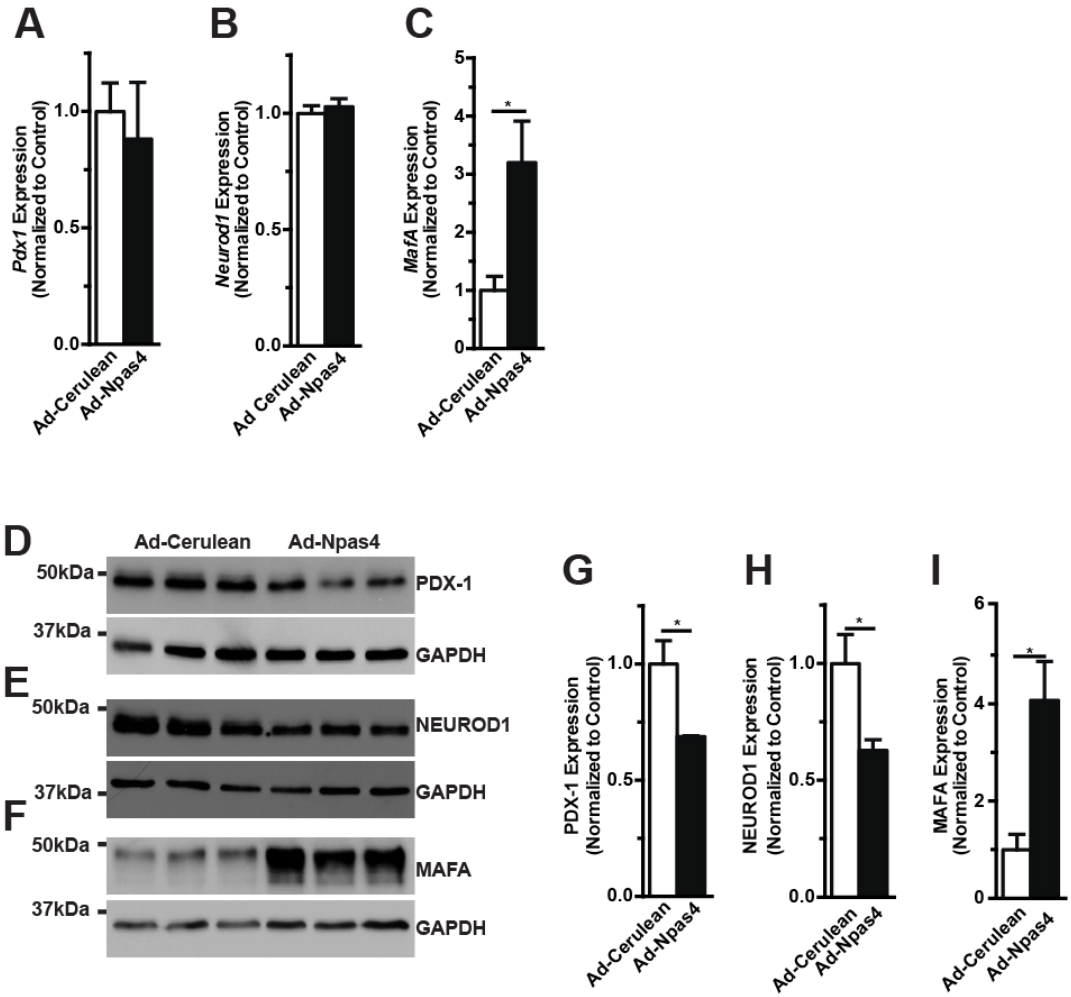

Figure 4.5: NPAS4 overexpression in MIN6 cells alters the expression of Pdx1, Neurod1 and MafA.
Npas4 transduction in MIN6 did not alter Pdx1 (A) or Neurod1 (B) mRNA expression but significantly decreased both at the protein level (n=3) (D,E,G,H). NPAS4 increased the expression of MafA at the message (L) and protein (F,I) level (n=3). Densiometric quantification of blots D-F can be found in G-I. * $p \leq 0.05$. Significance was established using a two tailed students t-test.

4.2.2 NPAS4 reduces GLP-1 stimulated cAMP production and insulin secretion

As NPAS4 overexpression substantially reduced insulin protein content in MIN6 cells, it was hypothesized that there would be subsequent defects in insulin secretion. Interestingly, when MIN6 cells or mouse islets infected with Ad-Npas4 were stimulated

with high glucose, no significant difference in insulin secretion was observed (Figures 4.6A&B). To better mimic *in vivo* postprandial conditions, in which beta cells are exposed to both glucose and incretin hormones, Npas4 transduced beta cells were also stimulated with glucose and varying concentrations of the GLP-1 receptor agonist, exendin-4. Whereas exendin-4 stimulated maximal insulin secretion at a concentration as low as 5 nM in control cells, exendin-4 had no potentiating effects in Ad-Npas4 transduced beta cells, even when used at a concentration of 50 nM (Figure 4.6B).

To determine whether the defect in exendin-4 potentiated secretion in Npas4 transduced beta cells was due to defective receptor signalling or downstream production of cAMP, a combination of forsokolin and IBMX was used to induce insulin secretion. Forskolin, an adenyl cyclase activator, and IBMX, an inhibitor of phosphodiesterase act to increase cAMP levels independent of the GLP-1 receptor, allowing for the examination of downstream events. Insulin secretion from Npas4-transduced MIN6 cells following stimulation with forskolin and IBMX (Figure 4.6B) was partially, but not completely, rescued. Suggesting that NPAS4 overexpression negatively impacts GLP-1 receptor signalling as well as pathways that lie downstream of cAMP production.

To more directly test whether NPAS4 reduced GLP-1 receptor-mediated cAMP production, Npas4 transduced MIN6 cells were stimulated with exendin-4 for 30 minutes, in the presence of IBMX, and cAMP content analyzed by ELISA. Across all concentrations of exendin-4 tested, Npas4 transduced beta cells had significantly reduced intracellular levels of cAMP (Figure 4.6C). Supporting the hypothesis that

impaired GLP-1 receptor signalling contributed to the reduced potentiating effect of exendin-4 in Npas4 transduced beta cells.

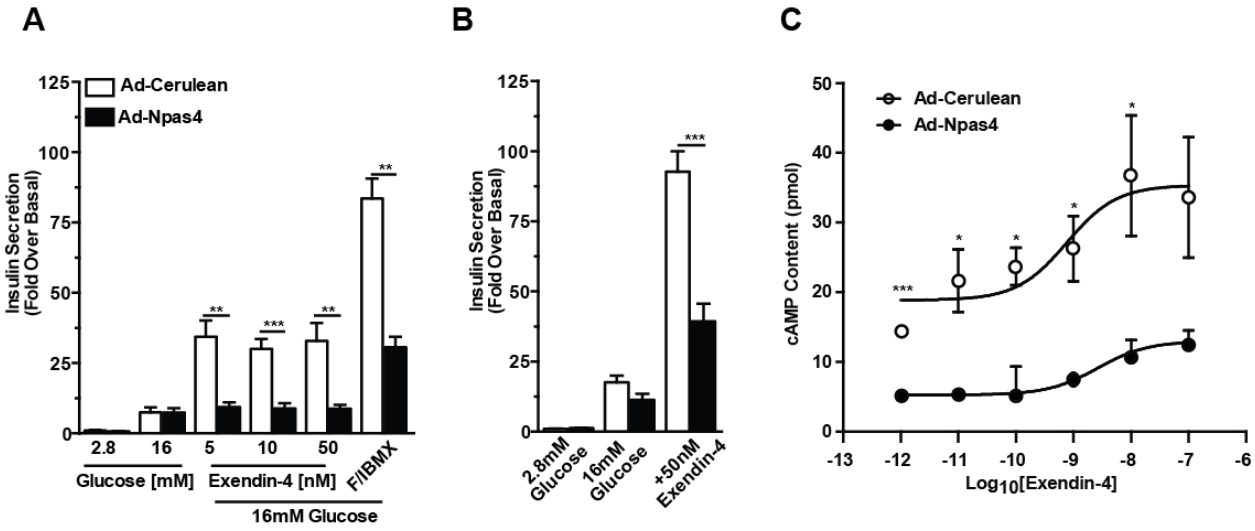

Figure 4.6: NPAS4 overexpression inhibits beta cell responsiveness to the GLP-1 receptor agonist, exendin-4.
MIN6 cells transduced with Ad-Cerulean (white bars) or Ad-Npas4 (black bars) displayed no significant difference in glucose-stimulated insulin secretion (n=3-5) (A). Similarly, insulin secretion from Ad-Cerulean or Ad-Npas4 transduced whole mouse islets displayed a similar insulin secretory response to elevated glucose (n=5-6) (B). However, in both MIN6 cells (A) and mouse pancreatic islets (B), exendin-4 was unable to potentiate glucose-induced secretion following Ad-Npas4 transduction, which could be partially rescued through stimulation with 10 μM forskolin and 100 μM IBMX. NPAS4 overexpression also decreases exendin-4-stimulated cAMP production in MIN6 cells (n=3) (C). * $p \leq 0.05$; ** $p \leq 0.01$; *** $p \leq 0.001$. Significance was established using a two-tailed Student's t-test.

4.2.3 NPAS4 increases expression of regulator of G-protein signaling 2 (Rgs2).

The observed impairment in exendin-4 stimulated cAMP production in Npas4 transduced beta cells raised the possibility that a target of NPAS4 may impair G-protein signalling. Ligand binding to the GLP-1 receptor results in the activation of the G protein subunit, GαS, by the exchange of GDP with GTP. This GTP-bound $G\alpha_S$ activates adenylate cyclase to stimulate cAMP generation. The inherent GTPase activity of $G\alpha_S$,

results in its return to an inactive, GDP-bound form. G-protein inactivation can be accelerated by the regulatory of G-protein signaling (RGS) proteins. As increased RGS2 expression in βTC3 cells has previously been shown to blunt GIP potentiated cAMP production and insulin secretion (236); it was hypothesized that NPAS4 may positively regulate Rgs2 expression.

To first determine whether depolarizing conditions that induce *Npas4* would lead to induction of *Rgs2*, MIN6 cells were depolarized with KCl. Under these conditions, *Rgs2* was significantly induced (Figure 4.7A) with delayed kinetics compared with *Npas4* (Figure 3.3B). Similar to *Npas4*, *Rgs2* was increased following two-hour exposure to elevated glucose concentrations in mouse islets (Figure 4.7B). RGS2 protein levels were also induced in response to membrane depolarization (Figure 4.7C). In agreement with other reports, forskolin also increased beta cell RGS2 expression (134,237,238).

As a positive correlation between *Npas4* and *Rgs2* was noted during beta cell depolarization, the effect of overexpressing NPAS4 on Rgs2 expression was subsequently assessed. In Npas4 transduced MIN6 cells, *Rgs2* expression levels were elevated 16-fold (Figure 4.8A). Similarly, Ad-Npas4 transduced whole mouse islets resulted in an 11-fold increase in *Rgs2*, compared to control infected islets (Figure 4.8B). Just as NPAS4 increased *Rgs2* message levels, a comparable increase in RGS2 protein was also appreciated (Figure 4.8C).

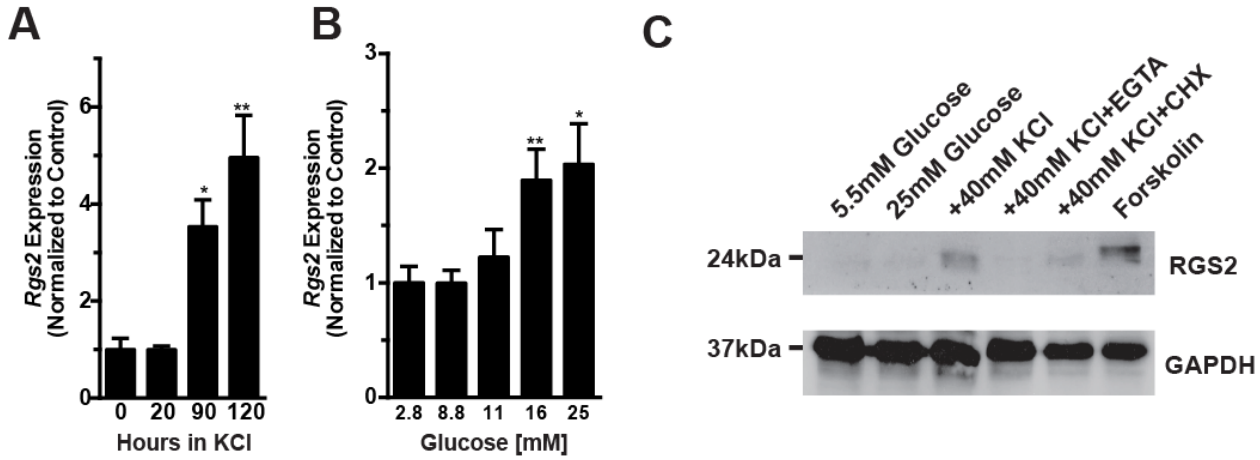

Figure 4.7: RGS2 is induced by membrane depolarization in beta cells. *Rgs2* expression was increased in a time-dependent manner in response to 40mM KCl in MIN6 cells (n=3) (A) as well as a two-hour exposure to various glucose concentrations in islets (n=3-8) (B). In MIN6 cells, RGS2 protein levels were increased in a calcium dependent manner by KCl as well as forskolin (C). * $p \leq 0.05$; ** $p \leq 0.01$. Significance was established using a one-way ANOVA with Dunnett's post-hoc analysis.

To assess whether this was a direct effect of NPAS4 on the Rgs2 promoter, ChIP assays were performed (a diagram of ChIP primer binding sites within the Rgs2 gene is available in appendix A). Following a 2-hour depolarization with 40 mM KCl, NPAS4 protein was enriched by 3- and 22-fold within intron 1 and at putative enhancer of the Rgs2 gene (239), respectively (Figure 4.8D). Taken together, these data suggest that Rgs2 may a genetic target of NPAS4 which inhibits GLP-1 receptor signalling and exendin-4 potentiated insulin secretion.

4.3 Discussion

To begin to understand the functional significance of NPAS4 expression within the pancreatic beta cell, studies within chapter 4 examined how NPAS4 influenced the expression and secretion of insulin. Following Npas4 transduction of beta cells, both *Insulin 1* and *Insulin 2* expression levels were significantly reduced. This was likely due to a combination of direct inhibition by Npas4 on the insulin promoter as well as indirect

regulation through decreased expression of PDX1 and NEUROD1. Despite the dramatically decreased insulin content, glucose stimulated insulin secretion from Npas4 transduced beta cells was not significantly impaired.

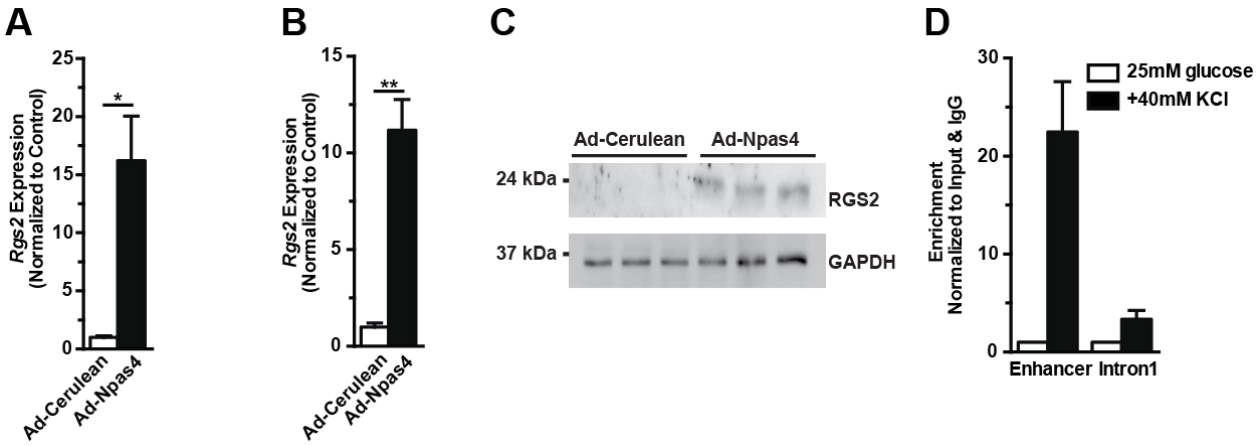

Figure 4.8: NPAS4 positively regulates RGS2 expression in beta cells. Overexpression of Npas4 in MIN6 cells (n=3) (A) and islets (n=3) (B) dramatically increased *Rgs2* mRNA expression as well as RGS2 protein levels in MIN6 cells (C). Performing ChIP on depolarized beta cells, NPAS4 was enriched at both a putative enhancer and a binding site within the first intron of Rgs2 in MIN6 cells (D). * $p \leq 0.05$; ** $p \leq 0.01$. Significance was established using a two-tailed Student's t-test.

However, the potentiating effects of the GLP-1 receptor agonist, exendin-4, were completely lost in MIN6 cells overexpressing NPAS4. At least part of this defect is believed to be due to the direct positive regulation of Rgs2, which acts as a negative regulator of G-protein signaling.

Prior to performing these studies, it was hypothesized that NPAS4 would act as a positive regulator of insulin expression. As data from chapter 3 demonstrated that NPAS4 is induced by beta cell activity and previous reports had observed elevated insulin expression in response to high glucose exposure (220,240). However, this was

not the case as experiments demonstrated an inhibitory effect of NPAS4 on the insulin promoter. At least part of this effect is mediated by direct inhibition. While the precise binding site within the insulin promoters was not determined; it seems likely that it is through E-box sites as these are present in both the Insulin 1 and Insulin 2 promoters and act as general binding sites for bHLH transcription factors such as NPAS4 and NEUROD1 (241). Although there have been reports of transcription factors that are positively regulated by beta cell activity and in turn, increase insulin expression (240) (200); this is one of the first reports of a glucose-induced transcription factor that acts to decrease insulin transcription. It is possible that beta cells express NPAS4 as a counter-regulatory mechanism during periods of extreme beta cell activity. NPAS4 may prevent the over-production of insulin mRNA which might overwhelm the ER; resulting in ER stress; although this remains to be experimentally determined.

While Npas4 transduced beta cells maintained a normal insulin secretory response to elevated glucose concentrations, there was a loss of responsiveness to exendin-4 potentiated insulin release. As bypassing the GLP-1 receptor through a combination of forskolin and IBMX could only partially rescue the defective insulin secretion, it is likely that NPAS4 overexpression inhibits signaling events up- and downstream of cAMP production. Further research suggested that NPAS4 reduced the exendin-4 mediated cAMP production and insulin secretion through the direct positive regulation of Rgs2. In other cell types RGS2 functions as a GTPase activating protein (GAP), which accelerates the hydrolysis of GTP to GDP by the Gα subunit (242). This function is conserved in beta cells as overexpression of RGS2 (and not RGS1,3 or 4) in βTC3 cells reduced GIP-1 stimulated cAMP production and insulin secretion (236). It is

therefore hypothesized that following beta cell depolarization, NPAS4 acts to increase RGS2 expression, which decreases GLP-1 receptor signaling by reducing activation of adenylate cyclases by $G\alpha_S$. Future studies should determine the actual contribution of RGS2 to the phenotype observed by NPAS4 overexpression. This could include a rescue experiment, wherein, RGS2 is knocked down to physiological levels in Npas4 transduced beta cells and incretin mediated cAMP production and insulin secretion assayed. It is hypothesized that knockdown of RGS2 would normalize the incretin effect in NPAS4 overexpressing beta cells.

In initial *in vitro* studies designed to determine how NPAS4 effects beta cell insulin expression and secretion demonstrate that, NPAS4 acts as a novel direct inhibitor of insulin promoter activity and while having minimal impact on glucose-stimulated insulin secretion, NPAS4 acts to blunt GLP1-mediated cAMP production and insulin secretion.

Chapter 5: Npas4 in beta cell dysfunction

5.1 Introduction

The beta cell dysfunction observed in T2D has been attributed to numerous stress pathways. As discussed in the introduction, chronic activation of the beta cell unfolded protein response (UPR) is considered one of the most relevant (69). While early UPR signaling is a homeostatic response, resulting in increased expression of ER protein chaperones and enzymes which degrade misfolded proteins (94); terminal UPR signaling results in programmed cell death (243). UPR driven apoptosis can occur through a number of pathways (243), however, the induction of the pro-apoptotic transcription factor, DDIT3 may be one of the most relevant in T2D. Islet expression of DDIT3 is significantly elevated in T2D (73,99) and deletion of Ddit3 is also sufficient to protect against the development of diabetes in *db/db*, Akita and HFD-fed mice (101,104).

Another pathway which may contribute to beta cell dysfunction in humans with T2D is increased transcriptional activity of the bHLH-PAS domain protein, hypoxia inducible factor 1α (HIF1α). Under normoxic conditions, HIF1α is degraded through hydroxylation by prolyl hydroxylase domain (PHD) containing enzymes while under conditions of reduced oxygen availability, HIF1α is stabilized (244). Short term activation of HIF1α under hypoxic conditions, such as those experienced during islet transplantation, is believed to be beneficial for graft survival and function (245). However, current research suggests that HIF1α may be chronically elevated within beta cells in T2D and contributing to the development of beta cell dysfunction and diabetes. For instance, increased beta cell HIF1α protein levels have been observed in the *db/db*

mouse model of T2D (144) and HIF1α is stabilized in beta cells following exposure to elevated glucose levels (143,144,237). Further in within islets from humans with T2D, at least two *bona fide* HIF1α targets, *LDHA and SOX9* are significantly elevated (246).

There are two pathways through which increased beta cell HIF1α activity in T2D negatively impacts cellular function and systemic glucose homeostasis through two pathways. The first is through a HIF1α mediated switch in glucose metabolism away from oxidative phosphorylation in favour of anaerobic glycolysis (247). As beta cells are heavily dependent on oxidative phosphorylation to generate ATP required to induce insulin secretion; this metabolic switch would impair glucose-stimulated insulin secretion. This HIF1α-mediated impairment in insulin secretion has been observed in multiple *in vivo* mouse studies in which HIF1α is rendered constitutively active within the beta cell (153-155). HIF1α stabilization can also disrupt beta cell function and insulin secretion through promoting beta cell dedifferentiation via one of its targets, Sox9. This transcription factor is normally expressed within pancreatic progenitors (248) and if its expression is elevated in mature beta cells, SOX9 is sufficient to drive dedifferentiation *in vivo* (127).

Studies within the CNS have implicated the loss of NPAS4 expression in dysregulated UPR signaling (163) and suggested that NPAS4 can inhibit the transcriptional activity of other bHLH-PAS domain proteins through competition with the common heterodimerization partner, ARNT (156). Therefore, it was hypothesized that within the beta cell, NPAS4 acts to maintain ER homeostasis in the face of increased stress and dampen HIF1α transcriptional activity. In order to test this hypothesis a series of *in vitro* experiments were performed.

5.2 Results

5.2.1 NPAS4 protects against ER stress in beta cells

To determine whether elevated NPAS4 expression was sufficient to alleviate ER stress, MIN6 cells were transduced with Ad-Npas4 or Ad-Cerulean for 48 hours before treatment with two separate ER stressors; thapsigargin or a combination of elevated glucose and palmitate.

In agreement with previous studies, both thapsigargin (249) or palmitate (250,251) treatment led to a concentration-dependent increase in *Ddit3* expression, which was significantly reduced in Npas4 transduced MIN6 cells (Figures 5.1A&B). Ad-Npas4 transduced cells had a 53% reduction in DDIT3 protein in when treated with 0.1 μM thapsigargin compared with Ad-Cerulean control virus (Figures 5.1C&D). Similarly, overexpression of NPAS4 in mouse islets reduced *Ddit3* mRNA levels following 24 hour thapsigargin exposure or 48-hour high glucose/palmitate treatment (Figures 5.1E&F). Conversely, the knockdown of NPAS4 with siRNAs led to a significant increase in *Ddit3* following 24-hour high glucose/palmitate exposure (Figure 5.1E). Finally, Npas4 transduction in MIN6 cells significantly reduced the number of apoptotic cells to 68.4% of control levels at 1 μM and 55% of control values following 10 μM thapsigargin treatment (Figure 5.1H).

To determine how NPAS4 overexpression protects against ER stress and the induction of DDIT3, the expression of two ER protective proteins, BiP (103) and Wfs-1 (252) was measured. Npas4 transduced MIN6 cells had significantly elevated expression of both *Wfs-1* and *BiP*, compared to Ad-Cerulean transduced beta cells

(Figures 5.2A&B); suggesting this may be one mechanism through which Npas4 transduced beta cells are protected from ER stress.

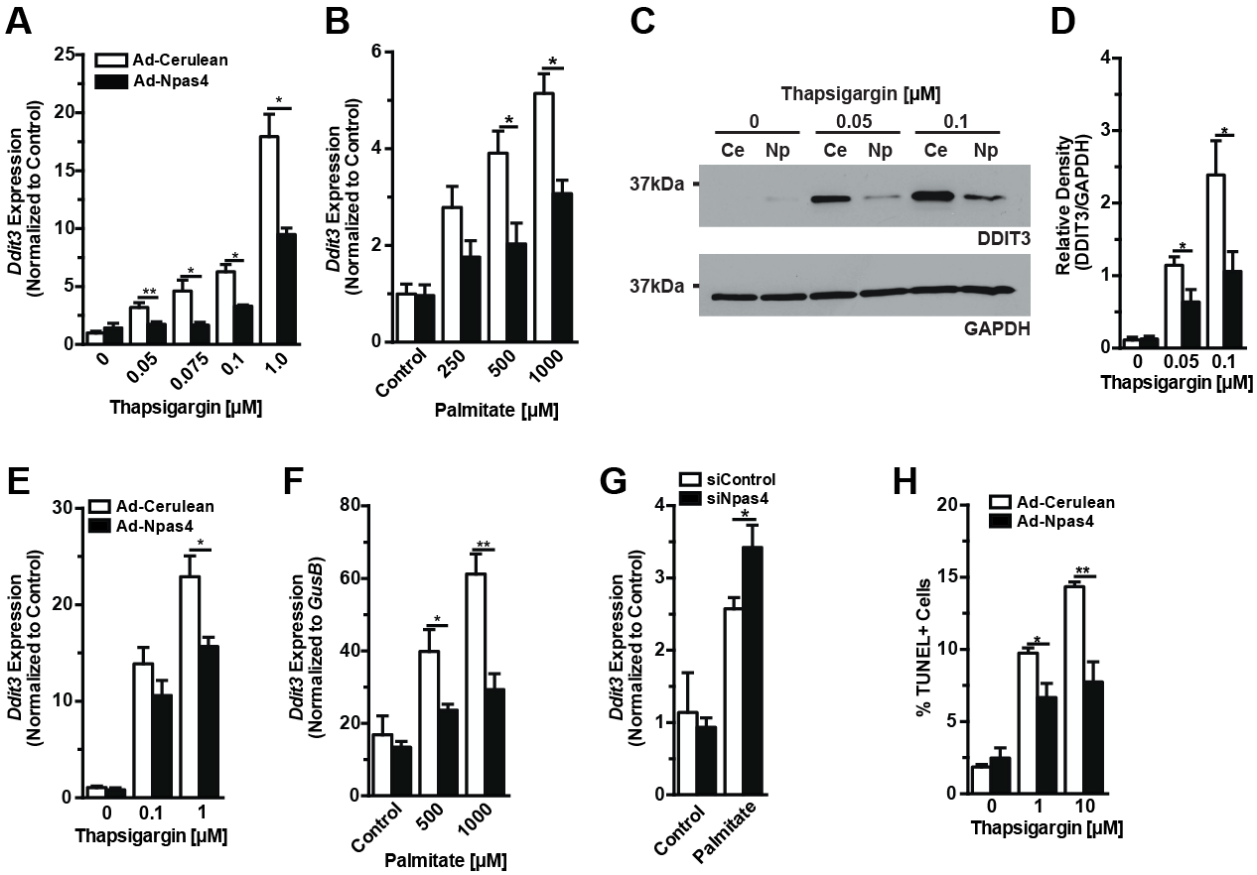

Figure 5.1: NPAS4 is protects against ER stress in pancreatic beta cells. NPAS4 overexpression (black bars) in MIN6 cells significantly reduced *Ddit3* induction following both thapsigargin (n=3-10) (A) and palmitate (n=3-5) (B) exposure compared with control virus (white bars). The reductions observed in *Ddit3* message level were also present at the protein level in thapsigargin treated Npas4 (Np) transduced MIN6 cells compared to cerulean (Ce) controls (n=3-4) (C&D). Ad-Npas4 transduced whole mouse islets similarly had reduced thapsigargin (n=3-6) (E) and palmitate (n=3) (F) mediated *Ddit3* induction. *Ddit3* mRNA levels were significantly elevated in MIN6 cells transfected with SiNpas4 and treated with palmitate (1000 μM) for 24 hours (n=6) (G). Ad-Npas4 infected cells had significantly reduced numbers of TUNEL+ MIN6 cells following exposure to 1 μM or 10 μM thapsigargin for 24 hours (n=3) (J). Significance was established using a two-tailed Student's t-test. * $p \leq 0.05$; ** $p \leq 0.01$.

Taken together these *in vitro* studies suggest that once induced, NPAS4 acts to protect beta cells against ER stress and subsequent apoptosis.

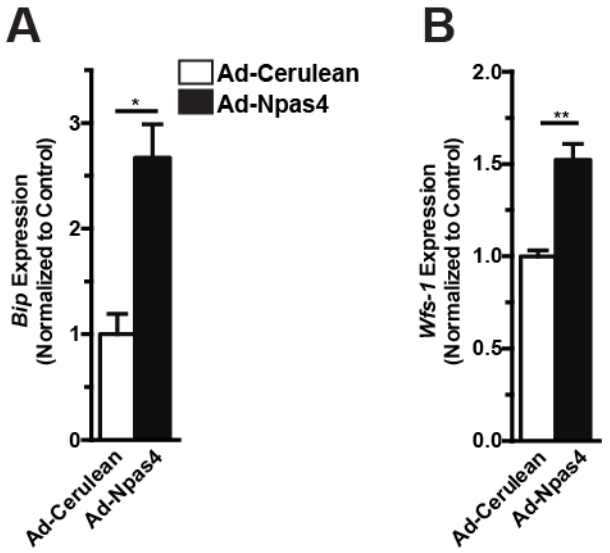

Figure 5.2: NPAS4 overexpression increases levels of protective factors, *Bip* & *Wfs-1*.
MIN6 cells transduced with Npas4 adenovirus had significantly elevated expression of the ER chaperone Bip (A) and Wfs-1 (B). (n=3). Significance was established using a two-tailed Student's t-test. * $p \leq 0.05$; ** $p \leq 0.01$.

5.2.2 Modulation of the beta cell hypoxic response by NPAS4

Based on data from chapter three and previously published reports (144,237), it is believed that following exposure to hyperglycemia, both NPAS4 and HIF1α are induced within the beta cell and compete for a common heterodimerization partner, ARNT. To determine whether elevated NPAS4 levels can dampen the hypoxic response, MIN6 cells were transfected with Ad-Npas4, exposed to low oxygen levels to induce HIF1α and the induction of validated HIF1α target genes measured with qPCR. Compared to Ad-GFP transduced beta cells cultured in control oxygen levels, there was robust induction of HIF1α target genes *Ldha*, *Mct4*, *Pdk1* and *Vegfa* following six hours of 1% O_2 exposure (Figures 5.3A-D). However, in Npas4 transduced beta cells, the induction of each HIF1α target was significantly reduced (Figures 5.3A-D).

As an immortalized cell line, MIN6 cells likely have alterations in glucose metabolism, characteristic of cancer cells (253); indeed compared to primary mouse islets, MIN6 cells express 5x as much *Ldha* and 20x as much *Mct4* (data not shown). Therefore, to validate the MIN6 data in primary tissues, similar experiments were performed in dispersed mouse islets. Following 24 hours of hypoxia (1% O_2) the induction of *Ldha* and *Mct4* was dramatically reduced in Npas4 transduced islet cells (Figures 5.3E&F). The induction of the HIF1α target (254) and pancreatic progenitor marker (248), *Sox9*, was similarly dampened by Npas4 transduction. Finally, dispersed islets from human cadaveric donors transduced with Ad-Npas4 also had a significantly reduced expression of *LDHA* and *SOX9* following 24 hours of hypoxia (1% O_2; Figure 5.3H&I). Demonstrating that NPAS4 overexpression in MIN6 cells, mouse and human islets is sufficient to dampen the cellular hypoxic response.

Just as elevated NPAS4 levels decreased the induction of HIF1α target genes, it was hypothesized that reduced NPAS4 expression would lead to an exaggerated hypoxic response. To test this, isolated islets from the Npas4 knockout mouse (termed the Npas4 PKO line and validated in chapter 6) were used. As NPAS4 expression levels are low under basal conditions, islets from control and Npas4 PKO mice were stimulated with 25 mM glucose, which only induces NPAS4 in control islets. Additionally, the PHD enzyme inhibitor JNJ-42041935 (195) was used to stabilize HIF1α by inhibiting HIF1α hydroxylation and subsequent degradation.

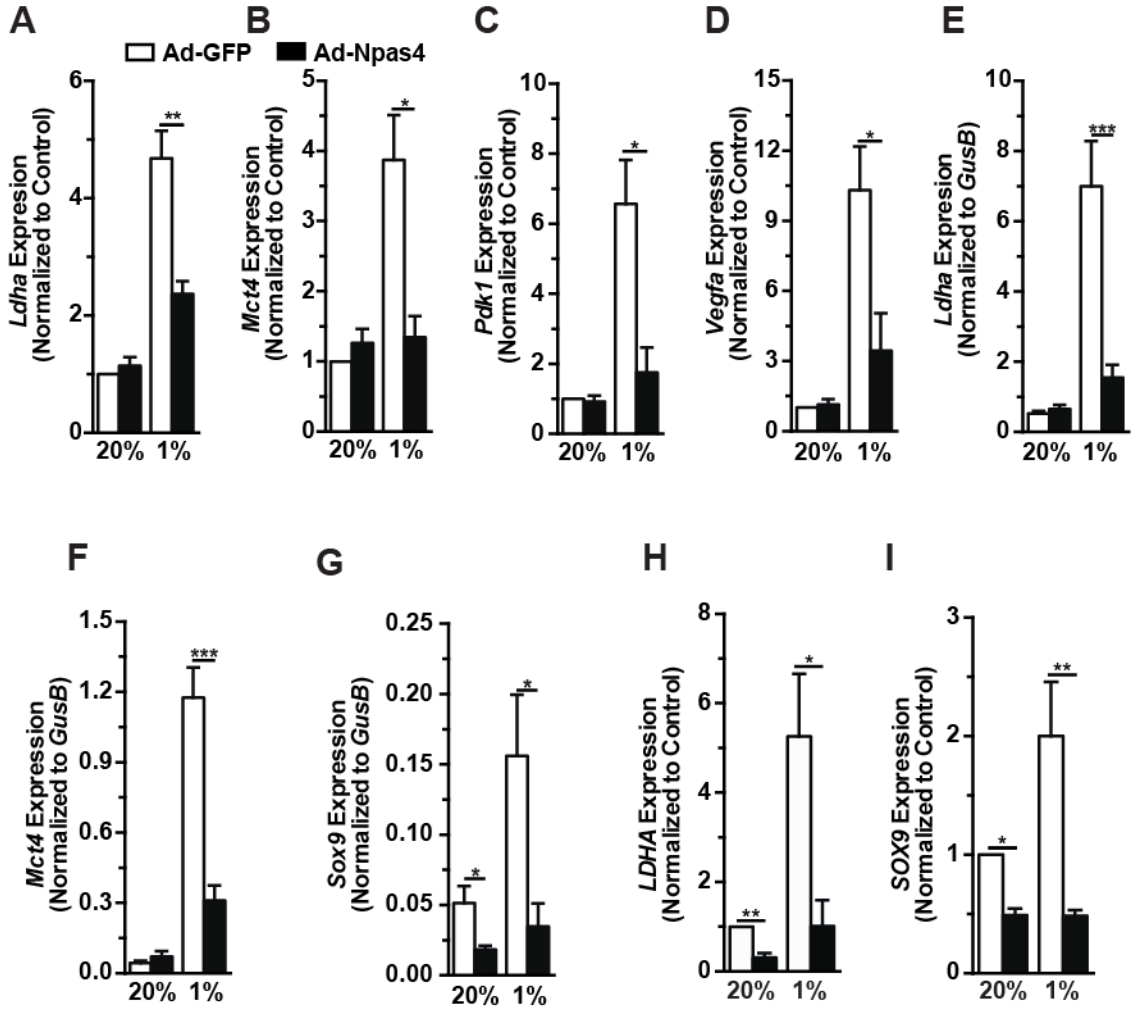

Figure 5.3: NPAS4 overexpression dampens the induction of HIF1α target genes in beta cells.
NPAS4 overexpression in MIN6 cells decreased the expression of the HIF1α target genes *Ldha*, *Mct4*, *Pdk1* & *Vegfa* following 6 hours of 1% or 20% O_2 exposure (n=4-5) (A-D). Npas4 transduced dispersed mouse islet cells had significantly impaired induction of *Mct4* (E), *Ldha* (F) and *Sox9* (G) following 24 hours of hypoxic exposure (n=5-12). Similarly, Npas4 transduction of dispersed human islets reduced the induction of *LDHA* (H) and *SOX9* (I) by 24-hour hypoxic exposure (n=4-5). * p≤ 0.05; ** p≤ 0.01; *** p≤ 0.001. Significance was established using a two-tailed Student's t-test.

JNJ-42041935 chosen to stabilize HIF1α in these experiments over hypoxic exposure as hypoxia inhibited Npas4 induction which would render it difficult to appreciate differences in control and Npas4 KO islets. Treating MIN6 cells with 100 μM JNJ-42041935 at 20% O_2 levels resulted in HIF1α stabilization (Figure 5.4A) and

induced the expression of HIF1α target genes *Ldha* and *Mct4* in wildtype islets (Figures 5.4B&C). Stimulating islets from control mice with 25 mM glucose for 2.5 hours in the presence of JNJ-42041935 at 20% O_2 levels led to a 2- and 3.5-fold increase in *Ldha* and *Mct4* levels, respectively (Figures 5.4D&E). Comparatively, islets from Npas4 PKO mice had significantly greater induction of these HIF1α targets (Figures 5.4D&E), suggesting reduced NPAS4 expression within beta cells, enhances HIF1α activity.

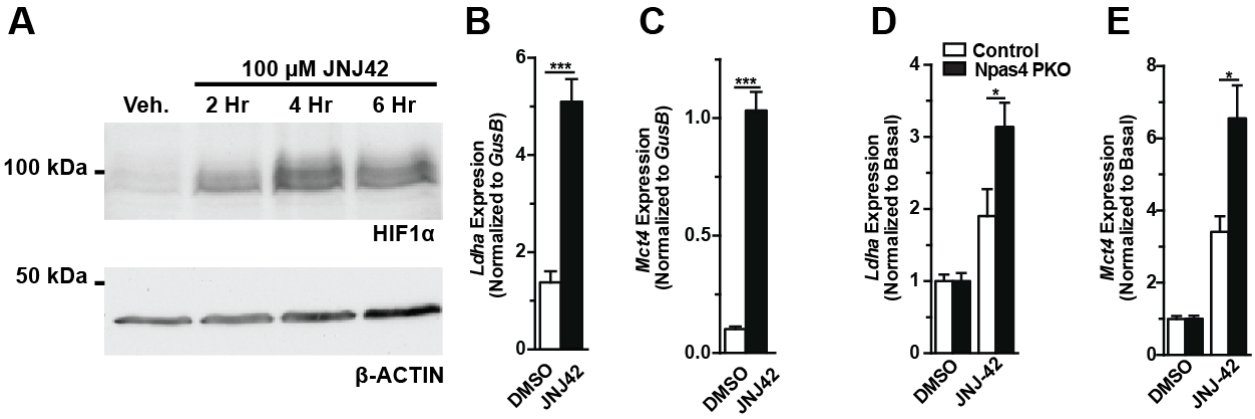

Figure 5.4: The PHD enzyme inhibitor JNJ-42041935 stabilizes HIF1α, and increases induction of HIF1α target genes in Npas4 KO islets.
MIN6 cells exposed to 100 μM JNJ-42041935 (JNJ42) had elevated levels of HIF1α protein after as little as 2 hours and persisted for up to six hours of treatment (A). Treating whole mouse islets with 100 μM JNJ-42041935 led to significant increases in *Ldha* (n=5) (B) and *Mct4* (n=5) (C). Treating isolated islets from control or Npas4 PKO mice to high glucose (25 mM) in the presence of 100 μM JNJ-42041935 for 2.5 hours significantly increased the induction of the HIF1α target genes *Ldha* and *Mct4* (n=4-9). Significance was established using two-tailed Student's t-tests. *p≤ 0.05, *** p≤ 0.001.

5.3 Discussion

The experiments presented within this chapter suggest that NPAS4 acts as a protective factor against two stresses relevant to the beta cell during the development of T2D; ER stress and inappropriate HIF1α activation. While no difference in the expression of the pro apoptotic transcription factor DDIT3, was observed under non stressed conditions, NPAS4 overexpression reduced *Ddit3* induction in the presence of

classical ER stressors: thapsigargin and palmitate. This protection against ER-stress-mediated *Ddit3* induction in Npas4 transduced beta cells was associated with decreased rates of apoptosis in response to thapsigargin treatment.

It is hypothesized that the reduced ER stress levels mediated by NPAS4 overexpression may be partially due to reduced insulin production. The most direct support for this hypothesis is that genetic deletion of all four insulin alleles from beta cells resulted in decreased expression certain ER stress markers, including *Ddit3* (129); demonstrating reduced insulin expression is sufficient to alleviate beta cell ER stress. NPAS4 also increased expression of *BiP* and *Wfs-1*, both of which have been shown to have protective roles within the beta cell (103,252,255).

The second T2D stress pathway that NPAS4 antagonized was the activation of HIF1α. Overexpression of NPAS4 in MIN6 cells, mouse and human islets reduced the induction of multiple HIF1α target genes. Conversely, reduced NPAS4 expression resulted in increased induction of the HIF1α targets; *Ldha* and *Mct4*. As all bHLH-PAS domain proteins must heterodimerize with ARNT, ARNT2 or BMAL1; it is expected that NPAS4 acts to dampen HIF1α activity through competitive binding with ARNT. The concept of competition between bHLH-PAS transcription factors has been proposed between other family members, including HIF1α and AHR. The hypoxia-mediated induction of HIF1α target genes could be dampened by activating AHR with dioxin (256,257). Conversely, stabilization of HIF1α with hypoxia, blocked AHR transcriptional activity and induction of AHR target genes (257,258). Furthermore, this competitive dynamic for ARNT heterodimerization has been noted to exist between NPAS4 and the bHLH-PAS domain protein, SIM2, for binding sites within the CNS midline element

(156). Based on the detrimental effects resulting from chronic HIF1α activation; it is hypothesized that one key function of NPAS4 within the beta cell, may be to titrate ARNT away from HIF1α in the postprandial period. Future experiments could perform co-immunopreciptiations to determine the degree of interaction between HIF1α, NPAS4 and ARNT in beta cells under varying glucose concentrations.

One final intriguing finding was that NPAS4 overexpression reduced Sox9 expression in mouse and human islets independent of oxygen availability. SOX9 is normally expressed at very low levels in mature beta cells (248) and its overexpression in mature beta cells leads to dedifferentiation (127). One interpretation of the data presented within chapters 3 and chapter 5 is that that in the postprandial state, beta cell membrane depolarization and stimulation of NPAS4 expression may suppress SOX9 expression and the dedifferentiation program it regulates. This pathway may be impaired in T2D as *NPAS4* expression is reduced under high glucose conditions (Figure 3.2.13) and *SOX9* was significantly elevated in laser micro-dissected beta cells of individuals with T2D (246).

In summary, the data presented within chapter 5 suggest that NPAS4 acts as a protective factor *in vitro* and reduces the beta cell ER stress and HIFα activity (Summary in Figure 5.5). These two pathways have been implicated in development of beta cell dysfunction during T2D pathogenesis and their antagonism by NPAS4 should preserve beta cell function, viability and differentiation. While these *in vitro* studies shed light on the possible functions of NPAS4, whether NPAS4 impacts any of these pathways *in vivo* was undetermined.

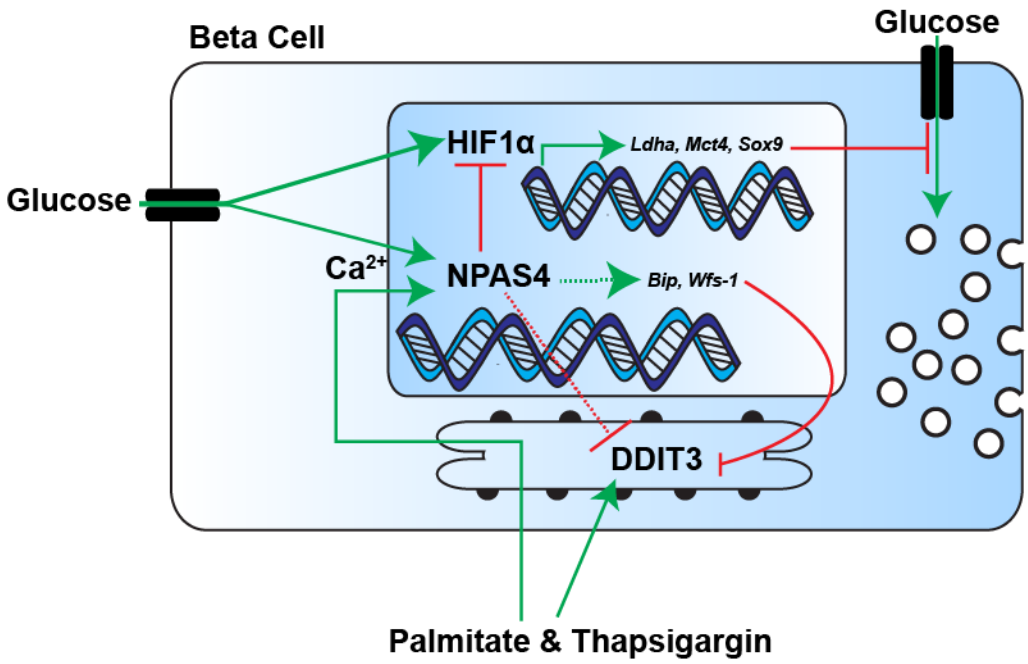

Figure 5.5: Model of NPAS4 regulated stress pathways in beta cells.
Npas4 expression is induced by glucose as well as thapsigargin and palmitate. Activation of NPAS4 inhibits HIF1α transcriptional activity and reduces ER stress driven *Ddit3* induction.

Chapter 6: Characterization of the Pdx1CreER Npas4 knockout mouse

6.1 Introduction

Previous *in vivo* studies that examined NPAS4 function have not detailed any perturbations in glucose homeostasis (163). However, as these characterizations focused on the role of NPAS4 within neurons, it is possible that subtle metabolic phenotypes were not detected. Following the *in vitro* characterization of the impact of NPAS4 on beta cell function presented within Chapter 5, experiments were undertaken to understand whether NPAS4 was important for the maintenance of glucose homeostasis *in vivo*.

As data from chapter 3 illustrated, NPAS4 is expressed at very low levels under basal conditions, which may render it difficult to detect differences between wild type and Npas4 knockout mice. Therefore, two approaches were taken in order to increase the likelihood of uncovering a metabolic phenotype in the Npas4 knockout mice. First was to age experimental cohorts for up to 44 weeks of age. As increased age is associated with glucose intolerance (259,260), this may unmask a subtle phenotype present within Npas4 knockout beta cells. Secondly, experimental cohorts were separated into two groups and fed either a standard rodent chow diet or a high fat/ high sucrose diet (HFD). Prolonged HFD-feeding results in increased insulin demands and results in increased insulin synthesis and secretion as well as elevated beta cell proliferation rates (261). Further, the combination of high fat and high sucrose was chosen as it has been shown to induce a greater degree of beta cell stress than either a high sucrose or high fat diet alone (262). These increased demands on beta cells was hypothesized to exacerbate any dysfunction caused by loss of NPAS4 expression.

Finally, the data from chapter 3 would suggest that HFD will increase NPAS4 expression levels by stimulating the beta cell free fatty acid receptor and subsequent release of intracellular calcium. This was expected to render any differences between control and knockouts more apparent.

6.1.1 Cre mediated recombination: promise and pitfalls

Biological research over the past 15 years has been greatly aided by the development of conditional alleles which allow for the study of a widely expressed gene within one cell type or tissue (263). The use of Cre/lox technology has been the most prevalent system of conditional recombination. Isolated from bacteriophage P1, Cre recombinase recognizes LoxP sites which consist of a 34bp sequence containing two 13bp inverted repeats flanking an 8bp nonpalindromic core (264). Cre will excise the intervening sequence between two LoxP sites and depending on the orientation of the 8p nonpalindromic sequence will lead to either excision or inversion.

Cre expression can be targeted to a specific cell type by placing the Cre recombinase sequence downstream of cell specific promoter (264). Additionally, the use of ligand activated Cre fusion proteins allows for the temporal control of gene deletion (264). The most common Cre fusion protein is a combination of Cre recombinase with a mutated estrogen receptor (ER) which is specifically induced by the synthetic ER ligand, tamoxifen (265).

There has been long-standing use of Cre-mediated recombination to study beta cell biology, with the majority of studies using either the rat insulin 2 or the Pdx1 promoter to drive Cre recombinase (266). However, one major caveat of these promoters is that both lack true beta cell specificity, as they are active in other sites;

including the hypothalamus (267-270). Within the hypothalamus, RIP2- and Pdx1-Cre transgenes are present within the arcuate nucleus (268), which is of particular importance for glucose homeostasis.

6.1.2 Neurons with the arcuate nucleus

The arcuate nucleus mediates its effects on glucose homeostasis and energy balance mainly through the actions of two neural cell types; Neuropeptide Y (NPY)/ Agouti-related peptide (AGRP) neurons and the proopiomelanocortin (POMC)/cocaine and amphetamine related transcript (CART) neurons (271). Functionally, the NPY/AGRP and POMC/CART neurons have opposing roles. The POMC/CART neurons decrease food intake mainly through processing POMC to generate melanocyte-stimulating hormones (MSH). When released by POMC/CART neurons, MSH then acts through its receptor, expressed on numerous secondary neurons in the paraventricular nucleus, ventromedial hypothalamus and lateral hypothalamus (271). Conversely, NPY/AGRP neurons stimulate food intake by acting as an antagonist to the MSH receptor and inhibiting POMC neuron function through the expression of the inhibitory neurotransmitter, GABA (271). Genetic studies targeting neurons of the arcuate have demonstrated that impaired function leads to disrupted glucose homeostasis, obesity and altered locomotor activity (272). Furthermore, the CNS activity of RIP2- and Pdx1-Cre transgenic mice is an important consideration for the investigation of glucose homeostasis phenotypes (266), as the CNS activity of both lines is sufficient to elicit metabolic phenotypes in mice (273-275) .

While recombination within the arcuate has been detected in both the Pdx1 and RIP2-Cre transgenic lines, there have been fewer reports of centrally driven phenotypes

within tamoxifen inducible Pdx1-CreER mouse lines. For this reason, the Pdx1-CreER line was used to delete Npas4 from Pdx1 expressing cells in male mice and the resultant phenotype characterized.

6.2 Results

6.2.1 Characterization of recombination within Pdx1CreER transgenic mice

To induce Cre activity, three doses of 8 mg tamoxifen (TMX) were administered to *Npas4*$^{flx/flx}$*Pdx1CreER*$^{-}$ (control) and *Npas4*$^{flx/flx}$ *Pdx1CreER*$^{+}$ (Npas4 PKO) mice at 6 weeks of age (An experimental timeline for the Pdx1CreER model is available in appendix B). This dosing scheme had previously been shown to induce high rates of beta cell recombination (276) and indeed, two weeks following TMX administration, islets from Npas4 PKO mice exhibited significantly reduced Npas4 mRNA and protein expression, compared to controls (Figures 6.1A-C).

To examine the proportion of recombined beta cells in islets from the Npas4 PKO mice, the Rosa26^{mTmG} Cre reporter allele (173) was crossed onto the Pdx1CreER background. Within Rosa26^{mTmG} mice, all cells express a membrane-bound red fluorescent dsTomato protein prior to Cre-mediated recombination. Following activation of Cre, the dsTomato cassette is excised, resulting in expression of a membrane-bound eGFP protein. In the absence of the PdxCreER transgene, no GFP immunofluorescence was detected in islets of Rosa26^{mTmG} mice transgene following tamoxifen administration (Figure 6.2A). In the absence of tamoxifen, islets from Rosa26^{mTmG} Pdx1CreER^{+} mice had a detectable population of recombined beta cells (Figure 6.2A); this tamoxifen-independent recombination has been observed previously in Pdx1CreER transgenics (277).

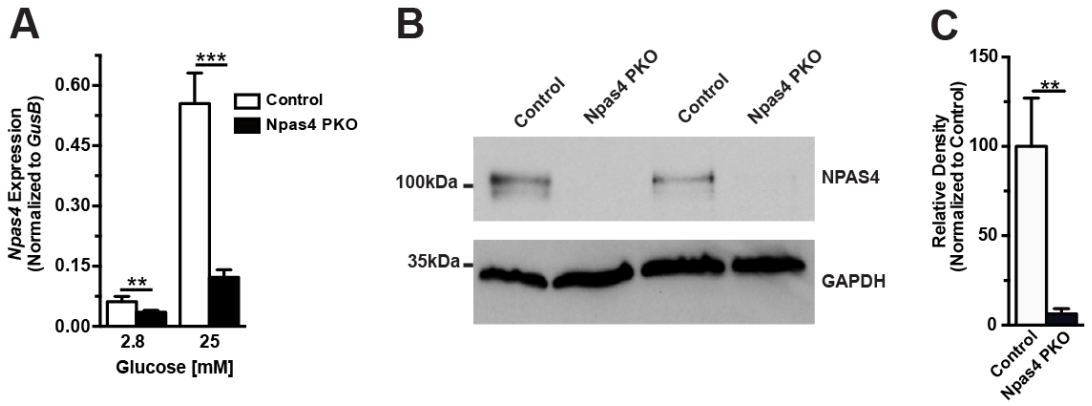

Figure 6.1: Npas4 expression is decreased in Npas4 PKO mice following tamoxifen administration.
Two weeks following tamoxifen administration, islets from Npas4 PKO mice had significantly reduced Npas4 expression following a two-hour stimulation at 2.8 mM or 25 mM glucose (n=6-11) (A). Following a two-hour stimulation in 25 mM glucose, whole islets from Npas4 PKO mice showed significantly reduced NPAS4 protein levels compared to controls (n=3-4) (B&C). Significance was established using a two-tailed Student's t-test. **=p≤ 0.01; ***=p≤ 0.001.

Two weeks following the administration of tamoxifen to Rosa26^{mTmG} Pdx1CreER^{+} mice, GFP immunofluorescence was detected in the vast majority of insulin expressing cells (Figure 6.2).

Besides recombination in beta cells of tamoxifen administered, Rosa26^{mTmG} Pdx1CreER^{+} mice, recombination was also detected in delta (Figures 6.3A&B) and alpha cells (Figures 6.4A&B)

A

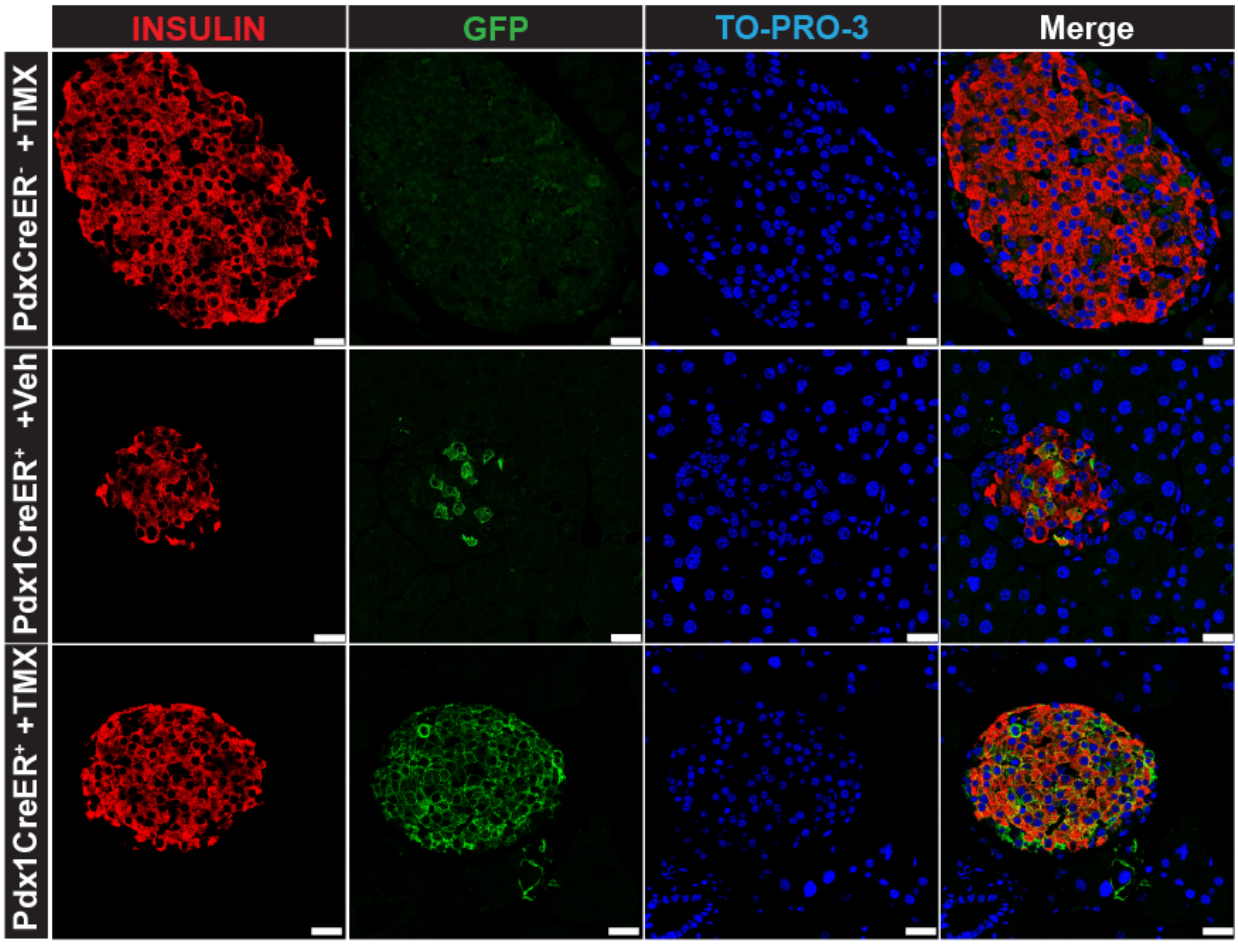

Figure 6.2: High beta cell recombination rates in Rosa26^{mTmG} Pdx1CreER mice. Two weeks following administration of either vehicle or tamoxifen to Rosa26^{mTmG} Pdx1CreER^{-} or Rosa26^{mTmG} Pdx1CreER^{+} mice, pancreas was harvested and paraffin sections stained for insulin and GFP. No Cre-mediated recombination was detected within beta cells of Pdx1CreER^{-} mice following tamoxifen administration (top three panels). A number of recombined beta cells were detected within islets from Pdx1CreER^{+} mice administered vehicle (middle three panels). Administration of tamoxifen to Pdx1CreER^{+} mice resulted in high rates of beta cell recombination (bottom three panels). Scale bars = 25µm.

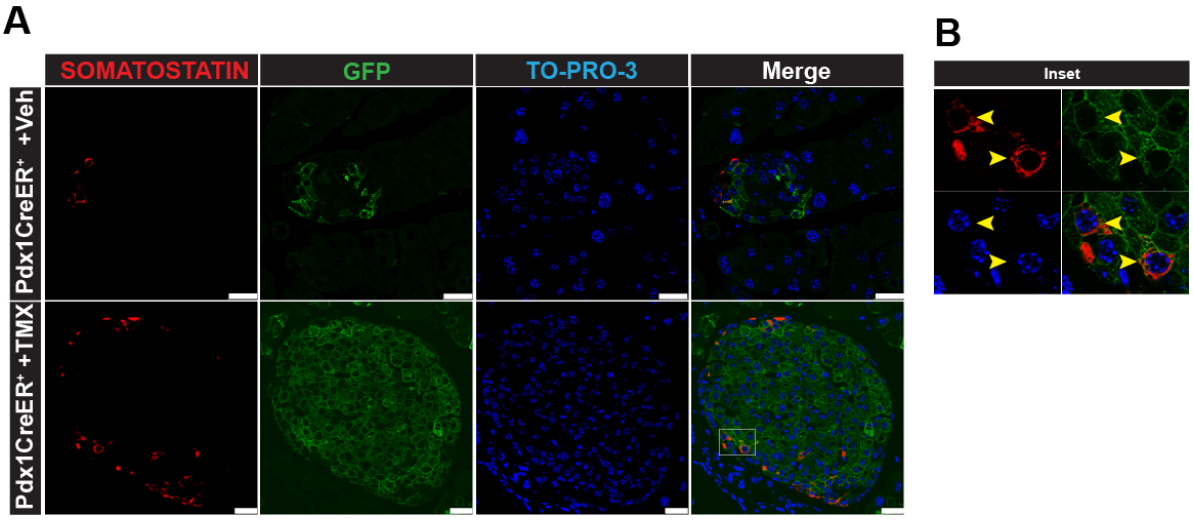

Figure 6.3: Tamoxifen induces recombination in somatostatin-expressing cells of Rosa26^{mTmG} Pdx1CreER mice.
Two weeks following administration of either vehicle or tamoxifen to Rosa26^{mTmG} Pdx1CreER^{+} mice, pancreas was harvested and paraffin sections stained for somatostatin and GFP. In the vehicle treated group, no GFP immunofluorescence was detected within somatostatin-positive delta cells (top three panels) (A). Following the administration of tamoxifen to Pdx1CreER^{+} mice, high rates of Cre-mediated recombination were detected within delta cells (bottom three panels) (A). Higher magnification of the inset box from (A) highlights GFP and somatostatin double-positive cells (yellow arrowheads) (B). Scale bars= 25 µm.

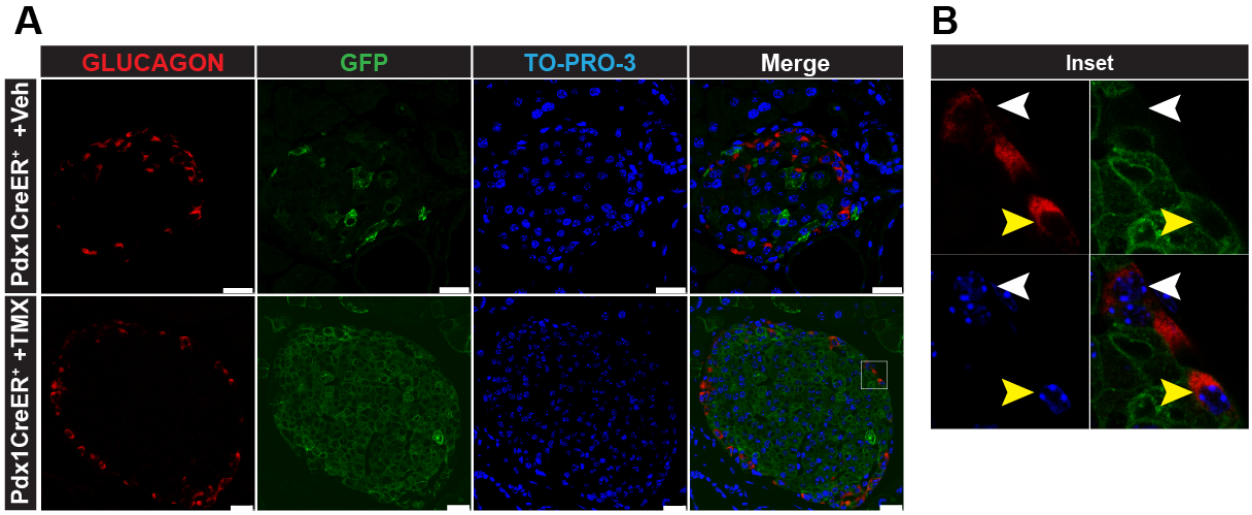

Figure 6.4: Low rates of recombination in alpha cells in Rosa26^{mTmG} Pdx1CreER mice.
Two weeks following administration of either vehicle or tamoxifen to Rosa26^{mTmG}Pdx1CreER^{+} mice, pancreas was harvested and paraffin sections stained for glucagon and GFP. Following vehicle administration to Rosa26^{mTmG} Pdx1CreER^{+} mice, no GFP expressing alpha cells were detected (top three panels) (A). Administration of tamoxifen to Rosa26^{mTmG} Pdx1CreER^{+} mice resulted in low but detectable numbers of recombined alpha cells (bottom three panels) (A). Higher magnification of the inset box from (A) highlights a single GFP^{+} (yellow arrowhead) and a GFP^{-} alpha cell (white arrowhead) (B). Scale bars = 25 µm.

Finally, as Cre activity within the arcuate nucleus has been detected within various Pdx1 transgenic mouse lines (267,268), coronal sections of the hypothalamus were assayed for GFP immunofluorescence. Two weeks following the administration of three doses of 8 mg tamoxifen, substantial recombination rates were detected in the arcuate nucleus of Rosa26^{mTmG} Pdx1CreER transgenic mice (Figures 6.5A&B). This immunofluorescence was not detected in the absence of primary GFP antibody (Figure 6.5B).

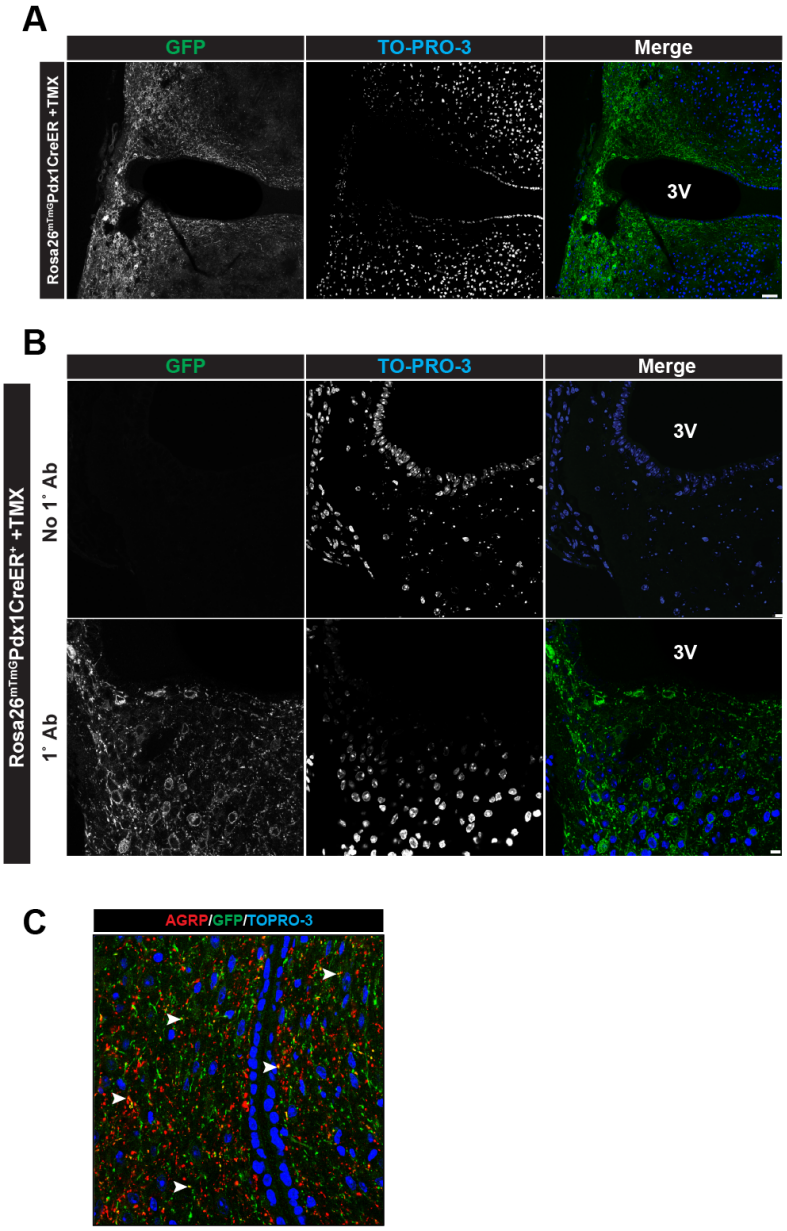

Figure 6.5: Recombination within the arcuate nucleus of the hypothalamus of Pdx1CreER transgenic mice.
Cre-mediated recombination was detected within the arcuate nucleus of Rosa26^{mTmG} Pdx1CreER mice two weeks following tamoxifen administration (A&B). No GFP immunofluorescence was detected in the absence of primary antibody (B). Co-staining of coronal brain cryosections for GFP and AGRP revealed some colocalization (white arrowheads); however, a high number of neural axons expressed either AGRP or GFP exclusively (C). Scale Bars = 25 µm.

Co-staining for the neuropeptide agouti-related peptide (AGRP) revealed colocalization within some, but not all, neural axons (Figure 6.5C). This is the first report of recombination of within the CNS of the Pdx1CreER line derived from the Melton laboratory (174).

Despite the recombination detected within the arcuate nucleus, *Npas4* expression levels were not significantly reduced in whole hypothalamic lysates (Figure 6.6A), although *Npas4* expression was substantially higher within the hypothalamus than some in other brain regions (Figure 6.6B). As the neurons within the arcuate nucleus constitute only a small proportion of the whole hypothalamus, it is possible that any reductions in *Npas4* within these cells were diluted by expression of *Npas4* in other hypothalamic neurons. Therefore, whether Npas4 is knocked out of neurons within the arcuate remains unknown but seems likely.

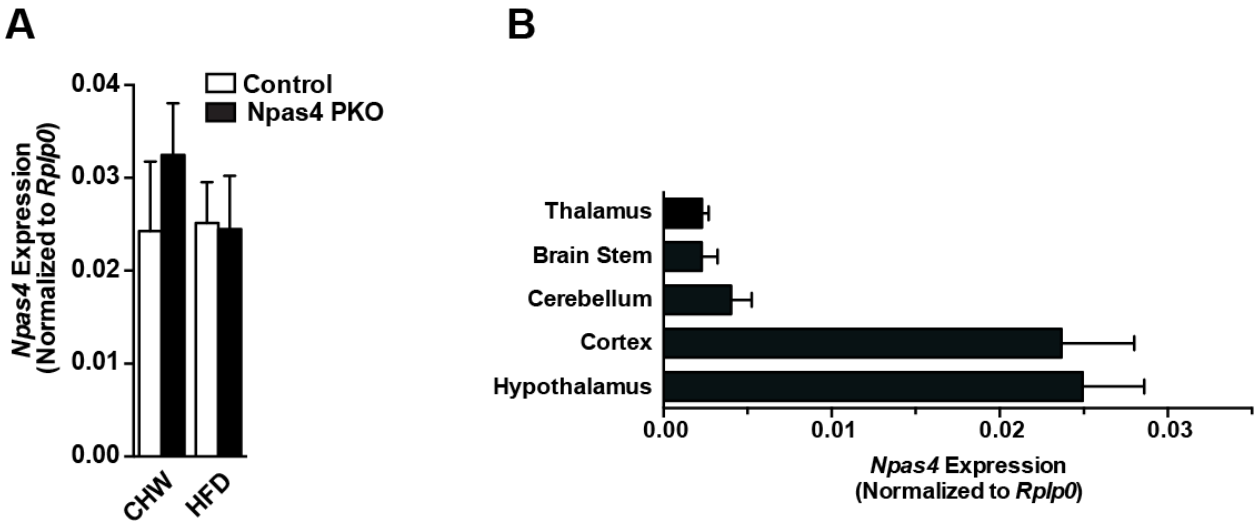

Figure 6.6: No decrease in whole hypothalamic *Npas4* expression in Npas4 PKO mice.
Npas4 expression was not significantly altered in whole hypothalamic extracts from control and Npas4 PKO mice (n=3-10) (A). Compared with the thalamus, brain stem and cerebellum, *Npas4* mRNA levels are substantially higher in whole hypothalamic extracts (n=7-13) (B).

Importantly, prior to characterization of the Npas4 PKO mice, HFD-fed Npas4$^{wt/wt}$ Pdx1CreER^{+} transgenic mice were characterized. However, no difference in weight gain, fasting or *ad libitum* glucose levels, glucose tolerance or glycerol tolerance was observed in Pdx1CreER^{+} transgenics compared to PdxCreER^{-} littermates (Figures 6.7A-G).

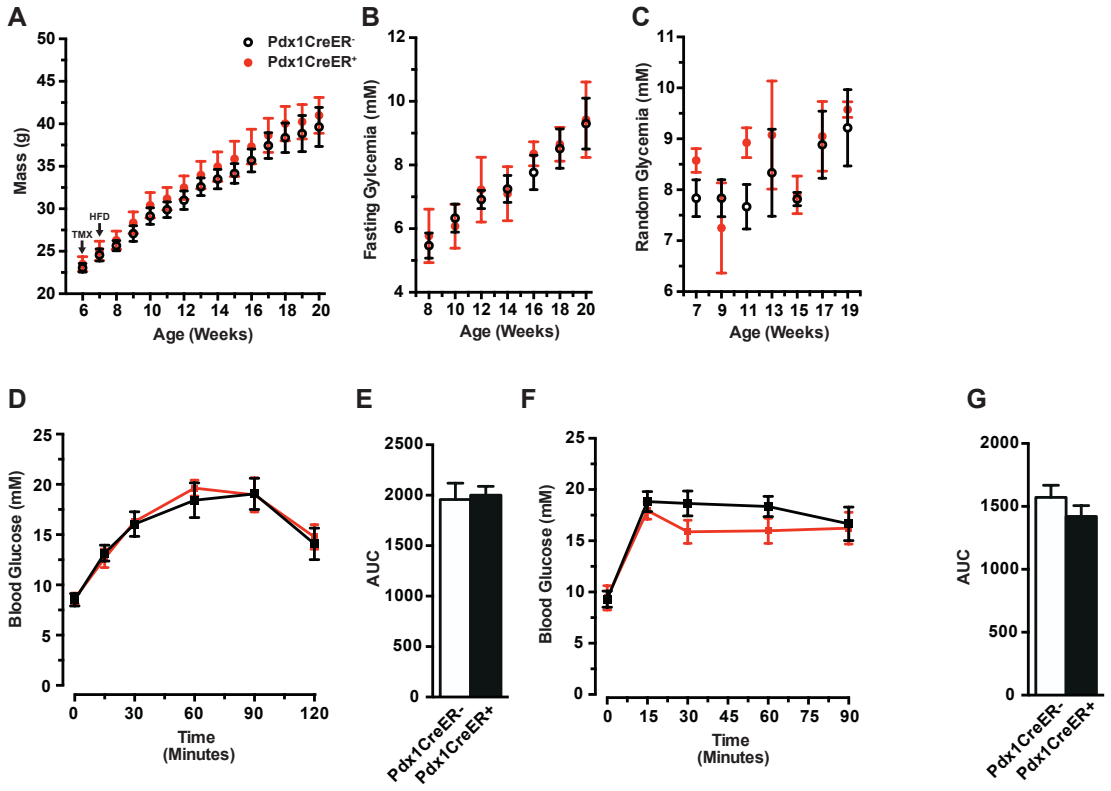

Figure 6.7: HFD-fed male transgenic Pdx1CreER^{+} mice demonstrate normal glucose phenotypes.
Male transgenic Pdx1CreER^{+} or littermate Pdx1CreER^{-} mice were administered three doses of 8 mg tamoxifen at 6 weeks of age and HFD was started one week following the last dose. Mass gain over 13 weeks of HFD-feeding was not different between transgenic and wildtype controls (A). Similarly, monitoring of blood glucose levels following an overnight fast (B) or random glycemia measured at 10AM (C) revealed no consistent differences between genotypes. Furthermore, changes in blood-glucose levels during a 2 g/kg glycerol tolerance test, performed at 11 weeks of HFD (D&E), or a 2 g/kg OGTT performed at 13 weeks of HFD (F&G), were also not statistically different between genotypes. (n=4-6).

6.2.2 Phenotype of the male Npas4 PKO mice

Over the course of the 25 weeks of HFD-feeding (timeline of experiments available in Appendix B), no major differences in mass were observed between control and Npas4 PKO mice (Figure 6.8A). However, there was a very modest but statistically significant increase in weight gain in both chow- (Figure 6.8B) and HFD-fed Npas4 PKO mice (Figure 6.8C) beginning at three weeks of HFD-feeding. While this persisted for several weeks, by nine weeks of HFD-feeding this difference was no longer significantly different.

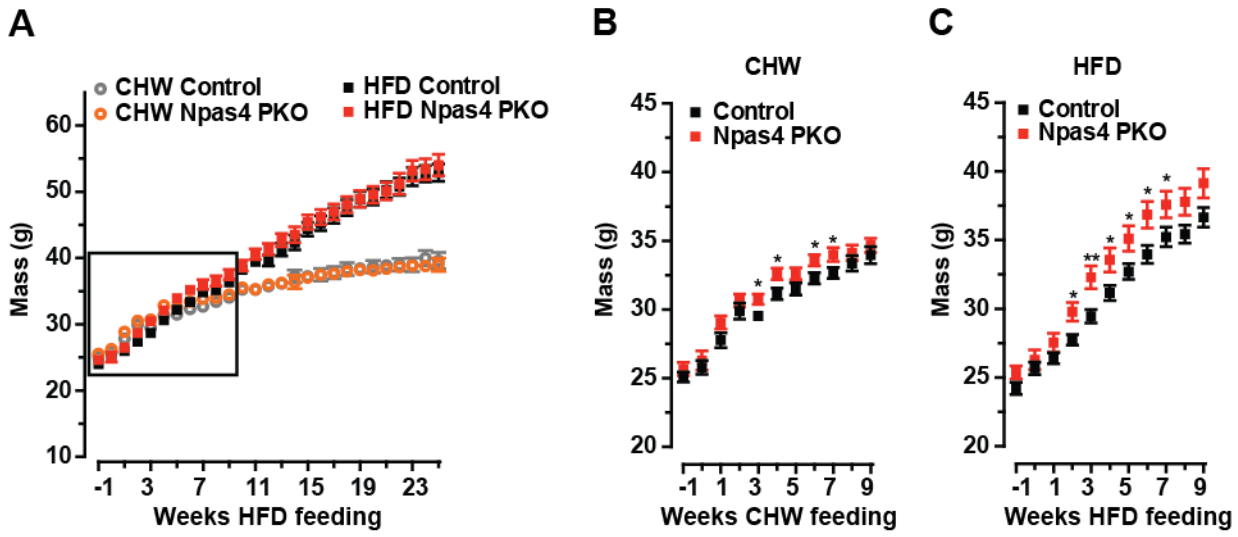

Figure 6.8: Npas4 PKO mice exhibit a slight increase in weight gain under both chow and high fat diet feeding.
Weekly body mass measurements of chow-fed Npas4 PKO mice (orange circles) and control mice (grey circles) and high fat diet fed Npas4 PKO mice (red squares) and control mice (black squares) from one week prior to HFD-feeding (start of tamoxifen administration) to 25 weeks of HFD-feeding (A). Mass gain in the nine weeks following tamoxifen administration (inset in A) was modestly elevated in both chow-fed (B) or high fat diet fed (C) control and Npas4 PKO mice (n=15-26). Significance was established using two-tailed Student's t-test. *=p ≤ 0.05; **=p ≤ 0.01.

As slight differences in mass were observed in the first weeks following tamoxifen administration, a more careful examination of body composition and behavior

was undertaken. The fat composition and total body weight of chow-fed Npas4 PKO mice not significantly different at seven weeks of diet feeding (Figure 6.9A). The behavior of chow-fed Npas4 PKO mice at the same time point revealed no significant differences in food or water consumption, locomotor activity patterns or respiratory exchange ratio (RER) (Figure 6.9 B-E).

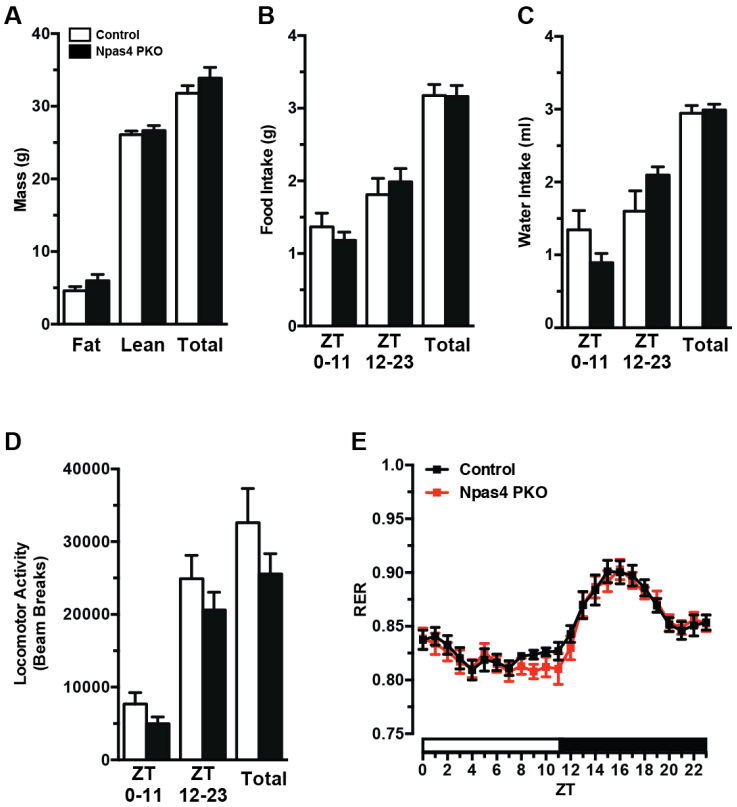

Figure 6.9: Normal body composition and metabolic cage behavior of chow-fed Npas4 PKO mice.
At 14 weeks of age the body composition and behavior of control and Npas4 PKO mice was analyzed. Npas4 PKO mice displayed a non-significant increase in fat and total body mass (A). No difference in food (B) or water (C) intake was observed. There was a trend towards decreased light (ZT0-11) and dark phase (ZT12-23) locomotor activity in Npas4 PKO mice (D), although this did not reach significance. No difference in respiratory exchange ratio (RER) was observed over a 24-hour period (E) (n=7-10).

A similar examination of the body composition and behavior of HFD-fed Npas4 PKO mice was undertaken at the same time point (7 weeks' diet). When compared to

HFD-fed controls, HFD-fed Npas4 PKO mice had higher total body mass due to significantly higher fat mass (Figure 6.10A). This may have been caused by a combination of increased light phase food intake, driven by increased meal size (Figures 6.10B-E) and reduced dark phase (ZT12-23) locomotor activity (Figures 6.10J&K). No significant differences in water intake (Figures 5.2.10F-I) or respiratory exchange ratio (Figure 6.10L) were noted. The altered feeding and locomotor behavior of HFD-fed Npas4 PKO mice raised the possibility that central recombination may contribute to the phenotype of these mice.

In parallel to weight measurements, glucose levels were monitored following an overnight fast and from *ad libitum* fed mice (referred to as 'random glycemia'). Three weeks following the onset of HFD-feeding, the fasting glycemia of Npas4 PKO mice was significantly elevated (Figure 6.11A). This fasting hyperglycemia persisted until the end of the experimental timeframe of 25 weeks of HFD-feeding and was not observed in chow-fed Npas4 PKO mice (Figure 6.11A). The cumulative hyperglycemic incidence, defined by two consecutive fasting glucose readings of 10 mM or higher, was approximately 25% in HFD-fed control mice, whereas 70% of HFD Npas4 PKO mice developed hyperglycemia (Figure 6.11B). Intriguingly, random glycemia in *ad libitum* fed mice did not reveal any significant differences between Npas4 PKO mice and controls on either diet (Figure 6.11C).

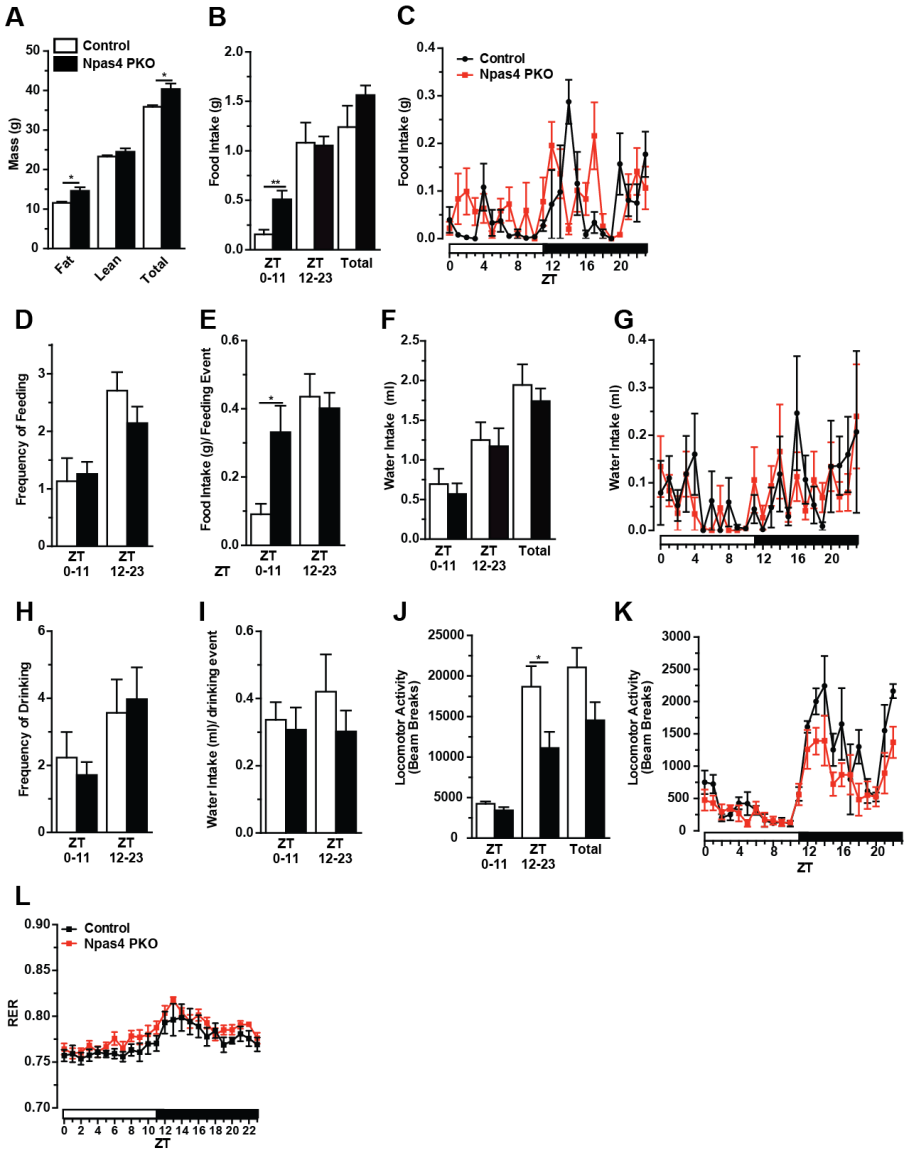

Figure 6.10: HFD-fed Npas4 PKO mice display increased fat mass and food intake with reduced locomotor activity.
8 weeks post tamoxifen administration (7 weeks HFD-feeding) Npas4 PKO mice were subjected to body mass composition and metabolic cage analysis. HFD-fed Npas4 PKO displayed significantly elevated fat and total body mass (A). HFD-fed Npas4 PKO mice also demonstrated a significant increase in light phase (ZT0-11) food intake which was not due to elevated feeding frequency (D) but food intake per feeding event (E). No alterations were observed in water intake (F-I). While daily locomotor activity was not different between controls and Npas4 PKO mice, dark phase (ZT12-23) activity was significantly reduced (J&K). The respiratory exchange ratio (RER) was not significantly elevated in HFD-fed Npas4 PKO mice (I) (n = 6-7). Significance was established using two-tailed Student's t-test * = $p \leq 0.05$; ** = $p \leq 0.01$.

Plotting the random and fasting glycemic values together, illustrated a rise in fasting glucose levels that was not paralleled by an equivalent increase in random glycemia in HFD Npas4 PKO mice (Figure 6.11E). This was not observed in either control or Npas4 PKO chow-fed mice or HFD-fed control animals (Figures 6.11D). The combination of fasting hyperglycemia and normal random glycemia made it difficult to determine whether a beta cell defect was present within Npas4 PKO mice.

As the fasting hyperglycemia present in HFD-fed Npas4 PKO mice may suggest impairments in beta cell function, glucose homeostasis was more robustly assessed by means of an oral glucose tolerance test (OGTT). Despite the presence of fasting hyperglycemia in HFD Npas4 PKO mice, their ability to clear glucose remained normal at seven weeks of HFD-feeding (Figures 6.12A&B). To more specifically test beta cell function, islets were isolated from both chow and HFD-fed animals and insulin release in response to glucose or KCl, assayed. While no significant differences between control and Npas4 PKO were observed, there was a trend towards increased insulin secretion in response to elevated glucose and KCl in chow-fed Npas4 PKO mice. However, islets from HFD-fed Npas4 PKO mice tended to secrete reduced amounts of insulin in response to elevated glucose concentrations (Figure 6.12C). To determine whether insulin levels were altered *in vivo* an additional OGTT was performed at 11 weeks of HFD-feeding and plasma collected at baseline and fifteen minutes following glucose injection. Similar to the OGTT performed at seven weeks, HFD-fed Npas4 PKO mice displayed normal glucose clearance, despite the presence of fasting hyperglycemia. (Figures 6.12D&E). Plasma insulin levels under fasting conditions and

following glucose administration were not significantly different between chow-fed Npas4 PKO and control mice.

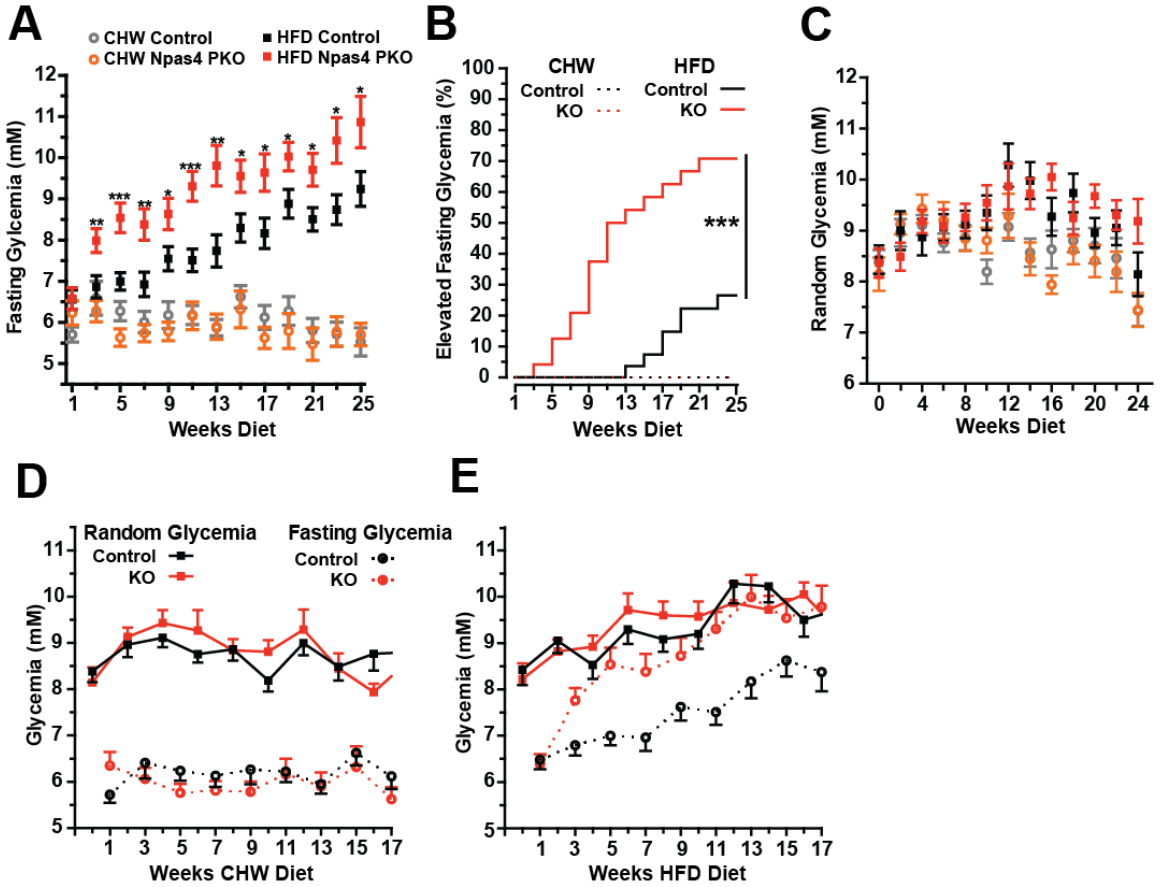

Figure 6.11: HFD-fed Npas4 PKO mice develop fasting hyperglycemia. HFD Npas4 PKO mice developed fasting hyperglycemia at three weeks of HFD, an effect not observed in chow-fed Npas4 PKO mice (A). Over the 25 weeks of monitoring, approximately 70% of HFD Npas4 PKO mice developed fasting hyperglycemia compared to 30% HFD controls and 0% of chow-fed animals (B). The *ad libitum* glucose levels of Npas4 PKO mice did not display significant differences from diet fed controls (C). Plotting fasting glycemia with random glycemia of the first 17 weeks of chow diet feeding, Npas4 PKO mice showed no differences from control mice (D). When plotting fasting glycemia with random glycemia of the first 17 weeks of HFD-feeding, Npas4 PKO mice had a specific increase in fasting glucose which was not observed in random glycemia (E) (n=15-26). Significance was established using a two-tailed Student's t-test or log-rank test for data plotted in (B). *=$p \leq 0.05$; **=$p \leq 0.01$; ***=$p \leq 0.001$.

However, HFD Npas4 PKO mice displayed fasting hyperinsulinemia, while insulin levels following administration of a glucose bolus were not significantly elevated (Figure

6.12F). The presence of fasting hyperglycemia and hyperinsulinemia but normal glucose tolerance raised further questions concerning the nature of the phenotype of HFD-fed Npas4 PKO mice.

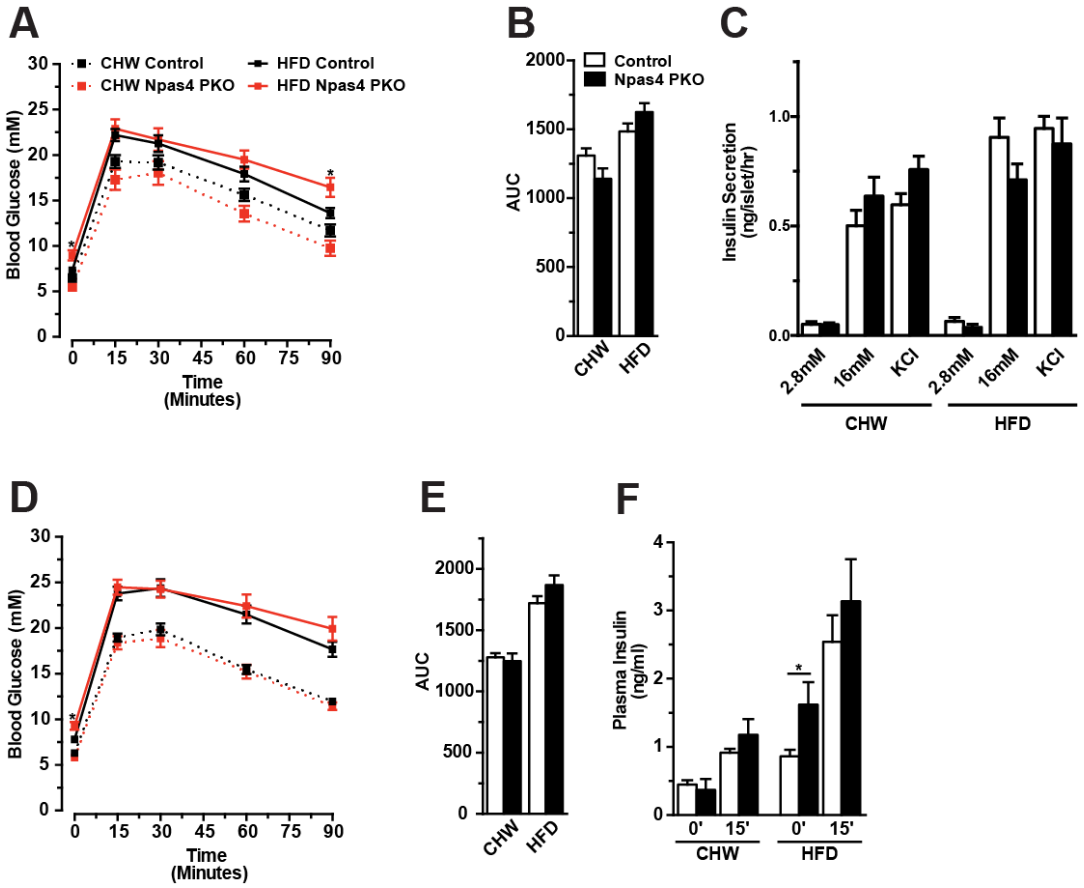

Figure 6.12: Normal glucose tolerance and insulin secretion in Npas4 PKO mice. Blood glucose values during a 2 g/kg OGTT following overnight fast in both chow and HFD-fed control and Npas4 PKO mice at 7 weeks of diet feeding (n=7-17) (A). Quantification of area under the glucose tolerance curve revealed no significant difference between control and knockout mice on either diet (B). Insulin secretion from isolated islets of chow or HFD-fed Npas4 PKO were not significantly altered compared to diet fed controls (n=4-6) (C). Similarly, no significant differences in glucose clearance (D) or in area under the curve (E) were observed during a 2 g/kg OGTT performed at 11 weeks of diet (n=10-21) (D&E). In chow-fed animals, no significant differences were observed in circulating insulin levels collected at baseline (0') and 15 minutes post glucose injection (15') (F). However, HFD-fed Npas4 PKO mice displayed significantly higher basal insulin levels with no significant difference in post-glucose circulating insulin (n=4-8) (F). Significance was established using two-tailed Student's t-tests. *=p≤ 0.05.

As elevated fasting insulin levels are correlated with insulin resistance in humans (278), the presence of hyperinsulinemia in HFD-fed Npas4 PKO mice suggested there may be impairments in insulin sensitivity. Therefore, to assess insulin sensitivity *in vivo*, all groups of mice were subject to two separate insulin tolerance tests (ITT). At seven weeks of HFD-feeding, none of the groups had significantly different responses following an IP administration of 0.75 U/kg insulin (Figures 6.13A&B). However, at 11 weeks of diet feeding, HFD-fed Npas4 PKO mice had a significantly reduced response to *in vivo* insulin administration (Figures 6.13C&D). Interestingly, chow-fed Npas4 PKO mice demonstrated a normal response to insulin in the first half of the ITT but in the latter half, had a more rapid return to baseline levels (Figure 6.13C). Quantification of area over the curve during the second ITT demonstrated that chow-fed Npas4 PKO mice were insulin resistant (Figure 6.13D).

As hepatic insulin resistance results in increased glucose output through elevated gluconeogenesis (279), the loss of insulin sensitivity in Npas4 PKO mice may have an impact on hepatic glucose production and release. In order to assess gluconeogenesis *in vivo*, the glucose precursors pyruvate and glycerol were injected into the peritoneal cavity of fasted mice and changes in blood-glucose monitored. Following IP injection of a 2 g/kg pyruvate bolus at seven weeks of diet feeding, HFD Npas4 PKO mice displayed a significantly elevated blood-glucose response, compared to HFD-fed controls (Figures 6.14A&B).

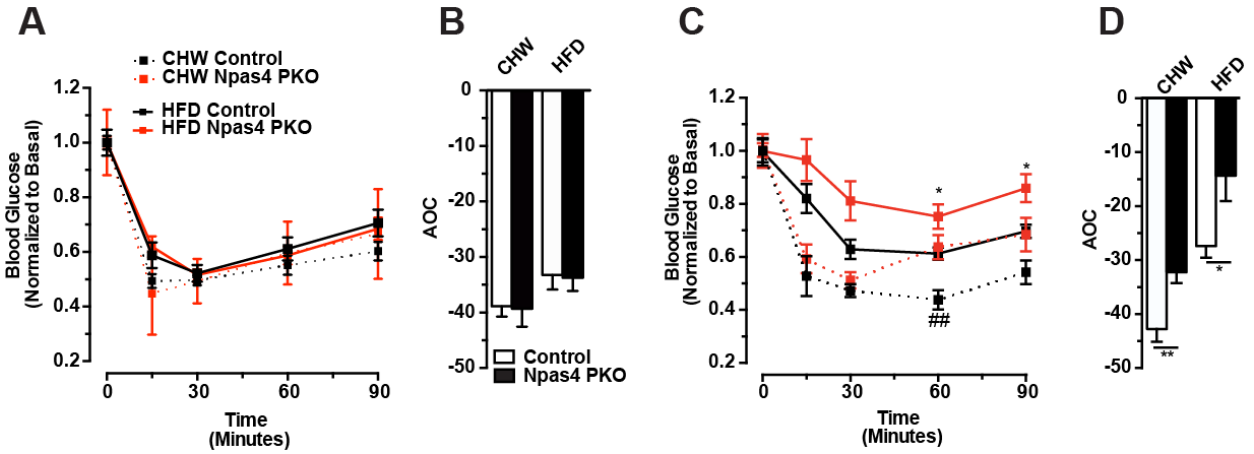

Figure 6.13: Npas4 PKO mice develop reduced sensitivity to insulin.
At seven weeks of diet feeding, neither chow or high fat diet fed Npas4 PKO mice displayed differences in blood-glucose levels during a 0.75 U/kg insulin tolerance test (n=7-21) (A&B). During a second insulin tolerance test, performed following 11 weeks of diet feeding, both HFD and chow-fed Npas4 PKO mice displayed impaired insulin tolerance (n=8-11) (C&D). Significance was established using two-tailed Student's t-test. For HFD control versus HFD Npas4 PKO mice; *=p ≤ 0.05; **=p ≤ 0.01. For chow control versus chow Npas4 PKO mice; ##=p ≤ 0.01.

Similarly, chow-fed Npas4 PKO mice also displayed an elevated glucose response to pyruvate, although this did not reach statistical significance (Figures 6.14A&B). At 11 weeks of age, both HFD and chow-fed Npas4 PKO mice displayed a significantly elevated glucose response to a 2 g/kg glycerol compared to the respective diet controls (Figures 6.14C&D). This elevation in gluconeogenic output may explain the fasting hyperglycemia observed in HFD Npas4 PKO mice.

As the liver acts as one of a few gluconeogenic organs (280), liver RNA was harvested from control and knockout mice under fasting conditions at seven weeks of diet feeding, the same age at which Npas4 PKO displayed an elevated response to pyruvate (Figure 6.14A). In agreement with the elevated response to gluconeogenic substrates in Npas4 PKO mice, the expression of *Ppargc1α*, a major transcriptional

coactivator of gluconeogenic enzymes (281), was increased within the liver of chow and HFD-fed Npas4 PKO mice (Figures 6.15A&B).

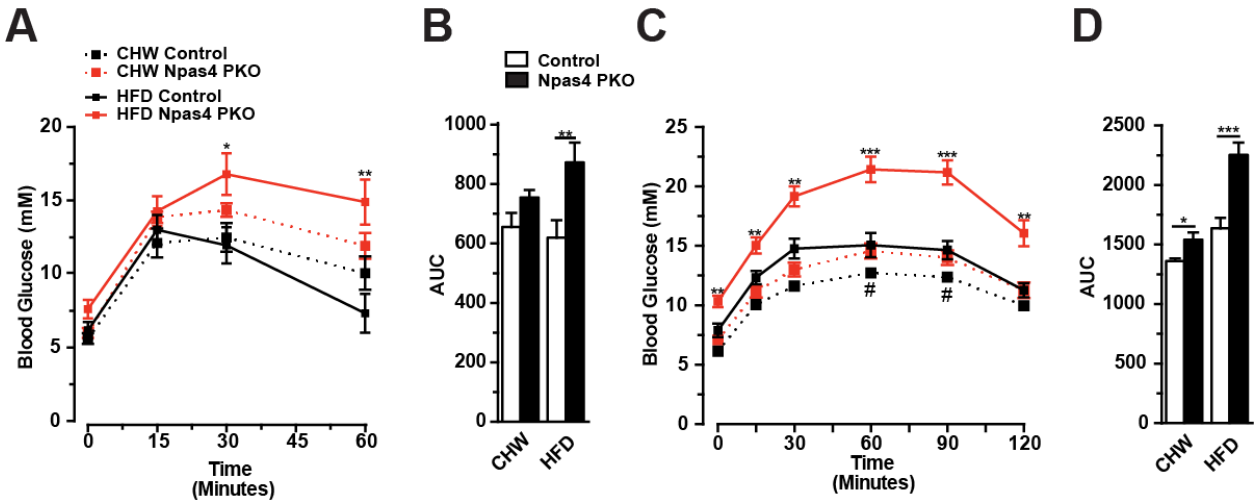

Figure 6.14: Npas4 PKO mice have elevated glucose responses to the administration of gluconeogenic substrates.
Both chow and HFD-fed Npas4 PKO mice had an elevated blood glucose response to the gluconeogenic substrate pyruvate during a 2 g/kg pyruvate tolerance test performed at seven weeks of diet feeding (n=6-12) (A&B). Similarly, following the administration of a 2 g/kg glycerol bolus, both chow and high fat diet fed Npas4 PKO mice had significantly elevated glucose responses as compared to the respective control diet during a 2 g/kg glycerol tolerance test performed at 11 weeks of diet feeding (n=12-15) (C&D). Significance was established using two-tailed Student's t-test. *= $p \leq 0.05$; **= $p \leq 0.01$; ***= $p \leq 0.001$.

A potential pathway through which loss of NPAS4 within the islet may be impacting hepatic gluconeogenesis is through increased glucagon secretion which promotes liver gluconeogenesis (282). However, at seven weeks of HFD-feeding, no significant differences in fasting glucagon or insulin levels were detected (Figures 6.16A&B); suggesting that loss of NPAS4 was not resulting in hyperglucagonemia and that perhaps loss of NPAS4 in another tissue was promoting increased hepatic gluconeogenesis.

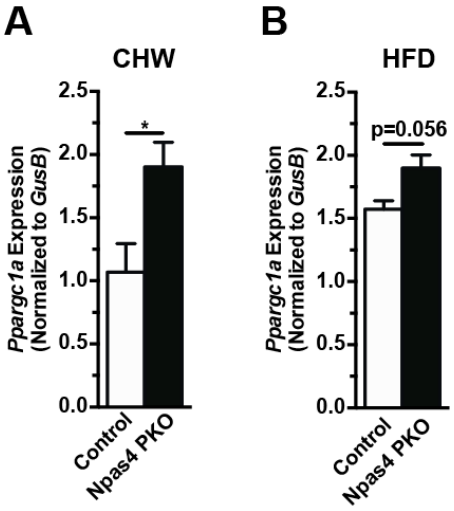

Figure 6.15: Increased liver *Ppargc1α* expression in Npas4 PKO mice.
Liver *Ppargc1α* expression was elevated in Npas4 PKO mice under fasting conditions compared to control mice following seven weeks of chow (A) or high fat diet-feeding (B) (n=4-8). Significance was established using two-tailed Student's t-tests. * = $p \leq 0.05$.

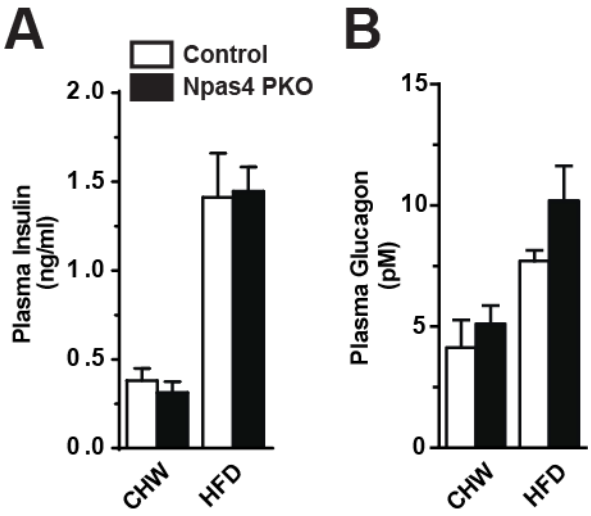

Figure 6.16: No difference in circulating glucagon or insulin levels at seven weeks of HFD-feeding in Npas4 PKO mice.
Plasma was collected under fasting conditions from both chow and HFD-fed control and Npas4 PKO mice at seven weeks of diet. Plasma insulin (A) and glucagon (B) levels were not significantly altered in chow or HFD-fed Npas4 PKO mice compared to diet fed controls (n=4-6).

While phenotyping of Npas4 PKO mice over the first 11 weeks of HFD-feeding did not produce an overt beta cell phenotype, it was hypothesized that with continued metabolic stress, beta cell failure would occur in Npas4 PKO mice. Therefore, monitoring was continued and beginning at 15 weeks of HFD, Npas4 PKO mice began to display glucose intolerance following a 2 g/kg oral glucose bolus (Figures 6.17A&B). The observed glucose intolerance does not seem to be due to due to specific defects in the incretin signalling, as HFD-fed Npas4 PKO mice displayed similar glucose intolerance following an IPGTT performed at 20 weeks of HFD-feeding, albeit with a smaller sample size (Figures 6.17C&D). Following 25 weeks of diet feeding, chow-fed Npas4 PKO mice continued to exhibit normal glucose tolerance, while HFD-fed Npas4 PKO mice developed a greater degree of glucose intolerance (Figures 6.17E&F). Increased age did not induce glucose intolerance in chow-fed Npas4 PKO mice, as a single cohort aged to 44 weeks remained glucose tolerant (Figures 6.17G&H).

To understand the underlying mechanism of the impaired glucose tolerance observed in HFD-fed Npas4 PKO mice, whole blood was collected during the 1 g/kg OGTT performed at 25 weeks of diet feeding and assayed for circulating insulin levels No significant difference in either fasting or post-glucose insulin levels was observed in chow-fed Npas4 PKO mice, compared with diet fed controls (Figure 6.18A). However, HFD-fed Npas4 PKO mice displayed a trend towards decreased post-glucose insulin without any alteration in fasting insulin levels (Figure 6.18A). To complement the *in vivo* insulin levels, isolated islet function was assessed during an *in vitro* insulin secretion assay.

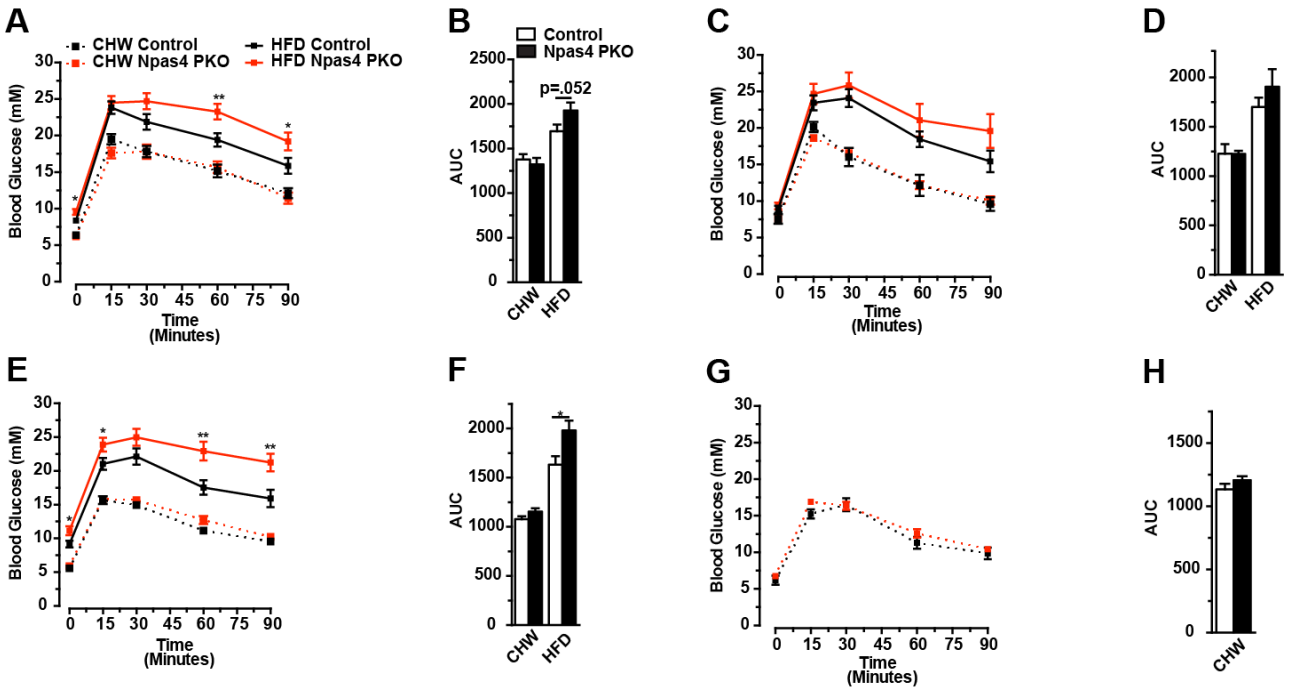

Figure 6.17: HFD-fed Npas4 PKO mice develop glucose intolerance.
At 15 weeks of HFD-feeding, Npas4 PKO mice display mildly impaired glucose tolerance following administration of a 2 g/kg oral glucose bolus (n=10-20) (A&B). No difference between genotypes was observed in chow-fed animals (A&B). Similarly, following the IP administration of a 2 g/kg glucose bolus at 20 weeks of age, HFD Npas4 PKO mice displayed a similar degree of glucose intolerance (n=4-8) (C&D). At 25 weeks of HFD-feeding, Npas4 PKO mice displayed more marked glucose intolerance during a 1 g/kg OGTT while chow-fed Npas4 PKO mice remained glucose tolerant (n=19-24) (E&F). Following a single cohort of chow-fed animals to 44 weeks of age did not reveal significant glucose intolerance in Npas4 PKO mice (n=3-4) (G&H). Significance was established using two-tailed Student's t-test. * = $p \leq 0.05$; ** = $p \leq 0.01$.

Islets from chow-fed Npas4 PKO mice secreted normal amounts of insulin under basal and stimulatory conditions (Figure 6.18B), however, islets from HFD-fed Npas4 PKO mice secreted significantly less insulin in response to high glucose (Figure 6.18B). The decreased *in vivo* and *in vitro* glucose stimulated insulin secretion from beta cells of HFD-fed Npas4 PKO mice are characteristic of beta cell dysfunction following prolonged stress and likely underlie the glucose intolerance observed in these mice.

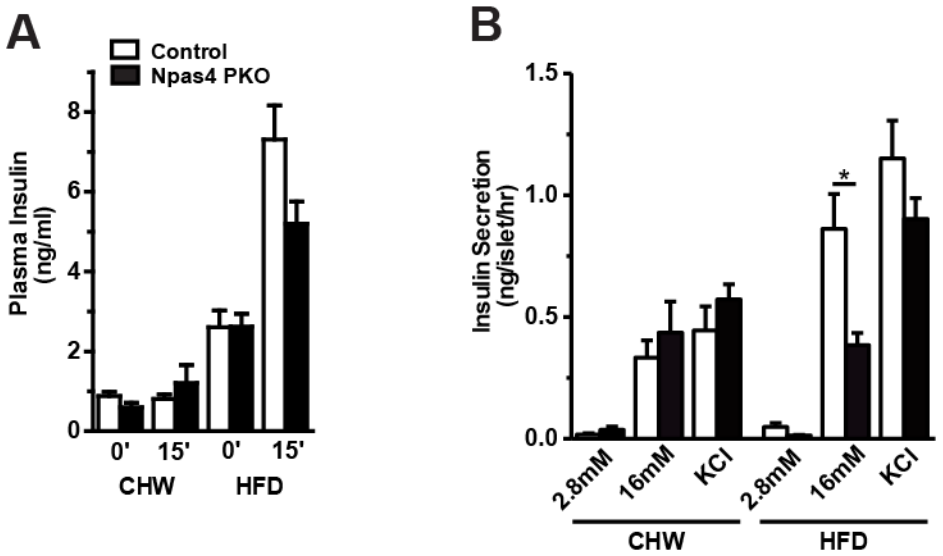

Figure 6.18: Decreased insulin secretion from HFD-fed Npas4 PKO mice. HFD but not chow-fed Npas4 PKO mice displayed a trend towards decreased circulating insulin levels following a 1 g/kg OGTT performed at 25 weeks of HFD (n=5-10) (A). Islets from 32 week old chow-fed Npas4 PKO mice had normal insulin secretion under basal and stimulatory conditions while islets from HFD-fed Npas4 PKO mice had significantly reduced glucose-stimulated insulin secretion (n=4-7) (B). Significance was established using a two-tailed Student's t-test. * = $p \leq 0.05$.

There are a number of possible mechanisms through which loss of NPAS4 may be impairing beta cell function and glucose intolerance in HFD-fed Npas4 PKO mice, including reduction in beta cell numbers due to impaired proliferation or increased rates of apoptosis. Conversely, beta cell mass may be maintained and functional deficits may the primary cause. To first address whether there were reductions in the number of beta cells in Npas4 PKO mice, pancreata from all groups were collect at the endpoint of 25 weeks of diet feeding and sections were stained for both insulin and glucagon. Following quantification, neither chow nor HFD-fed Npas4 PKO mice had significant differences in the number of alpha or beta cells, compared to age and diet fed controls (Figure 6.19A&B). Likely precluding a differences in apoptosis or proliferation rates in

Npas4 PKO mice and suggesting functional deficits were the primary cause of impaired glucose tolerance.

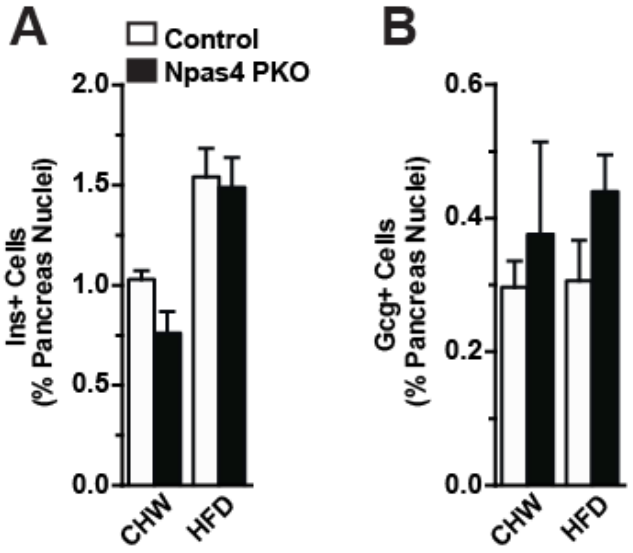

Figure 6.19: No significant differences in beta or alpha cell numbers in Npas4 PKO mice following 25 weeks of diet.
Paraffin sections, separated by 500 µm, were sampled from the pancreas of 32 week old chow and high fat diet fed control and Npas4 PKO mice and stained for either insulin (A) or glucagon (B). Sections were imaged and endocrine cells quantified and normalized to total pancreatic nuclei on the respective section (n=3-4).

Importantly, following a two-hour stimulation in 25 mM glucose, *Npas4* expression in islets from both chow and HFD-fed Npas4 PKO mice was significantly reduced (Figure 6.20A). The degree of knockout was highly similar to what was observed two weeks following tamoxifen administration (Figure 6.1A), suggesting that there was no dramatic loss of recombined cells or a dilution with non-recombined cells. Another possibility that may explain the reduced beta cell function in HFD-fed Npas4 PKO mice is beta cell dedifferentiation. As discussed within chapter 1, there are multiple pathways through which beta cells have been shown to dedifferentiate; including increased expression of the transcription factor, Sox9 (127).

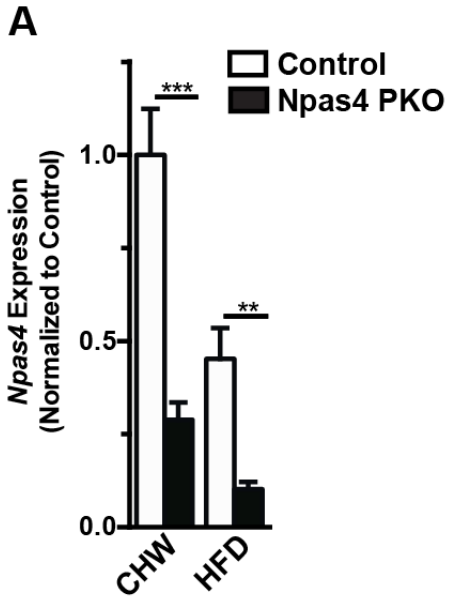

Figure 6.20: *Npas4* expression is reduced in islets from 32-week old Npas4 PKO mice.
Islets from chow and HFD-fed control and knockout mice were harvested at 32 weeks of age and stimulated *in vitro* for two hours with 25 mM glucose (A). *Npas4* expression was significantly reduced in both chow and HFD-fed Npas4 PKO mice (n = 5-10). Significance was established using a two-tailed Student's t-test. ** = $p \leq 0.01$; *** = $p \leq 0.001$.

Based on the studies in chapter 4, which suggested NPAS4 negatively regulates beta cell Sox9; its expression was subsequently measured within isolated islets of Npas4 PKO mice. Following 25 weeks of diet feeding, *Sox9* was elevated in both chow and high fat diet fed Npas4 PKO islets, although this only reached statistical significance in HFD-fed mice (Figure 6.21A). To investigate whether increased *Sox9* expression in the Npas4 PKO model was associated with beta cell dedifferentiation, lineage tracing analysis was conducted with the use of the Rosa26^{mTmG} reporter allele.

A

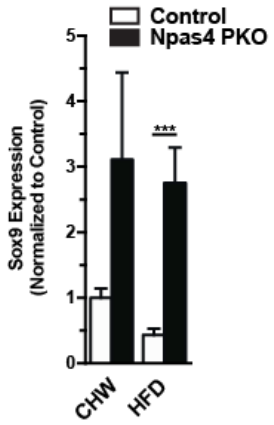

Figure 6.21: Npas4 PKO mice have increased islet expression of *Sox9*.
Islets isolated from Npas4 PKO mice following 25 weeks of HFD-feeding had significantly higher *Sox9* expression. While there was a trend towards increased *Sox9* expression in age matched, chow-fed Npas4 PKO mice, this did not reach statistical significance (n=4-9) (A). Significance was established using a two-tailed Student's t-test.*** = $p \leq 0.001$.

In control mice, 7.5% of all GFP immunoreactive islet cells were negative for insulin staining. It is likely that this GFP+/Insulin- population constitutes recombined alpha and delta cells as described above (Figures 6.3&4). In contrast, within islets from both chow and high fat diet fed Npas4 PKO mice, the number of GFP-labelled cells that were not immunoreactive for insulin increased to approximately 12% (Figures 6.22A&C). Next, to determine whether beta cells were transdifferentiating into glucagon-expressing cells, sections were co-stained for GFP and glucagon. In control mice, islet cells that were labelled with GFP and expressed glucagon constituted 3.5% of all glucagon immunoreactive cells. The number of these GFP, glucagon co-immunoreactive cells was significantly higher in both chow and HFD-fed Npas4 PKO mice, constituting 17% and 10% of the total GFP labelled cell population, respectively (Figures 6.22B&C). Suggesting that beta cell dedifferentiation or transdifferentiation

may contribute to the impaired beta cell function and glucose tolerance in HFD Npas4 PKO mice.

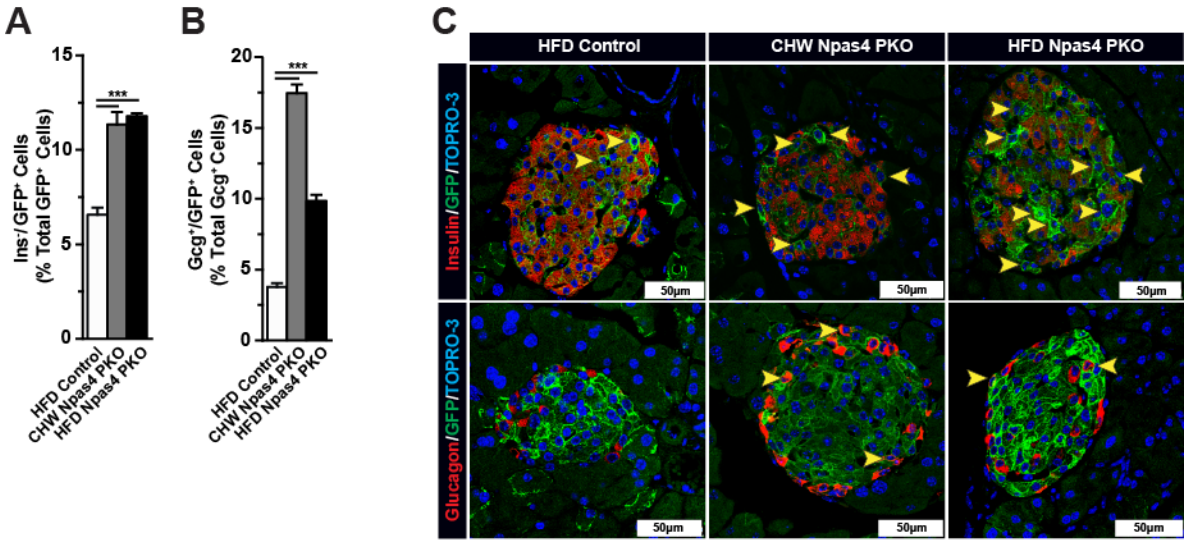

Figure 6.22: Increased rates of beta cell dedifferentiation and transdifferentiation in Npas4 PKO mice
Pancreatic sections from HFD-fed controls, and both chow and HFD-fed Npas4 PKO mice were stained for GFP and insulin or GFP and glucagon. Both chow and HFD-fed Npas4 PKO mice had increased numbers of GFP labelled cells that did not express detectable insulin protein, suggestive of a loss of beta cell maturation state (A). Furthermore, both chow and HFD-fed Npas4 PKO mice had increased numbers of GFP labelled cells expressing glucagon, suggestive of beta cell transdifferentiation (B) (n=3). Significance was a one-way ANOVA with Dunnett's post-hoc analysis. *** = $p \leq 0.001$.

6.3 Discussion

Based on the number of pathways that were influenced by *in vitro* overexpression of NPAS4 in beta cells, it was hypothesized that knockout of Npas4 would impair beta cell function or viability in response to stress. To test this, a novel Npas4 knockout mouse model was developed by crossing the Pdx1CreER transgenic line to the Npas4 floxed mouse and followed by tamoxifen administration at 6 weeks of age. Examination of Cre activity through the Rosa26^{mTmG} reporter strain revealed recombination within the pancreatic islet as well as within the hypothalamus. As these studies initially intended to

specifically examine the effect of reduced NPAS4 expression within the beta cell, the presence of Cre activity within this brain region complicates the interpretation of some of the observed phenotypes.

To understand the role of Npas4 in glucose homeostasis under metabolic stress, control and Npas4 PKO mice were separated into two experimental cohorts; one fed a standard rodent chow and the other fed a diet high in fat and sugar content. To rigorously characterize the long term consequences of genetic ablation of Npas4 from Pdx1-Cre expressing cells, weight gain, glycemia, feeding and locomotor activity were monitored over the course of 25 weeks of HFD-feeding as well as blood glucose response during glucose, insulin, pyruvate and glycerol tolerances tests. A number of phenotypes were observed in HFD-fed Npas4 PKO mice, including fasting hyperglycemia and elevated gluconeogenic output in response to the *in vivo* administration of pyruvate or glycerol. Metabolic cage analysis also revealed significant differences in feeding and locomotor behaviors in HFD-fed Npas4 PKO. The earliest phenotypes observed in the Npas4 PKO mice were slightly increased mass and fasting hyperglycemia and elevated gluconeogenesis with hyperinsulinemia and insulin resistance developing afterwards. Following prolonged HFD-feeding, Npas4 PKO mice also developed glucose intolerance associated with increased rates of beta cell dedifferentiation and transdifferentiation.

Based on the Cre activity within the CNS and the pancreatic islet and the types of phenotypes developed by Npas4 PKO mice; these *in vivo* experiments support a dual role for NPAS4 in the maintenance of glucose homoeostasis. One based on its

expression with the neurons of the arcuate and one based on a role within the pancreatic beta cell.

Regarding the role of NPAS4 within the beta cell, the data from the Npas4 PKO mice suggests that continued NPAS4 expression is required to suppress *Sox9* and maintain beta cell differentiation. While increased islet expression of *Sox9* and similar rates of beta cell dedifferentiation were observed regardless of diet, glucose intolerance and reduced insulin secretion was only observed in HFD-fed Npas4 PKO mice. This would suggest that HFD-feeding constitutes an additional beta cell stress and is required to precipitate disrupted glucose homeostasis in Npas4 PKO mice. There are multiple mechanisms through which HFD-feeding could exacerbate any dysfunction present within Npas4 PKO beta cells, such as driving beta cell proliferation (261), increasing ER stress levels (98), or decreasing the expression of the transcription factor MAFA (134). Alternatively, based on the competitive dynamic between NPAS4 and HIF1α illustrated in chapter 5, it is possible that HIF1α transcriptional activity is increased in Npas4 null beta cells due to decreased competition for ARNT. Furthermore, as HFD-feeding increased HIF1α protein levels in adipose (283) and liver (284), it is possible that beta cells express higher levels of HIF1α following HFD-feeding. It could be this increased HIF1α in HFD-fed Npas4 PKO beta cells that further exacerbates beta cell dysfunction and leads to glucose intolerance.

There were other phenotypes observed in Npas4 PKO mice that are not traditionally believed to be mediated by beta cell dysfunction, these include increased gluconeogenesis, insulin resistance and altered eating and locomotor behaviors. As recombination was detected within the arcuate nucleus, it raised the possibility that loss

of central Npas4 expression mediated these effects. Indeed, a number of studies using "beta cell specific" Cre lines have uncovered centrally mediated phenotypes which manifest as alterations in weight gain, food intake or insulin sensitivity (273,274,285-287).

There are several pathways that NPAS4 is known to regulate in other contexts which may be impacted in POMC or AGRP neurons of Npas4 PKO mice, resulting in the observed phenotypes. For instance, based on data from chapter 4, it is possible that loss of Npas4 may increase neural ER stress within the arcuate neurons, which has been implicated in the development of obesity and insulin resistance (288,289). Alternatively, NPAS4 promotes the generation of GABAergic synapses within hippocampal neurons (164) and it is possible it has a similar function within the hypothalamus; resulting in reduced GABA release from Npas4 PKO neurons. Impaired GABA secretion in Pdx1-CreER expressing neurons could contribute to the phenotype of the Npas4 PKO mouse as blocking GABA secretion from RIP-Cre neurons, resulted in increased weight gain on HFD (274). A final mechanism through which loss of Npas4 within the neurons of the arcuate could be impacting glucose homeostasis is by regulating intrinsic neural activity. The possibility that NPAS4 regulates neuron excitability in a cell autonomous fashion has currently only speculative (290), however, if true, would likely alter the function of multiple cell types within the ARC.

Importantly, attempts to demonstrate reduced hypothalamic *Npas4* mRNA expression in Npas4 PKO mice were unsuccessful. Therefore, it cannot be conclusively stated that Npas4 is expressed within the arcuate nucleus or that there is reduced Npas4 expression in the arcuate of Npas4 PKO mice; relegating this line of discussion

as one based on conjecture rather than empirical evidence. Future experiments will determine which neural types within the arcuate express NPAS4, whether its expression is altered by metabolic signals such as glucose or insulin within these neurons and the effect of reduced NPAS4 expression within these neurons on glucose homeostasis.

In conclusion, Pdx1CreER mediated genetic deletion of Npas4 leads to the development of several phenotypes, including elevations in gluconeogenesis, impaired insulin sensitivity and increased islet *Sox9* expression. These data support the importance of Npas4 in promoting glucose homeostasis. While the exact nature of these alterations was unresolved; it is hypothesized that loss of Npas4 within the islet and within an extra-islet cell type both contribute to the phenotype.

Chapter 7: Characterization of the AAV-Cre & Ins1Cre Npas4 knockout mouse

7.1 Introduction

The use of Pdx1CreER transgenics to genetically delete Npas4 from Pdx1-CreER expressing cells resulted in a number of phenotypes including; elevated gluconeogenesis, insulin resistance, altered feeding and locomotor behavior as well as beta cell dysfunction and dedifferentiation. However, the Cre recombinase activity in both the CNS and the beta cell of Pdx1CreER transgenic mice confounded the interpretation of some of the phenotypes of observed. Therefore, in order to exclude any contribution of reduced Npas4 expression within arcuate neurons and specifically examine the metabolic consequences of Npas4 ablation from the beta cell, two recent advancements in targeting Cre recombinase to beta cells were utilized.

One advancement is the delivery of Cre recombinase to beta cells through the use an adeno-associated viral (AAV) vector. AAVs consist of ~4.5kb single stranded DNA genome with Rep and Cap genes flanked by inverted terminal repeats (ITRs) on the 5' and 3' ends (291-293). The Rep and Cap genes can be removed and replaced with promoters and coding sequences of interest. Within the CNS, several studies have successfully used stereotaxic injections to deliver Cre recombinase to specific brain regions (159,294). In beta cells, AAVs have been used as gene delivery vectors in rodent models of type 1 or T2D (172,295-301) by either injecting AAV into the peritoneal cavity or, for more pancreas specific delivery, directly into the pancreatic duct. To date there have been no reports of AAV infecting neurons of the CNS following intraductal injection of AAVs targeting the beta cell.

The second tool that has improved targeting of Cre to beta cells is the development of novel mouse lines which express Cre under the control of the mouse Insulin 1 promoter. Compared to the insulin 2 allele, insulin 1 is restricted to the pancreatic beta cell (302) and the characterization of both a knock-in Ins1-Cre mouse line (175) and a transgenic Ins1-Cre mouse line (267,303,304) have failed to detect recombination within the CNS.

Both the Ins1-Cre and AAV-mediated systems offered distinct advantages; the Ins1-Cre mouse line results in Cre mediated recombination in nearly 100% of beta cells (175), while AAV-mediated gene delivery to beta cells has been shown to be substantially less efficient (172,300). However, as the insulin 1 allele is activated during pancreatic development (305) it does not offer the temporal control afforded through the use of AAV-mediated Cre delivery, unless a tamoxifen responsive Cre is used. Based on the advantages of the Ins1-Cre and the AAV approached, both were used to generate two separate models of beta cell Npas4 knockout mice and determine whether loss of Npas4 within the beta cells was sufficient to recapitulate the diverse phenotypes present in the Npas4 PKO model.

7.2 Results

7.2.1 Recombination within the Ins1Cre knock-in mice

Similar to the high beta cell Cre activity observed in Pdx1CreER transgenic mice following tamoxifen administration; examination of GFP immunofluorescence in $Ins1^{WT/Cre}$- $Rosa26^{mTmG}$ islets revealed recombination in essentially every beta cell and no alpha cells (Figure 7.1A). The expression of *Npas4* was also significantly reduced in $Ins1^{WT/Cre}Npas4^{flx/flx}$ (Npas4 IKO) mice compared to $Ins1^{WT/WT}Npas4^{flx/fx}$ (Control) mice

following two hour stimulation in 25 mM glucose (Figure 7.1B). Importantly, no recombination was detected within the arcuate nucleus (Figure 7.1C), demonstrating a high degree of beta cell specificity in this Cre line.

7.2.2 Characterization of male Npas4 IKO mice

As the Ins1-Cre knockin line demonstrated high rates of beta cell recombination with no detectable recombination within the arcuate nucleus, it was a suitable model to examine whether the loss of Npas4 within the beta cell lineage was responsible for the pleiotropic phenotypes within the Npas4 PKO mouse. Therefore, cohorts of male Npas4 IKO mice were split between standard rodent chow and HFD at seven weeks of age and monitored on a weekly basis.

In contrast to what was observed with the Npas4 PKO model, Npas4 IKO mice did not demonstrate any difference in weight gain (Figure 7.2A) and the fat mass of HFD Npas4 IKO mice was not significantly different from diet fed controls (Figure 7.2B). To examine feeding and locomotor behavior within the Npas4 IKO mouse, HFD-fed control and Npas4 IKO mice were placed into metabolic cages at seven weeks of diet feeding. While the HFD Npas4 PKO mice had increased light phase food intake and decreased dark phase locomotor activity no such phenotype was observed in the HFD-fed IKO knockout model (Figure 7.3A&C).

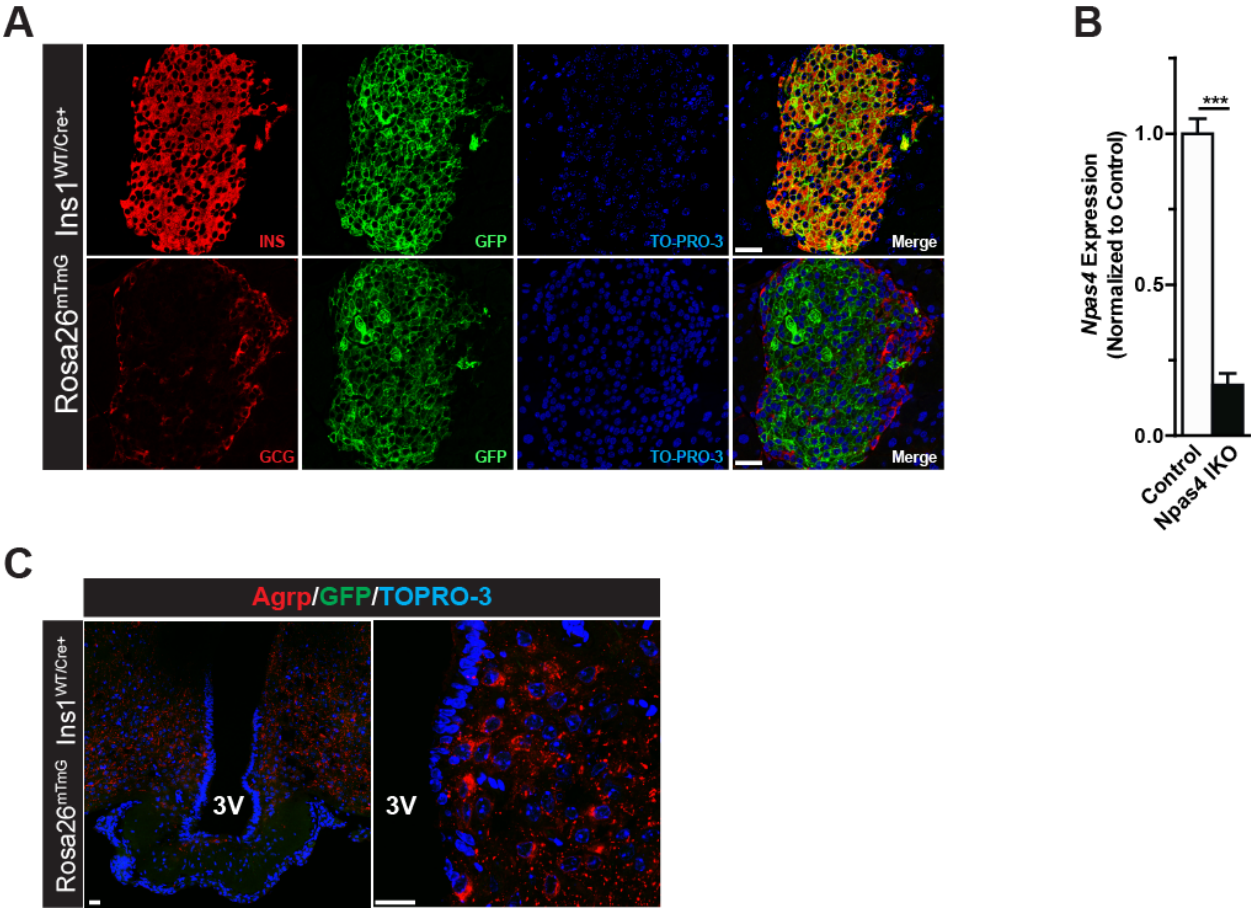

Figure 7.1: High rates of beta cell specific recombination in the Ins1$^{WT/Cre}$ mice. At 8 weeks of age, Ins1$^{WT/Cre}$Rosa26^{mTmG} mice were sacrificed, perfused with 4% PFA and pancreas and brain harvested for immunofluorescent staining. Stained paraffin sections from the pancreas revealed high rates of beta cell recombination and no detectable recombination within alpha cells (A). *Npas4* mRNA levels were significantly reduced within whole islets of Npas4 IKO mice following a two hour *in vitro* stimulation in 25 mM glucose (n=3-8) (B). Stained coronal cryosections of the brain from Ins1WT/CreRosa26mTmG mice did not yield GFP positive cells within the arcuate nucleus (C). 3V: Third Ventricle. Scale bars = 25 µm. Significance was established using two-tailed Student's t-tests. ***= p≤ 0.001.

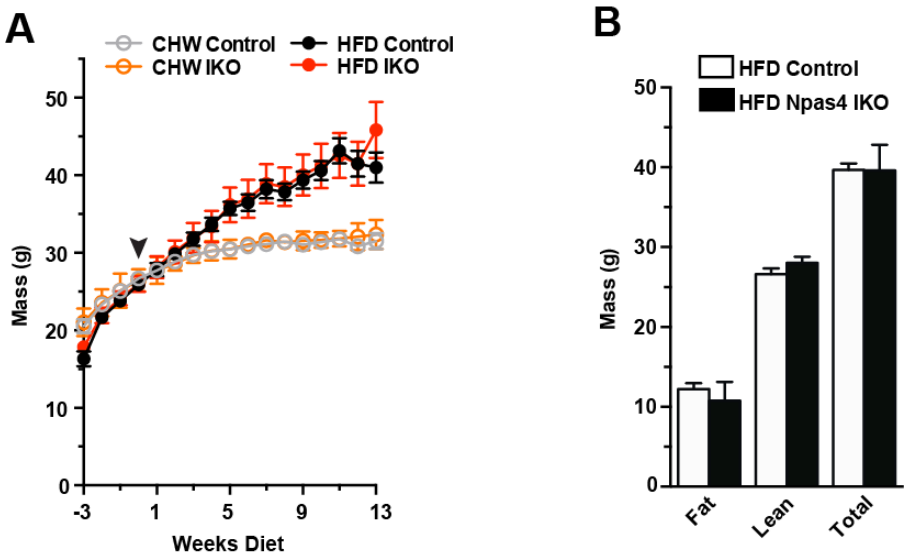

Figure 7.2: No difference in weight gain in Npas4 KO mice.
Body mass measurements taken weekly from one week post-weaning. Mice were placed on HFD at 7 weeks of age (black arrow head) however no difference in mass gain was observed in either chow or HFD-fed Npas4 IKO mice over 13 weeks of diet feeding (n≥5) (A). Neither the fat nor lean body mass composition of HFD-fed Npas4 IKO at seven weeks of HFD-feeding was significantly different from HFD-fed control mice (n=4) (B).

Furthermore, there were no significant differences in water intake or RER (Figure 7.3B&D). This metabolic cage data from the Npas4 IKO mode suggested that loss of Npas4 within beta cells is not sufficient to induce changes in locomotor activity or changes in feeding behavior.

To examine any alterations in glucose homeostasis in chow and HFD-fed Npas4 IKO mice; fasting and random glucose was monitored in an identical manner as the Npas4 PKO model. However, in contrast to the fasting hyperglycemia observed in Npas4 PKO mice, elevated fasting glucose levels did not develop in HFD-fed Npas4 IKO mice over the first 13 weeks of diet feeding (Figure 7.4A). No difference was observed in the random blood-glucose levels in *ad libitum* fed animals either (Figure 7.4B).

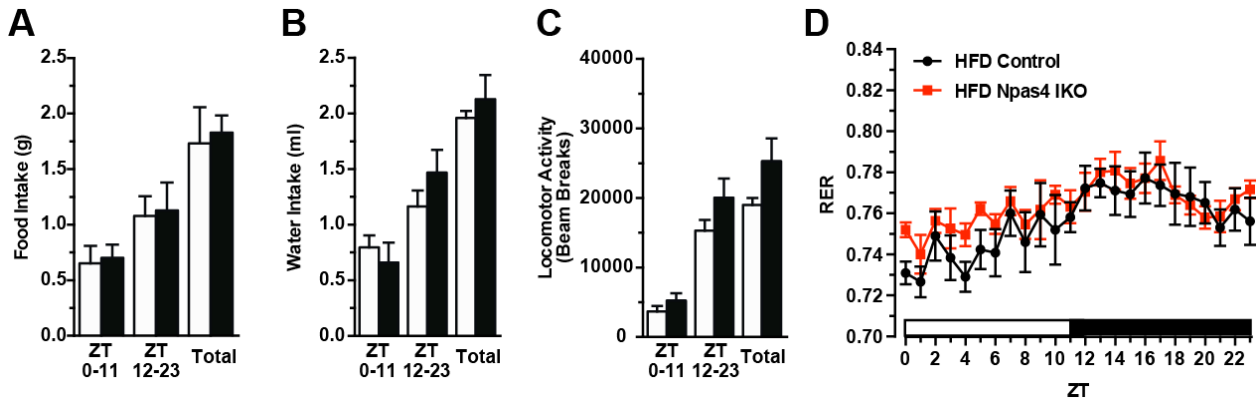

Figure 7.3: No alterations to the behavioral phenotype of HFD-fed Npas4 IKO mouse.
At seven weeks of HFD-feeding, male control and Npas4 IKO mice were subjected to metabolic cage analysis. No difference between the lean or fat mass in Npas4 IKO was detected (A). Food (B) and water (C) intake patterns were also unaltered in HFD Npas4 IKO mice. A non-significant trend toward increased locomotor activity was observed in HFD Npas4 IKO mice (D). Finally, the respiratory exchange ratio (RER) of HFD-fed Npas4 IKO mice was not significantly different than diet fed controls (n=4) (E).

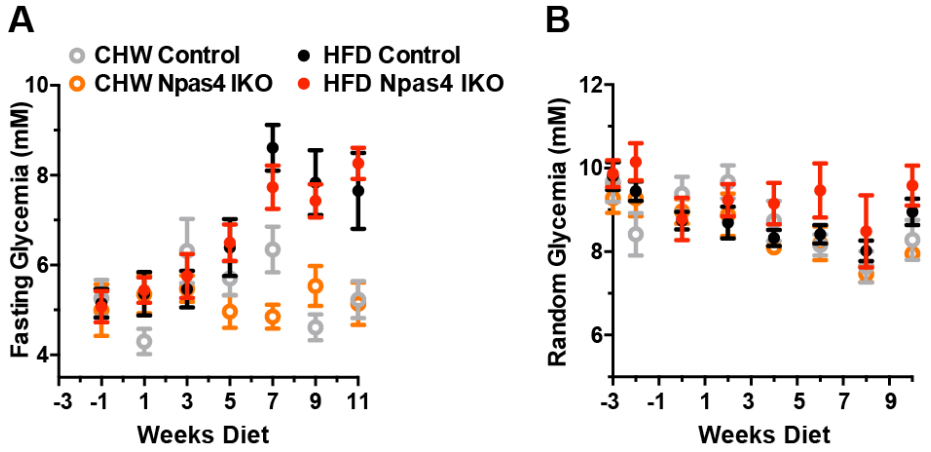

Figure 7.4: No change in random or fasting glycemia of Npas4 IKO mice
No significant difference in blood glucose following an overnight fast (A) or in ad libitum (B) fed Npas4 IKO mice on either chow or HFD compared to their respective diet fed controls (n≥5).

It was possible that normal fasting glucose levels may be maintained in the Npas4 IKO mice but there may be still be underlying elevations in hepatic glucose production. Therefore, to assay *in vivo* gluconeogenic output, both pyruvate and glycerol tolerance tests were performed at 7 and 11 weeks of HFD-feeding,

respectively. These time points match the age at which the pyruvate and glycerol tolerance tests were performed in the Npas4 PKO mice. In response to either pyruvate or glycerol, both CHW and HFD-fed Npas4 IKO mice displayed a normal glucose response, compared to their diet controls (Figures 7.5A&B).

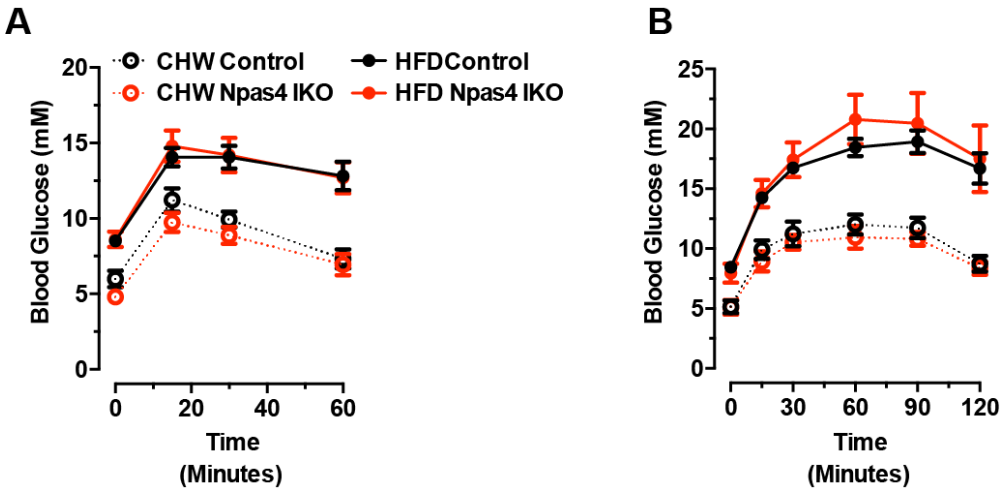

Figure 7.5: Npas4 IKO respond normally to *in vivo* administration of gluconeogenic substrates.
Both chow and HFD-fed Npas4 IKO mice have normal glucose responses during a 2 g/kg pyruvate tolerance test performed at seven weeks of HFD-feeding (n≥5) (A). Similarly, glucose response during a 2 g/kg glycerol tolerance test remained normal in Npas4 IKO mice compared to diet fed controls (n≥5) (B).

Similarly, the insulin resistance observed in Npas4 PKO mice after 11 weeks of high fat diet feeding was not observed in Npas4 IKO mice (Figure 7.6A). As HFD-fed Npas4 IKO mice did not develop fasting hyperglycemia, elevated gluconeogenic output or insulin resistance; this suggested that loss of Npas4 expression from the beta cell was not responsible for the development of these phenotypes within the PKO model.

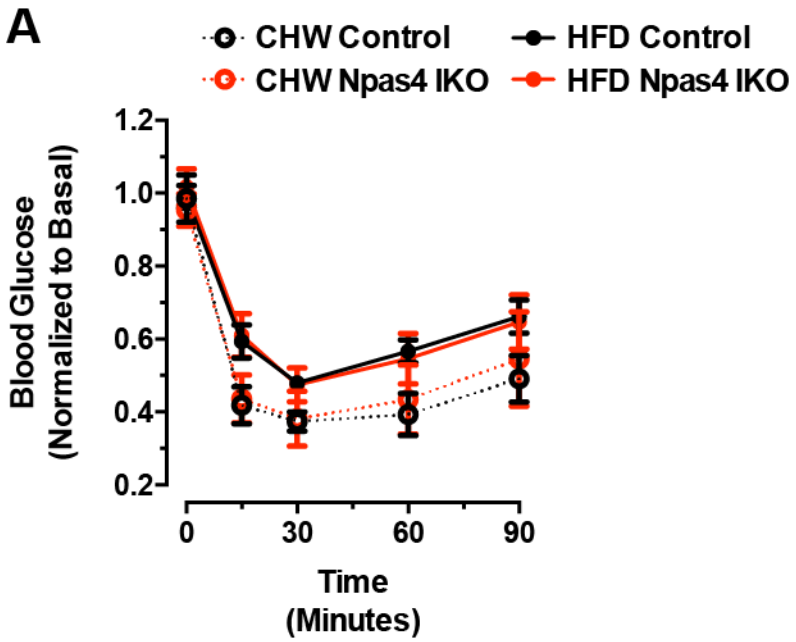

Figure 7.6: Npas4 IKO demonstrate normal glucose response to insulin. Compared to diet fed controls, Npas4 IKO mice display a normal response to insulin during a 0.75 U/kg ITT performed at 11 weeks of HFD-feeding (n≥5) (A).

7.2.2.1 Recombination in AAV-RIP2-Cre injected Rosa26^{mTmG} mice

As early expression of Cre driven by the Insulin 1 promoter resulted in deletion of Npas4 during pancreatic development, this may allow the beta cell to compensate for loss of NPAS4 and masking the development of a phenotype. In order to ablate Npas4 from mature beta cells in a manner more similar to what was performed with the Pdx1CreER model; an AAV-mediated approach was taken.

To this end, 1.5x10^{11} viral genomes (vg) of an adeno-associated virus (AAV) serotype 6 expressing Cre under control of the rat insulin 2 promoter was injected directly into the pancreatic duct. To determine the efficiency of beta cell recombination, pancreata from AAV-RIP-Cre injected Rosa26^{mTmG} mice were harvested two weeks following AAV delivery and Cre activity assessed through the presence of membrane bound GFP. Immunofluorescent examination of islets from AAV-RIP-Cre injected mice,

revealed Cre mediated recombination in both beta and alpha cells (Figure 7.7A) of pancreatic islets but not within the arcuate nucleus (Figure 7.7B).

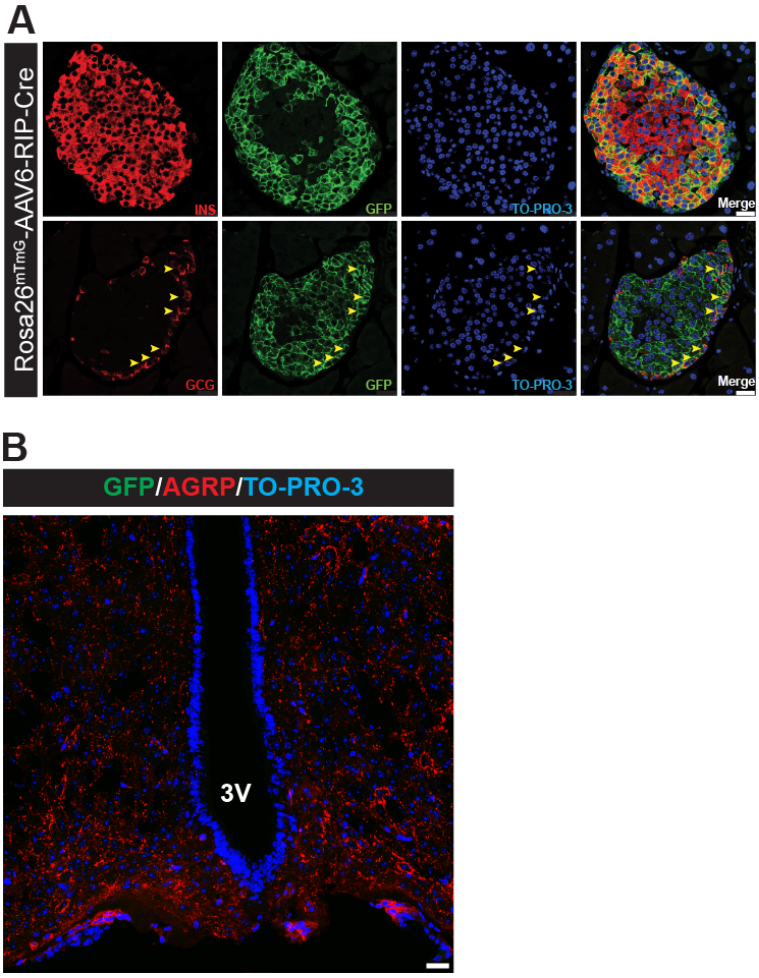

Figure 7.7: Islet specific recombination in AAV-RIP-Cre injected Rosa26^{mTmG} mice. Pancreas and whole brain were harvested for immunofluorescent analysis of Cre mediated recombination two weeks following injection of 1.5x10^{11}vg of AAV-RIP-Cre into the pancreatic duct of Rosa26^{mTmG} mice. Co-staining for GFP and insulin within the pancreas revealed higher rates of recombination on the periphery of the islet as opposed to the islet core (A). While the majority of recombined cells were insulin positive, a number of recombined alpha cells were also detected (yellow arrowheads) (A). Further, no recombination within the arcuate nucleus was detected (B). 3V: Third Ventricle. Scale bars = 25 µm.

7.2.3 Phenotype of Npas4 AAV-KO mice

To generate an AAV-mediated Npas4 KO model, $1.5x10^{11}$vg of AAV-RIP-Cre or a control virus which lacked the Cre recombinase sequence (AAV-RIP-Empty), were injected into the pancreatic duct of 8-10 week old Npas4$^{flx/flx}$ mice. Following the surgery, mice were maintained on standard chow diet for one week prior to transfer to high fat diet for the duration of the studies.

The weight gain on HFD was not as substantial as that observed in the Npas4 PKO or IKO models, likely due to a secondary effect of the surgery. However, no significant difference was observed between the two groups (Figure 7.8A). There was also no significant difference in fasting blood-glucose levels between RIP-Cre or RIP-Empty injected Npas4$^{flx/flx}$ mice (Figure 7.8B). Notably, the random blood glucose levels in *ad libitum* fed mice were non-significantly elevated in the first few weeks following the initiation of HFD-feeding, however, this normalized by six weeks of diet (Figure 7.8C). Further, the glucose response during either a pyruvate tolerance test, administered at 7 weeks of HFD-feeding or a glycerol tolerance test, performed at 11 weeks HFD-feeding, remained normal in AAV-RIP-Cre injected mice (Figure 7.8D-G).

While these mice were monitored for up to 25 weeks of HFD-feeding, no significant impairment in glucose tolerance was observed (Figure 7.9A). As the AAV-RIP-Cre injected Npas4$^{flx/flx}$ mice had the Cre reporter mTmG allele present, lineage tracing analysis was performed to examine recombination rates. At end point, 26 weeks post intraductal surgery, there were reduced proportions of recombined beta cells present in AAV-RIP-Cre injected Npas4$^{flx/flx}$ mice (Figure 7.9B) compared to what had been observed two weeks post-injection. Due to the reduced numbers of recombined

beta cells at this time point; it is difficult draw conclusions on the impact of reduced beta cell NPAS4 expression on glucose homeostasis. However, apparent loss of recombined beta cells suggests they were at a competitive disadvantage

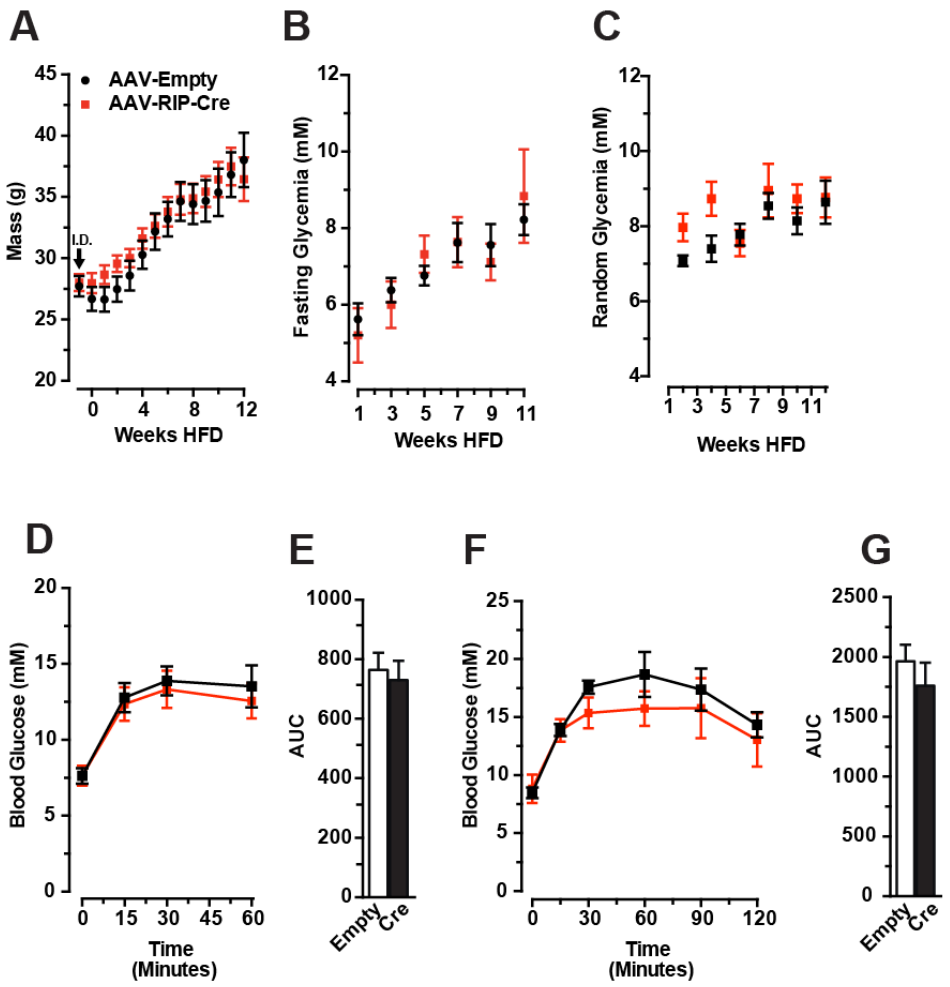

Figure 7.8: AAV-RIP-Cre injected Npas4$^{flx/flx}$ mice display normal weight gain, glycemia and response to gluconeogenic substrates.
One week following intraductal surgery (I.D.) standard diet was replaced with HFD and mice monitored for 12 weeks of HFD-feeding. AAV-RIP-Cre injected Npas4$^{flx/flx}$ mice display normal weight gain compared to AAV-RIP-Empty injected controls (A). Fasting glycemia was not significantly different between the two groups (B) and while there was trend towards elevated random glycemia in the first few weeks following the onset of HFD-feeding, this was no longer present by 6 weeks of HFD-feeding (C). AAV-RIP-Cre injected Npas4$^{flx/flx}$ mice demonstrated normal glucose responses during a 2 g/kg pyruvate tolerance test (D&E) and 2 g/kg glycerol tolerance test (n=5-6) (F&G).

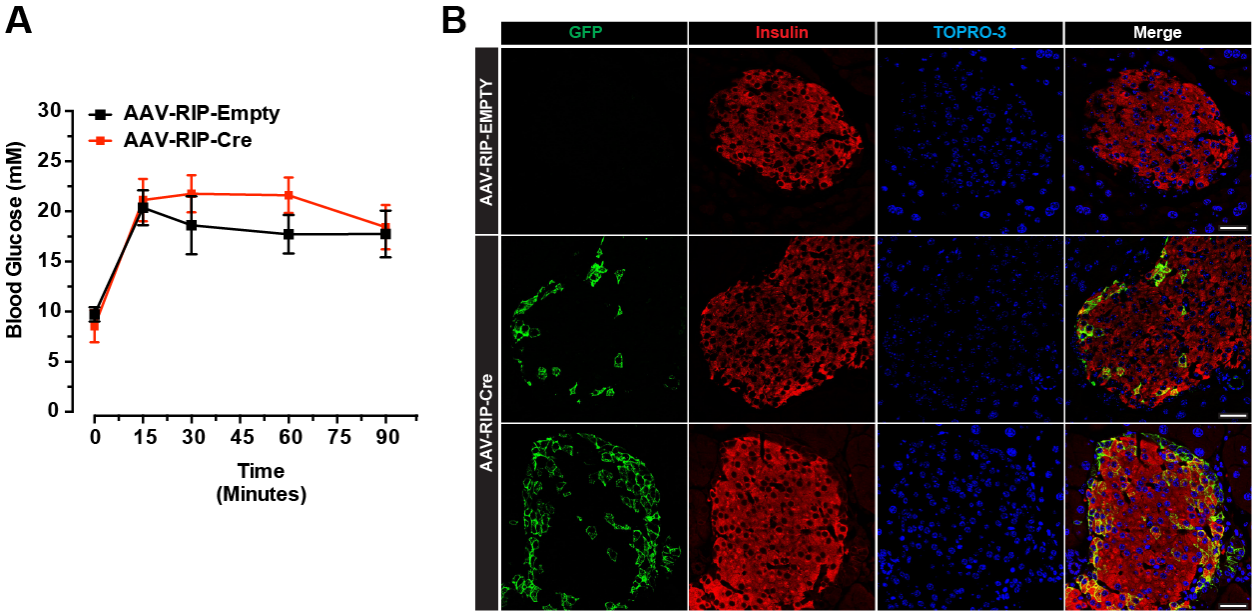

Figure 7.9: Following prolonged HFD-feeding, AAV-RIP-Cre injected Npas4$^{flx/flx}$ mice have reduced beta cell recombination rates.
Following 25 weeks of HFD-feeding, glucose clearance was similar following a 2 g/kg OGTT in AAV-RIP-Cre injected Npas4$^{flx/flx}$ mice compared to AAV-RIP-Empty injected controls (n=5-6) (A). Following 25 weeks of HFD, no Cre mediated recombination was detected in islets from AAV-RIP-Empty injected Npas4$^{flx/flx}$-Rosa26^{mTmG} mice (top row) (B); however, the proportion of recombined beta cells in AAV-RIP-Cre injected Npas4$^{flx/flx}$-Rosa26^{mTmG} mice was substantially lower than that observed two weeks following intraductal surgery (bottom two rows) (B).

7.3 Discussion

To decipher whether the metabolic phenotypes observed in the Pdx1CreER Npas4 KO model were due to loss of Npas4 expression within the beta cell or from another cell type; two novel Npas4 beta cell KO models were generated. Importantly, no Cre-mediated recombination was detected within the arcuate nucleus of the hypothalamus in either of these models; allowing for specific examination of the functional significance of Npas4 expression in beta cells.

While the Pdx1CreER Npas4 knockout model developed fasting glycemia associated with an elevated glucose response to gluconeogenic substrates such as pyruvate and glycerol; neither the Npas4 AAV-KO nor the Npas4 IKO knockout mice

developed this phenotype. Similarly, impaired insulin sensitivity and alterations in feeding behavior and locomotor activity in the HFD Npas4 PKO mice were not observed in the HFD Npas4 IKO mice. Combined these three models suggest that the early phenotype of the Pdx1CreER Npas4 model is likely due to Cre expression in cell types other than the beta cell. Supporting the position outlined in chapter 5 that recombination within the CNS may be driving some of the phenotypes of the Npas4 PKO mouse model.

A caveat of the AAV studies is that in comparison to the Pdx1CreER model, recombination rates were lower at the beginning of the study and the proportion of recombined beta cells seemed to decline following 25 weeks of HFD-feeding. Therefore, it is possible that the rates of recombination were not high enough at the outset of the studies to establish significant differences between control and knockout mice. However, the absence of even non-significant differences in fasting glycemia or in glucose response to pyruvate or glycerol in Npas4 AAV-KO mice would suggest that reduced numbers of recombined beta cells was not the primary reason a phenotype was not detected.

These studies also aimed to examine beta cell function within these two models of beta cell specific Npas4 knockout; however, the data is currently inconclusive. In the case of the AAV-mediated approach, the reduced proportion of recombined beta cells following 25 weeks of HFD-feeding make it difficult to assess the long term consequence to glucose homeostasis caused by genetic Npas4 ablation. One interpretation of this finding is that within this model, the beta cells which still express Npas4 are more capable of expansion following HFD-feeding; possibly due to increased

stress levels within the Npas4 null beta cell. While the Ins1Cre model would not be subject to the same limitations, unfortunately, due to the length of time required to age the Npas4 IKO mice; the beta cell phenotype for this model was not performed. Based upon the phenotype of beta cells in the Npas4 PKO it is believed that the Npas4 IKO beta cells will express higher levels of *Sox9*, dedifferentiate and impair systemic glucose homeostasis.

Chapter 8: Summary & conclusions

Research over the past twenty years has demonstrated that the etiology of T2D is highly complex, with both genetic and environmental contributions (306). The development of T2D is also marked by the dysfunction of multiple glucoregulatory organs (307) which all contribute to insulin resistance and hyperglycemia. The continued function of the pancreatic beta cell is critical for the promotion of euglycemia; failure in the beta cell compensatory response to increased metabolic demands precipitates the development of T2D.

Through the use of mouse models, multiple beta cell proteins and pathways have been identified which have essential roles in regulating beta cell function, viability and differentiation. Among these are the bHLH-PAS domain transcription factors and calcium signaling pathways. The bHLH-PAS domain proteins assume a unique role in beta cells as a critical component of the sensory machinery (244). Disruption of many of the bHLH-PAS domain proteins, including, HIF1α (149), ARNT (150), CLOCK (136,308) and BMAL1 (136,137) results in impaired insulin secretion and glucose intolerance in mice; demonstrating the importance of these proteins to beta cell function. Secondly, stimulation of beta cell calcium signaling pathways resulting in NFAT and CREB activation have also been shown to be critically important to beta cell; through their roles in promoting proliferation (201,202) and survival (196,309-311). Furthermore, disruption of CREB (196) or NFAT (204,205) activity, *in vivo*, impairs beta cell function leading to compromised glucose homeostasis; highlighting the immense importance of these proteins and their downstream targets.

Previous studies have demonstrated NPAS4 is calcium-induced bHLH-PAS domain protein and as such, resides at the intersection of these two essential beta cell pathways. Despite this, the role of NPAS4 within the beta cell or more broadly, glucose homeostasis has not yet been examined. The studies presented within this thesis were designed to answer three overarching questions. First, how is Npas4 expression regulated within the pancreatic beta cell in response to a number of relevant environmental stimuli? Secondly, within an *in vitro* model, how does NPAS4 regulate beta cell insulin expression and secretion and the cellular response to ER stress and HIF1α activation? Finally, within multiple *in vivo* models, how does reduced Npas4 expression impact glucose homeostasis and energy balance?

In answer to the first question, *Npas4* expression was detected within the developing pancreas but did not reach levels similar to what was observed in mature islets until e17.5. Within the adult beta cell, NPAS4 was expressed at very low levels under resting conditions and dramatically induced in response to stimulation with agents which result in insulin secretion such as glucose, KCl and palmitate. The induction of *Npas4* by KCl was shown to be dependent on calcium influx; likely laying downstream of CREB or NFAT activation. Importantly, *Npas4* expression was detected in the beta cells of multiple mammals including mouse, rat and humans and the induction of *Npas4* by membrane depolarization was observed in all beta cells tested. This similarity across different mammals may suggest that this pathway has enough functional importance to ensure it is conserved. There were also various pathways which reduced the induction of NPAS4, including the inhibition of Akt activity and reduced oxygen availability. Intriguingly, in islets from HFD-fed mice and individuals diagnosed with T2D, the

induction of *Npas4* by membrane depolarization was diminished. Raising the possibility that impairments in *Npas4* induction may contribute to beta cell dysfunction.

The experiments presented in chapters 4 and 5 used *in vitro* models to subsequently address which beta cell processes NPAS4 was regulating. Supraphysiologic NPAS4 levels significantly reduced the expression of both the mouse insulin 1 and insulin 2 genes. This inhibition of insulin production was likely due to a combination of direct regulation of insulin promoter activity by NPAS4 and indirect regulation through reduced PDX1 and NEUROD1 levels. While no effect on glucose-stimulated insulin release was observed in Npas4 transduced beta cells, the potentiating effects of the GLP-1 receptor agonist, exendin-4 were completely lost. This was likely mediated by increased expression of regulator of G-protein signaling protein 2 (RGS2). The expression of RGS2 was increased under the same conditions which lead to increased NPAS4 expression including high glucose or KCl treatment. Furthermore, NPAS4 overexpression in MIN6 cells or mouse islets significantly increased *Rgs2* expression due to direct binding of the Rgs2 promoter and putative enhancer.

Further studies were then performed to understand how NPAS4 influenced the beta cell stress response. In particular, the cellular response to ER stress and HIF1α activation were assessed as both have been shown to inhibit beta cell function and are relevant to T2D (99,127). Npas4 transduced beta cells had significantly reduced *Ddit3* expression following exposure to the ER stressors, palmitate or thapsigargin. The observed cytoprotective effects of NPAS4 corroborates the studies performed in neurons (163,312) and one separate examination of NPAS4 in beta cells (206).

Similarly, Npas4 transduction reduced the expression of multiple HIF1α target genes in beta cells including those considered to be “disallowed” (313), “forbidden” (314) and characteristic of dedifferentiated beta cells (127,315).

To determine whether reduced beta cell NPAS4 expression *in vivo* would result in dysfunction following metabolic stress, Npas4 was genetically ablated using the Pdx1CreER transgenic mouse line. Following HFD-feeding, this novel Npas4 knockout model developed a wide range of metabolic phenotypes including increased weight gain, altered feeding and locomotor behavior as well as fasting hyperglycemia, insulin resistance and increased hepatic gluconeogenesis. Furthermore, following prolonged HFD-feeding, these Npas4 PKO mice developed glucose intolerance, likely caused by increased *Sox9* expression and beta cell dedifferentiation.

Confounding the interpretation of the data from the Pdx1CreER model was the Cre-mediated recombination detected within the hypothalamus; a brain region of critical importance in the regulation of feeding and glucose homeostasis (316,317). Therefore, to determine whether any of the metabolic phenotypes observed in the Pdx1CreER Npas4 KO model were caused by reduced beta cell Npas4 expression, two separate beta cell Npas4 knockout models were developed. Characterization of the Ins1-Cre and AAV-RIP-Cre Npas4 knockout mice did not recapitulate the early metabolic phenotypes of the Pdx1CreER model, including insulin resistance, elevated gluconeogenesis or fasting hyperglycemia. Together these three Npas4 knockout models suggest that NPAS4 expression within the neurons of the hypothalamus and the beta cell is required for the maintenance of glucose homeostasis.

The sum of the experiments presented within this thesis demonstrate that *Npas4* expression in beta cells is tightly regulated and highly dynamic. Functionally, NPAS4 acts to temper cellular function through the reduced insulin production and secretion in response to GLP-1 receptor activation. At the same time, NPAS4 maintains long term beta cell viability and differentiation by reducing ER stress and limiting the transcriptional activity of HIF1α. Furthermore, as *NPAS4* expression under stimulatory conditions was reduced in islets from donors with T2D, these protective pathways are likely impaired and contribute to the beta cell deficits in T2D.

Finally, NPAS4 may be a tractable molecular target in the treatment of T2D in order to protect beta cells during periods of prolonged stress. The possibility of exploiting the endogenous beta cell homeostatic response to stress in order to preserve beta cell function in a prediabetic state is an attractive therapeutic avenue as it may delay or prevent the onset of T2D (318). Due to its dynamic expression levels, Npas4 may be well suited for manipulation by small molecules. This could be accomplished by increasing the activity of transcription factors which promote NPAS4 expression. Alternatively, inhibiting the proteins responsible for degrading NPAS4 would result in NPAS4 protein stabilization. Based on the studies contained within this thesis and other reports (163,206,312), it is hypothesized that increased NPAS4 expression in dysfunctional beta cells would reduce in stress levels and maintain an adequate level of functional beta cell mass to delay the progression of T2D. However, there are many questions which remain to be answered prior to NPAS4 manipulation being used to therapeutic ends in T2D, including how to target a small molecule to specifically increase NPAS4 expression and not other similarly regulated proteins in beta cells. The

second and perhaps most important question is what are the long term effects of elevated beta cells NPAS4 expression *in vivo*? These experiments will be addressed in future studies however, regardless of whether NPAS4 is amenable to therapeutic ends, continued examination of beta cell homeostatic responses will yield a better understand beta cell biology in health and disease and identify further potential targets for the treatment and prevention of T2D.

8.1 Future directions

The data presented within this thesis demonstrate that NPAS4 expression is increased in response to beta cell depolarization and that it promotes a cytoprotective transcriptional program. As these are the first studies on the regulation of glucose homeostasis by NPAS4, there are numerous future research avenues which would offer further clarity into the regulation and function of NPAS4 in both the pancreatic beta cell and the neurons of the arcuate nucleus.

For instance, while the requirement for calcium has been established, further studies could offer greater mechanistic detail to the induction of NPAS4 in beta cells. These experiments may include, determining transcription factor binding sites within the Npas4 promoter required for depolarization-dependent *Npas4* expression. This could be performed through a series of promoter truncations to narrow down the relevant promoter region. Subsequently, site-directed-mutagenesis of the Npas4 promoter could be used to identify specific transcription factor binding sites. In conjunction, chromatin immunoprecipitation (ChIP) experiments for calcium regulated transcription factors such factors as NFAT proteins or CREB could be performed. Together, these mechanistic

studies may help facilitate the development of small molecules aimed at increasing the activity of transcription factors which induce NPAS4. in order to increase NPAS4 expression to protect beta cells under stressed conditions.

The studies within this thesis identified the insulin and Rgs2 genes as direct targets of NPAS4 in beta cells. In order to uncover further NPAS4 targets in a non-biased approach, human islets could be depolarized through high glucose exposure for two hours and Chromatin immunopreciptitation (ChIP) performed. Subsequently, the NPAS4 ChIP DNA library could be sequenced to identify genome-wide NPAS4 binding sites within human beta cells. To further complement this ChIP-Seq data set, and better identify *bona fide* NPAS4 targets, cDNA libraries from Npas4 null beta cells and beta cells overexpressing NPAS4 could also be sequenced. These three data sets would offer a comprehensive overview of directly regulated NPAS4 target genes within the beta cell and could be used to offer a more thorough understanding of how NPAS4 protects against cell stress as well as identifying novel cellular processes regulated by NPAS4.

A third research avenue would be a further characterization of the beta cell specific Npas4 knockout mouse model. The Pdx1CreER Npas4 knockout model displayed increased islet expression of *Sox9* and rates of beta cell dedifferentiation, however due to the Cre activity within other cell types, most notably the neurons of the hypothalamus, a careful examination of beta cells from the Npas4 IKO model is required. This characterization should include HFD-feeding for a 32 week period, followed by assessment of glucose tolerance and *in vitro* insulin secretion assays. Further to determine whether beta cell dedifferentiation occurs in this Npas4 knockout

model, immunofluorescent analysis of lineage traced beta cells as well as quantification of dedifferentiation markers including *Sox9* should be performed.

Alternatively, the impact of beta cell NPAS4 overexpression *in vivo* could also be examined. The *in vivo* overexpression could be accomplished through the use of a viral approach such as an AAV or lentivirus vector. Alternatively, a transgenic approach could be used in which the Npas4 sequence could be placed downstream of the insulin 1 promoter. The characterization of these mice could include how increased beta cell NPAS4 expression impacts glucose tolerance and insulin secretion *in vivo* under non stressed settings. Furthermore, HFD-feeding or STZ administration could be used to determine whether increased NPAS4 expression *in vivo* protects against beta cell stress and preserves glucose homeostasis. Crossing the NPAS4 overexpression mouse strain to genetic models of diabetes such as the Akita or *db/db* mouse would also bolster findings from the HFD and STZ models.

Finally, expression analysis of *Npas4* in the CNS revealed high expression levels in the hypothalamus, compared to some other brain regions. Therefore, a further characterization of the hypothalamic neurons which express Npas4 should be performed. This could be done through immunofluorescent staining for NPAS4 protein or the generation of a knock-in mouse strain which expressed GFP downstream of the Npas4 promoter. This initial characterization should also include how metabolic signals such as glucose or insulin impact Npas4 expression within these neurons. As Npas4 is similarly regulated as the other IEG c-fos (165) it is likely that under fasting conditions Npas4 would be upregulated in NPY/AGRP cells while under fed conditions Npas4 should be induced in POMC neurons (319). To understand whether NPAS4 expression

within the arcuate is required for the maintenance of glucose homeostasis; the Npas4 floxed mouse line could be crossed to the Agrp and Pomc –Cre transgenics. These novel Npas4 knockout mice could then be fed a HFD and their weight gain, fasting glucose, insulin and glucose tolerance monitored on a regular basis. Alternatively a more wide-spread Cre strain could be used as examination of Pdx1-Cre expression patterns within the arcuate nucleus did not yield a large degree of overlap with POMC or AGRP neurons (275). Therefore broader hypothalamic Cre lines such as the kisspeptin-Cre (320), Sim1-Cre (321) and Esr1-Cre (322) may be more effective at targeting the Pdx1-Cre neurons.

Despite the progress made in understanding a role for NPAS4 within the beta cell, there is still many unanswered questions. The studies outlined above will add greater mechanistic detail to what is known about NPAS4 and open completely new areas of scientific inquiry into how Npas4 expression in the beta cell and brain contribute to the promotion of glucose homeostasis.

Bibliography

1. Brissova M. Assessment of Human Pancreatic Islet Architecture and Composition by Laser Scanning Confocal Microscopy. Journal of Histochemistry and Cytochemistry. 2005 May 27;53(9):1087–97.

2. Cryer PE. Minireview: Glucagon in the Pathogenesis of Hypoglycemia and Hyperglycemia in Diabetes. Endocrinology. 2012 Feb 21;153(3):1039–48.

3. Braun M, Ramracheya R, Bengtsson M, Zhang Q, Karanauskaite J, Partridge C, et al. Voltage-Gated Ion Channels in Human Pancreatic Beta-Cells: Electrophysiological Characterization and Role in Insulin Secretion. Diabetes. 2008 Jun 1;57(6):1618–28.

4. Henquin JC. Triggering and amplifying pathways of regulation of insulin secretion by glucose. Diabetes. 2000 Nov;49(11):1751–60.

5. Fu Z, Gilbert ER, Liu D. Regulation of insulin synthesis and secretion and pancreatic Beta-cell dysfunction in diabetes. Curr Diabetes Rev. 2013 Jan 1;9(1):25–53.

6. Ferdaoussi M, Dai X, Jensen MV, Wang R, Peterson BS, Huang C, et al. Isocitrate-to-SENP1 signaling amplifies insulin secretion and rescues dysfunctional β cells. J Clin Invest. 2015 Sep 21;:1–14.

7. Nolan CJ, Madiraju MSR, Delghingaro-Augusto V, Peyot ML, Prentki M. Fatty Acid Signaling in the -Cell and Insulin Secretion. Diabetes. 2006 Nov 27;55(Supplement 2):S16–S23.

8. Mancini AD, Poitout V. The fatty acid receptor FFA1/GPR40 a decade later: how much do we know? Trends in Endocrinology & Metabolism. Elsevier Ltd; 2013 Aug 1;24(8):398–407.

9. Hsu WH, Xiang HD, Rajan AS, Kunze DL, Boyd AE. Somatostatin inhibits insulin secretion by a G-protein-mediated decrease in Ca2+ entry through voltage-dependent Ca2+ channels in the beta cell. Journal of Biological Chemistry. ASBMB; 1991;266(2):837–43.

10. Kawai K, Yokota C, Ohashi S, Watanabe Y, Yamashita K. Evidence that glucagon stimulates insulin secretion through its own receptor in rats. Diabetologia. 1995 Mar;38(3):274–6.

11. Rask-Madsen C, Kahn CR. Tissue-Specific Insulin Signaling, Metabolic Syndrome, and Cardiovascular Disease. Arteriosclerosis, Thrombosis, and Vascular Biology. 2012 Aug 15;32(9):2052–9.

12. Saltiel AR, Kahn CR. Insulin signalling and the regulation of glucose and lipid metabolism. Nature. Nature Publishing Group; 2001;414(6865):799–806.

13. American Diabetes Association. Diagnosis and Classification of Diabetes Mellitus. Diabetes Care. 2012 Dec 20;36(Supplement_1):S67–S74.

14. Brownlee M. The pathobiology of diabetic complications: a unifying mechanism. Vol. 54, Diabetes. 2005. pp. 1615–25.

15. Daneman D. Type 1 diabetes. Lancet. Elsevier; 2006;367(9513):847–58.

16. Atkinson MA, Eisenbarth GS, Michels AW. Type 1 diabetes. Lancet. 2014.

17. Polak M, Cavé H. Neonatal diabetes mellitus: a disease linked to multiple mechanisms. Orphanet J Rare Dis. 2007;2(1):12.

18. Zimmet P, Alberti KG, Shaw J. Global and societal implications of the diabetes epidemic. Nature. 2001 Dec 13;414(6865):782–7.

19. MD DAGT, PhD CH, MD WR, PhD EJB, PhD PMK. Diabetes 1 Prediabetes: a high-risk state for diabetes development. Lancet. Elsevier Ltd; 2012 Jun 16;379(9833):2279–90.

20. Alberti KGMM, Zimmet PZ. Definition, diagnosis and classification of diabetes mellitus and its complications. Part 1: diagnosis and classification of diabetes mellitus. Provisional report of a WHO consultation. Diabetic medicine. Wiley Online Library; 1998;15(7):539–53.

21. Aguiree F, Alberti K, Brown A, Zimmet P, Cho NH, Shaw J, et al. IDF diabetes atlas. 2013.

22. Wild S, Roglic G, Green A, Sicree R, King H. Global prevalence of diabetes: estimates for the year 2000 and projections for 2030. Diabetes Care. 2004 May;27(5):1047–53.

23. Association CD. An economic tsunami: the cost of diabetes in Canada. 2009.

24. Dall TM, Yang W, Halder P, Pang B, Massoudi M, Wintfeld N, et al. The Economic Burden of Elevated Blood Glucose Levels in 2012: Diagnosed and Undiagnosed Diabetes, Gestational Diabetes Mellitus, and Prediabetes. Diabetes Care. 2014 Nov 20;37(12):3172–9.

25. Connolly V, Unwin N, Sherriff P, Bilous R. Diabetes prevalence and socioeconomic status: a population based study showing increased prevalence of type 2 diabetes mellitus in deprived areas. Journal of Epidemiology …. 2000.

26. Larranaga I, Arteagoitia JM, Rodriguez JL. Socio-economic inequalities in the prevalence of Type 2 diabetes, cardiovascular risk factors and chronic diabetic complications in the Basque Country, Spain. Diabetic …. 2005.

27. Espelt A, Borrell C, Roskam AJ, Rodríguez-Sanz M, Stirbu I, Dalmau-Bueno A,

et al. Socioeconomic inequalities in diabetes mellitus across Europe at the beginning of the 21st century. Diabetologia. 2008 Sep 9;51(11):1971–9.

28. Roper NA, Bilous RW, Kelly WF, Unwin NC, Connolly VM. Excess mortality in a population with diabetes and the impact of material deprivation: longitudinal, population based study. BMJ. 2001 Jun 9;322(7299):1389–93.

29. Taylor SI. Deconstructing type 2 diabetes. Cell. 1999.

30. Nolan CJ, Damm P, Prentki M. Type 2 diabetes across generations: from pathophysiology to prevention and management. Lancet. 2011.

31. Yoon KH, Ko SH, Cho JH, Lee JM, Ahn YB, Song KH, et al. Selective β-Cell Loss and α-Cell Expansion in Patients with Type 2 Diabetes Mellitus in Korea. Journal of Clinical Endocrinology & Metabolism. 2003 May;88(5):2300–8.

32. Rahier J, Goebbels RM, Henquin JC. Cellular composition of the human diabetic pancreas. Diabetologia. 1983;24(5).

33. Baron AD, Schaeffer L, Shragg P, Kolterman OG. Role of hyperglucagonemia in maintenance of increased rates of hepatic glucose output in type II diabetics. Diabetes. Am Diabetes Assoc; 1987;36(3):274–83.

34. Unger RH, Aguilar-Parada E, Müller WA, Eisentraut AM. Studies of pancreatic alpha cell function in normal and diabetic subjects. J Clin Invest. 1970 Apr 1;49(4):837–48.

35. Yamauchi T, Kamon J, Waki H, Terauchi Y, Kubota N, Hara K, et al. The fat-derived hormone adiponectin reverses insulin resistance associated with both lipoatrophy and obesity. Nature Medicine. 2001 Aug;7(8):941–6.

36. Steppan CM, Bailey ST, Bhat S, Brown EJ, Banerjee RR, Wright CM, et al. The hormone resistin links obesity to diabetes. Nature. 2001 Jan 18;409(6818):307–12.

37. Esposito K. Inflammatory Cytokine Concentrations Are Acutely Increased by Hyperglycemia in Humans: Role of Oxidative Stress. Circulation. 2002 Sep 30;106(16):2067–72.

38. Lumeng CN, Bodzin JL, Saltiel AR. Obesity induces a phenotypic switch in adipose tissue macrophage polarization. J Clin Invest. 2007 Jan 2;117(1):175–84.

39. Weisberg SP, McCann D, Desai M, Rosenbaum M, Leibel RL, Ferrante AW Jr. Obesity is associated with macrophage accumulation in adipose tissue. J Clin Invest. 2003 Dec 15;112(12):1796–808.

40. Ehses JA, Perren A, Eppler E, Ribaux P, Pospisilik JA, Maor-Cahn R, et al.

Increased Number of Islet-Associated Macrophages in Type 2 Diabetes. Diabetes. 2007 Jun 11;56(9):2356–70.

41. Larsen CM, Faulenbach M, Vaag A, Vølund A, Ehses JA, Seifert B, et al. Interleukin-1-receptor antagonist in type 2 diabetes mellitus. N Engl J Med. 2007 Apr 12;356(15):1517–26.

42. Obici S, Zhang BB, Karkanias G, Rossetti L. Hypothalamic insulin signaling is required for inhibition of glucose production. Nature Medicine. 2002 Nov 11;8(12):1376–82.

43. Pocai A, Lam TKT, Gutierrez-Juarez R, Obici S, Schwartz GJ, Bryan J, et al. Hypothalamic K(ATP) channels control hepatic glucose production. Nature. 2005 Apr 21;434(7036):1026–31.

44. Plum L. Central insulin action in energy and glucose homeostasis. J Clin Invest. 2006 Jul 3;116(7):1761–6.

45. Puglianiello A, Cianfarani S. Central Control of Glucose Homeostasis. Rev Diabetic Stud. 2006;3(2):54–4.

46. Perry RJ, Zhang X-M, Zhang D, Kumashiro N, Camporez J-PG, Cline GW, et al. Leptin reverses diabetes by suppression of the hypothalamic-pituitary-adrenal axis. Nature Medicine. Nature Publishing Group; 2014 Jun 15;:1–7.

47. Coppari R, Ichinose M, Lee CE, Pullen AE, Kenny CD, McGovern RA, et al. The hypothalamic arcuate nucleus: A key site for mediating leptin's effects on glucose homeostasis and locomotor activity. Cell Metabolism. 2005 Jan;1(1):63–72.

48. Obici S, Feng Z, Morgan K, Stein D, Karkanias G, Rossetti L. Central administration of oleic acid inhibits glucose production and food intake. Diabetes. 2002 Feb;51(2):271–5.

49. Lam T, Gutierrez-Juarez R, Pocai A, Rossetti L. Regulation of blood glucose by hypothalamic pyruvate metabolism. Science. 2005.

50. Mighiu PI, Yue JTY, Filippi BM, Abraham MA, Chari M, Lam CKL, et al. Hypothalamic glucagon signaling inhibits hepatic glucose production. Nature Medicine. Nature Publishing Group; 2013 May 19;19(6):766–72.

51. Sandoval DA, Bagnol D, Woods SC, D'Alessio DA, Seeley RJ. Arcuate Glucagon-Like Peptide 1 Receptors Regulate Glucose Homeostasis but Not Food Intake. Diabetes. 2008 Jul 28;57(8):2046–54.

52. Pocai A, Obici S, Schwartz GJ, Rossetti L. A brain-liver circuit regulates glucose homeostasis. Cell Metabolism. 2005 Jan;1(1):53–61.

53. Prentki M. Islet cell failure in type 2 diabetes. J Clin Invest. 2006 Jul 3;116(7):1802–12.

54. Muoio DM, Newgard CB. Mechanisms of disease: Molecular and metabolic mechanisms of insulin resistance and β-cell failure in type 2 diabetes. Nat Rev Mol Cell Biol. 2008 Mar;9(3):193–205.

55. Halban PA, Polonsky KS, Bowden DW, Hawkins MA, Ling C, Mather KJ, et al. β-Cell Failure in Type 2 Diabetes: Postulated Mechanisms and Prospects for Prevention and Treatment. Diabetes Care. 2014 May 22;37(6):1751–8.

56. Kültz D. MOLECULAR AND EVOLUTIONARY BASIS OF THE CELLULAR STRESS RESPONSE. Annu Rev Physiol. 2005 Mar 17;67(1):225–57.

57. Ubeda M, Rukstalis JM, Habener JF. Inhibition of cyclin-dependent kinase 5 activity protects pancreatic beta cells from glucotoxicity. J Biol Chem. 2006 Sep 29;281(39):28858–64.

58. Maedler K, Spinas GA, Lehmann R, Sergeev P, Weber M, Fontana A, et al. Glucose induces β-cell apoptosis via upregulation of the Fas receptor in human islets. Diabetes. Am Diabetes Assoc; 2001;50(8):1683–90.

59. Donath MY, Gross DJ, Cerasi E, Kaiser N. Hyperglycemia-induced beta-cell apoptosis in pancreatic islets of Psammomys obesus during development of diabetes. Diabetes. 1999 Apr;48(4):738–44.

60. Maedler K, Sergeev P, Ris F, Oberholzer J, Joller-Jemelka HI, Spinas GA, et al. Glucose-induced β cell production of IL-1β contributes to glucotoxicity in human pancreatic islets. J Clin Invest. 2002 Sep 15;110(6):851–60.

61. Oprescu AI, Bikopoulos G, Naassan A, Allister EM, Tang C, Park E, et al. Free Fatty Acid Induced Reduction in Glucose-Stimulated Insulin Secretion: Evidence for a Role of Oxidative Stress In Vitro and In Vivo. Diabetes. 2007 Nov 27;56(12):2927–37.

62. Bollheimer LC, Skelly RH, Chester MW, McGarry JD, Rhodes CJ. Chronic exposure to free fatty acid reduces pancreatic beta cell insulin content by increasing basal insulin secretion that is not compensated for by a corresponding increase in proinsulin biosynthesis translation. J Clin Invest. 1998 Mar 1;101(5):1094–101.

63. Carpentier A, Mittelman SD, Bergman RN, Giacca A, Lewis GF. Prolonged elevation of plasma free fatty acids impairs pancreatic beta-cell function in obese nondiabetic humans but not in individuals with type 2 diabetes. Diabetes. 2000 Mar;49(3):399–408.

64. El-Assaad W, Buteau J, Peyot M-L, Nolan C, Roduit R, Hardy S, et al. Saturated Fatty Acids Synergize with Elevated Glucose to Cause Pancreatic β-Cell Death.

Endocrinology. 2003 Sep;144(9):4154–63.

65. Jacqueminet S, Briaud I, Rouault C, Reach G, Poitout V. Inhibition of insulin gene expression by long-term exposure of pancreatic beta cells to palmitate is dependent on the presence of a stimulatory glucose concentration. Metab Clin Exp. 2000 Apr;49(4):532–6.

66. Arnush M, Heitmeier MR, Scarim AL, Marino MH, Manning PT, Corbett JA. IL-1 produced and released endogenously within human islets inhibits beta cell function. J Clin Invest. 1998 Aug 1;102(3):516–26.

67. Mandrup-Poulsen T, Bendtzen K, Nerup J, Dinarello CA, Svenson M, Nielsen JH. Affinity-purified human interleukin I is cytotoxic to isolated islets of Langerhans. Diabetologia. 1986 Jan;29(1):63–7.

68. Mandrup-Poulsen T, Bendtzen K, Nielsen JH, Bendixen G, Nerup J. Cytokines cause functional and structural damage to isolated islets of Langerhans. Allergy. 1985 Aug;40(6):424–9.

69. Donath MY, Ehses JA, Maedler K, Schumann DM, Ellingsgaard H, Eppler E, et al. Mechanisms of beta-cell death in type 2 diabetes. Diabetes. 2005 Dec;54 Suppl 2:S108–13.

70. Han J, Song B, Kim J, Kodali VK, Pottekat A, Wang M, et al. Antioxidants Complement the Requirement for Protein Chaperone Function to Maintain β-Cell Function and Glucose Homeostasis. Diabetes. 2015 Jul 23;64(8):2892–904.

71. Westwell-Roper C, Dai DL, Soukhatcheva G, Potter KJ, van Rooijen N, Ehses JA, et al. IL-1 Blockade Attenuates Islet Amyloid Polypeptide-Induced Proinflammatory Cytokine Release and Pancreatic Islet Graft Dysfunction. The Journal of Immunology. 2011 Aug 19;187(5):2755–65.

72. Masters SL, Dunne A, Subramanian SL, Hull RL, Tannahill GM, Sharp FA, et al. Activation of the NLRP3 inflammasome by islet amyloid polypeptide provides a mechanism for enhanced IL-1β in type 2 diabetes. Nat Immunol. 2010 Sep 12;11(10):897–904.

73. Huang CJ, Lin CY, Haataja L, Gurlo T, Butler AE, Rizza RA, et al. High Expression Rates of Human Islet Amyloid Polypeptide Induce Endoplasmic Reticulum Stress Mediated -Cell Apoptosis, a Characteristic of Humans With Type 2 but Not Type 1 Diabetes. Diabetes. 2007 Aug 1;56(8):2016–27.

74. Martindale JL, Holbrook NJ. Cellular response to oxidative stress: signaling for suicide and survival. J Cell Physiol. 2002 Jul;192(1):1–15.

75. Pi J, Bai Y, Zhang Q, Corkey BE, Wong V, Floering LM, et al. Reactive Oxygen Species as a Signal in Glucose-Stimulated Insulin Secretion. Diabetes. 2007 Jun 27;56(7):1783–91.

76. Lenzen S, Drinkgern J, Tiedge M. Low antioxidant enzyme gene expression in pancreatic islets compared with various other mouse tissues. Free Radic Biol Med. 1996;20(3):463–6.

77. Lenzen S. Oxidative stress: the vulnerable β-cell. Biochem Soc Trans. 2008 Jun 1;36(3):343.

78. Robertson RP. Chronic Oxidative Stress as a Central Mechanism for Glucose Toxicity in Pancreatic Islet Beta Cells in Diabetes. Journal of Biological Chemistry. 2004 Jul 16;279(41):42351–4.

79. Leinonen J, Lehtimäki T, Toyokuni S, Okada K, Tanaka T, Hiai H, et al. New biomarker evidence of oxidative DNA damage in patients with non-insulin-dependent diabetes mellitus. FEBS Lett. Federation of European Biochemical Societies; 1997 Nov 3;417(1):150–2.

80. Dandona P, Thusu K, Cook S, Snyder B, Makowski J, Armstrong D, et al. Oxidative damage to DNA in diabetes mellitus. Lancet. 1996 Feb 17;347(8999):444–5.

81. Sakuraba H, Mizukami H, Yagihashi N, Wada R, Hanyu C, Yagihashi S. Reduced beta-cell mass and expression of oxidative stress-related DNA damage in the islet of Japanese Type II diabetic patients. Diabetologia. 2002 Jan;45(1):85–96.

82. Harmon JS, Bogdani M, Parazzoli SD, Mak SSM, Oseid EA, Berghmans M, et al. β-Cell-Specific Overexpression of Glutathione Peroxidase Preserves Intranuclear MafA and Reverses Diabetes in db/dbMice. Endocrinology. 2009 Nov;150(11):4855–62.

83. Kubisch HM, Wang J, Bray TM, Phillips JP. Targeted overexpression of Cu/Zn superoxide dismutase protects pancreatic β-cells against oxidative stress. Diabetes. 1997.

84. Clark A, Saad MF, Nezzer T, Uren C, Knowler WC, Bennett PH, et al. Islet amyloid polypeptide in diabetic and non-diabetic Pima Indians. Diabetologia. 1990 May;33(5):285–9.

85. Zhao H-L, Lai FMM, Tong PCY, Zhong D-R, Yang D, Tomlinson B, et al. Prevalence and clinicopathological characteristics of islet amyloid in chinese patients with type 2 diabetes. Diabetes. 2003 Nov;52(11):2759–66.

86. Butler AE, Janson J, Bonner-Weir S, Ritzel R, Rizza RA, Butler PC. β-Cell deficit and increased β-cell apoptosis in humans with type 2 diabetes. Diabetes. Am Diabetes Assoc; 2003;52(1):102–10.

87. Westwell-Roper CY, Ehses JA, Verchere CB. Resident Macrophages Mediate Islet Amyloid Polypeptide-Induced Islet IL-1 Production and -Cell Dysfunction.

Diabetes. 2014 Apr 22;63(5):1698–711.

88. Huang CJ, Haataja L, Gurlo T, Butler AE, Wu X, Soeller WC, et al. Induction of endoplasmic reticulum stress-induced -cell apoptosis and accumulation of polyubiquitinated proteins by human islet amyloid polypeptide. Am J Physiol Endocrinol Metab. 2007 Oct 23;293(6):E1656–62.

89. Janson J, Ashley RH, Harrison D, McIntyre S, Butler PC. The mechanism of islet amyloid polypeptide toxicity is membrane disruption by intermediate-sized toxic amyloid particles. Diabetes. Am Diabetes Assoc; 1999;48(3):491–8.

90. Potter KJ, Abedini A, Marek P, Klimek AM, Butterworth S, Driscoll M, et al. Islet amyloid deposition limits the viability of human islet grafts but not porcine islet grafts. Proc Natl Acad Sci USA. 2010 Mar 2;107(9):4305–10.

91. Butler AE, Jang J, Gurlo T, Carty MD, Soeller WC, Butler PC. Diabetes due to a progressive defect in beta-cell mass in rats transgenic for human islet amyloid polypeptide (HIP Rat): a new model for type 2 diabetes. Diabetes. 2004 Jun;53(6):1509–16.

92. Janson J, Soeller WC, Roche PC, Nelson RT, Torchia AJ, Kreutter DK, et al. Spontaneous diabetes mellitus in transgenic mice expressing human islet amyloid polypeptide. Proc Natl Acad Sci USA. 1996 Jul 9;93(14):7283–8.

93. Eizirik DL, Cnop M. ER stress in pancreatic β cells: the thin red line between adaptation and failure. Sci Signal. 2010.

94. Papa FR. Endoplasmic Reticulum Stress, Pancreatic -Cell Degeneration, and Diabetes. Cold Spring Harbor Perspectives in Medicine. 2012 Sep 4;2(9):a007666–6.

95. Harding HP, Ron D. Endoplasmic reticulum stress and the development of diabetes a review. Diabetes. Am Diabetes Assoc; 2002;51(suppl 3):S455–61.

96. Zhang K, Kaufman RJ. From endoplasmic-reticulum stress to the inflammatory response. Nature. 2008 Jul 24;454(7203):455–62.

97. Cnop M, Foufelle F, Velloso LA. Endoplasmic reticulum stress, obesity and diabetes. Trends in Molecular Medicine. Elsevier Ltd; 2012 Jan 1;18(1):59–68.

98. Omikorede O, Qi C, Gorman T, Chapman P, Yu A, Smith DM, et al. ER stress in rodent islets of Langerhans is concomitant with obesity and b-cell compensation but not with b-cell dysfunctionand diabetes. Nutrition & Diabetes. Nature Publishing Group; 2013 Oct 1;3(10):e93–9.

99. Laybutt DR, Preston AM, Åkerfeldt MC, Kench JG, Busch AK, Biankin AV, et al. Endoplasmic reticulum stress contributes to beta cell apoptosis in type 2 diabetes. Diabetologia. 2007 Feb 1;50(4):752–63.

100. Marchetti P, Bugliani M, Lupi R, Marselli L, Masini M, Boggi U, et al. The endoplasmic reticulum in pancreatic beta cells of type 2 diabetes patients. Diabetologia. 2007 Sep 30;50(12):2486–94.

101. Oyadomari S, Koizumi A, Takeda K, Gotoh T, Akira S, Araki E, et al. Targeted disruption of the Chop gene delays endoplasmic reticulum stress–mediated diabetes. J Clin Invest. 2002 Feb 15;109(4):525–32.

102. Ozcan U. Chemical Chaperones Reduce ER Stress and Restore Glucose Homeostasis in a Mouse Model of Type 2 Diabetes. Science. 2006 Aug 25;313(5790):1137–40.

103. Teodoro-Morrison T, Schuiki I, Zhang L, Belsham DD, Volchuk A. GRP78 overproduction in pancreatic beta cells protects against high-fat-diet-induced diabetes in mice. Diabetologia. 2013 Mar 9;56(5):1057–67.

104. Song B, Scheuner D, Ron D, Pennathur S, Kaufman RJ. Chop deletion reduces oxidative stress, improves β cell function, and promotes cell survival in multiple mouse models of diabetes. J Clin Invest. 2008 Oct 1;118(10):3378–89.

105. Meier JJ, Bonadonna RC. Role of Reduced -Cell Mass Versus Impaired -Cell Function in the Pathogenesis of Type 2 Diabetes. Diabetes Care. 2013 Jul 23;36(Supplement_2):S113–9.

106. Clark A, Jones LC, de Koning E, Hansen BC, Matthews DR. Decreased insulin secretion in type 2 diabetes: a problem of cellular mass or function? Diabetes. 2001 Feb;50 Suppl 1:S169–71.

107. Rahier J, Guiot Y, Goebbels RM, Sempoux C, Henquin JC. Pancreatic β-cell mass in European subjects with type 2 diabetes. Diabetes, Obesity and Metabolism. 2008 Nov;10:32–42.

108. Marchetti P, Del Guerra S, Marselli L, Lupi R, Masini M, Pollera M, et al. Pancreatic Islets from Type 2 Diabetic Patients Have Functional Defects and Increased Apoptosis That Are Ameliorated by Metformin. Journal of Clinical Endocrinology & Metabolism. 2004 Nov;89(11):5535–41.

109. Cohen GM. Caspases: the executioners of apoptosis. Biochem J. 1997 Aug 15;326 (Pt 1):1–16.

110. Masini M, Marselli L, Bugliani M, Martino L, Masiello P, Marchetti P, et al. Ultrastructural morphometric analysis of insulin secretory granules in human type 2 diabetes. Acta Diabetol. 2012 Nov 25;49(S1):247–52.

111. Marselli L, Suleiman M, Masini M, Campani D, Bugliani M, Syed F, et al. Are we overestimating the loss of beta cells in type 2 diabetes? Diabetologia. 2013 Nov 15;57(2):362–5.

112. Ward WK, LaCava EC, Paquette TL, Beard JC, Wallum BJ, Porte D. Disproportionate elevation of immunoreactive proinsulin in type 2 (non-insulin-dependent) diabetes mellitus and in experimental insulin resistance. Diabetologia. 1987 Sep;30(9):698–702.

113. Greenwood RH, Mahler RF, Hales CN. Improvement in insulin secretion in diabetes after diazoxide. Lancet. 1976.

114. Guldstrand M, Grill V, Björklund A, Lins PE, Adamson U. Improved beta cell function after short-term treatment with diazoxide in obese subjects with type 2 diabetes. Diabetes Metab. 2002 Dec;28(6 Pt 1):448–56.

115. Laedtke T, Kjems L, Pørksen N, Schmitz O, Veldhuis J, Kao PC, et al. Overnight inhibition of insulin secretion restores pulsatility and proinsulin/insulin ratio in type 2 diabetes. Am J Physiol Endocrinol Metab. 2000 Sep;279(3):E520–8.

116. Weir GC, Aguayo-Mazzucato C, Bonner-Weir S. β-cell dedifferentiation in diabetes is important, but what is it? islets. 2014 Oct 27;5(5):233–7.

117. Blau HM, Baltimore D. Differentiation requires continuous regulation. J Cell Biol. 1991 Mar;112(5):781–3.

118. Szabat M, Lynn FC, Hoffman BG, Kieffer TJ, Allan DW, Johnson JD. Maintenance of -Cell Maturity and Plasticity in the Adult Pancreas: Developmental Biology Concepts in Adult Physiology. Diabetes. 2012 May 22;61(6):1365–71.

119. Stoffers DA, Zinkin NT, Stanojevic V, Clarke WL, Habener JF. Pancreatic agenesis attributable to a single nucleotide deletion in the human IPF1 gene coding sequence. Nat Genet. 1997 Jan;15(1):106–10.

120. Jonsson J, Carlsson L, Edlund T, Edlund H. Insulin-promoter-factor 1 is required for pancreas development in mice. Nature. Nature Publishing Group; 1994;371(6498):606–9.

121. Gao T, McKenna B, Li C, Reichert M, Nguyen J, Singh T, et al. Pdx1 Maintains β Cell Identity and Function by Repressing an α Cell Program. Cell Metabolism. 2014 Feb;19(2):259–71.

122. Sander M, Sussel L, Conners J, Scheel D, Kalamaras J, Cruz Dela F, et al. Homeobox gene Nkx6.1 lies downstream of Nkx2.2 in the major pathway of beta-cell formation in the pancreas. Development. 2000 Dec;127(24):5533–40.

123. Hang Y, Yamamoto T, Benninger RKP, Brissova M, Guo M, Bush W, et al. The MafA Transcription Factor Becomes Essential to Islet -Cells Soon After Birth. Diabetes. 2014 May 22;63(6):1994–2005.

124. Schaffer AE, Taylor BL, Benthuysen JR, Liu J, Thorel F, Yuan W, et al. Nkx6.1

Controls a Gene Regulatory Network Required for Establishing and Maintaining Pancreatic Beta Cell Identity. Grapin-Botton A, editor. PLoS Genet. 2013 Jan 31;9(1):e1003274–15.

125. Nishimura W, Takahashi S, Yasuda K. MafA is critical for maintenance of the mature beta cell phenotype in mice. Diabetologia. 2014 Dec 13;58(3):566–74.

126. Talchai C, Xuan S, Lin HV, Sussel L, Accili D. Pancreatic β Cell Dedifferentiation as a Mechanism of Diabetic β Cell Failure. Cell. Elsevier Inc; 2012 Sep 14;150(6):1223–34.

127. Puri S, Akiyama H, Hebrok M. VHL-mediated disruption of Sox9 activity compromises -cell identity and results in diabetes mellitus. Genes & Development. 2013 Dec 2;27(23):2563–75.

128. Wang Z, York NW, Nichols CG, Remedi MS. Pancreatic β Cell Dedifferentiation in Diabetes and Redifferentiation following Insulin Therapy. Cell Metabolism. 2014 May;19(5):872–82.

129. Szabat M, Page MM, Panzhinskiy E, Skovsø S, Mojibian M, Fernandez-Tajes J, et al. Reduced Insulin Production Relieves Endoplasmic Reticulum Stress and Induces β Cell Proliferation. Cell Metabolism. 2015 Nov.

130. Guo S, Dai C, Guo M, Taylor B, Harmon JS, Sander M, et al. Inactivation of specific β cell transcription factors in type 2 diabetes. J Clin Invest. 2013 Jul 1;123(8):3305–16.

131. Cinti F, Bouchi R, Kim-Muller JY, Ohmura Y, Rodrigo Sandoval P, Masini M, et al. Evidence of β-cell Dedifferentiation in Human Type 2 Diabetes. Journal of Clinical Endocrinology & Metabolism. 2015 Dec 29;:jc.2015–860.

132. Butler AE, Dhawan S, Hoang J, Cory M, Zeng K, Fritsch H, et al. Beta-cell deficit in Obese Type 2 Diabetes, a Minor Role of Beta-cell Dedifferentiation and Degranulation. Journal of Clinical Endocrinology & Metabolism. 2015 Dec 23;:jc.2015–3566.

133. Taylor BL, Zhulin IB. PAS domains: internal sensors of oxygen, redox potential, and light. Microbiol Mol Biol Rev. 1999 Jun;63(2):479–506.

134. Blanchet E, Van de Velde S, Matsumura S, Hao E, LeLay J, Kaestner K, et al. Feedback Inhibition of CREB Signaling Promotes Beta Cell Dysfunction in Insulin Resistance. CellReports. The Authors; 2015 Feb 24;10(7):1149–57.

135. Turek FW. Obesity and Metabolic Syndrome in Circadian Clock Mutant Mice. Science. 2005 May 13;308(5724):1043–5.

136. Marcheva B, Ramsey KM, Buhr ED, Kobayashi Y, Su H, Ko CH, et al. Disruption of the clock components CLOCK and BMAL1 leads to hypoinsulinaemia and

diabetes. Nature. Nature Publishing Group; 2010 Jul 19;466(7306):627–31.

137. Lee J, Moulik M, Fang Z, Saha P, Zou F, Xu Y, et al. Bmal1 and -Cell Clock Are Required for Adaptation to Circadian Disruption, and Their Loss of Function Leads to Oxidative Stress-Induced -Cell Failure in Mice. Molecular and Cellular Biology. 2013 May 8;33(11):2327–38.

138. Perelis M, Marcheva B, Moynihan Ramsey K, Schipma MJ, Hutchison AL, Taguchi A, et al. Pancreatic cell enhancers regulate rhythmic transcription of genes controlling insulin secretion. Science. 2015 Nov 5;350(6261):aac4250–0.

139. Jaakkola P, Mole DR, Tian YM, Wilson MI, Gielbert J, Gaskell SJ, et al. Targeting of HIF-alpha to the von Hippel-Lindau Ubiquitylation Complex by O2-Regulated Prolyl Hydroxylation. Science. 2001 Apr 20;292(5516):468–72.

140. Maxwell PH, Wiesener MS, Chang GW, Clifford SC, Vaux EC, Cockman ME, et al. The tumour suppressor protein VHL targets hypoxia-inducible factors for oxygen-dependent proteolysis. Nature. 1999 May 20;399(6733):271–5.

141. Salceda S, Caro J. Hypoxia-inducible Factor 1 (HIF-1) Protein Is Rapidly Degraded by the Ubiquitin-Proteasome System under Normoxic Conditions: ITS STABILIZATION BY HYPOXIA DEPENDS ON REDOX-INDUCED CHANGES. Journal of Biological Chemistry. 1997 Sep 5;272(36):22642–7.

142. Wenger RH, Stiehl DP, Camenisch G. Integration of Oxygen Signaling at the Consensus HRE. Science Signaling. 2005 Oct 18;2005(306):re12–2.

143. Sato Y, Endo H, Okuyama H, Takeda T, Iwahashi H, Imagawa A, et al. Cellular Hypoxia of Pancreatic -Cells Due to High Levels of Oxygen Consumption for Insulin Secretion in Vitro. Journal of Biological Chemistry. 2011 Apr 1;286(14):12524–32.

144. Bensellam M, Duvillie B, Rybachuk G, Laybutt DR, Magnan C, Guiot Y, et al. Glucose-Induced O2 Consumption Activates Hypoxia Inducible Factors 1 and 2 in Rat Insulin-Secreting Pancreatic Beta-Cells. Gaetano C, editor. PLoS ONE. 2012 Jan 3;7(1):e29807–15.

145. Chandel NS, Maltepe E, Goldwasser E, Mathieu CE, Simon MC, Schumacker PT. Mitochondrial reactive oxygen species trigger hypoxia-induced transcription. Proc Natl Acad Sci USA. 1998 Sep 29;95(20):11715–20.

146. Chandel NS, McClintock DS, Feliciano CE, Wood TM, Melendez JA, Rodriguez AM, et al. Reactive Oxygen Species Generated at Mitochondrial Complex III Stabilize Hypoxia-inducible Factor-1 during Hypoxia: A MECHANISM OF O2 SENSING. J Biol Chem. 2000 Aug 18;275(33):25130–8.

147. Guzy RD, Hoyos B, Robin E, Chen H, Liu L, Mansfield KD, et al. Mitochondrial complex III is required for hypoxia-induced ROS production and cellular oxygen

sensing. Cell Metabolism. 2005 Jun;1(6):401–8.

148. Majmundar AJ, Wong WJ, Simon MC. Hypoxia-inducible factors and the response to hypoxic stress. Molecular cell. 2010 Oct 22;40(2):294–309.

149. Cheng K, Ho K, Stokes R, Scott C, Lau SM, Hawthorne WJ, et al. Hypoxia-inducible factor-1α regulates β cell function in mouse and human islets. J Clin Invest. 2010 Jun 1;120(6):2171–83.

150. Gunton JE, Kulkarni RN, Yim S, Okada T, Hawthorne WJ, Tseng Y-H, et al. Loss of ARNT/HIF1β Mediates Altered Gene Expression and Pancreatic-Islet Dysfunction in Human Type 2 Diabetes. Cell. 2005 Aug;122(3):337–49.

151. Pillai R, Huypens P, Huang M, Schaefer S, Sheinin T, Wettig SD, et al. Aryl Hydrocarbon Receptor Nuclear Translocator/Hypoxia-inducible Factor-1 Plays a Critical Role in Maintaining Glucose-stimulated Anaplerosis and Insulin Release from Pancreatic -Cells. Journal of Biological Chemistry. 2011 Jan 7;286(2):1014–24.

152. Pillai R, Paglialunga S, Hoang M, Cousteils K, Prentice KJ, Bombardier E, et al. Deletion of ARNT/HIF1β in pancreatic beta cells does not impair glucose homeostasis in mice, but is associated with defective glucose sensing ex vivo. Diabetologia. 2015 Sep 26;:1–11.

153. Cantley J, Selman C, Shukla D, Abramov AY, Forstreuter F, Esteban MA, et al. Deletion of the von Hippel–Lindau gene in pancreatic β cells impairs glucose homeostasis in mice. J Clin Invest. Am Soc Clin Investig; 2009;119(119 (1)):125–35.

154. Zehetner J, Danzer C, Collins S, Eckhardt K, Gerber PA, Ballschmieter P, et al. pVHL is a regulator of glucose metabolism and insulin secretion in pancreatic cells. Genes & Development. 2008 Nov 15;22(22):3135–46.

155. Puri S, Cano DA, Hebrok M. A Role for von Hippel-Lindau Protein in Pancreatic -Cell Function. Diabetes. 2008 Nov 4;58(2):433–41.

156. Ooe N, Saito K, Mikami N, Nakatuka I, Kaneko H. Identification of a novel basic helix-loop-helix-PAS factor, NXF, reveals a Sim2 competitive, positive regulatory role in dendritic-cytoskeleton modulator drebrin gene expression. Molecular and Cellular Biology. Am Soc Microbiol; 2004;24(2):608–16.

157. Moser M, Knoth R, Bode C, Patterson C. LE-PAS, a novel Arnt-dependent HLH-PAS protein, is expressed in limbic tissues and transactivates the CNS midline enhancer element. Molecular Brain Research. 2004 Sep;128(2):141–9.

158. Kim T-K, Hemberg M, Gray JM, Costa AM, Bear DM, Wu J, et al. Widespread transcription at neuronal activity-regulated enhancers. Nature. Nature Publishing Group; 2011 Jan 5;465(7295):182–7.

159. Bloodgood BL, Sharma N, Browne HA, Trepman AZ, Greenberg ME. The activity-dependent transcription factor NPAS4 regulates domain-specific inhibition. Nature. Nature Publishing Group; 2014 Apr 9;503(7474):121–5.

160. Ibi D, Takuma K, Koike H, Mizoguchi H, Tsuritani K, Kuwahara Y, et al. Social isolation rearing-induced impairment of the hippocampal neurogenesis is associated with deficits in spatial memory and emotion-related behaviors in juvenile mice. J Neurochem. 2008 May;105(3):921–32.

161. Yun J, Koike H, Ibi D, Toth E, Mizoguchi H, Nitta A, et al. Chronic restraint stress impairs neurogenesis and hippocampus-dependent fear memory in mice: possible involvement of a brain-specific transcription factor Npas4. J Neurochem. 2010 Sep 2;114(6):1840–51.

162. Shamloo M, Soriano L, Schack von D, Rickhag M, Chin DJ, Gonzalez-Zulueta M, et al. Npas4, a novel helix-loop-helix PAS domain protein, is regulated in response to cerebral ischemia. European Journal of Neuroscience. 2006 Nov;24(10):2705–20.

163. Ooe N, Motonaga K, Kobayashi K, Saito K, Kaneko H. Functional Characterization of Basic Helix-Loop-Helix-PAS Type Transcription Factor NXF in Vivo PUTATIVE INVOLVEMENT IN AN “ON DEMAND” NEUROPROTECTION SYSTEM. Journal of Biological Chemistry. ASBMB; 2009;284(2):1057–63.

164. Lin Y, Bloodgood BL, Hauser JL, Lapan AD, Koon AC, Kim T-K, et al. Activity-dependent regulation of inhibitory synapse development by Npas4. Nature. 2008 Sep 24;455(7217):1198–204.

165. Ramamoorthi K, Fropf R, Belfort GM, Fitzmaurice HL, McKinney RM, Neve RL, et al. Npas4 Regulates a Transcriptional Program in CA3 Required for Contextual Memory Formation. Science. 2011 Dec 23;334(6063):1669–75.

166. Unfried C, Burbach G, Korf H-W, Gall von C. Melatonin receptor 1-dependent gene expression in the mouse pars tuberalis as revealed by cDNA microarray analysis and in situhybridization. Journal of Pineal Research. 2010 Mar;48(2):148–56.

167. Human Variants in the Neuronal Basic Helix-Loop-Helix/Per-Arnt-Sim (bHLH/PAS) Transcription Factor Complex NPAS4/ARNT2 Disrupt Function. PLoS ONE. 2014;9(1):e85768.

168. Floor K, Barøy T, Misceo D, Kanavin ØJ, Fannemel M, Frengen E. A 1 Mb de novo deletion within 11q13.1q13.2 in a boy with mild intellectual disability and minor dysmorphic features. European Journal of Medical Genetics. 2012 Dec;55(12):695–9.

169. Luo J, Deng Z-L, Luo X, Tang N, Song W-X, Chen J, et al. A protocol for rapid

generation of recombinant adenoviruses using the AdEasy system. Nat Protoc. 2007 May;2(5):1236–47.

170. Ohta Y, Kosaka Y, Kishimoto N, Wang J, Smith SB, Honig G, et al. Convergence of the Insulin and Serotonin Programs in the Pancreatic -Cell. Diabetes. 2011 Nov 21;60(12):3208–16.

171. Riddelle KS, Green KJ, Jones JC. Formation of hemidesmosomes in vitro by a transformed rat bladder cell line. J Cell Biol. 1991 Jan;112(1):159–68.

172. Wang Z, Zhu T, Rehman KK, Bertera S, Zhang J, Chen C, et al. Widespread and stable pancreatic gene transfer by adeno-associated virus vectors via different routes. Diabetes. 2006 Apr;55(4):875–84.

173. Muzumdar MD, Tasic B, Miyamichi K, Li L, Luo L. A global double-fluorescent Cre reporter mouse. genesis. 2007;45(9):593–605.

174. Gu G, Dubauskaite J, Melton DA. Direct evidence for the pancreatic lineage: NGN3+ cells are islet progenitors and are distinct from duct progenitors. Development. The Company of Biologists Limited; 2002;129(10):2447–57.

175. Thorens B, Tarussio D, Maestro MA, Rovira M, Heikkilä E, Ferrer J. Ins1 Cre knock-in mice for beta cell-specific gene recombination. Diabetologia. 2014 Dec 11;58(3):558–65.

176. Mitchell KJ, Lai FA, Rutter GA. Ryanodine Receptor Type I and Nicotinic Acid Adenine Dinucleotide Phosphate Receptors Mediate Ca2+ Release from Insulin-containing Vesicles in Living Pancreatic -Cells (MIN6). J Biol Chem. 2003 Mar 28;278(13):11057–64.

177. Fill M, Copello JA. Ryanodine Receptor Calcium Release Channels. Physiological Reviews. 2002 Oct 1;82(4):893–922.

178. Mikoshiba K. IP 3receptor/Ca 2+channel: from discovery to new signaling concepts. J Neurochem. 2007 Sep;102(5):1426–46.

179. Blondel O, Moody MM, Depaoli AM. Localization of inositol trisphosphate receptor subtype 3 to insulin and somatostatin secretory granules and regulation of expression in islets and insulinoma cells. 1994.

180. Chin D, Means AR. Calmodulin: a prototypical calcium sensor. Trends in cell biology. 2000.

181. Clapham DE. Calcium Signaling. Cell. 2007 Dec;131(6):1047–58.

182. Berridge MJ. Calcium signalling remodelling and disease. Biochem Soc Trans. 2012 Apr 1;40(2):297–309.

183. Zieg J, Greer PL, Greenberg ME. SnapShot: Ca2+-Dependent Transcription in Neurons. Cell. 2008 Sep;134(6):1080–2.

184. Okuno H. Regulation and function of immediate-early genes in the brain: Beyond neuronal activity markers. Neuroscience Research. Elsevier Ireland Ltd and Japan Neuroscience Society; 2011 Mar 1;69(3):175–86.

185. Gilon P, Chae H-Y, Rutter GA, Ravier MA. Calcium signaling in pancreatic β-cells in health and in Type 2 diabetes. Cell Calcium. Elsevier Ltd; 2014 Nov 1;56(5):340–61.

186. Wilson ME, Scheel D, German MS. Gene expression cascades in pancreatic development. Mechanisms of development. 2003.

187. Lytton J, Westlin M, Hanley MR. Thapsigargin inhibits the sarcoplasmic or endoplasmic reticulum Ca-ATPase family of calcium pumps. Journal of Biological Chemistry. 1991.

188. Burant CF. Activation of GPR40 as a Therapeutic Target for the Treatment of Type 2 Diabetes. Diabetes Care. 2013 Jul 23;36(Supplement_2):S175–9.

189. Szkudelski T. The mechanism of alloxan and streptozotocin action in B cells of the rat pancreas. Physiol Res. 2001;50(6):537–46.

190. Robbins MJ, Sharp RA, Slonim AE, Burr IM. Protection against streptozotocin-induced diabetes by superoxide dismutase. Diabetologia. Springer; 1980;18(1):55–8.

191. O'Brien BA, Harmon BV, Cameron DP, Allan DJ. Beta-cell apoptosis is responsible for the development of IDDM in the multiple low-dose streptozotocin model. J Pathol. 1996 Feb;178(2):176–81.

192. Kröncke KD, Fehsel K, Sommer A, Rodriguez ML, Kolb-Bachofen V. Nitric oxide generation during cellular metabolization of the diabetogenic N-methyl-N-nitroso-urea streptozotozin contributes to islet cell DNA damage. Biol Chem Hoppe-Seyler. 1995 Mar;376(3):179–85.

193. Schneider-Poetsch T, Ju J, Eyler DE, Dang Y, Bhat S, Merrick WC, et al. Inhibition of eukaryotic translation elongation by cycloheximide and lactimidomycin. Nat Chem Biol. 2010 Mar;6(3):209–17.

194. Safran M, Kaelin WG Jr. HIF hydroxylation and the mammalian oxygen-sensing pathway. J Clin Invest. 2003 Mar 15;111(6):779–83.

195. Barrett TD, Palomino HL, Brondstetter TI, Kanelakis KC, Wu X, Haug PV, et al. Pharmacological Characterization of 1-(5-Chloro-6-(trifluoromethoxy)-1H-benzoimidazol-2-yl)-1H-pyrazole-4-carboxylic Acid (JNJ-42041935), a Potent and Selective Hypoxia-Inducible Factor Prolyl Hydroxylase Inhibitor. Molecular

Pharmacology. 2011 May 17;79(6):910–20.

196. Jhala US, Canettieri G, Screaton RA, Kulkarni RN, Krajewski S, Reed J, et al. cAMP promotes pancreatic beta-cell survival via CREB-mediated induction of IRS2. Genes & Development. 2003 Jul 1;17(13):1575–80.

197. Bernal-Mizrachi E, Wice B, Inoue H, Permutt MA. Activation of Serum Response Factor in the Depolarization Induction of Egr-1 Transcription in Pancreatic Islet -Cells. J Biol Chem. 2000 Aug 18;275(33):25681–9.

198. Persaud SJ, Liu B, Sampaio HB, Jones PM, Muller DS. Calcium/calmodulin-dependent kinase IV controls glucose-induced Irs2 expression in mouse beta cells via activation of cAMP response element-binding protein. Diabetologia. 2011 Feb 8;54(5):1109–20.

199. Demozay D, Tsunekawa S, Briaud I, Shah R, Rhodes CJ. Specific Glucose-Induced Control of Insulin Receptor Substrate-2 Expression Is Mediated via Ca2+-Dependent Calcineurin/NFAT Signaling in Primary Pancreatic Islet -Cells. Diabetes. 2011 Oct 24;60(11):2892–902.

200. Lawrence MC, Bhatt HS, Watterson JM, Easom RA. Regulation of insulin gene transcription by a Ca(2+)-responsive pathway involving calcineurin and nuclear factor of activated T cells. Mol Endocrinol. 2001 Oct;15(10):1758–67.

201. Liu B, Barbosa-Sampaio H, Jones PM, Persaud SJ, Muller DS. The CaMK4/CREB/IRS-2 Cascade Stimulates Proliferation and Inhibits Apoptosis of β-Cells. Tsilibary EC, editor. PLoS ONE. 2012 Sep 25;7(9):e45711–9.

202. Wang P, Alvarez-Perez J-C, Felsenfeld DP, Liu H, Sivendran S, Bender A, et al. A high-throughput chemical screen reveals that harmine-mediated inhibition of DYRK1A increases human pancreatic beta cell replication. Nature Medicine. 2015 Mar 9;21(4):383–8.

203. Shen W, Taylor B, Jin Q, Van Nguyen-Tran, Meeusen S, Zhang Y-Q, et al. Inhibition of DYRK1A and GSK3B induces human β-cell proliferation. Nat Commun. Nature Publishing Group; 2015 Oct 17;6:1–11.

204. Goodyer WR, Gu X, Liu Y, Bottino R, Crabtree GR, Kim SK. Neonatal β cell development in mice and humans is regulated by calcineurin/NFAT. Developmental Cell. 2012 Jul 17;23(1):21–34.

205. Heit JJ, Apelqvist ÅA, Gu X, Winslow MM, Neilson JR, Crabtree GR, et al. Calcineurin/NFAT signalling regulates pancreatic β-cell growth and function. Nature. 2006 Sep 21;443(7109):345–9.

206. Speckmann T, Sabatini PV, Nian C, Smith RG, Lynn FC. Npas4 Transcription Factor Expression Is Regulated by Calcium Signaling Pathways and Prevents Tacrolimus-induced Cytotoxicity in Pancreatic Beta Cells. Journal of Biological

Chemistry. 2016 Feb 5;291(6):2682–95.

207. Welsh M, Nielsen DA, MacKrell AJ, Steiner DF. Control of insulin gene expression in pancreatic beta-cells and in an insulin-producing cell line, RIN-5F cells. II. Regulation of insulin mRNA stability. Journal of Biological Chemistry. ASBMB; 1985;260(25):13590–4.

208. Knoch K-P, Bergert H, Borgonovo B, Saeger H-D, Altkrüger A, Verkade P, et al. Polypyrimidine tract-binding protein promotes insulin secretory granule biogenesis. Nat Cell Biol. 2004 Feb 22;6(3):8–214.

209. Pautz A, Linker K, Hubrich T, Korhonen R, Altenhofer S, Kleinert H. The Polypyrimidine Tract-binding Protein (PTB) Is Involved in the Post-transcriptional Regulation of Human Inducible Nitric Oxide Synthase Expression. Journal of Biological Chemistry. 2006 Sep 5;281(43):32294–302.

210. Xu M, Hecht NB. Polypyrimidine Tract Binding Protein 2 Stabilizes Phosphoglycerate Kinase 2 mRNA in Murine Male Germ Cells by Binding to Its 3'UTR. Biology of Reproduction. 2007 May 22;76(6):1025–33.

211. Tillmar L. Control of Insulin mRNA Stability in Rat Pancreatic Islets. REGULATORY ROLE OF A 3'-UNTRANSLATED REGION PYRIMIDINE-RICH SEQUENCE. Journal of Biological Chemistry. 2001 Nov 5;277(2):1099–106.

212. Wang M, Li J, Lim GE, Johnson JD. Is Dynamic Autocrine Insulin Signaling Possible? A Mathematical Model Predicts Picomolar Concentrations of Extracellular Monomeric Insulin within Human Pancreatic Islets. Maedler K, editor. PLoS ONE. 2013 Jun 14;8(6):e64860–10.

213. Deb TB, Coticchia CM, Dickson RB. Calmodulin-mediated Activation of Akt Regulates Survival of c-Myc-overexpressing Mouse Mammary Carcinoma Cells. J Biol Chem. 2004 Sep 3;279(37):38903–11.

214. Danciu TE, Adam RM, Naruse K, Freeman MR, Hauschka PV. Calcium regulates the PI3K-Akt pathway in stretched osteoblasts. FEBS Lett. 2003 Jan 22;536(1-3):193–7.

215. Dart C, Standen NB. Activation of ATP-dependent K+ channels by hypoxia in smooth muscle cells isolated from the pig coronary artery. The Journal of Physiology. 1995.

216. Kanatous SB, Mammen PPA, Rosenberg PB, Martin CM, White MD, DiMaio JM, et al. Hypoxia reprograms calcium signaling and regulates myoglobin expression. AJP: Cell Physiology. 2008 Dec 31;296(3):C393–C402.

217. Blodgett DM, Nowosielska A, Afik S, Pechhold S, Cura AJ, Kennedy NJ, et al. Novel Observations from Next Generation RNA Sequencing of Highly Purified Human Adult and Fetal Islet Cell Subsets. Diabetes. 2015 Apr 30;:db150039–

10.

218. Shiao MS, Liao BY, Long M, Yu HT. Adaptive Evolution of the Insulin Two-Gene System in Mouse. Genetics. 2008 Feb 1;178(3):1683–91.

219. Melloul D, Marshak S, Cerasi E. Regulation of insulin gene transcription. Diabetologia. Springer; 2002;45(3):309–26.

220. Andrali SS, Sampley ML, Vanderford NL, Özcan S. Glucose regulation of insulin gene expression in pancreatic β-cells. Biochem J. 2008 Oct 1;415(1):1.

221. Lu M, Seufert J, Habener JF. Pancreatic β-Cell-specific Repression of Insulin Gene Transcription by CCAAT/Enhancer-binding Protein β INHIBITORY INTERACTIONS WITH BASIC HELIX-LOOP- …. Journal of Biological Chemistry. 1997.

222. TAYLOR KW, PARRY DG, SMITH GH. BIOSYNTHETIC LABELLING OF MAMMALIAN INSULINS IN VITRO. Nature. 1964 Sep 12;203:1144–5.

223. PARRY DG, TAYLOR KW. The effects of sugars on incorporation of [3H)leucine into insulins. Biochem J. 1966 Jul;100(1):2C–4C.

224. Muller D. Identification of Insulin Signaling Elements in Human -Cells: Autocrine Regulation of Insulin Gene Expression. Diabetes. 2006 Oct 1;55(10):2835–42.

225. Alarcon C, Verchere CB, Rhodes CJ. Translational Control of Glucose-Induced Islet Amyloid Polypeptide Production in Pancreatic Islets. Endocrinology. 2012 Apr 20;153(5):2082–7.

226. Schuit FC, In't Veld PA, Pipeleers DG. Glucose stimulates proinsulin biosynthesis by a dose-dependent recruitment of pancreatic beta cells. Proc Natl Acad Sci USA. 1988 Jun;85(11):3865–9.

227. Goodison S, Kenna S, Ashcroft SJ. Control of insulin gene expression by glucose. Biochem J. 1992 Jul 15;285 (Pt 2):563–8.

228. German MS, Moss LG, Rutter WJ. Regulation of insulin gene expression by glucose and calcium in transfected primary islet cultures. J Biol Chem. 1990 Dec 25;265(36):22063–6.

229. Lawrence MC, Borenstein-Auerbach N, McGlynn K, Kunnathodi F, Shahbazov R, Syed I, et al. NFAT Targets Signaling Molecules to Gene Promoters in Pancreatic β-Cells. Mol Endocrinol. 2015 Feb;29(2):274–88.

230. Newsholme P, Cruzat V, Arfuso F, Keane K. Nutrient regulation of insulin secretion and action. J Endocrinol. 2014 May 27;221(3):R105–20.

231. Drucker DJ, Sherman SI, Gorelick FS, Bergenstal RM, Sherwin RS, Buse JB.

Incretin-Based Therapies for the Treatment of Type 2 Diabetes: Evaluation of the Risks and Benefits. Diabetes Care. 2010 Jan 26;33(2):428–33.

232. Drucker DJ. The biology of incretin hormones. Cell Metabolism. Elsevier; 2006;3(3):153–65.

233. Seino Y, Fukushima M, Yabe D. GIP and GLP-1, the two incretin hormones: Similarities and differences. Journal of Diabetes Investigation. 2010 Apr 22;1(1-2):8–23.

234. Holst JJ. Role of incretin hormones in the regulation of insulin secretion in diabetic and nondiabetic humans. AJP: Endocrinology and Metabolism. 2004 Aug 1;287(2):E199–E206.

235. Spiegel I, Mardinly AR, Gabel HW, Bazinet JE, Couch CH, Tzeng CP, et al. Npas4 Regulates Excitatory-Inhibitory Balance within Neural Circuits through Cell-Type-Specific Gene Programs. Cell. Elsevier Inc; 2014 May 22;157(5):1216–29.

236. Tseng CC, Zhang XY. Role of regulator of G protein signaling in desensitization of the glucose-dependent insulinotropic peptide receptor. Endocrinology. 1998 Nov;139(11):4470–5.

237. Van de Velde S, Hogan MF, Montminy M. mTOR links incretin signaling to HIF induction in pancreatic beta cells. Proc Natl Acad Sci USA. 2011 Oct 11;108(41):16876–82.

238. Klinger S, Poussin C, Debril M-B, Dolci W, Halban PA, Thorens B. Increasing GLP-1-induced beta-cell proliferation by silencing the negative regulators of signaling cAMP response element modulator-alpha and DUSP14. Diabetes. 2008 Mar;57(3):584–93.

239. Tennant BR, Robertson AG, Kramer M, Li L, Zhang X, Beach M, et al. Identification and analysis of murine pancreatic islet enhancers. Diabetologia. 2012 Dec 14;56(3):542–52.

240. Ban N, Yamada Y, Someya Y, Ihara Y, Adachi T, Kubota A, et al. Activating transcription factor-2 is a positive regulator in CaM kinase IV-induced human insulin gene expression. Diabetes. 2000 Jul;49(7):1142–8.

241. Jones S. An overview of the basic helix-loop-helix proteins. Genome Biol. 2004;5(6):226.

242. Kehrl JH, Sinnarajah S. RGS2: a multifunctional regulator of G-protein signaling. The International Journal of Biochemistry & Cell Biology. 2002 May;34(5):432–8.

243. Szegezdi E, Logue SE, Gorman AM, Samali A. Mediators of endoplasmic reticulum stress-induced apoptosis. EMBO Rep. 2006 Sep;7(9):880–5.

244. Sabatini PV, Lynn FC. All-encomPASsing regulation of. Trends in Endocrinology & Metabolism. Elsevier Ltd; 2015 Jan 1;26(1):49–57.

245. Stokes RA, Cheng K, Deters N, Lau SM, Hawthorne WJ, O'Connell PJ, et al. Hypoxia-Inducible Factor-1α (HIF-1α) Potentiates β-Cell Survival After Islet Transplantation of Human and Mouse Islets. cell transplant. 2013 Feb 1;22(2):253–66.

246. Marselli L, Thorne J, Dahiya S, Sgroi DC, Sharma A, Bonner-Weir S, et al. Gene Expression Profiles of Beta-Cell Enriched Tissue Obtained by Laser Capture Microdissection from Subjects with Type 2 Diabetes. Westermark P, editor. PLoS ONE. 2010 Jul 13;5(7):e11499.

247. Denko NC. Hypoxia, HIF1 and glucose metabolism in the solid tumour. Nat Rev Cancer. 2008.

248. Seymour PA, Freude KK, Tran MN, Mayes EE, Jensen J, Kist R, et al. SOX9 is required for maintenance of the pancreatic progenitor cell pool. Proc Natl Acad Sci USA. 2007 Feb 6;104(6):1865–70.

249. Luciani DS, Gwiazda KS, Yang TLB, Kalynyak TB, Bychkivska Y, Frey MHZ, et al. Roles of IP3R and RyR Ca2+ Channels in Endoplasmic Reticulum Stress and -Cell Death. Diabetes. 2009 Jan 26;58(2):422–32.

250. Karaskov E. Chronic Palmitate But Not Oleate Exposure Induces Endoplasmic Reticulum Stress, Which May Contribute to INS-1 Pancreatic -Cell Apoptosis. Endocrinology. 2006 Apr 20;147(7):3398–407.

251. Jeffrey KD, Alejandro EU, Luciani DS, Kalynyak TB, Hu X, Li H, et al. Carboxypeptidase E mediates palmitate-induced beta-cell ER stress and apoptosis. Proc Natl Acad Sci USA. 2008 Jun 17;105(24):8452–7.

252. Fonseca SG, Ishigaki S, Oslowski CM, Lu S, Lipson KL, Ghosh R, et al. Wolfram syndrome 1 gene negatively regulates ER stress signaling in rodent and human cells. J Clin Invest. 2010 Mar 1;120(3):744–55.

253. Annibaldi A, Widmann C. Glucose metabolism in cancer cells. Current Opinion in Clinical Nutrition and Metabolic Care. 2010 Jul;13(4):466–70.

254. Amarilio R, Viukov SV, Sharir A, Eshkar-Oren I, Johnson RS, Zelzer E. HIF1 regulation of Sox9 is necessary to maintain differentiation of hypoxic prechondrogenic cells during early skeletogenesis. Development. 2007 Oct 3;134(21):3917–28.

255. Yamada T, Ishihara H, Tamura A, Takahashi R, Yamaguchi S, Takei D, et al. WFS1-deficiency increases endoplasmic reticulum stress, impairs cell cycle progression and triggers the apoptotic pathway specifically in pancreatic beta-cells. Human Molecular Genetics. 2006 May 15;15(10):1600–9.

256. Takacova M, Holotnakova T, Vondracek J, Machala M, Pencikova K, Gradin K, et al. Role of aryl hydrocarbon receptor in modulation of the expression of the hypoxia marker carbonic anhydrase IX. Biochem J. 2009 Apr 15;419(2):419–25.

257. Gradin K, McGuire J, Wenger RH, Kvietikova I, fhitelaw ML, Toftgård R, et al. Functional interference between hypoxia and dioxin signal transduction pathways: competition for recruitment of the Arnt transcription factor. Molecular and Cellular Biology. 1996 Oct;16(10):5221–31.

258. Vorrink SU, Severson PL, Kulak MV, Futscher BW, Domann FE. Hypoxia perturbs aryl hydrocarbon receptor signaling and CYP1A1 expression induced by PCB 126 in human skin and liver-derived cell lines. Toxicology and Applied Pharmacology. Elsevier Inc; 2010 Mar 18;274(3):408–16.

259. Wang Y, Perfetti R, Greig NH, Holloway HW, DeOre KA, Montrose-Rafizadeh C, et al. Glucagon-like peptide-1 can reverse the age-related decline in glucose tolerance in rats. J Clin Invest. 1997 Jun 15;99(12):2883–9.

260. Li L, Trifunovic A, Köhler M, Wang Y, Petrovic Berglund J, Illies C, et al. Defects in β-cell Ca2+ dynamics in age-induced diabetes. Diabetes. 2014 Dec;63(12):4100–14.

261. Mosser RE, Maulis MF, Moullé VS, Dunn JC, Carboneau BA, Arasi K, et al. High-fat diet-induced β-cell proliferation occurs prior to insulin resistance in C57Bl/6J male mice. Am J Physiol Endocrinol Metab. 2015 Apr 1;308(7):E573–82.

262. Omar B, Pacini G, Ahrén B. Differential Development of Glucose Intolerance and Pancreatic Islet Adaptation in Multiple Diet Induced Obesity Models. Nutrients. 2012 Dec;4(12):1367–81.

263. Kwan K-M. Conditional alleles in mice: Practical considerations for tissue-specific knockouts. genesis. 2002 Feb 14;32(2):49–62.

264. Nagy A. Cre recombinase: the universal reagent for genome tailoring. genesis. 2000 Feb;26(2):99–109.

265. Danielian PS, Muccino D, Rowitch DH, Michael SK, McMahon AP. Modification of gene activity in mouse embryos in utero by a tamoxifen-inducible form of Cre recombinase. Curr Biol. 1998 Dec 3;8(24):1323–6.

266. Magnuson MA, Osipovich AB. Pancreas-Specific Cre Driver Lines and Considerations for Their Prudent Use. Cell Metabolism. Elsevier Inc; 2013 Jul 2;18(1):9–20.

267. Wicksteed B, Brissova M, Yan W, Opland DM, Plank JL, Reinert RB, et al. Conditional gene targeting in mouse pancreatic ß-Cells: analysis of ectopic Cre transgene expression in the brain. Diabetes. 2010 Dec;59(12):3090–8.

268. Song J, Xu Y, Hu X, Choi B, Tong Q. Brain expression of Cre recombinase driven by pancreas-specific promoters. genesis. 2010 Oct 19;48(11):628–34.

269. Harno E, Cottrell EC, White A. Perspective. Cell Metabolism. Elsevier Inc; 2013 Jul 2;18(1):21–8.

270. Honig G, Liou A, Berger M, German MS, Tecott LH. Precise pattern of recombination in serotonergic and hypothalamic neurons in a Pdx1-cre transgenic mouse line. Journal of Biomedical Science. 2010;17(1):82.

271. Grayson BE, Seeley RJ, Sandoval DA. Wired on sugar: the role of the CNS inthe regulation of glucose homeostasis. Nature Publishing Group; 2012 Dec 12;:1–14.

272. Könner AC, Klöckener T, Brüning JC. Control of energy homeostasis by insulin and leptin: Targeting the arcuate nucleus and beyond. Physiology & Behavior. Elsevier Inc; 2009 Jul 14;97(5):632–8.

273. Wang L, Opland D, Tsai S, Luk CT, Schroer SA, Allison MB, et al. deletion in RIP-Cre neurons protects against type 2 diabetes by activating the anti-inflammatory reflex. Nature Medicine. Nature Publishing Group; 2014 Apr 20;20(5):490–8.

274. Kong D, Tong Q, Ye C, Koda S, Fuller PM, Krashes MJ, et al. GABAergic RIP-Cre Neurons in the Arcuate Nucleus Selectively Regulate Energy Expenditure. Cell. Elsevier Inc; 2012 Oct 26;151(3):645–57.

275. Kim ER, Wu Z, Sun H, Xu Y, Mangieri LR, Tong Q. Hypothalamic Non-AgRP, Non-POMC GABAergic Neurons Are Required for Postweaning Feeding and NPY Hyperphagia. Journal of Neuroscience. 2015 Jul 22;35(29):10440–50.

276. Reinert RB, Kantz J, Misfeldt AA, Poffenberger G, Gannon M, Brissova M, et al. Tamoxifen-Induced Cre-loxP Recombination Is Prolonged in Pancreatic Islets of Adult Mice. Maedler K, editor. PLoS ONE. 2012 Mar 28;7(3):e33529.

277. Liu Y, Suckale J, Masjkur J, Magro MG, Steffen A, Anastassiadis K, et al. Tamoxifen-Independent Recombination in the RIP-CreER Mouse. Federici M, editor. PLoS ONE. 2010 Oct 22;5(10):e13533.

278. Olefsky J, Farquhar JW, Reaven G. Relationship between fasting plasma insulin level and resistance to insulin-mediated glucose uptake in normal and diabetic subjects. Diabetes. 1973 Jul;22(7):507–13.

279. Michael MD, Kulkarni RN, Postic C, Previs SF. Loss of insulin signaling in hepatocytes leads to severe insulin resistance and progressive hepatic dysfunction. Molecular cell. 2000.

280. Gerich JE, Meyer C, Woerle HJ, Stumvoll M. Renal Gluconeogenesis Its

importance in human glucose homeostasis. Diabetes Care. Am Diabetes Assoc; 2001;24(2):382–91.

281. Finck BN. PGC-1 coactivators: inducible regulators of energy metabolism in health and disease. J Clin Invest. 2006 Mar 1;116(3):615–22.

282. Jiang G, Zhang BB. Glucagon and regulation of glucose metabolism. Am J Physiol Endocrinol Metab. 2003 Apr 1;284(4):E671–8.

283. Hosogai N, Fukuhara A, Oshima K, Miyata Y, Tanaka S, Segawa K, et al. Adipose Tissue Hypoxia in Obesity and Its Impact on Adipocytokine Dysregulation. Diabetes. 2007 Mar 29;56(4):901–11.

284. Burgueño AL, Burgueño AL, Gianotti TF, Mansilla NG, Gianotti TF, Pirola CJ, et al. Cardiovascular disease is associated with high-fat-diet-induced liver damage and up-regulation of the hepatic expression of hypoxia-inducible factor 1α in a rat model. Clin Sci. 2013 Jan;124(1):53–63.

285. Rother E, Belgardt BF, Tsaousidou E, Hampel B, Waisman A, Myers MG, et al. Acute selective ablation of rat insulin promoter-expressing (RIPHER) neurons defines their orexigenic nature. Proc Natl Acad Sci USA. 2012 Oct 30;109(44):18132–7.

286. Choudhury AI, Heffron H, Smith MA, Al-Qassab H, Xu AW, Selman C, et al. The role of insulin receptor substrate 2 in hypothalamic and β cell function. J Clin Invest. 2005 Mar 24;115(4):940–50.

287. Mori H, Inoki K, MUnzberg H, Opland D, Faouzi M, Villanueva EC, et al. Critical Role for Hypothalamic mTOR Activity in Energy Balance. Cell Metabolism. Elsevier Ltd; 2009 Apr 8;9(4):362–74.

288. Cakir I, Cyr NE, Perello M, Litvinov BP, Romero A, Stuart RC, et al. Obesity Induces Hypothalamic Endoplasmic Reticulum Stress and Impairs Proopiomelanocortin (POMC) Post-translational Processing. J Biol Chem. 2013 Jun 14;288(24):17675–88.

289. Williams KW, Liu T, Kong X, Fukuda M, Deng Y, Berglund ED, et al. Xbp1s in Pomc Neurons Connects ER Stress with Energy Balance and Glucose Homeostasis. Cell Metabolism. Elsevier Inc; 2014 Sep 2;20(3):471–82.

290. Sun X, Lin Y. Npas4: Linking Neuronal Activity to Memory. Trends in Neurosciences. Elsevier Ltd; 2016 Apr 1;39(4):264–75.

291. Prasad K-M, Yang Z, Bleich D, Nadler JL. Adeno-associated virus vector mediated gene transfer to pancreatic beta cells. Gene Therapy. Nature Publishing Group; 2000;7(18):1553–61.

292. Wu Z, ASOKAN A, SAMULSKI R. Adeno-associated Virus Serotypes: Vector

Toolkit for Human Gene Therapy. Molecular Therapy. 2006 Sep;14(3):316–27.

293. Daly TM. Overview of adeno-associated viral vectors. Methods Mol Biol. 2004;246:157–65.

294. Kaspar BK, Vissel B, Bengoechea T, Crone S, Randolph-Moore L, Muller R, et al. Adeno-associated virus effectively mediates conditional gene modification in the brain. Proc Natl Acad Sci USA. 2002 Feb 19;99(4):2320–5.

295. Jimenez V, Ayuso E, Mallol C, Agudo J, Casellas A, Obach M, et al. In vivo genetic engineering of murine pancreatic beta cells mediated by single-stranded adeno-associated viral vectors of serotypes 6, 8 and 9. Diabetologia. 2011 Feb 11;54(5):1075–86.

296. Montane J, Bischoff L, Soukhatcheva G, Dai DL, Hardenberg G, Levings MK, et al. Prevention of murine autoimmune diabetes by CCL22-mediated Treg recruitment to the pancreatic islets. J Clin Invest. 2011 Aug 1;121(8):3024–8.

297. Poungvarin N, Lee JK, Yechoor VK, Li MV, Assavapokee T, Suksaranjit P, et al. Carbohydrate response element-binding protein (ChREBP) plays a pivotal role in beta cell glucotoxicity. Diabetologia. 2012 Mar 3;55(6):1783–96.

298. Riedel MJ, Gaddy DF, Asadi A, Robbins PD, Kieffer TJ. DsAAV8-mediated expression of glucagon-like peptide-1 in pancreatic beta-cells ameliorates streptozotocin-induced diabetes. Gene Therapy. Nature Publishing Group; 2009 Oct 29;17(2):171–80.

299. Johnson MC, Garland AL, Nicolson SC, Li C. β-Cell–Specific IL-2 Therapy Increases Islet Foxp3+ Treg and Suppresses Type 1 Diabetes in NOD Mice. Diabetes. 2013.

300. Gaddy DF, Riedel MJ, Pejawar-Gaddy S, Kieffer TJ, Robbins PD. In Vivo Expression of HGF/NK1 and GLP-1 From dsAAV Vectors Enhances Pancreatic -Cell Proliferation and Improves Pathology in the db/db Mouse Model of Diabetes. Diabetes. 2010 Nov 29;59(12):3108–16.

301. Gaddy DF, Riedel MJ, Bertera S, Kieffer TJ, Robbins PD. dsAAV8-mediated gene transfer and β-cell expression of IL-4 and β-cell growth factors are capable of reversing early-onset diabetes in NOD mice. Gene Therapy. 2012 Aug;19(8):791–9.

302. Mehran AE, Templeman NM, Brigidi GS, Lim GE, Chu K-Y, Hu X, et al. Hyperinsulinemia Drives Diet-Induced Obesity Independently of Brain Insulin Production. Cell Metabolism. Elsevier Inc; 2012 Dec 5;16(6):723–37.

303. Tamarina NA, Roe MW, Philipson LH. Characterization of mice expressing Ins1 gene promoter driven CreERT recombinase for conditional gene deletion in pancreatic β-cells. islets. 2014 Jan 14;6(1):e27685–10.

304. Oropeza D, Jouvet N, Budry L, Campbell JE, Bouyakdan K, Lacombe J, et al. Phenotypic Characterization of MIP-CreERT 1LphiMice With Transgene-Driven Islet Expression of Human Growth Hormone. Diabetes. 2015 Oct 22;64(11):3798–807.

305. Jiang F-X, Mehta M, Morahan G. Quantification of insulin gene expression during development of pancreatic islet cells. Pancreas. 2010 Mar;39(2):201–8.

306. Murea M, Ma L, Freedman BI. Genetic and environmental factors associated with type 2 diabetes and diabetic vascular complications. Rev Diabet Stud. 2012;9(1):6–22.

307. Lin Y, Sun Z. Current views on type 2 diabetes. J Endocrinol. 2009 Dec 8;204(1):1–11.

308. Rudic RD, McNamara P, Curtis A-M, Boston RC, Panda S, Hogenesch JB, et al. BMAL1 and CLOCK, Two Essential Components of the Circadian Clock, Are Involved in Glucose Homeostasis. Plos Biol. 2004;2(11):e377.

309. Shin S, Le Lay J, Everett LJ, Gupta R, Rafiq K, Kaestner KH. CREB mediates the insulinotropic and anti-apoptotic effects of GLP-1 signaling in adult mouse β-cells. Molecular Metabolism. Elsevier GmbH; 2014 Nov 1;3(8):803–12.

310. Soleimanpour SA, Crutchlow MF, Ferrari AM, Raum JC, Groff DN, Rankin MM, et al. Calcineurin Signaling Regulates Human Islet -Cell Survival. J Biol Chem. 2010 Dec 10;285(51):40050–9.

311. Johnson JD, Ao Z, Ao P, Li H, Dai L-J, He Z, et al. Different Effects of FK506, Rapamycin, and Mycophenolate Mofetil on Glucose-Stimulated Insulin Release and Apoptosis in Human Islets. cell transplant. 2009 Aug 1;18(8):833–45.

312. Qiu J, Tan Y-W, Hagenston AM, Martel M-A, Kneisel N, Skehel PA, et al. Mitochondrial calcium uniporter Mcu controls excitotoxicity and is transcriptionally repressed by neuroprotective nuclear calcium signals. Nat Commun. 2013;4:2034.

313. Pullen TJ, Khan AM, Barton G, Butcher SA, Sun G, Rutter GA. Identification of genes selectively disallowed in the pancreatic islet. islets. 2014 Oct 27;2(2):89–95.

314. Pullen TJ, Rutter GA. When less is more: the forbidden fruits of gene repression in the adult β-cell. Diabetes, Obesity and Metabolism. 2013 Jun;15(6):503–12.

315. Yoshihara E, Wei Z, Lin CS, Fang S, Ahmadian M, Kida Y, et al. ERRγ Is Required for the Metabolic Maturation of Therapeutically Functional Glucose-Responsive β Cells. Cell Metabolism. Elsevier Inc; 2016 Apr 12;23(4):622–34.

316. Lam CKL, Chari M, Lam TKT. CNS Regulation of Glucose Homeostasis. Physiology. 2009 Jun 9;24(3):159–70.

317. Kalra SP. Appetite and body weight regulation: is it all in the brain? Neuron. 1997.

318. Bonora E. Protection of pancreatic beta-cells: Is it feasible? Nutrition, Metabolism and Cardiovascular Diseases. 2008 Jan;18(1):74–83.

319. Wu Q, Lemus MB, Stark R, Bayliss JA, Reichenbach A, Lockie SH, et al. The Temporal Pattern of cfos Activation in Hypothalamic, Cortical, and Brainstem Nuclei in Response to Fasting and Refeeding in Male Mice. Endocrinology. 2014 Mar;155(3):840–53.

320. Cravo RM, Margatho LO, Osborne-Lawrence S, Donato J Jr, Atkin S, Bookout AL, et al. Characterization of Kiss1 neurons using transgenic mouse models. Neuroscience. 2011 Jan;173:37–56.

321. Balthasar N, Dalgaard LT, Lee CE, Yu J, Funahashi H, Williams T, et al. Divergence of Melanocortin Pathways in the Control of Food Intake and Energy Expenditure. Cell. 2005 Nov;123(3):493–505.

322. Lee H, Kim D-W, Remedios R, Anthony TE, Chang A, Madisen L, et al. Scalable control of mounting and attack by Esr1+ neurons in the ventromedial hypothalamus. Nature. Nature Publishing Group; 2014 May 20;509(7502):627–32.

Appendices

Appendix A : diagram of ChIP primers used in the Chapter 3

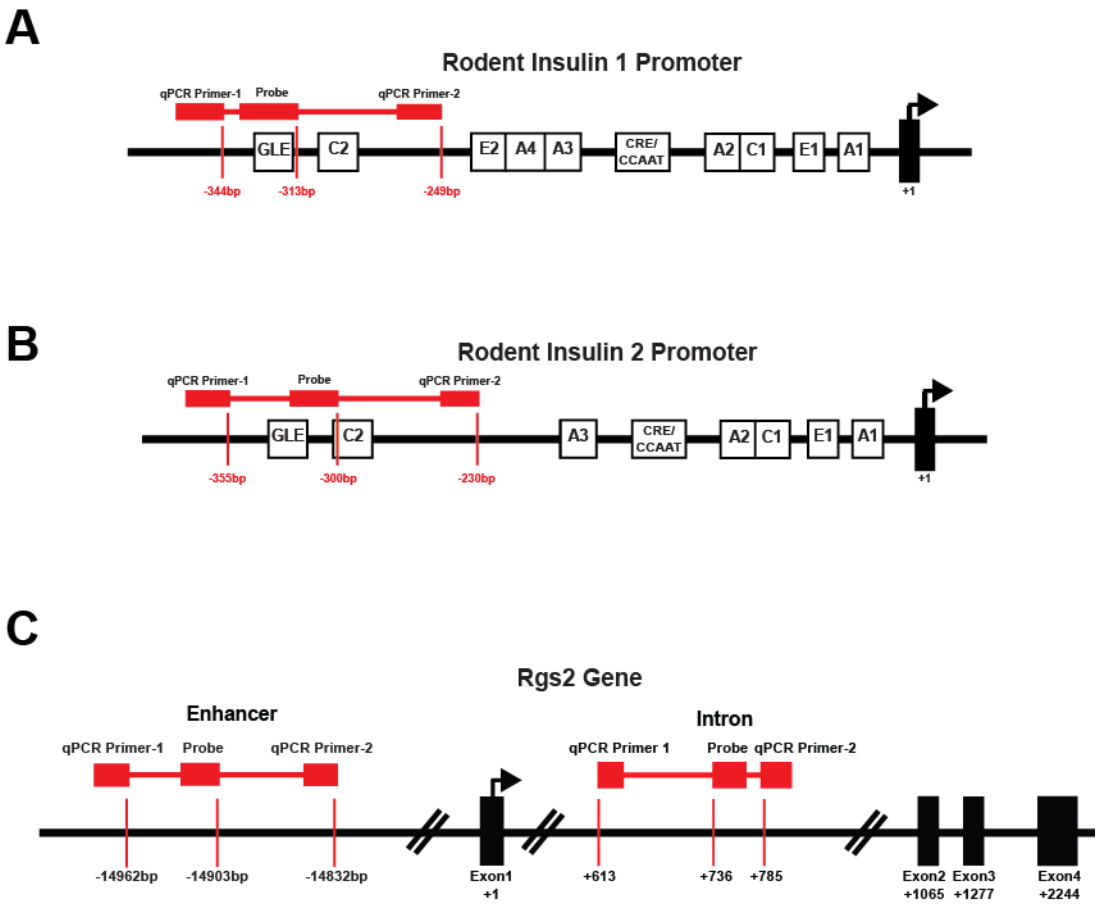

Appendix B : timeline for Pdx1CreER Npas4 KO mice